



Final Technical Report

The Water-to-Wire (W2W) Project

*Funding Opportunity Number: DE-FOA-000069
Contract #: DE-EE0002652*

DOE EERE Advanced Water Power (AWP) Program

FFP CAGE Code: 584M1

FFP Company Address:
239 Causeway St, Suite 300
Boston, MA 02114
Fax: 617-367-3372

FFP Principal Investigator: Dr. Edward C. Lovelace (formerly CTO & EVP of Engineering)

FFP Administrative Contact: Daniel Lissner, General Counsel
978-252-7111, dlissner@free-flow-power.com

Proprietary Data Legend:

The data contained in pages (none) of this report have been submitted in confidence and contain trade secrets or proprietary information, and such data shall be used or disclosed only for evaluation purposes, provided that if this applicant receives an award as a result of or in connection with the submission of this application, DOE shall have the right to use or disclose the data herein to the extent provided in the award. This restriction does not limit the Government's right to use or disclose data obtained without restriction from any source, including the applicant.

1 Executive Summary

The purpose of the Free Flow Power (FFP) Water-to-Wire Project (Project) was to evaluate and optimize the performance, environmental compatibility, and cost factors of FFP hydrokinetic turbines through design analyses and deployments in test flumes and riverine locations.

Specific objectives of the Project were:

- Design, fabrication, and testing of a full-scale prototype hydrokinetic turbine (Endpoint: functional generating hardware)
- In-river deployment and testing of the full-scale prototype turbine (Endpoint: test data demonstrating performance, river environment, and resource potential)
- Design and analyses for the commercial scale infrastructure and identification of viable sites (Endpoint: refined cost and design for complete array systems to provide launch point for next TRL level deployments)

The Project was intended to address the challenge that there are no commercially operating hydrokinetic river systems in existence in the United States, and therefore uncertainty exists about the performance of hydrokinetic turbine equipment in a relevant environment, commercial cost of capital and O&M for practical systems, and the amount of generation that is practically achievable from the available resource. The Project was conducted in conjunction with FFP’s regulatory activities in furtherance of the licensing of more than 50 potential hydrokinetic sites in the Mississippi River, the largest river system in the United States.

The Project results, summarized in this report and in additional filings publicly available through the Federal Energy Regulatory Commission’s (FERC) electronic docket system (eLibrary), provide a pathway and supporting data and demonstration results from FFP’s hydrokinetic turbine that will assist all hydrokinetic developers in addressing the design and cost challenges associated with turbine siting, installation, and maintenance, with particular emphasis on commercial-scale riverine applications.

The results from the Project were:

- Design and fabrication of a full-scale (3-meter diameter, 40kW in 3.5 m/sec free stream flow) axial ducted hydrokinetic turbine;
- Initial operational validation of the hydrokinetic turbine at Conte Anadromous Fish Research Laboratory (CAFRL) in Turner Falls, Massachusetts;
- Deployment of the hydrokinetic turbine in 2011 on a floating test platform in the Mississippi River near Baton Rouge, Louisiana, where it generated power continuously for several months, validating turbine performance predictions and the consistent river flow rate potential;
- Attempted re-deployment of the hydrokinetic turbine in 2012 with enhanced instrumentation from the National Renewable Energy Laboratory (NREL) through a Cooperative Research and Development Agreement, which was concluded when damage resulted to the four-year-old floating platform, necessitating repairs that would have exceeded the budget of the Project.

- Analysis of more than 50 potential hydrokinetic commercial sites in the Mississippi River, including preliminary design of commercial arrays, identification of feasible locations for infrastructure deployment, and assessment of environmental factors relevant to hydrokinetic deployments.
- Array energy assessments conducted in collaboration with Sandia National Laboratory (SNL) to investigate net energy output and impact on the flow behavior of the river.



FFP hydrokinetic turbine deployed on the Mississippi River

The Project supported the de-risking of hydrokinetic project development and technology deployment in the Lower Mississippi River (LMR), the more significant potential riverine hydrokinetic resource in the United States. The resource assessment information developed through the Project will support technology selection and project feasibility analyses for the LMR, a major potential source of renewable energy for the South-Central region of the United States. The information discussed in this report, as well as additional information available through FERC’s eLibrary that is accessible as described herein, will facilitate future commercial development activities of the nation’s premier hydrokinetic river system and will more broadly support technology development and activities in furtherance of the development of hydrokinetic renewable energy projects.

2 Overview

2.1 Technical Approach

Phase I of the Project addressed the challenge of identifying optimal locations for installation of hydrokinetic turbine generators within a riverine environment, and assessing the performance of and the effect of the environment on, and by, installed turbines. The methods utilized during Phase I included design, operation, and deployment of a full-scale prototype hydrokinetic turbine, including performance data collection and comparison to analytical predictions. Other methods utilized for the analysis of potential hydrokinetic commercial-scale deployment locations included analysis of river bathymetry, overlaying of competing-use GIS layers, and locating of pilings to maximize potential build out of multiple LMR sites. In addition, velocity transects obtained through field collection were analyzed in connection with historical river stage and flow data to develop velocity duration curves and location-specific velocity distributions at the deployment site.

Phase II of the Project addressed the challenge of developing and deploying a durable, cost-efficient mounting technology that will facilitate installation and maintenance of hydrokinetic turbine generators without disrupting navigation or creating other adverse consequences. The scope of this phase built upon the piling and turbine placement efforts of Phase I, which were expanded in Phase III to include piling, yoke, and cable design efforts. Methods utilized during Phase II included conceptual mechanical design, loading analysis, operational analysis for normal and faulted behavior, and supply chain costing analysis.

The Project effort was unique because it focused on the challenges of developing a commercial-scale hydrokinetic installation across a range of riverine sites. Information developed and lessons learned through the Project will provide valuable resources in furtherance of the key issues relevant to the development of commercial-scale (as opposed to demonstration or pilot) hydrokinetic projects, including resource potential, practical generation capacity, equipment design and performance for the environment, and both capital and operational costs.

2.2 Project Plan/Schedule

The Project was conducted over the course two years, from 3Q 2010 to 3Q 2012. Project milestones are reported below in reference to Federal fiscal quarters, and deviations from originally anticipated milestone dates are reflected where appropriate. Results of the Project activities are discussed below in Section 3 – Technical Discussion.

3Q10 (including activities retrospective to February 15, 2010)

- Executed Project contract and certified NEPA compliance
- Completed initial operational testing of 3-meter turbine at CAFRL test flume
 - o Verified cut-in speed
 - o Verified structural integrity at maximum flow
 - o Verified open circuit flow vs. rpm
- Commenced electric generator installation on 3-meter turbine
- Completed first FERC environmental study report for Mississippi River sites
 - o Infrastructure siting study – developed proposed turbine field boundaries for 51 sites, a screening assessment strategy for barge-mounted deployments, and conceptual plan for piling-based test deployment site
 - o Hydraulic study – developed overview of baseline data to constitute input parameters for CFD modeling and proposal for phase 2D and 3D modeling of hydraulic effects, and preliminary plan for estimating effects of vibration on existing structures
 - o Navigation study – developed study matrix to assess relevant data and stakeholder comments
 - o Damaged turbine and debris risk study – developed preliminary design of support structures and installation approaches and assessment of characteristics of river debris
 - o Fish entrainment study – developed proposal of methodologies and fish species, age classes, and sizes for controlled entrainment testing, discussed available data

- from USACE’s Engineer Research and Development Center, Environmental Laboratory (ERDC-EL) for population analysis
- Acoustic energy study – provided analysis of acoustic energy resulting from pile driving, sensitivity of fish species to acoustic species, and plan for measuring acoustic fields
- Electromagnetic fields study – provided proposed list of fish species of focus and assessment of electromagnetic fields (EMF) potential at representative sites

4Q10

- Completed generator installation on 3-meter turbine at CAFRL test flume
- Finalized floating mount design modifications to accommodate 3-meter turbine
- Completed second FERC environmental study report for Mississippi River sites
 - Infrastructure siting study – analyzed water surface elevation and historical bathymetry at five sites, revised conceptual plan for piling-based test deployment site
 - Hydraulic study – developed plan for documenting hydraulic and sediment conditions during test deployment, revised plan for estimating effects of vibration on existing structures
 - Navigation study – provided plan for data collection to address traffic survey study requirement
 - Damaged turbine and debris risk study – developed preliminary assessment of risk to turbines, plan for analysis of potential effects of debris on turbines and piling mounting systems, and preliminary design of piling mounting structures and analysis of loads and vibrations
 - Fish entrainment study – provided revised methodology for laboratory entrainment testing and discussed literature review on causes of injury and mortality
 - Electromagnetic fields study – analyzed potential of turbine components to generate EMF

1Q11

- Completed electrical generator testing of 3-meter turbine at CAFRL test flume

2Q11

- Completed third FERC environmental study report (Initial Study Report) for Mississippi River sites
 - Infrastructure siting study – developed proposed piling locations and turbine quantity calculations for five lead sites
 - Hydraulic study – refined study methodologies in consultation with USACE Independent Technical Review Team (ITRT)
 - Navigation study – discussed USACE’s Waterborne Commerce Statistics Center (WCSC) data and provided photographic record of traffic observations at single site
 - Damaged turbine and debris risk study – provided photographic record of observations of debris and detailed plan for analysis of effects of debris on barge-mounted systems

- Fish entrainment study – provided methodology for analyzing population-level effects utilizing ERDC-EL data and revised methodology for controlled entrainment testing at CAFRL
- Acoustic energy study – provided assessment of characteristics and amplitude of acoustic energy in project construction, maintenance, and operation
- Completed piling-based concept design and equipment Request for Quotations

3Q11

- Completed fabrication of floating platform design modifications (originally scheduled 1Q11)
- Deployed 3-meter turbine on floating platform at Mississippi River site (originally scheduled 1Q11)
 - Verified turbine coefficient of performance
 - Verified other turbine operational parameters
 - Recorded debris, fish, and navigation data
 - Recorded and analyze resource variation over time
- Analyzed costs and risks of equipment for piling-based deployment

4Q11

- Conducted periodic monitoring and survey of turbine deployment and candidate piling-based site (originally scheduled 2Q11)
- Removed turbine and floating mount during low river stage for teardown assessment following 3+ months deployment
- Completed fourth FERC environmental study report for Mississippi River sites
 - Infrastructure siting study – developed refined proposed turbine field boundaries for 51 sites to address competing uses, controlling works, and substation locations
 - Hydraulic study – developed preliminary 2D analysis of near-field hydraulic effects
 - Navigation study – provided consultation results and discussion of navigational data from WCSC
 - Damaged turbine and debris risk study – provided results from riverine deployment of turbine, including observations regarding in-river debris, fish, and navigation
 - Fish entrainment study – provided discussion of ERDC-EL data set and proposed biostatistics approach to analysis
 - Acoustic energy study – provided results of consultation regarding acoustic energy in project construction, operation, and maintenance
 - Electromagnetic fields study – provided results of navigation survey and analysis of EMF frequencies generated by turbine equipment

1Q12

- Completed selection of site for piling-based deployment
- Conducted array flow analysis in cooperation with SNL
- Designed instrumentation system in cooperation with NREL
- Completed turbine deployment effort and removed floating mount system

2Q12

- Completed fifth FERC environmental study report for Mississippi River sites
 - o Infrastructure siting study – developed refined proposed piling locations and turbine quantity calculations for 51 sites
 - o Hydraulic study – provided refined 2D analysis of near-field hydraulic effects
 - o Navigation study – analyzed WCSC navigational traffic data and discussion of US Coast Guard (USCG) compliance
 - o Damaged turbine and debris risk study – analyzed debris impact
 - o Fish entrainment study – provided biostatistics analysis of ERDC-EL dataset and report on fish distribution
 - o Electromagnetic fields study – discussed EMF baseline and fish and aquatic sensitivity to EMF

3Q12

- Completed sixth FERC environmental study report for Mississippi River sites
 - o Infrastructure siting study – developed refined methodologies and cost estimates for test deployment, including plans for monitoring of fish population, fish entrainment, hydraulics, acoustics, and navigation
 - o Hydraulic study – provided preliminary 2D analysis of field-field hydraulic effects
 - o Damaged turbine and debris risk study – provided zone categorization and methodology for seismic analysis

2.3 Technical Accomplishments and Progress

Technical goals accomplished through the Project include the following:

1. FFP successfully deployed the prototype hydrokinetic turbine, generating electricity immediately upon deployment, and transitioned to continuous 24-hour per day generating operation. This is significant because it was the first hydrokinetic deployment funded under the AWP program to generate electricity, and because the turbine operated successfully, with no performance degradation over the course of the Project, and met design coefficient of performance predictions.
2. FFP developed detailed piling-based deployment locations and energy generation projections for multiple potential hydrokinetic sites on the Mississippi River, utilizing a combination of historical data, information developed through direct consultation with regulators and stakeholders, and field data collected through the deployment. This information was published in FFP’s FERC study reports and provides a blueprint for future development activities across a large reach of the LMR.
3. FFP completed conceptual mechanical design of a durable, cost-efficient mounting technology, including design of pilings, yokes, and cabling, that will enable installation and maintenance of piling-based hydrokinetic turbine generators in a manner that is compatible with environmental conditions and existing uses of a river, including navigation.

2.4 Identification of Challenges

FFP experienced and addressed the following challenges while conducting the Project:

1. Construction and deployment of a robust floating platform test bed for an extended duration was constrained by the available budget for the Project, and ultimately the riverine deployment phase of the Project was concluded when the structural viability of the floating platform was compromised.
2. Delays in commencing the deployment phase of the Project resulted from factors beyond the control of the Project, including a six-month deviation from the original schedule while awaiting regulatory approval for the deployment premised in part upon the recession of high-water conditions.

2.5 Approaches to Resolving Issues or Challenges

FFP managed the challenges faced during the Project primarily through contingency planning, both on schedule and cost.

One significant challenge was the cancelling of the riverine re-deployment of the floating mount and turbine in 2012. Mechanical failures of components of the floating mount (but not the hydrokinetic turbine) increased the cost of the re-deployment by an additional \$150,000, which exceeded the budget allocated to this phase of the Project.

- Necessity of back-up mechanical systems – the floating mount platform was designed with multiple back-up systems to prevent loss of the hydrokinetic turbine in the event of unpredicted risks. The turbine was secured to the floating mount with substantially independent subsystems: four separate stay cables (overhead left, overhead right, bow left, and bow right) and four mechanical rotating arms (two left, two right). When the mechanical arms failed, the turbine remained connected to the floating mount and was retrieved by means of the stay cables. A lesson reinforced by this challenge is that back-up systems are necessary for critical risks, and chain falls are the most useful tool for raising and lowering hydrokinetic turbine equipment when primary systems do not function as planned. Chains falls should be installed consistently as a back-up system for secondary raising and lowering.
- Repetitive structural inspections – the floating mount platform was deployed for three separate study periods over the course of three years: for six continuous months from July 2009 to January 2010; again from May 2011 to September 2011; and a third time in February 2012, when it finally experienced mechanical failure. During these deployments the hydrokinetic turbine was raised/lowered by means of the mechanical arms more than 100 times, with accumulated in-water immersion of more than 12 months. Following removal of the floating mount from the water after the second deployment in September 2011, an inspection was conducted in October 2011, at which time corrosion on the load-bearing bolts was not visible. Subsequently, a re-deployment was scheduled for February

2012 due to the availability of National Laboratory experience and an opportunity to obtain additional field measurements under similar river stage and loading conditions as previously tested successfully. After the mechanical failure of the mechanical arms in February 2012, the floating mount was removed to land and retired, at which time corrosion was visible on some of the load-bearing bolts. While the root cause of the mechanical failure during the February 2012 deployment is unknown, it is possible that primary corrosion may have occurred but not been visible at the time of the October 2011 inspection, or that the corrosion occurred after this inspection but prior to the re-deployment. A lesson reinforced by this challenge is that frequent, redundant inspections are necessary to fully assess risks of riverine deployments, and that the condition of equipment utilized in challenging underwater environments may deteriorate rapidly. Where the floating mount platform used in the Project was not designed to be a permanent mounting solution for FFP’s hydrokinetic deployments, FFP’s primary focus for risk mitigation was installation of redundant back-up systems as opposed to detailed prospective assessments of the life expectancy of floating mount components, such as those performed for the turbine and piling-based components in FFP’s Damaged Turbine and Debris Risk Study. These back-up systems operated as planned.

- Alternate plan for allocation of resources – the re-deployment of the floating mount and turbine in February 2012 was a modification to the originally conceived study plan that became possible when National Laboratory resources and expertise became available for the Project. When the re-deployment was cancelled as a result of its projected cost (including necessary floating mount repairs) exceeding the available budget, FFP refocused its efforts to the Phase 2 design and cost analysis for pre-production piling-based systems. A lesson reinforced by this challenge is that development of a Project plan should seek to utilize available opportunities that may arise during the course of execution of the Project, but a back-up (in this case, original) alternative plan should be conceived in the event that these opportunities do not fully materialize.

A second significant challenge was the delay of the 2011 deployment as a result of record high river conditions. During the spring of 2011, the Mississippi River experienced unprecedented flood-stage conditions, requiring the USACE to open flood control structures that have never before been utilized in order to control the flows. FFP felt that these conditions rendered the river unsafe to attempt deployment at the intended dock facility, so efforts were suspended until river stages had subsided to safer levels. The lesson reinforced by this challenge was that river conditions can be variable, particularly in free-flowing hydrokinetic environments, and that safety must be prioritized first and foremost, as it was in this case.

2.6 Research Integration

The resource potential for river hydrokinetics is addressed through seasonal deployment, river velocity surveys, and analytical velocity/depth modeling at various river stages. Identification and solution to barriers is achieved through the design, analysis, and implementation of river hydrokinetic systems targeted towards eventual commercially licensed projects.

This Project is a critical-path contributor to commercializing hydrokinetics along the Mississippi River. FFP already had under environmental study and site design, the largest project pipeline worldwide for hydrokinetics. The performance of the prototype turbine and associated river environment data informs the design and implementation of subsequent larger scale deployments beyond this Project.

FFP participated in dissemination of results with individual briefings to the DOE, collaboration with the National Lab AWP projects, DOE-sponsored events, and general public events focused on hydropower, renewable energy, and the green economy.

3 Technical Discussion

The following discusses the results of operational testing performed on FFP’s 3-meter hydrokinetic turbine (3M01) throughout the course of the Project, the design of piling systems to support installations of hydrokinetic turbines in riverine environments, and the study efforts that assessed the effects of the environment on hydrokinetic infrastructure as well as the effects of such infrastructure on environmental resources.

3.1 Flume Testing of Turbine Operation

FFP developed and tested its 3M01 at the indoor water flume at CAFRL in February 2010 and November 2010.

In February 2010, FFP tested the assembled 3M01 rotor and housing, without a generator, including rotor speed under a variety of flow conditions. Results of those tests are summarized in Appendix 1.

In November 2010, FFP incorporated the electric generator into the 3M01 and tested performance characteristics of the completed hydropower turbine/generator system, including tip speed ratio and power generation under low- and high-flow scenarios. Results of those tests are summarized Appendix 2.

3.2 Riverine Testing of Turbine Operation

In the fall of 2010, FFP began construction of a floating mount platform (FM) to deploy the 3M01 in a live river environment on the Mississippi River for additional testing. The FM was constructed by re-using parts from an original FM that had been utilized for the deployment of a 1.4-meter proof-of-concept prototype from July 2009 to January 2010. FM construction and integration of the 3M01 were completed in May 2011.

At the time that FFP was fabricating the FM, FFP applied for, and subsequently obtained, a USACE Nationwide Permit to authorize the continuous mooring of the FM at a private dock in the main channel of the Mississippi River. FFP had initially planned to utilize a different mooring site, identified in the permit application as Site 28; however, this site proved to be

inadequate due to a long-term repair and construction effort at the industrial dock. An alternate industrial owner then made its site available to FFP; the permit application was therefore modified to conform to this new site, located approximately 23 miles downstream in Site 25, near Baton Rouge, Louisiana.

Velocity surveys were conducted at Site 25 on February 8, 2011, prior to deployment, to project expected velocities at the site during the deployment, as depicted in the figures below. The velocities were in the range of 0.8 to 1.4 m/s on a day that the Baton Rouge gage was at 9.6 feet. The B-R gage “Surface Mean Velocity” at the same height was 0.98 m/s, indicating that at least similar or better velocities should be expected at the moored deployment site.

The spring of 2011 brought record flooding to the Mississippi River Basin; as a result, FFP elected to delay its FM deployment after consultation with USACE, USCG, and the industrial dock owner. The delay lasted until the river stage and flooding control activities had returned to normal operations and the river stage receded with a reasonable forecast of ongoing descent.

The FM system was towed into the river channel for final configuration and system testing operations on May 10, 2011 and May 13, 2011. On the first deployment, the FM was deployed in areas where available velocities were below the cut-in speed of the 3M01 rotor. When lowered into the water on May 13, 2011, the 3M01 successfully generated power.

On June 20, 2011, the FM system was ferried from the shipyard to the main channel and moored at the industrial dock. FFP performed testing operations by traveling to the mooring site (boat access by river only), lowering and operating the turbine, and then raising the turbine. The FM system remained at the mooring site until September 2011, when the river was at or near its lowest seasonal stage, and therefore lowest velocity, at which time it was decommissioned.

During the course of the deployment at the industrial dock site, FFP collected data and obtained measurements related to river conditions and the performance of the turbine. Results from those measurements are summarized below.

3.2.1 Flow Velocity Measurement

During the course of the deployment, velocities were monitored on per minute intervals from June 20, 2011 to July 18, 2011. Average daily velocities ranged from 1.7 meters per second to 1.48 meters per second, declining steadily over the course of the deployment in line with expectations.

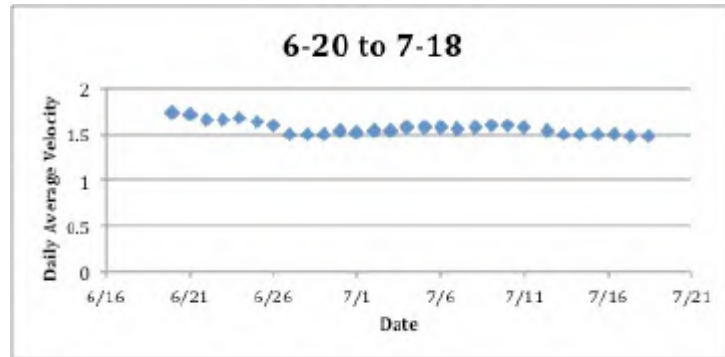


Figure 2: Daily Average Velocity by Date

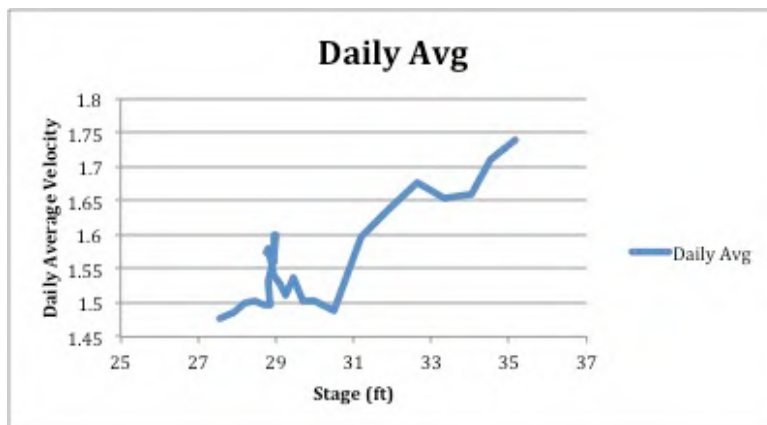


Figure 3: Daily Average Velocity by River Stage

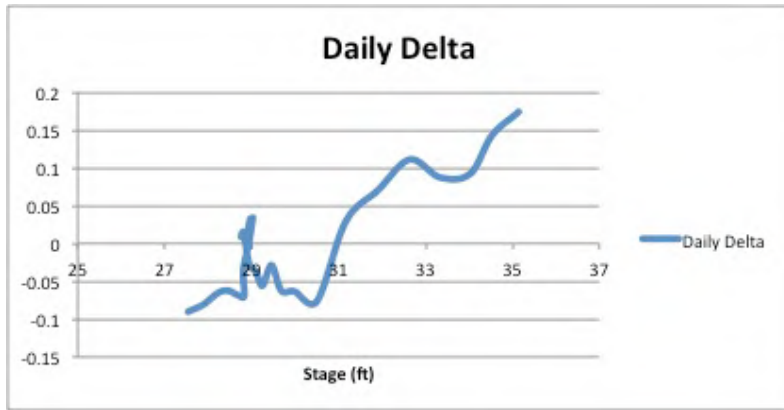


Figure 4: Daily Average Velocity Change by River Stage

3.2.2 Turbine Performance Testing

The 3M01 generated power consistent with expectations for the given flow velocities during the period of deployment. Data regarding average current, rotor speed, mechanical power, and power are summarized in Appendix 3.

3.2.3 Environmental Studies

The Project supported the study of the effects of a freshwater, riverine environment on the 3M01 turbine through the demonstration deployment, while also supporting further study of the effect of the 3M01 on the environment. The environmental components of the Project were undertaken carefully order to ensure conformity of the Project scope with the National Environmental Policy Act and consisted primarily of analysis of existing available data and literature review. Where compatible and appropriate, these study activities were complemented by field measurements and observations.

Study activities were collected and reported publicly in the following study reports, which were filed by FFP with the FERC in connection with FFP’s licensing of proposed hydrokinetic sites on the LMR. Complete copies of each study report are available for download from FERC’s eLibrary by either of the following methods:

- Docket Search: Visit http://elibrary.ferc.gov/idmws/docket_search.asp and search under Docket Number “P-12829” for a chronological listing of all documents, including the study reports, organized by subdocket.
- Accession Number Search: Visit <http://elibrary.ferc.gov/idmws/search/fercadvsearch.asp> and enter the Accession Number of each document in the “Accession Number” field, under the category “Numbers” (Note: confirm that the check box next to the “Date” field is empty or that the range of dates includes the date filed for the relevant document)

Study Report	Date Filed	Accession Number
First Study Report	April 30, 2010	20100430-5006 (Part 1) 20100430-5010 (Part 2) 20100430-5013 (Part 3)
Second Study Report	August 2, 2010	20100802-5099
Initial (Third) Study Report	January 19, 2011	20110119-5037
Fourth Study Report	August 1, 2011	20110801-5016
Fifth Study Report	February 1, 2012	20120201-5031
Sixth Study Report	July 31, 2012	20120731-5170

Of particular relevance to the scope of the Project were the Infrastructure Siting Study, the Hydraulic Study, the Navigation Study, the Damaged Turbine and Debris Risk Study, and the Fish Entrainment Study. In addition to the Infrastructure Siting Study reflecting one of the primary goals of the Project – the identification of viable site for hydrokinetic infrastructure deployment – the information and experienced collected during the Project’s riverine deployment was instrumental in refining and validating conclusions developed in the course of the other study activities. The design of piling-based turbine infrastructure, another primary goal of the Project, is reflected in the design of the *in situ* deployment, reported in the Infrastructure Siting study. This design reflects the paramount benefit of the interrelationship between the Project’s objectives and FFP’s ongoing study activities for purposes of FERC licensing, in that it reflects extensive consultation with stakeholders and practical consideration of the effects of actual proposed hydrokinetic projects that were the subject of ongoing licensing activity.

3.2.3.1 Infrastructure Siting Study

The goals of the Infrastructure Siting Study were:

- To determine the number and locations of turbines that can be deployed at each of FFP’s proposed commercial-scale hydrokinetic sites without adverse impact to other important LMR uses and resources;
- To determine the location of other infrastructure, such as associated cabling, substations, access roads, and construction staging areas; and
- To determine the location and configuration for the FERC-mandated *in situ* deployment.

The Infrastructure Siting Study included the majority of activities relating to a primary goal of the Project – design and analysis of commercial scale infrastructure and identification of viable sites. During the course of this study, FFP investigated the feasibility of hydrokinetic installations at more than 60 sites, conducted extensive consultation with stakeholders including the USACE and USCG regarding restrictions that would be placed on potential siting locations, and then refined initial projects to identify specific piling/turbine locations within each of the sites. Further, the design of the infrastructure itself was advanced through the layout of the proposed *in situ* deployment, which FERC mandated to be representative of a full-scale commercial deployment in terms of equipment and configuration.

The following summarizes key results identified through the course of the Infrastructure Siting Study:

- The outsides of river bends are optimal locations for piling-based hydrokinetic turbine installations, since these locations typically correspond to both greatest depths and highest velocities. The majority of the sites for which FFP prepared proposed turbine locations included river bends, and the majority of the areas suitable for hydrokinetic turbine deployment were located along the outside of these bends.
- The Mississippi River is a highly engineered water system, including measures utilized by the USACE to control flooding and erosion (including structures such as levees and revetments and activities such as dredging), numerous bridges and utility and pipeline crossings, and many areas designed by the USACE or USCG for anchorages or other purposes. Identification of these areas of competing uses and negotiation of strategies for mitigating effects of hydrokinetic installations is an essential component of infrastructure siting. Frequently, the only acceptable form of mitigation that will be considered is avoidance.
- Deployment of hydrokinetic turbines on pilings will require that infrastructure must be submerged to a depth that will ensure that it is safe from collision with navigational traffic or other competing uses. This allowable distance will be the subject of consideration by the USACE, USCG, FERC, and potentially other stakeholders. After extensive consultation on this point, FFP proposed siting its hydrokinetic turbine infrastructure at a depth of not less than 20 feet below Low Water Reference Plane (LWRP) in the shallow-draft sections of the LMR (upriver approximately from Baton Rouge, Louisiana), and 65 feet below LWRP in the deep-draft sections of the LMR (downriver approximately from Baton Rouge, Louisiana). Uncertainty about future river stage levels will complicate this analysis, particularly where the term of an original

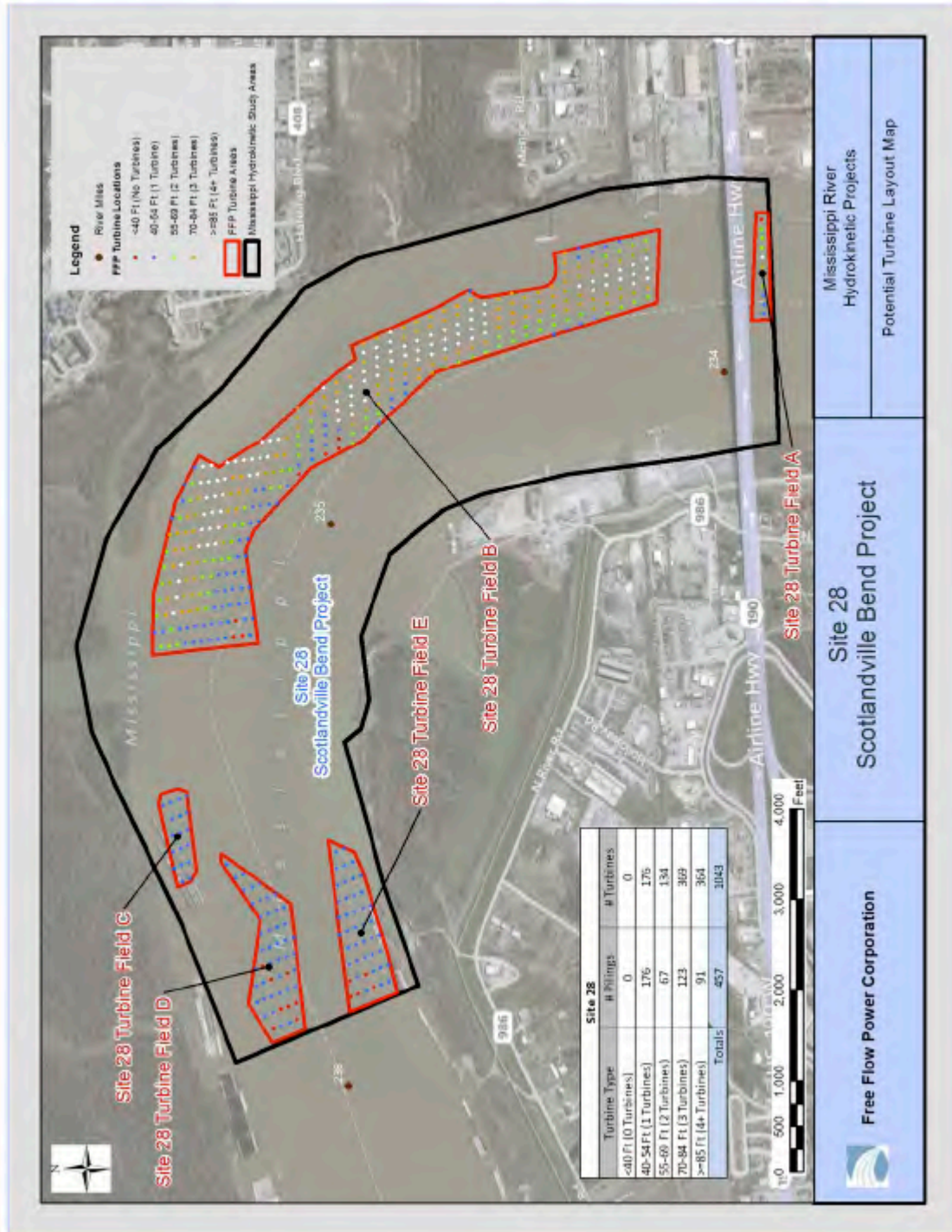
FERC license is 30 to 50 years but where the LMR has recently experienced historic levels of drought.

- Deployment of hydrokinetic turbines by suspending them from floating structures, such as barges, was an approach considered but ultimately foregone by FFP. FFP determined that the requirement to avoid surface-level uses of the LMR (such as barge navigation) would render only a few locations feasible for hydrokinetic deployments, as opposed to the greater potential scale of piling-based deployments.

The figure below depicts a representative commercial-scale hydrokinetic site, consisting of piling-based deployments, screened for allowable depth and avoidance of competing uses. This particular site is Site 28, Scotlandville Bend, located near Baton Rouge, Louisiana. The assessment was based on the turbine field boundary, as established by bathymetric analysis, with a turbine density arrangement of 90-feet transverse piling spacing, 150-longitudinal piling spacing, with each row offset by 50%. The turbine density grid pattern was overlaid over the turbine field area and rotated to roughly match the stream flow orientation. Then the grid point were matched to the closest bathymetric data point to obtain the number of turbines that can be stacked on one piling.

Additional turbine siting maps were published in the Fifth Study Report under the Infrastructure Siting Study.

(Continued on Next Page)



The analysis that was incorporated into the turbine siting activities included assessment of available bathymetric and hydraulic data, site-specific mapping of competing uses, and

assessment of viable locations for on-shore substation infrastructure. Where available, additional site-specific information was collected and utilized. Site 28 provides one example where additional field studies of flow information by ADCP were incorporated into the assessment. Such additional effort was allocated to Site 28 due to its consideration as a prospective site for the *in situ* deployment. The following figures reflect additional analysis of Site 28, focusing on available flows and the appropriate location for siting turbine infrastructure to maximize electricity output within the site boundaries.

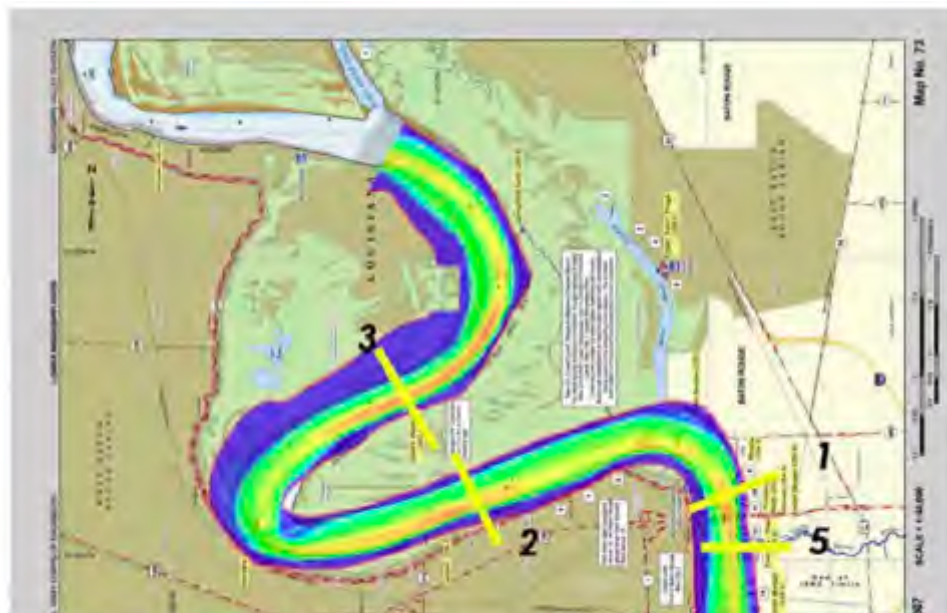
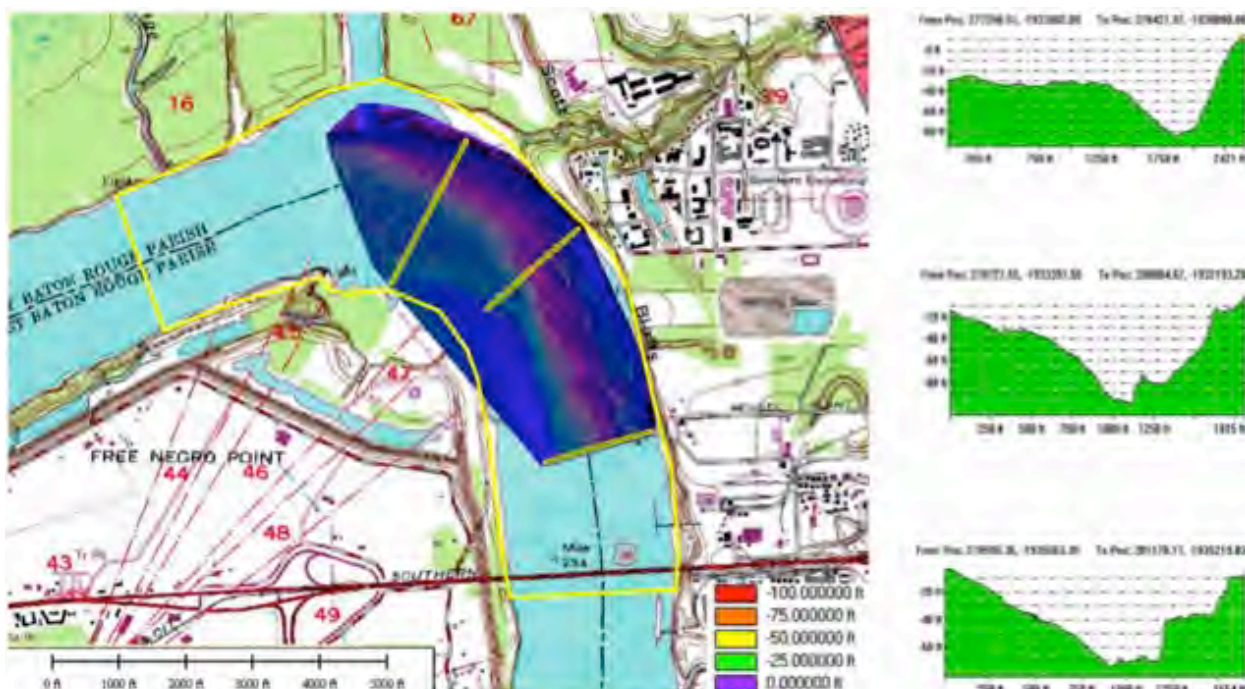


Figure 1.21. Relative 2D Averaged Velocities at Scotlandville Bend



Figure 1.22. Analysis of Available Depth at Scotlandville Bend



Bathymetry at Site 28, Scotlandville Bend

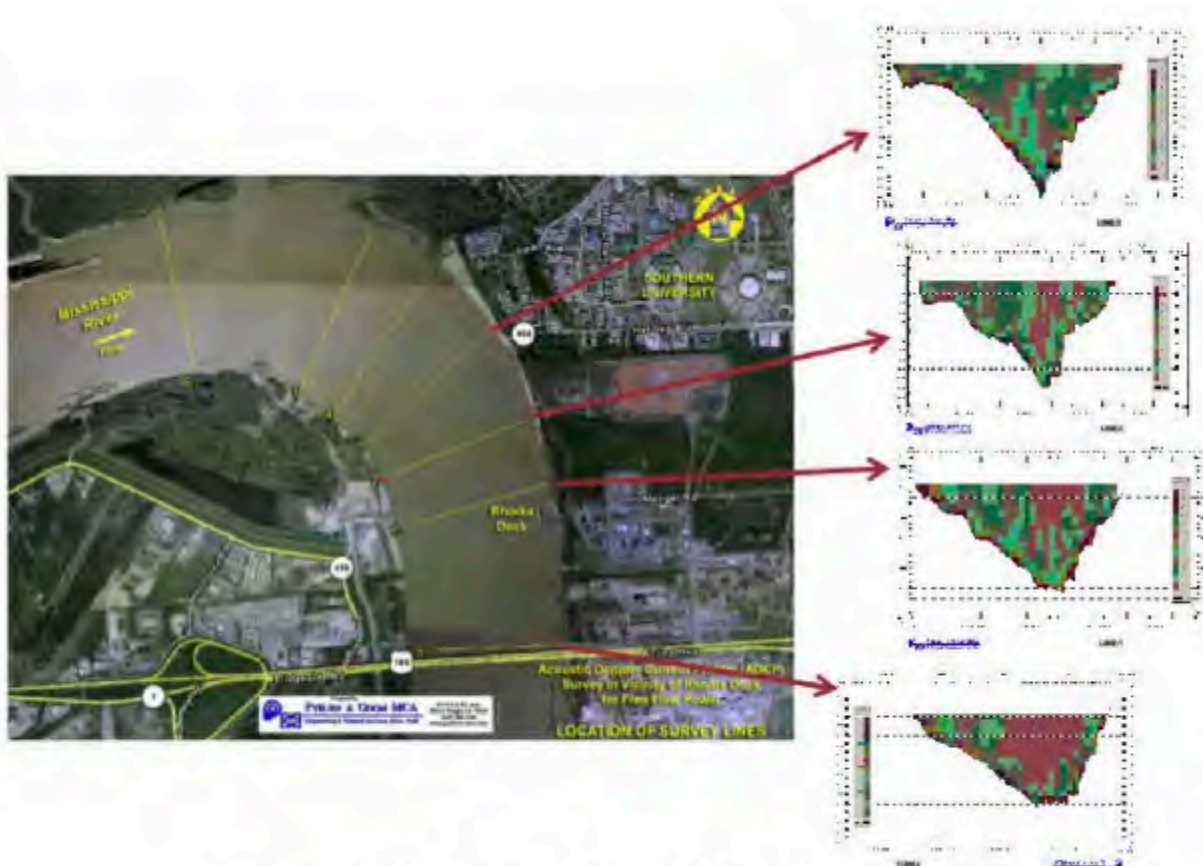


Figure 1.23. ACDP transects taken July 24, 2009 (low water)

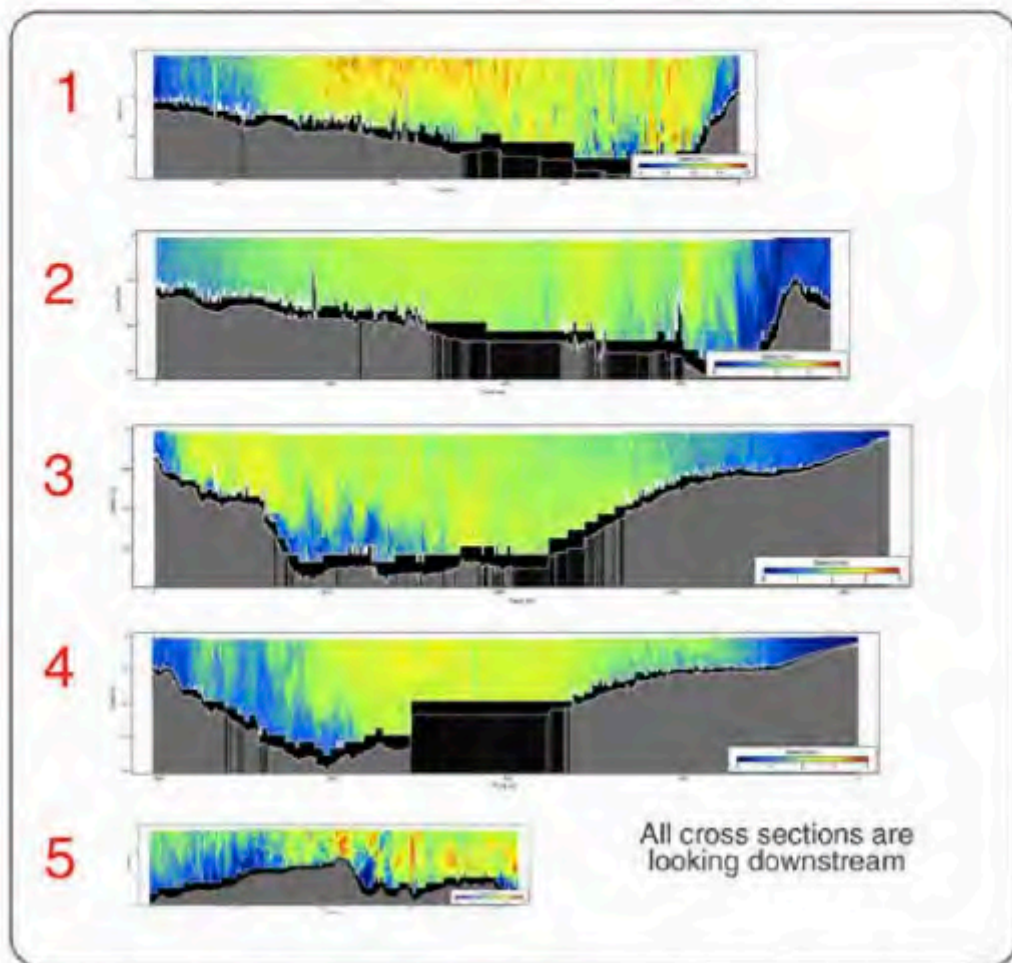
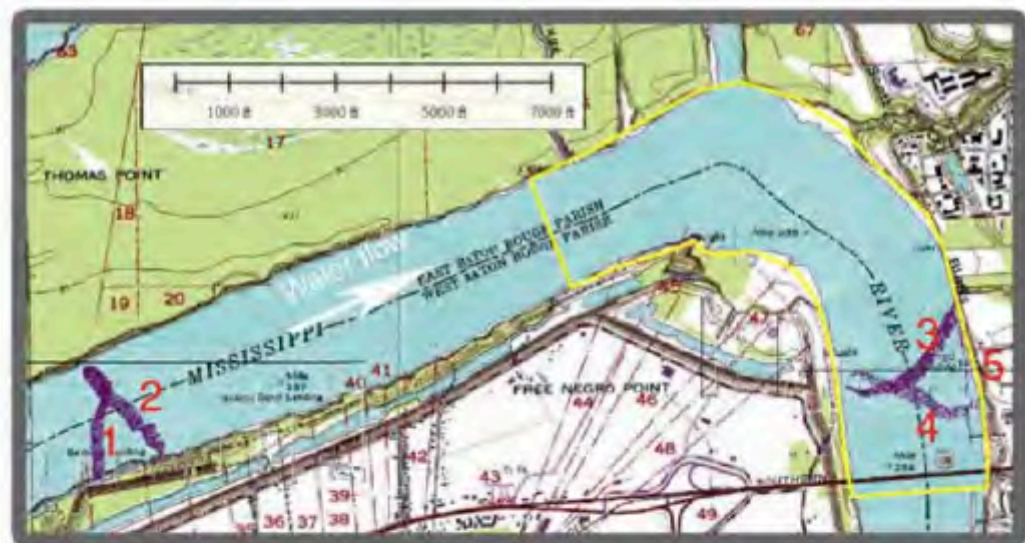


Figure 1.24. ADCP transects at Scotlandville Bend taken Feb 17, 2010 (high water)

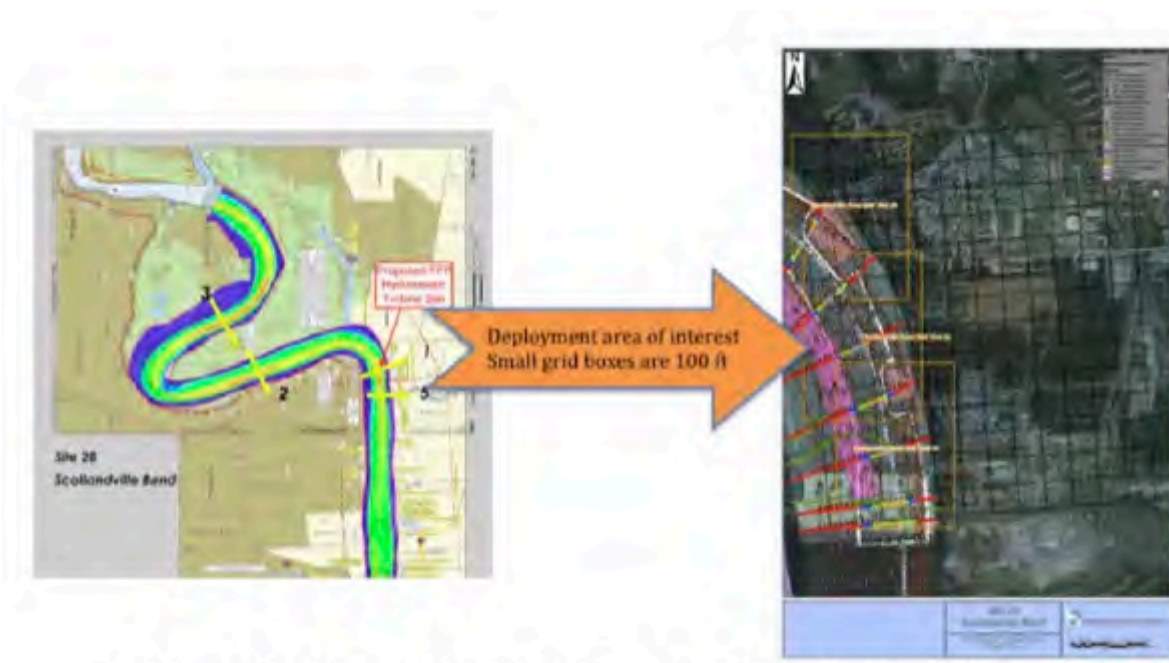


Figure 1.25. Proposed in-situ deployment location at Scotlandville Bend



Figure 1.26. Detailed bathymetry and competing use map of in-situ deployment location at Scotlandville Bend with planned boundaries noted

3.2.3.1.1 Barge-Mounted Deployments

The Project provided sufficient information and field experience to enable FFP to determine that barge-mounted deployment were not a feasible conceptual alternative for the LMR sites for which it held FERC permits. Initially, FFP’s FERC preliminary permit applications proposed an assessment of both piling-based deployments and surface-mounted deployments from barges or other floating structures. Below are photographs of FFP’s 3M01 hydrokinetic turbine deployed from the FM, depicting a design alternative considered for barge-mounted deployments and one which was conducted for test deployments prior to and during the Project.



FFP’s initial consultation with stakeholders, including those representing the navigation industry, expressed reservations regarding the feasibility of surface-mounted deployments on a widespread basis. Evidence was provided indicating that barge pilots frequently utilized the majority of the river column when navigating river bends, and that navigation activities are not restricted to a specific latitudinal channel of the river. Further, FFP’s observations of buoyant debris on the surface of the river, combined with prior experience deploying its sub-scale prototype turbine in the Mississippi River, indicated that management of debris would be a challenge in a full-scale surface-mounted hydrokinetic installation. These concerns were offset in part by the observation that river flows at the surface exceed those found at greater depths, and the fact that surface-mounted hydrokinetic turbines are more easily accessed for maintenance and repair than piling-based installations.

The Project’s deployment was an essential activity in evaluating the trade offs among these two deployment approaches. During the course of the Project’s deployment, FFP maintained logs of debris and navigational traffic in the vicinity of the deployment site in order to assess the feasibility of mitigation approaches to addressing these challenges. These logs were published in the FERC’s study reports, including the Initial Study Report.

Ultimately, FFP determined that a barge-mounted deployment strategy was not the preferred alternative for full-scale development of the majority of LMR sites for which FFP held FERC preliminary permits. FFP made the determination, published in the Fifth Study Report, that it was deprioritizing barge-mounted deployments in favor of further development of the design of piling-based installations through the *in situ* deployment. The Project was an essential laboratory in enabling FFP to make this determination.

3.2.3.1.2 *In Situ* Deployment Design

Throughout the course of the Project and its FERC licensing activities, FFP refined its design of the piling-based turbine infrastructure through the development, in consultation with stakeholders, of a proposal for the *in situ* deployment required by FERC’s Study Plan Determination order. This *in situ* deployment consisted of four turbines installed on pilings with associated infrastructure, including cabling, in accordance with the spacing and configuration of a larger commercial-scale array. The following figures illustrate the design of the *in situ* deployment developed through this approach.

The baseline configuration of the piling-based array consists of turbines assembled dry in pairs on a yoke, and then turbine-yoke assemblies installed over permanent piles and removed for dry maintenance. Alternative configurations could include shallow installations with turbines mounted side-by-side to a horizontal beam between pilings, bridge pier mounts, and mounts upstream or downstream of existing dams.

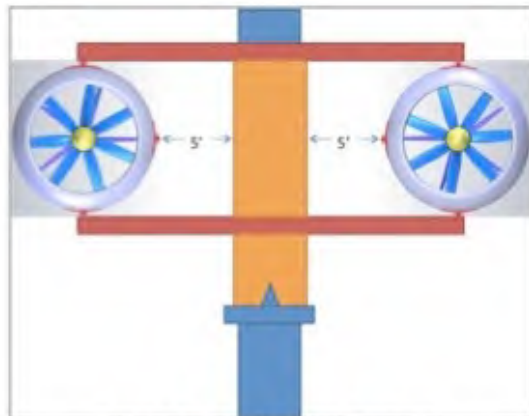


Figure 4.3. Turbine-yoke layout with two turbines

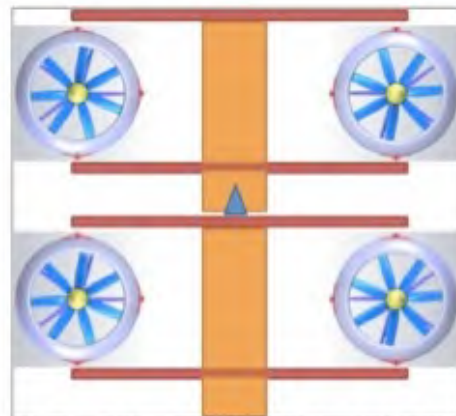


Figure 4.4. Turbine-yoke layout with stacked pairs of turbines (higher stacks possible)

The steps for installing the turbines-yoke-piling systems include the following:

1. Align and start installation of two piling sections
2. Connect additional piling sections above water level
3. Drive additional piling sections
4. Add “follower” to last section above water level
5. Utilize “follower” to drive to desired depth
6. Align two-turbine yoke array to “follower” and pulley yoke down
7. Secure turbine yoke to piling
8. Remove “follower”

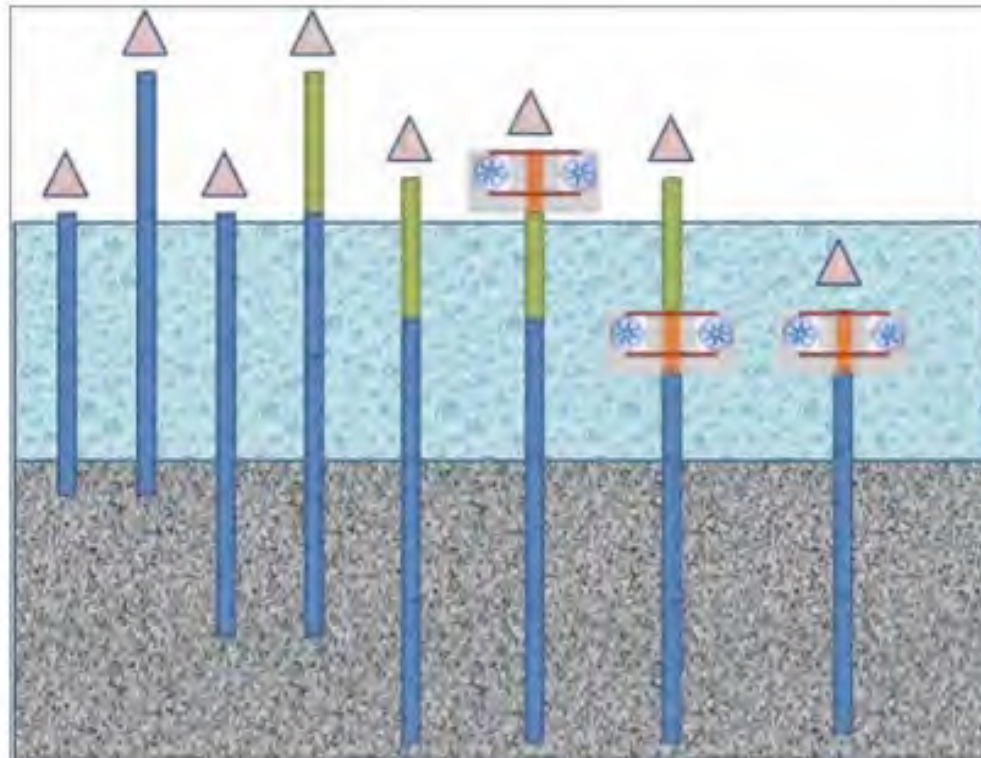


Figure 4.15. Notional piling installation steps

Electrical cabling would then be installed from the river infrastructure to an on-shore substation. An electrical service loop on the turbine-yoke-piling assembly would enable the raising of the turbine-yoke pairs to the water surface for maintenance without disconnection. Underwater cables would be buried either by self-burying, trenching, or vibratory-burying. DC combiners would be attached either to the pilings or the yoke assembly. Shore infrastructure would be equivalent to commercial scale solar PV grid interconnection systems.

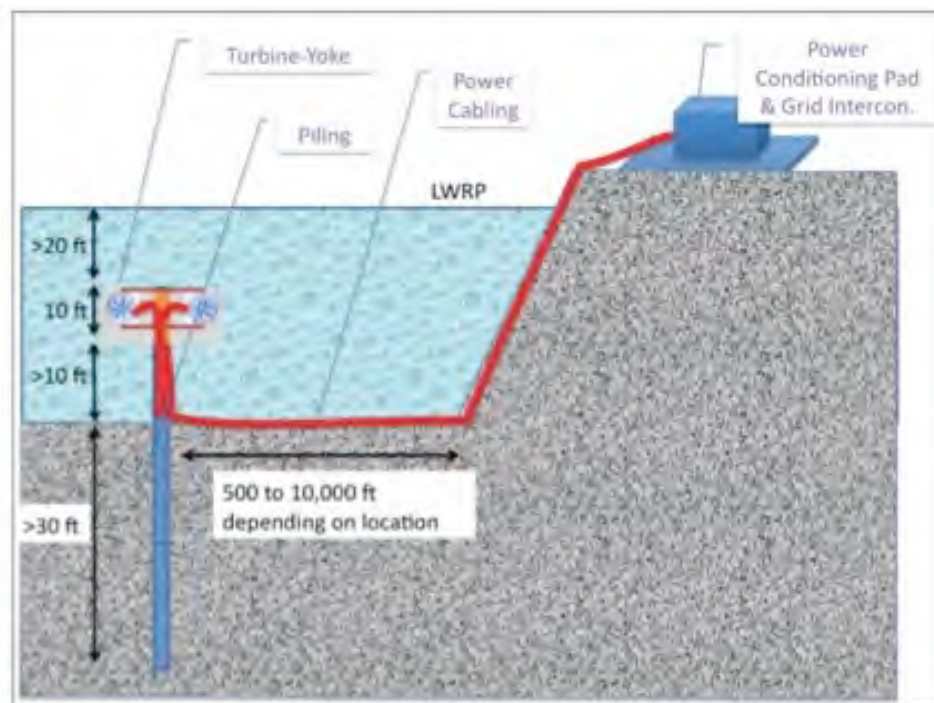
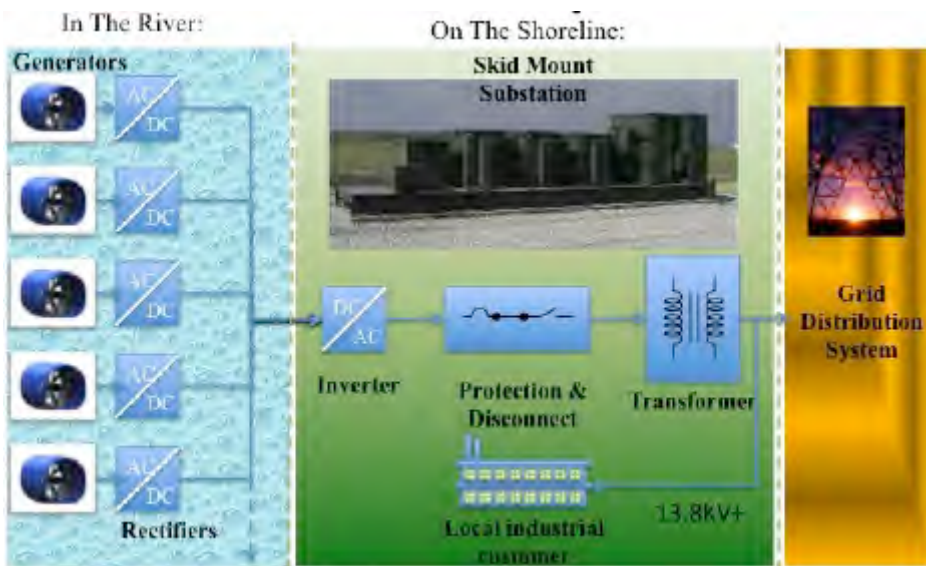
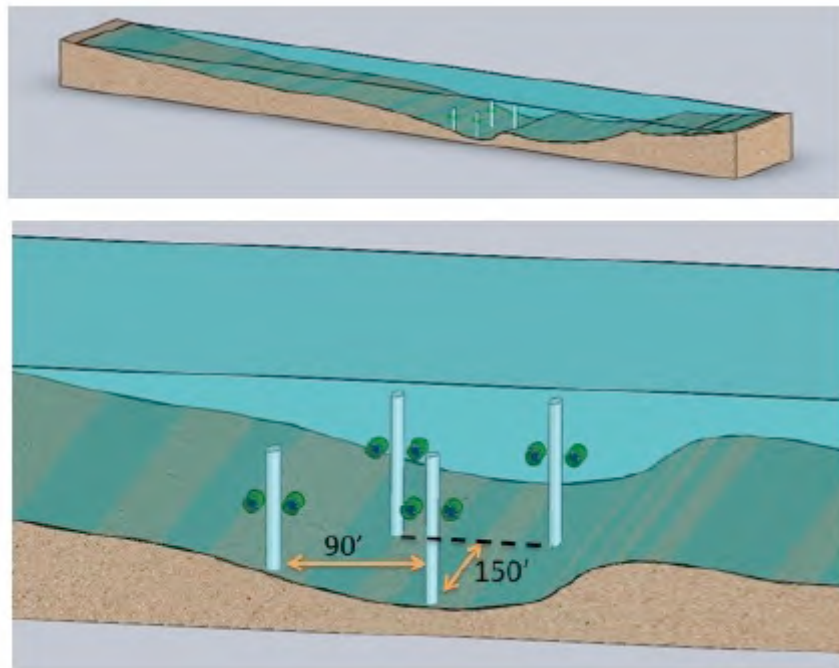


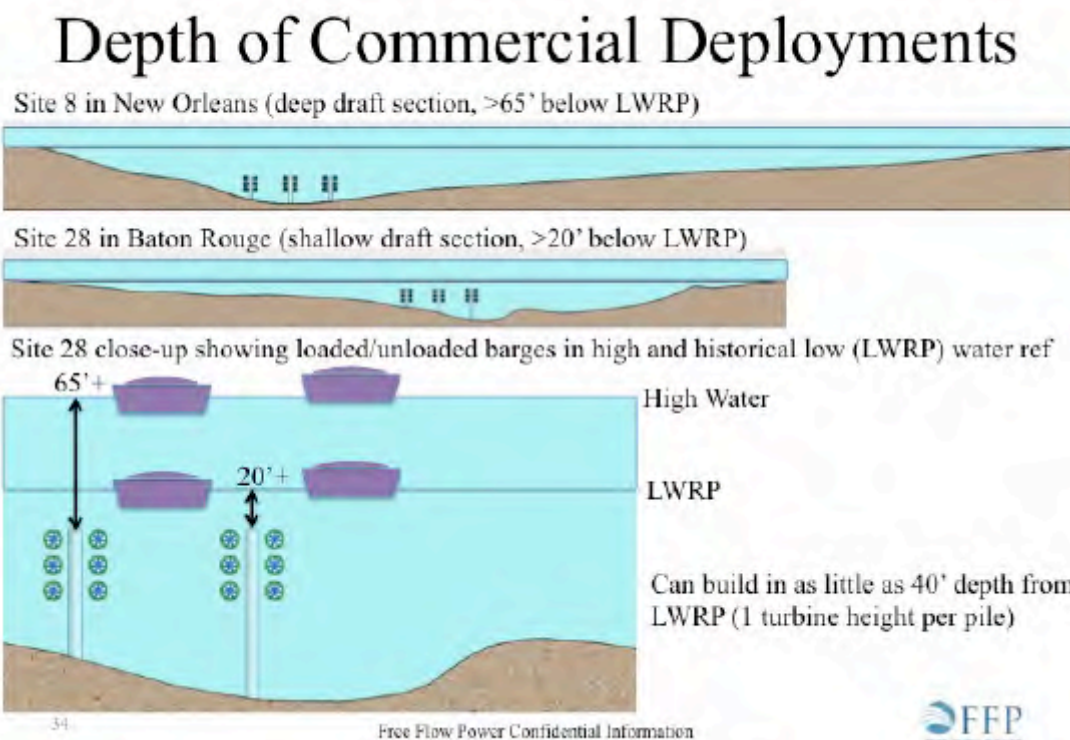
Figure 4.6. SmarTurbine™ system layout



The spacing of the turbine/piling systems would be 90 feet transverse spacing and 150 feet downstream spacing, with a 45 feet longitudinal offset from upstream piles, as shown below.



The depth of the installed pilings would be in reference to LWRP, as shown in the figure below.



3.2.3.2 Hydraulic Study

The goals of the Hydraulic Study were:

- To determine metrics for measuring impact on flows and on sedimentation;
- To determine thresholds for impact;
- To determine the force or “drag” from a single turbine and small groups of turbines and effects on flow energy and behavior; and
- To assess the impact of turbine deployment on flow conditions and sedimentation, including effects from fouling and debris loading;
- To use computation fluid dynamics (CFD) methods to evaluate hydraulic impact associated with decreased efficiency of the turbine over time; and
- To evaluate effects on navigation, USACE structures, natural riverbank stability, floodwater elevations, and aquatic habitat.

A significant component of the Hydraulic Study effort was dedicated to consultation between FFP and the USACE’s Independent Technical Review Team, which was constituted by the USACE to review and comment upon FFP’s study methodologies and results. Through this consultation, FFP developed a plan for combining 1D, 2D, and 3D far field, near-mid field, and near field modeling to address the goals discussed above. Specifically, FFP created a near-field model of the hydrokinetic turbine and used a model to define an “equivalent turbine” with similar drag and wake characteristics, and then transferred the model into a 2D far field hydraulic modeling to simulate the effects of many turbines at a given site. The modeled results would then be validated with additional data collected through ADCP, with hand calculations, and with measurements taken at the *in situ* deployment.

The Hydraulic Study was an ongoing effort reflected throughout each of the FERC Study Reports, but in particular two reports summarize the extent of the results developed through the course of the Project:

- The Fifth Study Report included responses to comments from the FERC and USACE; a consideration of induced velocities from ship propellers; near field flow model results of areas around and behind the turbine; findings regarding deteriorated turbine performance; findings regarding the effects that a locked rotor or blocked inlet would have on turbine performance; a description of a CFD prediction of turbine shear stress; discussion of the Project’s riverine deployment; and additional national hydraulic study efforts. This section of the Fifth Study Report is included as Appendix 4.
- The Sixth Study Report included a hydraulic modeling report for a representative site, Site 42 near Memphis, Tennessee, which is provided as Appendix 5.

In addition, in the Sixth Study Report, FFP proposed a methodology for monitoring hydraulic effects at the *in situ* deployment. This proposed study methodology, including projected costs, is attached as Appendix 6.

3.2.3.3 Navigation Study

The goals the Navigation Study were:

- To assess existing river navigation patterns relevant to commercial-scale hydrokinetic projects;
- To determine construction and maintenance practices that would minimize impacts to all major forms of river transportation and risks to public safety.

Through the Navigation Study FFP assessed potential sources of information regarding traffic on the LMR, including data collected by the USACE’s WCSC and compiled and analyzed by FFP. FFP conducted additional activities, including limited navigational surveys, to assess the representativeness of the WCSC data. Whether the WCSC data ultimately would provide information satisfactory to address the FERC’s requirement of a one-year traffic survey was undetermined at the conclusion of the Project. Accordingly, in its Sixth Study Report, FFP proposed a methodology for monitoring navigational traffic in the vicinity of the *in situ* deployment. This proposed study, including projected costs, is attached as Appendix 7.

The necessity of compatibility of the proposed hydrokinetic installations, whether surface-mounted or piling-based, was among several paramount considerations in the design of commercial deployments. In order to assess the multiple, and multi-dimensional, factors necessary to assess this compatibility, FFP prepared and consulted with navigational industry stakeholders regarding the comment matrix presented below, which FFP and stakeholder both adopted as a useful tool to investigating this critical issue.

Technology-Specific Site Evaluation		Project Phases				
Parameters		Siting/Testing	Construction	Operations	Maintenance	Decommissioning
1 Visual Navigation						
2 Maneuverability						
3 Current Factors						
4 Traffic Density						
5 Misc. Non-Transit Uses						
6 Recreational Uses						
7 Commercial Fishing						
8 Crossings						
9 Fleeting and Anchorages						
10 Surrounding Infrastructure						
11 Strategic Importance of Area						
12 Future Use Factors						
13 Communications						
14 Emergency Response						
15 Environmental						
16 USACE Factors						
17 ATON Factors						
18 Floating Hazards						
19 Staging Areas						
		High Water	Low Water	High Wind	Seasonal Variance	
						Environmental Variables

3.2.3.4 Damaged Turbine and Debris Risk Study

The goals of the Damaged Turbine Recovery and Debris Risk Study were:

- To assess the risk of damage to turbines or other infrastructure as a result of debris or other foreseeable conditions, including the probabilities of occurrence of such damage;

- To determine any adverse impacts associated with damaged turbine features, including abandoned pilings, broken turbine housings or blades and, if necessary, to determine how damaged turbines would be recovered from the river.

The results of the Damaged Turbine study included analyses of the continuous, chronic, intermittent, and episodic loads that the hydrokinetic turbine, pilings, and other infrastructure would be expected to encounter in a deployment. These forces, together with FFP’s planned design life and maintenance protocols, are further described as follows:

Continuous

- This includes normal axial, vertical, and side loads on structures.
- The FFP equipment will be designed for 30+ year life for this type.

Chronic

- This includes normal continuous effects that are cumulative such as vibration, sediment and small debris collection, wear, corrosion, and bio-fouling.
- The removable FFP equipment will be designed for seven-year life with one-year maintenance for this load type, and 30+ years life with for permanent equipment.

Intermittent

- This includes normal large debris that may be seasonal or vary with river stage, such as logs, ice, and nets.
- The removable FFP equipment will be designed for one-year maintenance with potential component replacement during normal maintenance for this type of load. The permanent equipment will be designed for 30+ years life. If the debris stops the turbine, the shore power conversion unit will be designed to identify the stopped turbine through individual turbine communication (nominally a coded powerline signal). Maintenance procedures will dictate the number of stopped turbines and/or accumulated time period that dictates unscheduled maintenance.

Episodic

- This includes extreme and rare occurrences such as anchors and extremely large debris.
- The FFP equipment will be designed using industry standards for anchor attachment for the various size classes of ships.

During the riverine deployment phase of the Project, the 3M01 and FM functioned as a laboratory of sorts for validation of the expectations documented in this study. Throughout the course of the Project deployment, the 3M01 functioned as expected. Ultimately, the mechanical failure that contributed to the retirement of the FM in February 2012 pertained to the FM’s mechanical arms, an element of the testing platform which was not incorporated into the commercial project design and therefore not the subject of the reporting of the Damaged Turbine Study.

The Initial Study Report contains discussion of the Project’s deployment under the Damaged Turbine Study section, the results of which are discussed throughout this report.

In the Fifth Study Report, FFP provided an analysis of studies of damage to the hydrokinetic turbine caused by debris, focusing on the forward shroud. This report is provided as Appendix 8.

3.2.3.5 Fish Entrainment Study

The goals the Fish Entrainment, Movement, Behavior, Habitat Use, and Population Effect Estimation Study were:

- To quantify the blade rotation rate, rotor blade tip speed, shear stress, pressure changes, turbulence, and cavitation associated with the turbine generator using CFD modeling techniques;
- To determine the range of fish species in the Mississippi River that may be affected by turbine deployment, based on literature review and assessment of fish distribution data collected by the USACE;
- To assess the probability of strike-related injuries and mortality for representative species, based on a laboratory-based or *in situ* testing program (with an expressed preference for a laboratory-based program, if feasible);
- To develop risk-based projections of population effects for several fish species.

Extensive efforts in the Fish Study were allocated to determining the number of and list of representative species to be studied, including a formal dispute resolution procedure invoked by US Fish and Wildlife Service and adjudicated by FERC. The fish study also incorporated the data from an extensive project of the USACE ERDC-EL to inventory pallid sturgeon and other fish along the LMR for over a decade. FFP, through consultation with resource agencies, endeavored to utilize this prior data and develop an assessment protocol that would facilitate river-wide analysis of fish populations. Together the results of laboratory-based entrainment tests which were planned (but not conducted), an assessment of fish entrainment and mortality would be possible.

In its Fifth Study Report, FFP presented a detailed analysis of the ERDC-EL data set and proposed a methodology for statistical analysis, together with an expert report discussing the applicability of the ERDC-EL data across all of FFP’s permitted sites. This study report is attached as Appendix 9.

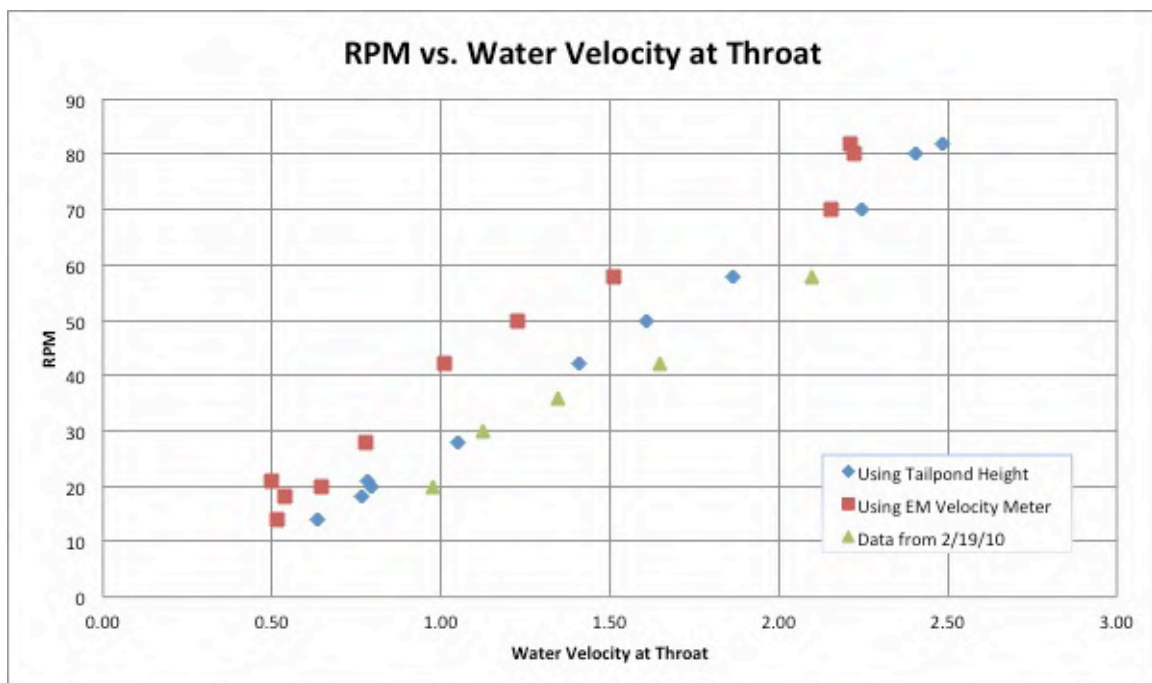
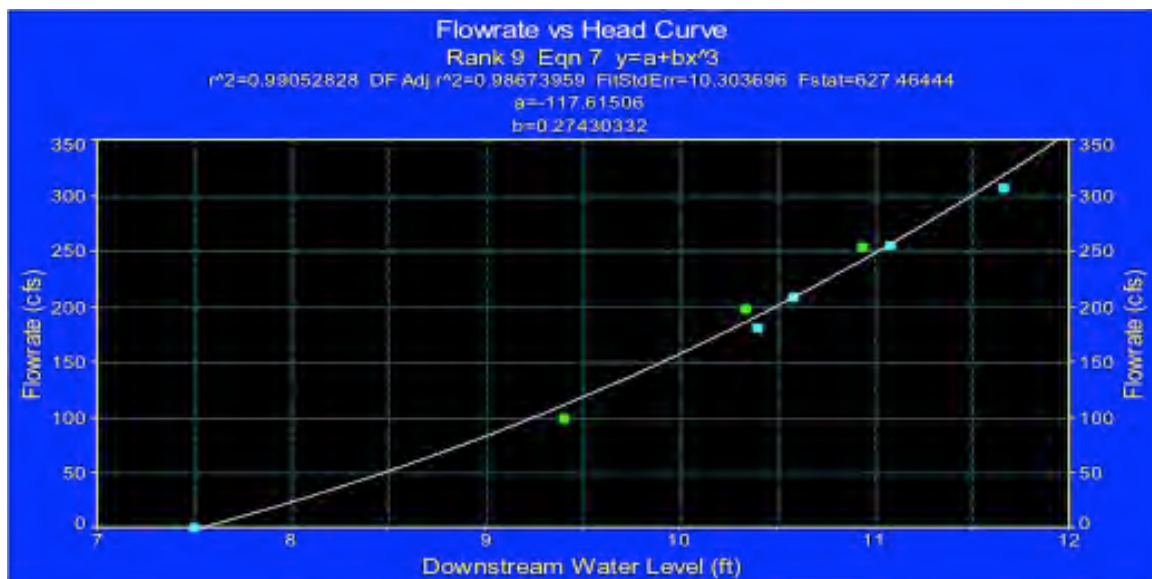
Notwithstanding the extensive fish population data available through ERDC-EL, FFP expected that additional monitoring at the *in situ* deployment would be required to validate the study findings and observe fish behavior in the vicinity of the installed turbines. In its Sixth Study Report, FFP proposed a methodology for monitoring fish effects at the *in situ* deployment. This proposed study, including projected costs, is attached as Appendix 10.

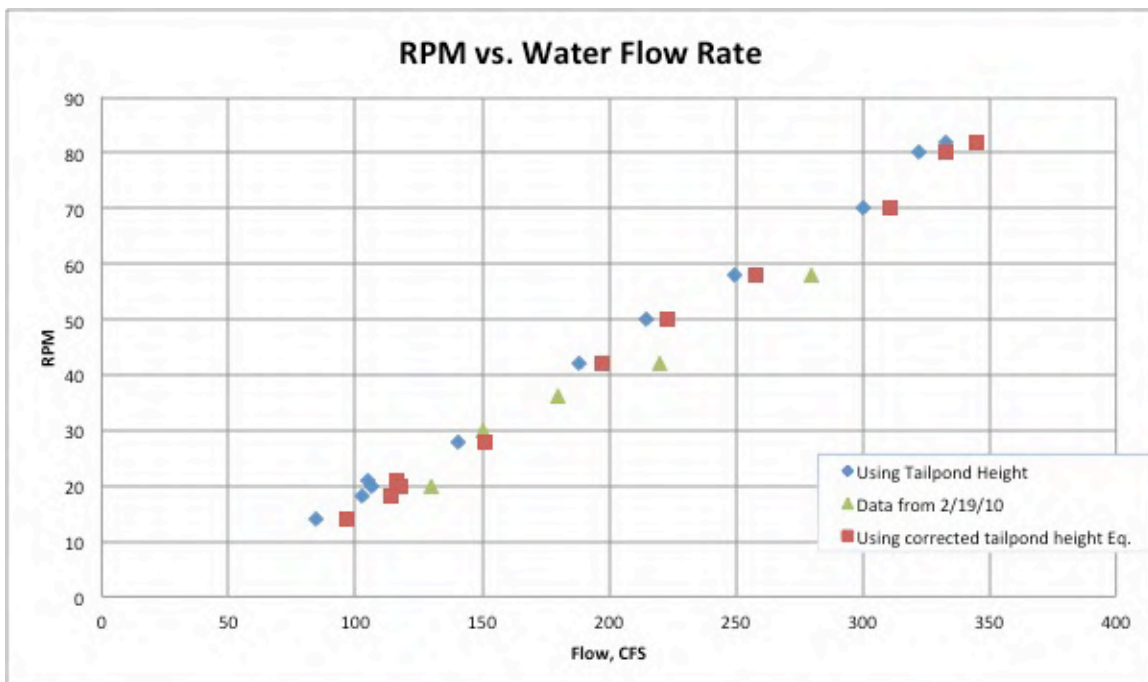
4 Appendices

- 4.1 Appendix 1: Conte Test Results February 2010
- 4.2 Appendix 2: Conte Test Results November 2010
- 4.3 Appendix 3: Project Deployment Test Results Summer 2011
- 4.4 Appendix 4: Hydraulic Study 5th Report
- 4.5 Appendix 5: Hydraulic Study 6th Report
- 4.6 Appendix 6: Hydraulic Monitoring Methodology
- 4.7 Appendix 7: Navigation Monitoring Methodology
- 4.8 Appendix 8: Damaged Turbine Study 5th Report
- 4.9 Appendix 9: Fish Study 5th Report
- 4.10 Appendix 10: Fish Monitoring Methodology

Appendix 1

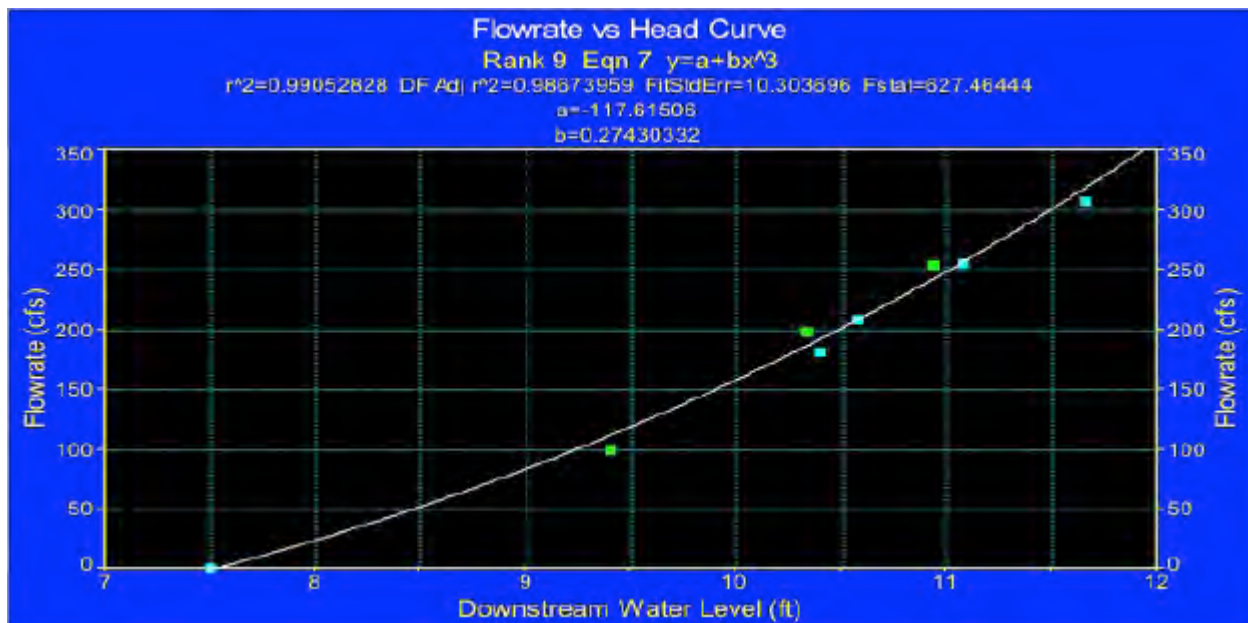
CAFRL Testing Results February 2010



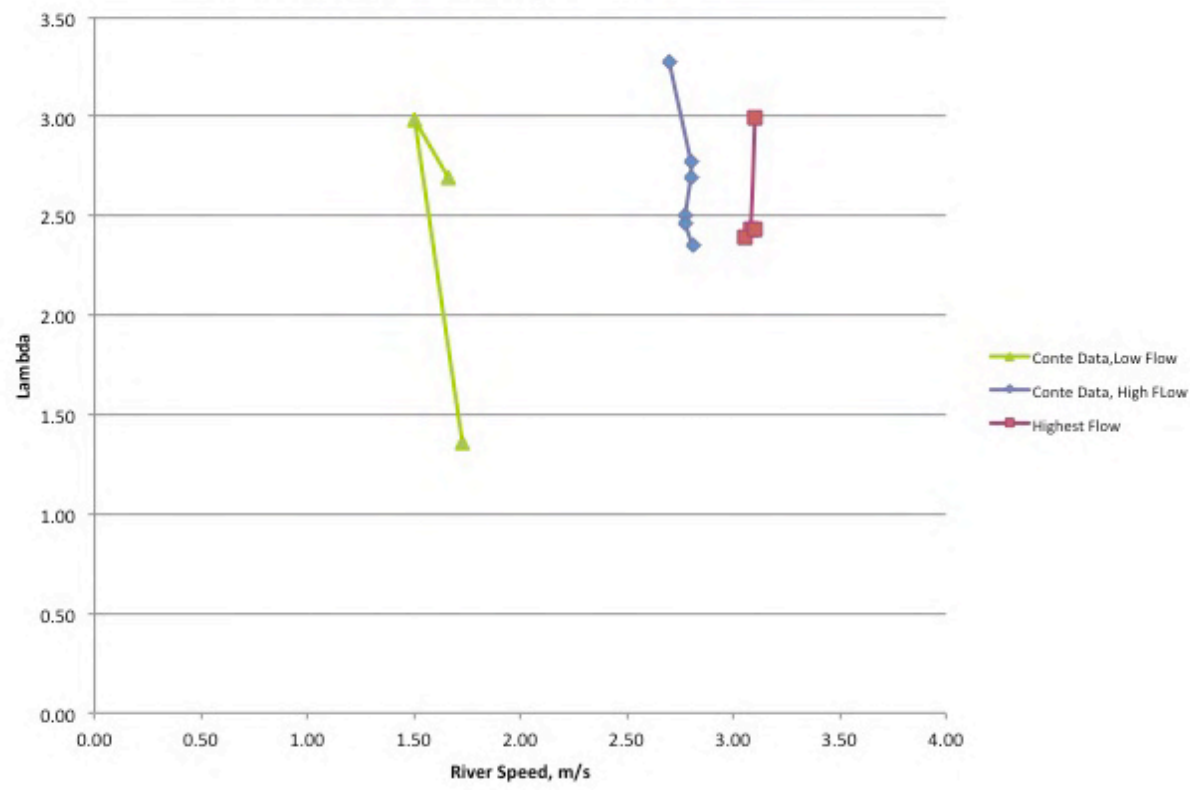


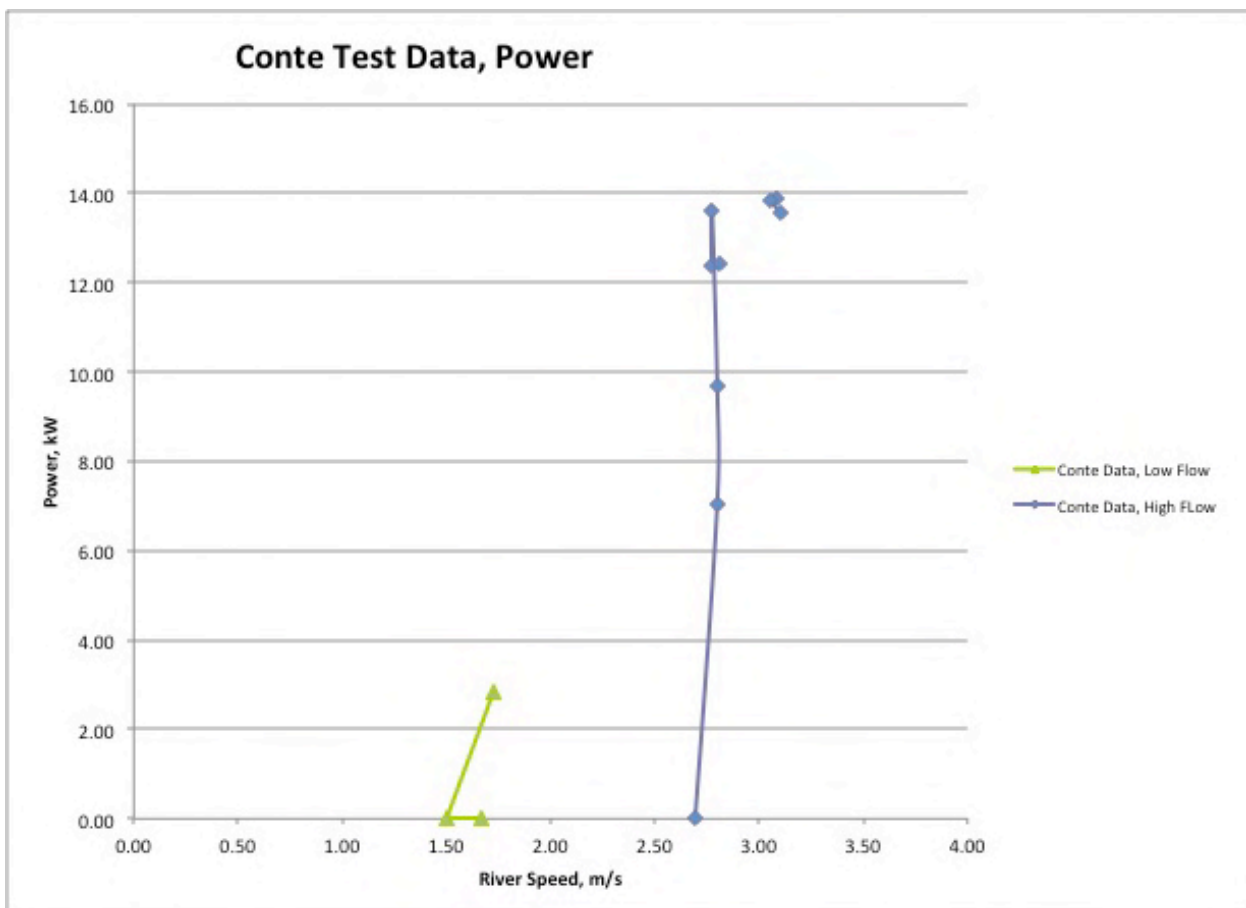
Appendix 2

CAFRL Testing Results November 2010

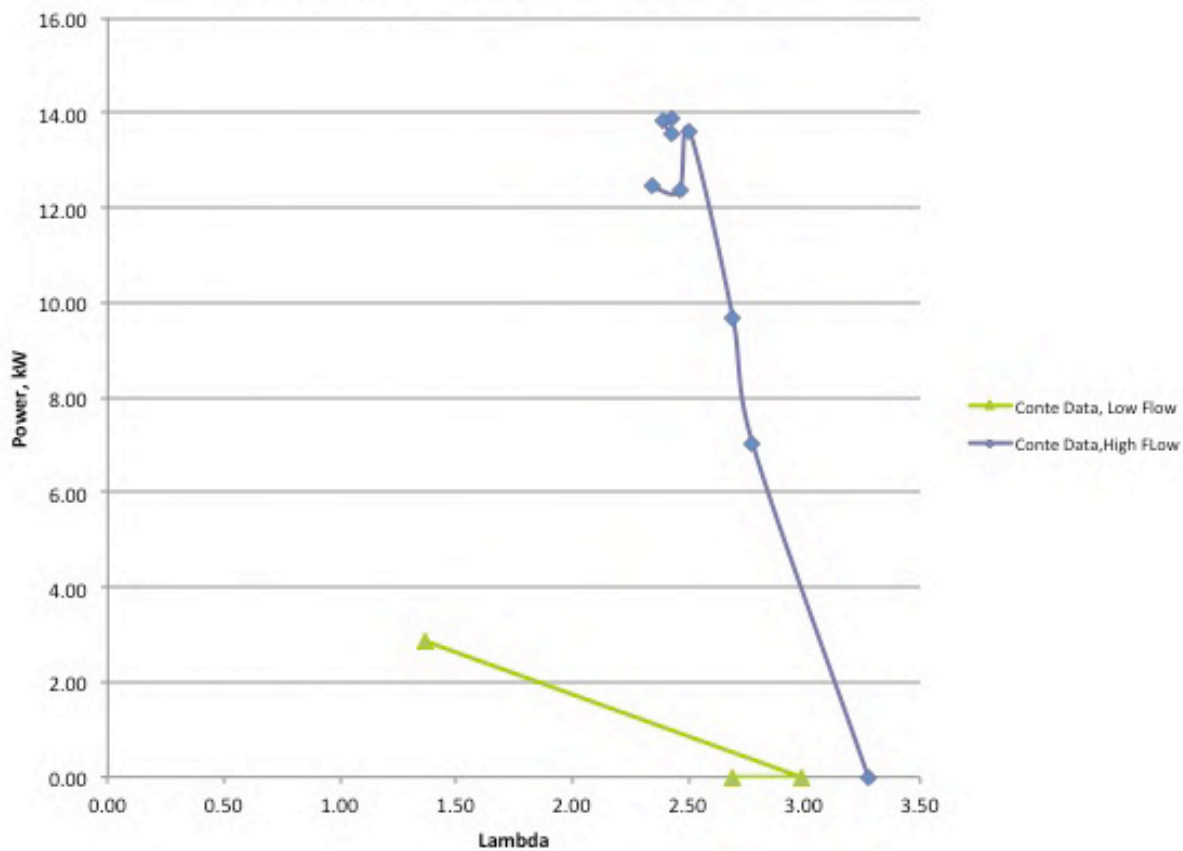


Conte Test Data, Tip Speed Ratio

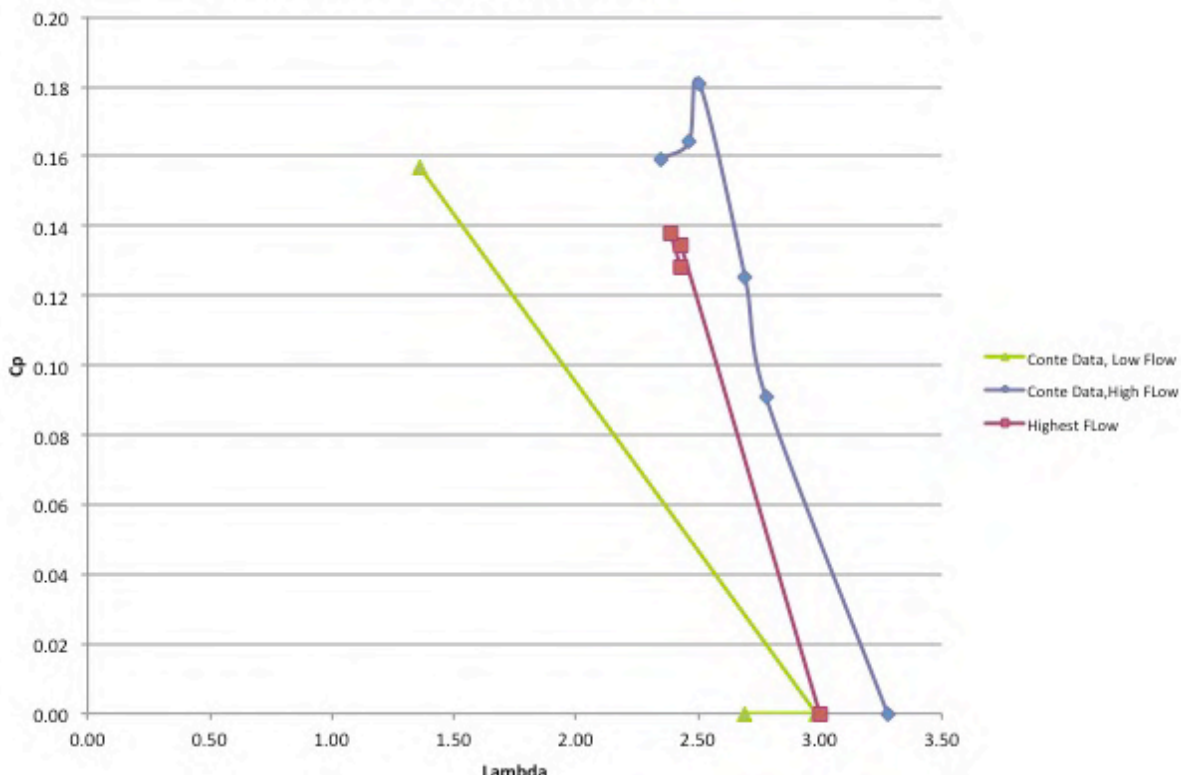




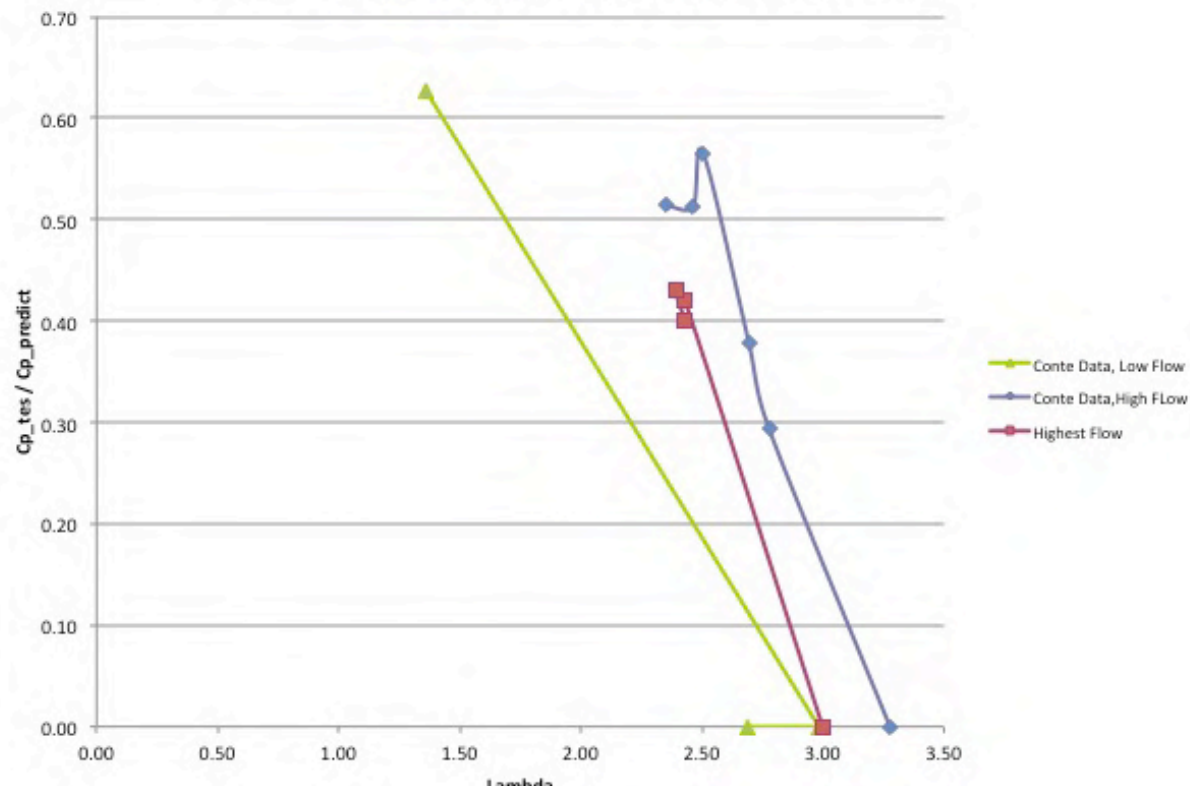
Conte Test Data, Power vs. Lambda

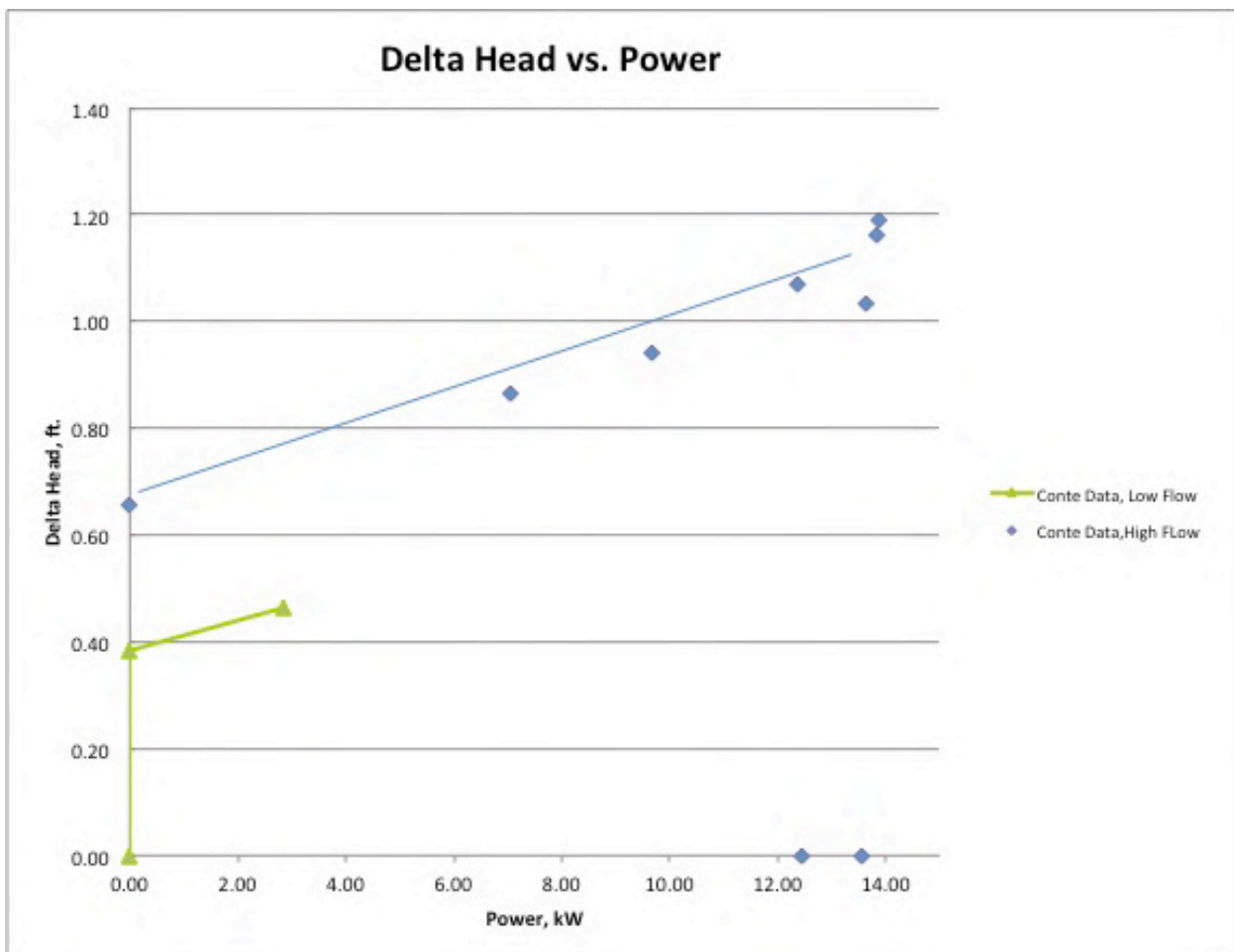


Conte Test Data, Cp vs. Lambda

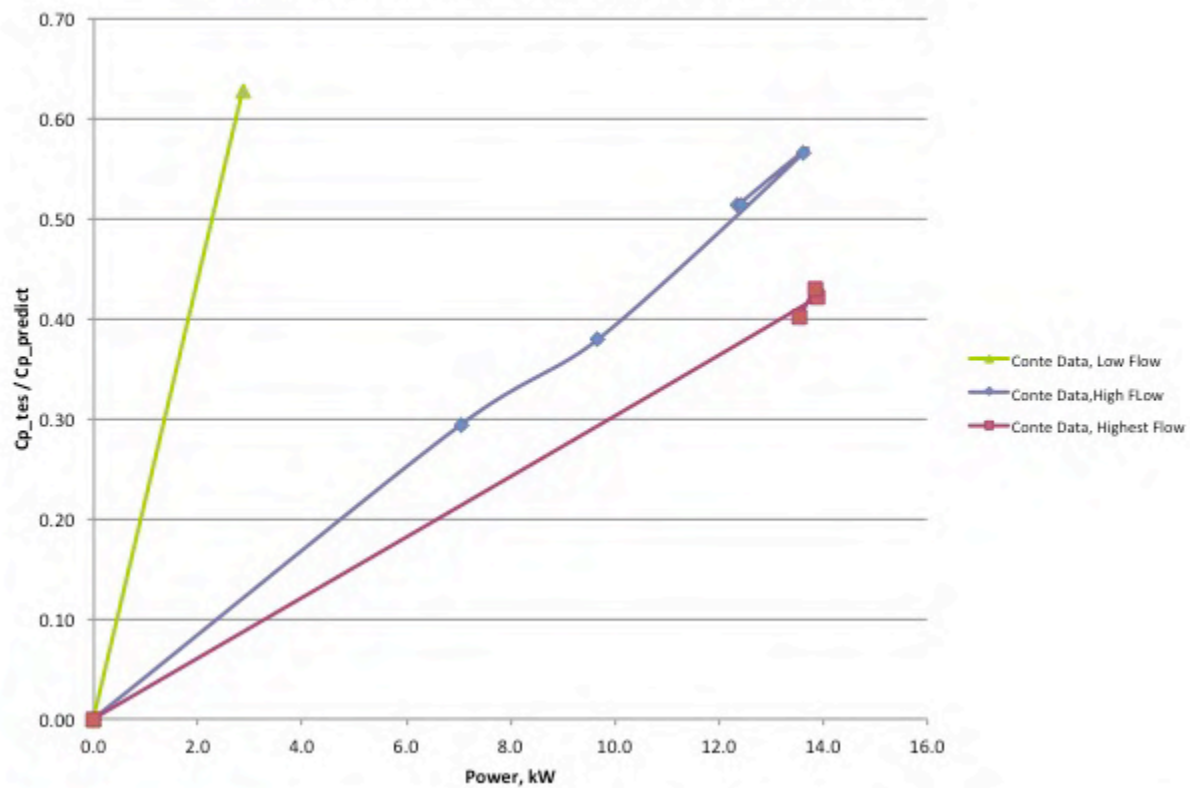


Conte Test Data, Cp test/Cp predicted vs Lambda



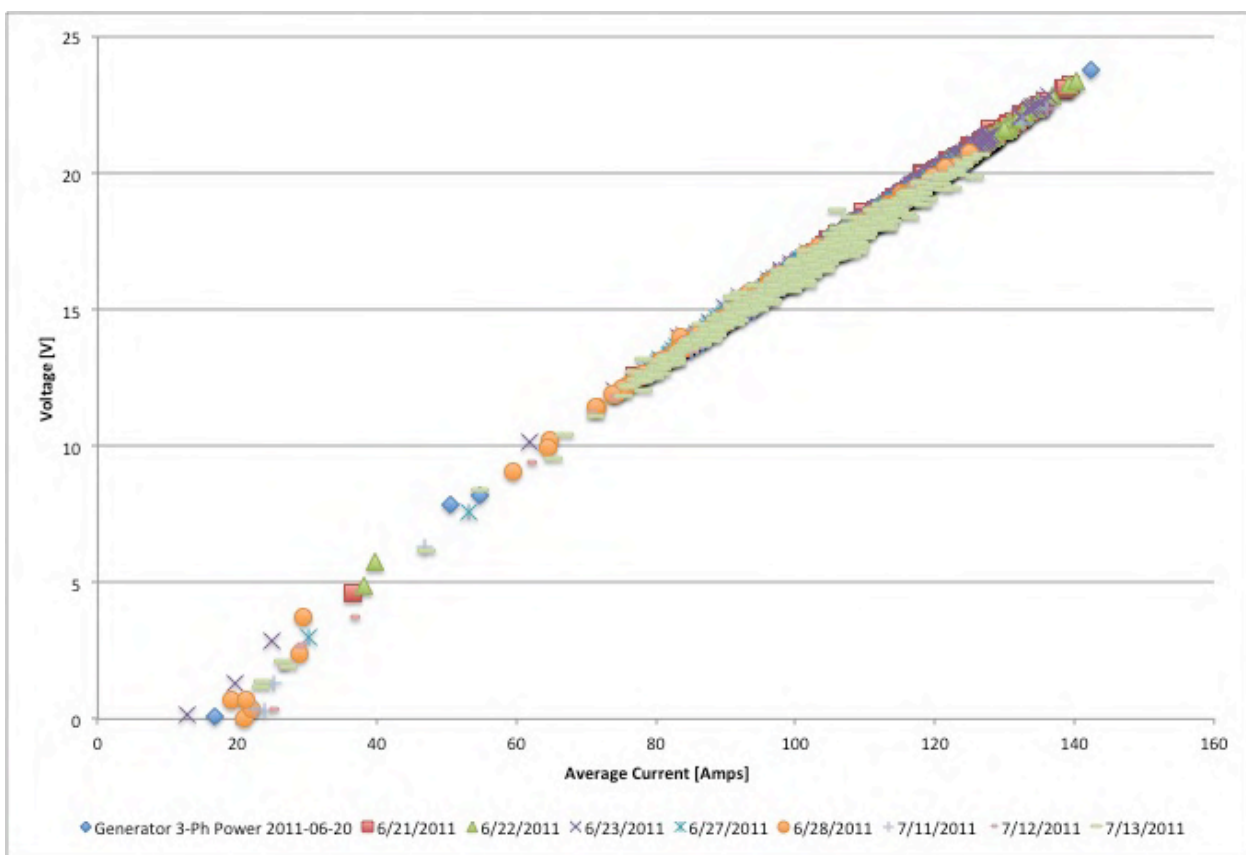


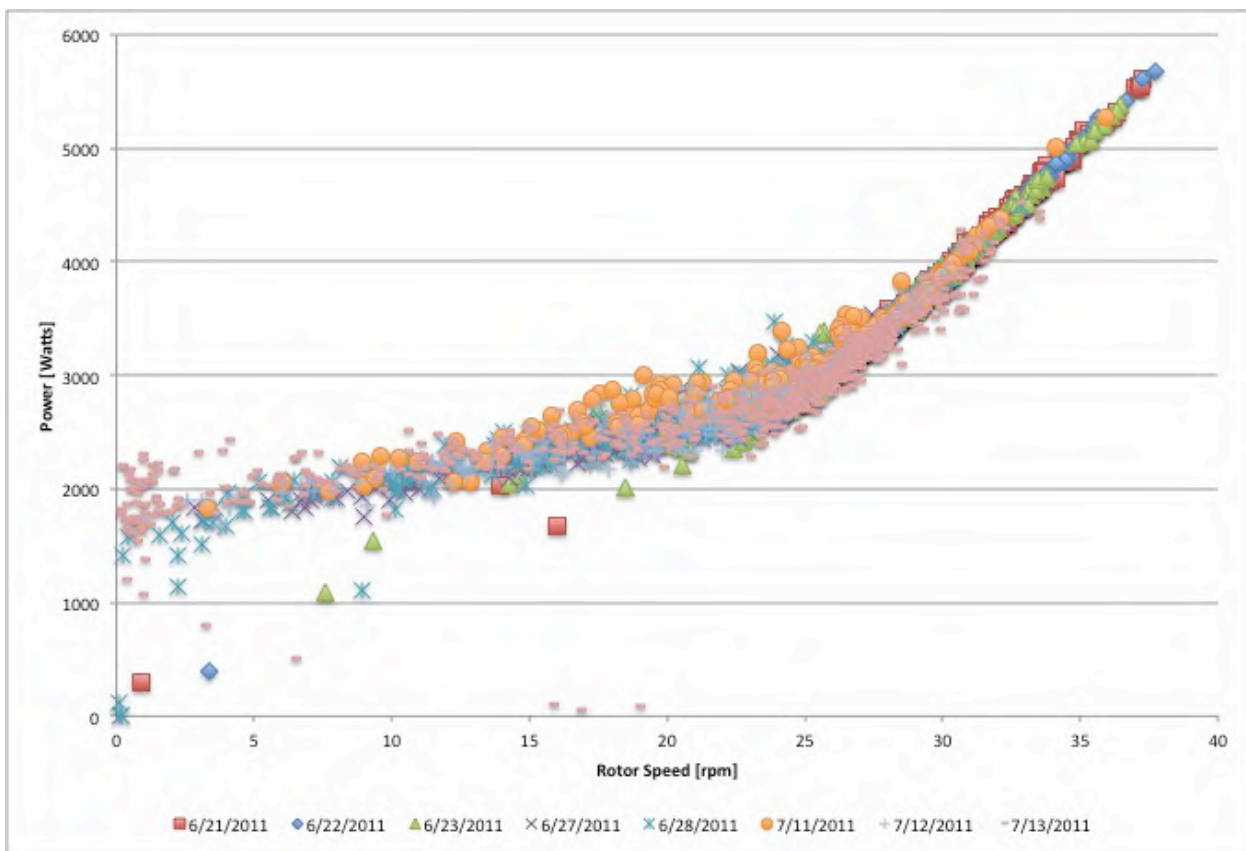
Conte Test Data, Cp test/Cp predicted vs Power



Appendix 3

LMR Testing Results Summer 2011









APPENDIX 4

HYDRAULIC STUDY FIFTH REPORT

SECTION 2**Hydraulic Study**

The goals of Free Flow Power's (FFP) Hydraulic Study are as follows:

- To determine metrics for measuring impact on flows and on sedimentation;
- To determine thresholds for impact;
- To determine the force or “drag” from a single turbine and small groups of turbines and effects on flow energy and behavior; and
- To assess the impact of turbine deployment on flow conditions and sedimentation, including effects from fouling and debris loading;
- To use computation fluid dynamics (CFD) methods to evaluate hydraulic impact associated with decreased efficiency of the turbine over time; and
- To evaluate effects on navigation, U.S. Army Corps of Engineers (USACE) structures, natural riverbank stability, floodwater elevations, and aquatic habitat.

In the First Quarterly Study Report (1Q Report), FFP provided an overview of available baseline data to constitute input parameters for CFD modeling, a description of FFP's proposal for phased 2D and 3D modeling of hydraulic effects, and a preliminary proposed plan for estimating the potential effects of vibration on USACE structures.

In the Second Quarterly Study Report (2Q Report), FFP provided a plan for documenting hydraulic and sediment conditions before and during the *in situ* deployment, a synthesis of hydraulic data on debris, and a plan for evaluating potential effects of vibration on USACE structures.

In the Initial Study Report, FFP described its consultation with the Independent Technical Review Team (ITRT) convened by the USACE New Orleans District to evaluate the hydraulic elements of the FFP Projects. The ITRT is comprised from the USACE's River Engineering Branch, Engineering Research and Development Center (ERDC). The main emphasis of the consultation was on the tools to perform the hydraulic and sedimentation modeling, particularly with respect to 1D, 2D, and 3D far field, near-mid field, and near field modeling as described in previous study reports. Specifically, FFP intends to create a near field model of the turbine and use the model to define an “equivalent turbine” with simpler geometry but similar drag and wake characteristics, then to transfer a simplified model into the 2D far field hydraulic model to simulate the effects of many turbines at a given site. Using ADCP and existing river data on flow and gage heights, the model will be validated without the turbines and then with the turbines, where data collected in the course of the *in situ* deployment will be integrated into the validation process for the with-turbine case. Calculations of scour, debris loading on pilings, and vibrations on USACE structures will be performed by hand using established methodologies, rather than by CFD.

In the Fourth Study Report, FFP provided additional information regarding its preliminary efforts at utilizing two-dimensional analysis of the flow field around the simulated geometry of FFP's three-meter hydrokinetic turbine. This analysis is broken down into the following segments. The analysis included an explanation of the utility of Manning's Roughness

Coefficient to describe resistance to flow in an open channel; an explanation of the effects of water discharge and changes in water surface elevation; a description of kinematic eddy velocity and its applicability to the FFP Projects; and an explanation of the numerical model that FFP plans to utilize in its hydraulic calculations.

In this Fifth Study Report, FFP provides additional results from near field flow analysis, particularly for drag and local flow characteristics around and through the FFP 3 meter turbine, and effects due to deterioration over time. Comments regarding issues raised in previous Study Reports are also addressed. This Hydraulic Study Report includes the following:

- A summary of consultation conducted regarding the 4SR, including responses to comments received from the Commission and the USACE – Section 2.1;
- An analysis of the hydraulic effects of induced velocities from ship propellers – Section 2.2;
- Near Field flow analysis around and behind the turbine – Section 2.3;
- A report on findings regarding deteriorated turbine performance (non-acoustic) – Section 2.4;
- A report on a study of the effects that a locked rotor or a blocked inlet would have on turbine performance – Section 2.5
- A description of a Computational Flow Dynamics (CFD) prediction of turbine shear stress – Section 2.6;
- A report providing updates on FFP’s in-river testing – Section 2.7;
- An update on national efforts in the field of hydrokinetic modeling and their applicability to FFP’s modeling efforts.

Since the last report, FFP has completed significant work on predicting and quantifying the near field flow around, through, and behind the turbine using the ANSYS CFX program. As stated in previous Study Plans, the goal of this effort is to generate an equivalent turbine that can be used in detailed 3D CFD modeling to evaluate the influence of turbines on the flow field, to model a turbine-piling assembly, and to assess the flow details of a turbine-piling array. Furthermore, the 3D results will be used to refine the turbine-piling models used in the 2D models so that the simpler models will properly capture the physics of the turbines effects on flow and energy extraction. The 3D model will be the basis for “tuning” the turbine-piling model used in the 2D studies.

Analysis of internal flow details through the rotating turbine blades are of interest in regards to potential fish or ZMEL injury from shear stress and pressure field variations, and the results of the analyses are presented. Although there is data in the literature for effects from shear stress and pressure changes in conventional hydropower turbines, little exists for much slower hydrokinetic devices, and FFP’s results are a step in quantifying flow field effects.

Efforts have begun on Mid Field modeling, including details to be used for the *in-situ* deployment and predictions, but FFP will be incorporating these analyses in its next Study Report, along with more integrated results. A significant part of the Mid Field and Far Field modeling is in the modeling of the river and river bed so that the CFD models capture the

geometry, flow, and velocity distribution adequately. FFP's utilization of existing USACE data (transects, multi-beam, and ADCP), coupled with FFP's additional (and ongoing) ADCP measurements, will lead to FFP's CFD models based on site data for the river bed and flow conditions.

2.1 Consultation Summary and Outreach

2.1(a) Commission's Comments on 4SR

In the Fourth Interim Report (page 2-9, table 2-6), the dimensions of the variables on both sides of the relationship between n (turbine) and drag coefficient seem to be inconsistent. Please double check this formula and make any appropriate corrections.

This formula should be unit-less, and updates are shown below in the original table with changes marked in red. The formula is restated with improved clarity, and the dimensions of Φ are explicitly described. The 4SR provided “ Φ is dimensional coefficient” as a description, but the dimensions were not listed.

[CONTINUED ON NEXT PAGE]

Input	Unit	Value	Comment
Width	ft	2,500	Average river width.
Length	ft	10,000	Four times the width.
Depth	ft	60	Average depth of flow for average discharge at Baton Rouge.
Elevation of Channel Bed	ft	-37.5	Approximate value.
LWRP	ft	2.5	From USACE hydrographic survey.
n (channel)	()	0.032	Manning's roughness coefficient in the main channel based on Error! Reference source not found.
n (turbine)	()	0.300	Manning's roughness coefficient around the turbine obtained from turbine drag coefficient using $n = [(C_D * H^{(1/3)} * \Phi^2) / g]^{(1/2)}$ Where C_D is turbine drag, H is depth of water above the turbine, Φ is equal to 1.486 $ft^{(1/3)}/s$ in English units and 1.0 $m^{(1/3)}/s$ in SI units, g is the acceleration of gravity.
v_t	ft^2/s	varies	This quantity varies with local velocity and flow depth. The EEV (Estimated Eddy Viscosity) approach was used in SMS-AdH with K=0.5 in isotropic mode.
Upstream boundary condition Q	cfs	549,000	
Downstream boundary condition WS EI.	ft	22.50	
Number of nodes	()	5136	
Number of elements	()	10036	
Average element size	ft^2	2491	
Average element size Δx	ft	70.5	

Revised 4SR Table 2-6, originally located on Page 2-9 of the 4SR. Inputs in FFP's numerical model.

In the Second Interim Report (page 2-4, first full paragraph), you state: “FFP...will evaluate available Corps [U.S. Army Corps of Engineers] and USGS [U.S. Geological Survey] data resources for hydraulic, sediment, and geometric information that was collected during that time of year at Scotlandville Bend. Then, in the course of construction of the *in situ* [test] deployment, FFP will collect similar data at the site during the installation period and for a period of one month after the completion of installation, to allow for compensation in flow changes over time and comparison between actual versus predicted effects.” We are concerned that existing available data may not accurately reflect conditions that exist at the time of deployment at a sufficient level of detail to assess effects of the *in situ* test deployment on hydraulic conditions and bathymetry. Therefore, please collect the following data prior to the *in situ* test deployment: (1) Acoustic Doppler Current Profiler (ADCP) velocity profiles, preferably

under a range of flow conditions; (2) detailed water surface profiles upstream and downstream of the test site under a range of flow conditions; and (3) river bed bathymetry shortly prior to the in situ test deployment. These data are required to define bathymetric and hydraulic conditions that exist at the in situ test deployment site before the pilings and turbines are installed.

FFP plans to collect all requested data. Additionally, this comment suggests that the bed and hydraulic conditions contain a temporal component, an assertion with which FFP strongly agrees; seasonal changes due to erosion and sedimentation occur, as do long term morphology due to accumulated affects and differences in flow from year-to-year. It is important to gather existing data to understand the natural rates of change so that local effects due to pilings and turbines can be isolated from the naturally occurring bed dynamics, and having some measure of this will aid in the validation of the CFD modeling for the *in situ* site. It is worth highlighting that one of the major reasons to perform the *in situ* deployment is to validate CFD predictions from the effects of pilings with the measured values. Therefore, it is critical to capture as much data as possible to integrate into that model, and to ensure sure the model is functioning properly before a determination is made regarding which measurements should be made and where they should be made. Specifically, FFP will model the site with high bed resolution using available data before construction begins.

FFP strongly agrees with the Commission’s recommendation that early measurements be taken before physical work is initiated to deploy hardware in the river. We believe that there exist important benefits to integrating existing data both for pre-construction optimization and to aid in quantifying morphological changes. Additionally, existing data will be highly useful in validating CFD models that can then be used with confidence when the latest bed geometry is available. Having the historical data serves as a very good reference for quantifying the effects of FFP’s turbines: predicting relative changes from the turbines and pilings is much more significant than an absolute reference. It will be important to separate incremental effects from other global effects, and having as much historical data will greatly aid in this effort.

In the Second Interim Report (page 2-4, last paragraph), you state: “Further, ADCP measurements taken following deployment of the turbines/pilings will be utilized to evaluate any localized changes in flow velocity in the vicinity of the infrastructure; such measurements will consist of full-river width scans at the following three locations: (1) 20 feet forward of the piling located furthest up-river; (2) 20 feet behind the piling located furthest down-river; and (3) 200 feet behind the piling located furthest down-river.” In developing your in situ test deployment plan, please add more ADCP transects in a reach between 20 feet upstream of the site and 200 feet downstream of the site so that velocity maps at 2 feet, 5 feet, and 10 feet below the water surface can be developed for comparison purposes. Comparison of velocity in these depths will be useful for evaluating potential effects on navigation.

FFP agrees with the Commission’s recommendation, and will perform these additional measurements.

In the First Interim Report (page 2-21, paragraph 3), you state: “The results are 65%, 102%, 48%, and 164% variation from the actual, in the stated range of desired accuracy for 1D codes

[one-dimensional] (50%–200%).” Please explain what variable or variables are referred to for the above-stated accuracy. We are concerned that the above-stated accuracy is acceptable for only a few variables, but not others.

This passage from the First Interim Report derives from a discussion of the results that other researchers had obtained with 1D modeling compared to their measurements. The difference in predicted and measured bed loads can vary by the amounts stated. The materials that were used to provide this information also correlated surface elevation between the 1D model and observed values. A 2003 calibration had not more than 6% variation in height, while a 1999/2000 set had contained data points within 6% and two others that were within 17 to 21%, likely due to the level of bed sediment.

In the First Interim Report (page 2-25, paragraph 3), you state: “The boundary conditions will be most important on the upstream part of the model and will include velocity (magnitude and direction) across the span, flow (must match the velocity versus location), and river height.” Please explain why the boundary conditions will be most important on the upstream part of the model (as opposed to the downstream end of the model) in a subcritical flow system like the Mississippi River. We are concerned this statement is contrary to common methods of numerical modeling of similar rivers.

After further refinement, FFP offers the following revision in order to address the previous version’s deficiencies, as described in the comment:

“The 2D model will be prepared by importing the bathymetry data along the entire bend and some upstream and downstream distances. For distance, the Corps has recommended utilizing a 15-mile reach; alternatively, FFP recommends that better results may obtain from modeling a domain of three river bends. The model will be meshed to subdivide the geometry into small segments and volumes, and boundary conditions will be applied. The boundary conditions will be flow rate at the upstream boundary, and river height on the downstream part of the model; the converged solution will require that downstream mass flow match the inlet value. For computational efficiency involving fewer elements and higher grid resolution, FFP would prefer a model that contains a developed velocity profile at the inlet. One manner in which to accomplish this is with the use of an inlet mass flow condition featuring one of two velocity profiles: 1) a normalized profile that will keep the ratio of local velocity/average velocity; or 2) the creation of a long reach upstream whose discharge velocity is transferred to the inlet of the 3 river bend model. The most effective approach to integrating the inlet velocity profile will be evaluated as efforts progress and with consultation with the USACE. As a general modeling note, the 2D code averages velocity, and upstream conditions will automatically be corrected by the CFD code to balance the losses in the flow, predominantly through adjusting the river height at the inlet.”

In the First Interim Report (page 2-25, paragraph 4), you state: “In addition, hand calculations will be performed to provide references and predictions that will be compared to model results. The 2D [two-dimensional] code will be run iteratively until there is acceptable agreement between the modeled results and the calculated results.” Please explain how you are using hand

calculations to compare model results. Modern 2D models normally provide much more accurate results than anything but extremely detailed hand calculations. We would like to know the advantages of the proposed calibration procedures as compared to standard model calibration procedures.

A favored synergy for hand calculations and model results is for determining intermediate details in a model. The primary tools for adjusting the 2D model are the losses and loss model used. The losses will primarily be frictional and bend losses, with the frictional component being bed and bank components, which are controlled by roughness. When specific data for roughness is lacking, “typical” values are normally employed, but these may not always provide a good match to actual data; therefore, roughness values will be iterated until there is good correlation between the model and the data. The values are often implemented on a large scale to capture an average, but at times there may be other information may be available to aid in defining local roughness values. In particular, most of the models are set up from transect data and ADCP data, which may have large spacing between them. At times, other data between the transects may be available to allow refinement of intermediate and local bed conditions. Specifically, when there is multi-beam data available, it is possible to calculate actual roughness, such as sand waves, sharp objects, and holes. Using hand calculations, this data can then be converted into an equivalent Manning’s coefficient. Hand calculations of roughness can then be used as input into the model, either as an average over a distance, or as a localized gradient in roughness. Mesh scale will determine how best to average the roughness in a region, but the mesh can be refined in local areas to capture extreme changes and local “hot spots”.

In the First Interim Report (page 2-25, paragraph 4), you state: “Ultimately, the matching of downstream velocity and gage height with known values will establish correlation. FFP will seek a highly correlated result, which will be done by beginning with a well-understood loss model already available for this area and then refining the mesh model sufficiently that the loss model does not have to change between runs.” Please provide the expected number of locations where velocity and gage height correlation will be examined.

Because FFP is in the process of initiating our model generation, we request that our answer to this comment be deferred until we research this issue further. Generally, a model benefits from the use of as many stations as possible. However, these projects present a small challenge in that at some sites, only widely spaced gage locations are available. Gage stations are particularly useful to obtain flow rate, which is a dominant input variable used in modeling; however, they lack the details of velocity that available in the ADCP data set. Flow rate can also be determined by integrating ADCP velocity measurements. The ADCP data includes river height, which makes possible accurate modeling by coupling the available data.

In the First Interim Report (page 2-25, paragraph 5), you state: “Since the 2D model is capable of piecewise solutions, with the discharge conditions being used for the input boundary conditions for a subsequent downstream solution, this approach could [be] employed if necessary to provide more detail over a large distance, or to section a local area for comparison with the details of the small-scale 3D [three-dimensional] solution (i.e., similar mesh refinement).” Please explain the functionality of downstream boundary condition, i.e., whether

modeling of a section of the river will require the results from its immediate downstream section to set its downstream boundary condition. If the answer is no, explain why. If the answer is yes, please describe whether iterative procedures will be required.

The answer to the Commission's question is that modeling a section of the river will indeed require the results from its immediate downstream boundary section to set its downstream boundary condition. The downstream boundary condition is river height, and this is primarily determined by the conditions downstream of that boundary. If no changes are made to a river segment, such as by adding turbine installations, no real change would be expected at the downstream height. It would then be possible to solve one segment, and to then use the converged upstream height value from this calculation as the downstream boundary condition for the next upstream segment model. This process, which is incremental, and therefore not iterative, could be marched upstream to arrive at an accumulated solution. However, the correct inlet details, primarily velocity distribution for the downstream segment, are not known until the upstream segment is solved. Therefore, this approach would be highly iterative, necessitating the use of the discharge from the upstream segment as the new velocity inlet. This could change inlet height, and then require the use of this new height to resolve the upstream segment with the new height boundary condition. This would then be repeated on every segment until a stable solution emerges. The 2D code incorporating the length desired will perform the equilibrium calculations to dispense with the need to perform iteration.

In the First Interim Report (page 2-26, paragraph 4), you state: “The ANSYS CFD [computational fluid dynamics software developed by ANSYS, Inc.] code is hydrostatic, meaning in this context that every term of the constituent equations is solved in the code. By comparison, non-hydrostatic 3D code often is used to model mid-field river hydrodynamics, though buoyancy (i.e., gravity) may be turned off in ANSYS if desired. The non-hydrostatic codes simplify the vertical equations (i.e., small compared to the main-stream variable) to allow a faster solution time, while still solving river height and free surface equations.” Please double check whether you have inadvertently reversed hydrostatic and non-hydrostatic in the statements above and throughout.

This comment correctly indicates that the terms hydrostatic and non-hydrostatic were inverted in this passage. FFP offers this revised version below:

“The ANSYS CFD [computational fluid dynamics software developed by ANSYS, Inc.] code is **non**-hydrostatic, meaning in this context that every term of the constituent equations is solved in the code. By comparison, **a** **non**-hydrostatic 3D code often is used to model mid-field river hydrodynamics. The **non**-hydrostatic codes simplify the vertical equations (i.e., small compared to the main-stream variable) to allow a faster solution time, while still solving river height and free surface equations.”

In the First Interim Report (page 2-27, paragraph 3), you state: “If the code is already validated for a similar geometry and bed conditions, FFP will use the code directly on the relevant location.” Please clarify whether you propose to skip model calibration in cases where you have validated the code elsewhere in areas of the Mississippi River with similar geometry

and bed conditions. Sediment transport modeling is generally very site specific and coefficients for the model can vary significantly even with small changes in local conditions. As such, we suggest that, as a matter of generally accepted modeling practice, the recommendations with regard to hydraulic model calibration, validation, and sensitivity evaluation (Study Plan Determination, pages A-12 to A-13) should also apply to sediment transport modeling.

FFP appreciates the Commission's insight and guidance on this issue. FFP acknowledges the challenges inherent in sedimentation modeling, and that it can be sensitive to variations. The processes of validation and sediment modeling will be highly interactive, as FFP believes that it is optimal to work closely with the Corps to benefit from its experience, data, and expertise.

In the First Interim Report (page 2-28, paragraph 5), you state: “FFP proposes that if, and only if, significant differences between the 2D and 3D models’ hydraulic bed conditions (i.e., shear stress) are observed will FFP consider performing detailed 3D sedimentation analyses.” Please propose a criterion to define significant differences in these conditions.

FFP has not yet defined criteria for determining the need or benefits of utilizing 3D sediment analyses, nor have we developed the computational base to define significant differences. FFP expects that refinements to these approaches will be a continuing and evolving process. FFP will gain greater insight after gaining experience using the various models, particularly with reference to existing data for global and site sediment measurements. We do envision a process that tightly integrates the Stakeholder feedback and guidance in developing a threshold. FFP anticipates that the criteria will not be limited to the differences in shear stress values, but will also include the extent of these.

2.1(b) USACE Comments on 4SR

Table 2-1 purports to show all stream gages in the Mississippi River near FFP proposed project sites. Please note that other gages exist near proposed project sites, such as Algiers Lock, IHNC Lock, and Alliance.

FFP appreciates the Corps' correction that other Gages do exist near FFP's proposed HK (Hydrokinetic) sites beyond those shown in Table 2-1. Hydraulic modeling will include far-field and very far field in the 2D and 1D models, and incorporating the largest data set of flow and gage height will be an important part of model validation.

(A) The Manning's roughness coefficients described in Figure 2-4 include energy losses due to channel irregularity and changes in alignment that are at least partially resolved by multi-dimensional models, such as AdH. The selection of a roughness coefficient for input to a multi-dimensional model must consider the internal algorithms applied in the model and may not precisely match values obtained from a one-dimensional analysis. The multi-dimensional model should be able to reproduce the average longitudinal energy loss observed in nature or computed from a one-dimensional analysis.

(B) It should be noted that Figure 2-4 does not describe longitudinal variations in Manning's roughness over approximately 1,000 miles of the Lower Mississippi River.

FFP is agreement with the comments regarding the use of Manning's coefficient, and the variations that will occur span-wise and length-wise at various locations, and between 1D averaged, 2D, and 3D models. Applying the best local measurements is absolutely desirable when such data exists, and ultimately stage and velocity data will be used for calibrating the final values of n. In the end all the models should have agreement with values of average energy loss, particularly to agree with measured (natural) data.

(A) A depth-integrated Elder (1959) form of the vertical distribution of eddy viscosity may be reasonable for wide shallow channels; however, this form assumes that the depth is the controlling length scale for mixing.

(B) Additional discussion or consultation on methods for assigning eddy viscosity values for model input is warranted. In the two-dimensional, shallow-water version of AdH, the assignment of horizontal eddy viscosity must consider constituent transport as well as hydrodynamic computations.

FFP greatly appreciates the guidance offered in assigning and implementing eddy viscosity values in hydraulic river modeling. Having the physical and coding experience and expertise of the Corps to assist FFP's hydraulic modeling efforts will greatly improve the accuracy of our results and the cumulative modeling time to get these solutions; this generous support is something which FFP anticipates will be an integral part of the transparent and collaborative hydraulic modeling effort. In short, FFP desires to arrive at the highest level of accuracy in our modeling, and the assistance of the Corps will be invaluable.

Figure 2-4 shows riverbed roughness as a function of stage. Technically, this relationship probably exhibits hysteresis (i.e. loop effect), though this may not be significant for FFP's purposes. The ERDC ITR team may be able to comment further.

FFP welcomes the valuable comments of ERDC ITR regarding this topic, and FFP looks forward to collaborating with the Corps on this issue.

(A) A more detailed description of the mesh and model inputs, e.g., "How many nodes or elements were used to define the turbine?" or "What is the surface area over which an n-value of 0.3 was applied?", would be useful in understanding the model results.

FFP's turbine model employed 4 nodes with 2 finite elements, in an area sized 10 ft x 10 ft.

(B) Normally, when Manning's bottom friction is used to represent obstructions, the ratio of the projected area of the obstruction to the area of the computation cell or element is used to scale the Manning's value. The value of 0.3 may be reasonable however, it is scale dependent.

(C) Additional discussion or consultation on methods for assigning roughness coefficients to represent turbines is warranted. The reported model results describing a relatively small impact of a single turbine on river stage and currents were not unexpected. A more detailed description of the computation and application of Manning's *n*-value for the turbine is needed in order to determine if this approach can be scaled to an entire turbine field over a wide range of flow and turbine operating conditions. Alternate approaches that may provide a more robust and accurate computation, including approaches being developed through on-going research funded by the Department of Energy, should be considered and discussed in future reports.

Use of Mannings friction coefficient: FFP again welcomes and appreciates the Corps' valuable comments regarding this topic and we look forward to further discussions and model review on this and other modeling topics. In Section 2.8, FFP discusses Sandia National Labs EFDC-SNL modeling efforts and those of Pacific Northwest National Laboratory's 3D FVCOM, and agree that the DoE's supported efforts are extremely helpful, and provide immediate benefits to FFP's modeling.

Document reads "FFP expects the magnitude and extent of these effects to decrease when using actual river bathymetry data ... " Please explain why.

The magnitude of variations in water surface elevation and velocity were small directly above the turbine and dissipated quickly within 100 feet downstream of the turbine. Water surface elevation disturbance was 0.04 feet (12 mm); this value is less than the height of surface wind waves (ripples) typically observed in the Mississippi River (3 in = 0.33 ft = 75 mm). A localized velocity decrease of 0.3 ft/s was observed directly above the turbine. At a distance of 100 feet from the turbine, the variation in water surface elevation was less than 0.005 feet (1.5 mm). The velocity variation after 100 feet from the turbine was 0.2 ft/s. These results suggest that, by carefully optimizing the arrangement of the turbine field, it is possible to minimize the interaction between turbines and thereby decrease any additive effect. The previously mentioned values were obtained using a simplified geometry of a channel with depths significantly lower than those found in the proposed locations of the turbine fields. It is expected that the increased depths at the actual turbine fields will act as a buffer reducing the effects (water surface elevation changes and velocity changes) perceived at the water surface.

2.2 Induced Velocity from Ship Propellers

As outlined in Section 4.3 of the Damaged Turbine section of the Second Interim Report, there exist ambiguities and complexities in evaluating the wakes of vessels' propellers. This analysis generally begins by determining representative operating conditions, and then by determining what an extreme case would comprise. A ship's propeller provides thrust to the vessel by increasing the energy and velocity of water through the propeller, and resulting in a jet wake behind the propeller. FFP has calculated a velocity increase of 4.5 - 9.3 m/s based on a 6 foot diameter propeller attached to a 2,000 HP engine. This figure is valid at peak operating conditions only, and would be lower at normal conditions. These values are added to river

velocity; therefore, in the case of a river velocity measuring 3 m/s, the total maximum velocity that could be anticipated would be in the range of 7.5 – 12.3 m/s. These calculations are available in Appendix 2-1.

The reason that as relatively large of a range as 4.5 – 9.3 m/s has been calculated is that thrust is generated in a propeller by accelerating fluid through it. The general equation is:

$$\text{Eq. 2.2.1: } T = m * dV_x$$

Where m is the mass flow rate (mdot) and dV_x is the change in velocity in the direction of thrust. For the sake of clarity, we will only consider flow that moves in the direction of the propeller's axis and ignore swirl that is in the wake. This will allow us to assume that dV infers velocity in the direction of thrust only. (NOTE: this is a reasonable assumption with the swirl component being treated as a reduction in propeller efficiency from the ideal value).

Another equation needs to be referenced to give insight into mass flow rate, m . This is:

$$\text{Eq. 2.2.2: } m = \rho * A * V$$

Where ρ = density, A = reference area, and V is the velocity. Density and area are fixed (density of water and the reference area of the propeller) while V can vary.

We see m , mass flow, in both equations 2.2.1 and 2.2.2. In the simplest form, if a ship has a relative velocity (speed of ship to the moving water) of 1 m/s and the relative velocity is then increased by a factor of 2 (to 2 m/s), the mass flow doubles (Eq. 2.2.2). AT a fixed value of thrust, Eq. 2.2.1 tells us that the value of dV is reduced by a factor of 2 to provide the same thrust. This gives us a very important conclusion: high thrust at low relative speed will require a large increase in velocity, while at high speed high thrust requires a smaller increase in velocity.

Next we consider operational conditions, which ties in the above conclusion. Thrust is needed for two conditions: (1) accelerating; and (2) overcoming resistance during steady operation, where resistance in this case is the drag of the vessel. High drag conditions would be at high relative speed, a very large tow, or some combination of the two. It is also useful to differentiate power from thrust. The equation for power is:

$$\text{Eq 2.2.3: } P = T * V$$

Where P = Power, T = Thrust, and V = Velocity.

High thrust can be generated at low speed, but this is typically at a fraction of the peak power available from the engine. Conversely, at high velocity, peak power does not necessarily mean high thrust. An analogy is illustrative. A high torque (what generates thrust) automobile will use thrust to accelerate quickly, but then has to reduce the acceleration (thrust) and power to keep from going too fast for the prevailing conditions. As the vehicle approaches a hill, however, the driver steps on the accelerator to maintain speed; because velocity remains the same, both thrust and power increase. At its limit, with the accelerator fully depressed, the thrust is used to

overcome the resistance of the grade and the speed is set by the available power. As the slope increases, the driver has to change to a lower gear, increasing thrust while lowering speed. The previous is a prelude to stating that high thrust at low river speeds is likely rare and brief. This most often would occur when a tug accelerates quickly, but then has must throttle back to restrict vessel speed. Similarly, continuous high thrust is also limited to high river velocities, much like the slope of the hill.

Returning to fluid dynamics and evaluating the effects of a propeller on the water, Table 2.1-1 lists the calculated velocities induced at different conditions, based either on maximum thrust or maximum power (listed as High and compared to average operation). This is calculated, but is reasonable, because the alternative, measuring propeller velocities in a fast moving river, would be difficult and potentially dangerous. Note that the values listed as “Average” are only estimates, based on 20% of the peak value. Absolute velocities expected from normal ship operation are quite low at low river velocities. The methodologies used to generate this table are discussed later in this section.

V _{river} , m/s	V _{ship_rel} , m/s	V _{ship, absolute, m/s}	V _{wake, relative, m/s}		V _{wake, absolute, m/s}	
			Average , m/s	High, m/s	Average , m/s	High, m/s
1	3	2	1.86	9.30	2.86	10.30
1	5	4	1.32	6.60	2.32	7.60
1	7	6	0.90	4.50	1.90	5.50
2	3	1	1.86	9.30	3.86	11.30
2	5	3	1.30	6.50	3.30	8.50
2	7	5	0.90	4.50	2.90	6.50
3	3	0	1.86	9.30	4.86	12.30
3	5	2	1.30	6.50	4.30	9.50
3	7	4	0.90	4.50	3.90	7.50

Table 2.1-1. Calculated velocities

FFP proposes to evaluate two conditions:

1. A ship traveling at 5 m/s (11.2 mph) relative to shore in a flow of 2 m/s (4.5 mph) with an absolute wake velocity of 6.5 m/s (14.5 mph).
2. A ship traveling at 2 m/s (4.5 mph) relative to shore in a flow of 3 m/s (6.7 mph) with an absolute wake velocity of 9.5 m/s (21.2 mph).

Other modes would be a reversing propeller or a ship travelling down river. In each case the induced velocity would subtract from the river velocity and is therefore lower in magnitude than the cases proposed. Also, when traveling downriver, the river carries the ship, leaving less need for thrust or power.

The question is then to calculate the velocity from a propeller wake that could impinge on a turbine or piling. This requires calculating the velocity and dissipation of the propeller discharge with distance and depth. The degree to which it dissipates will be determined using CFD methods.

To quantify the effects of propeller induced velocity FFP will be using CFD to approximate the jet wakes and the induced velocities from this as a function of distance vertically to the wake and downstream from the propeller. The primary variables that FFP will use to set up this model are proposed as:

- River velocity: 2 m/s and 3 m/s;
- Ship velocity (relative to water): 7 m/s and 5 m/s;
- Velocity increase across propeller: 4.5 m/s and 6.5 m/s;
- Propeller diameter: 6’;
- Distance from surface to bottom of propeller: 9’ (3’ from top of propeller to surface);
- River turbulence kinetic energy: 10%;
- Propeller angle from horizontal: 3 degrees upward (axis points skyward in upstream direction).

For modeling purposes, the other conditions will be:

- A fixed surface with free slip;
- No swirl in the wake;
- The propeller will be an equivalent propeller that has the diameter listed previously and adds the acceleration to the flow to provide the velocity listed.

The use of a free surface approach for this analysis would be difficult and would add little value to the flow dynamics occurring under the water. Observation of tows on the Mississippi River at high load show very complex wakes, including a significant “fountain” behind the propeller where the wake is tossed many feet in the air. Capturing this detail is not beneficial to our needs. Disregarding the residual swirl is likely a conservative assumption, meaning that the effect of swirl is likely to increase the wake dissipation. Therefore, ignoring it will show at worst a wake that is longer and deeper than will actually occur. If the results indicate the need for including swirl, this can be evaluated later, but for now FFP plans to incorporate swirl simply as a loss in propeller efficiency. With propeller efficiency, FFP is assuming a relatively low value. The rationale for this assumption is that craft in the shallow draft section of the river typically incorporate a large upturn in the hull just forward of the propellers, which will negatively affect

the flow entering the propellers. These propellers are likely designed for very high loading (thrust coefficients) which tends to reduce efficiency, because more efficient, larger propellers are more costly and run deeper in the water.

The methodology and rationale for the values in Table 2.1-1 are based upon the following: the SPD requires FFP to calculate the effects of a ship's propeller on turbines x ft below the surface. Propeller information can be used to translate thrust or horsepower values into approximate jet velocities that are then run in CFD to determine their extents (lengthwise) and influence (depth-wise). The goal is to create a uniform jet of a diameter equal to that of a representative propeller (typically 6' in the shallow draft region) and then to normalize the results to diameter. The results can be applied to turbines at different depths below the waterline. Importantly, although this study is focused on shallow draft ships, the normalized results can be applied to deep water sections with ships having much larger diameter propellers.

The attached copy of a MATHCAD calculations shows the velocity value and how FFP arrived at the values stated. The basis is the momentum equation listed in Equation 2.2.1, but is more complex than simply using relative speed to capture actual mass flow through the propeller (the higher the mass flow, the lower the speed increase). This complexity arises from the physics of propeller (or fan) operation; because a propeller will increase the velocity both behind and in front of the blades, therefore capturing the actual flow requires the inclusion of the induced upstream velocity. Equation 2.2.4 (Theodorsen) is an implicit equation with the desired solution variable (dV_{prop}) appearing on both sides. FFP solved this iteratively to arrive at the values listed.

Eq. 2.2.4:

To calculate the thrust value in the above equation, FFP utilized two methods and averaged their results. The first method used a value of 20 lbf./HP and a 2,000 HP engine to arrive at the thrust, and the second assumed peak power and calculated thrust from Eq. 2.2.3. Details are in the MATHCAD file included in Appendix 2-2.

FFP will create a CFD solution for two cases using an equivalent propeller to accelerate the flow as calculated using the methods described. From this, a chart of velocity versus depth and velocity versus distance can be generated, which can then be normalized to propeller diameter and power and then applied to known turbine locations. If sufficient changes in velocity are expected on a turbine or a piling, then further steps will be employed to calculate the drag forces and stresses, and the loads will be incorporated into the design with adequate margin.

On the issue of impingement, real world operating conditions must be evaluated. High velocities have been observed at high river stage and when a tug is accelerating from rest. High river stage means that turbines and pilings are much farther below the surface than they are at low water

(20' below LWRP), so the jet from the propeller wake is likely to be highly dissipated. CFD will show this value. A tug that is using maximum acceleration at low velocity is likely going to be a brief occurrence; this raises the issue of the frequency at which this could occur in a location where turbines are mounted. FFP will continue to evaluate the likelihood of this occurrence as we finalize turbine mounting details.

2.3 Near Field Flow

Near Field Flow describes the detail of the turbine hydrodynamics, in particular the effect of the turbine on flow around, through, and behind the device. The hydrodynamic design of the turbine was generated in the ANSYS CFX program, a general use commercial CFD code. In the ISP, FFP presented results of the design and analysis, including the performance factors calculated. Testing of the turbine is thus far showing very good correlation to the predictions, but that model did not include the wake behind the turbine, which is a significant flow component required for river and installation modeling. FFP presents the results of our near field flow model in several sections below, beginning with the wake model.

From a highly-detailed design, FFP has generated an “equivalent” turbine which replaces the complex geometry of the blades and struts (de-swirl vanes) with a simple loss model, and shows that excellent correlation with the detailed model has been achieved.

The detailed equivalent turbine model described above includes a turbine shroud. The shroud’s inclusion is beneficial for analyzing the flow interactions between turbines and pilings, while remaining mesh intensive to capture the shroud flow and details. When we transition from the very near flow field to a Mid Field Flow model, and attempt to capture the 3D effects of numerous turbines and pilings, we will need only a simple actuator disk type model. The actuator disk removes the same flow energy as the turbine, and has the same flow field characteristics, but with far fewer mesh details. FFP presents the results of that CFD analysis below.

2.3(a) Near Field Flow

FFP’s turbine is a 3 meter diameter (appx. 10') device incorporating a flow duct, a turbine rotor, and de-swirl vanes/struts, whose purpose is to transfer kinetic energy from the flow into rotational energy for extraction by a generator. The changes in flow will create drag on the device and result in reduced energy flow behind the turbine. Figures 2.3-1 and 2.3-2 show two views of the machine and the flow, with the first image of a longitudinal cross section, and the second of an isometric view showing flow on a cylindrical surface (slice). Note that the velocities shown for the rotor are in the relative (rotating) reference frame, thus the magnitude and vector orientation.

These images were developed from the design study of the device, using ANSYS CFX. This model is a 1/7th sector model: there are 7 blades on the turbine, and the model is accordingly created in 7 longitudinal “pie” sections with periodic boundaries in the circumferential direction.

The use of the sector model applies a highly refined mesh in the region of interest, rather than a coarser mesh over a full 360° model. Figure 2.3-3 shows a slice through the mesh and size of the domain. As a modeling note, the boundary conditions are fixed velocity at the inlet, a pressure boundary on the exit, and fixed RPM on the rotor.

Because the flow-field is not carried downstream for many turbine diameters, this model does not capture the wake effect, which is critical for the river modeling. FFP extended this model and recalculated the larger flow field to capture the wake details. FFP's analyses are also performed in the ANSYS CFX code; we have purchased ANSYS CFD, which includes both CFX and FLUENT.

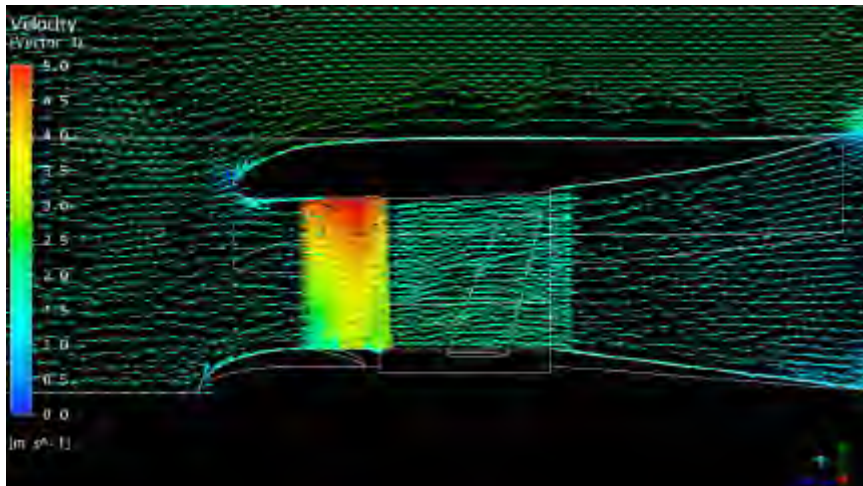


Figure 2.3-1. Longitudinal Cross Section with Flow Vectors

[CONTINUED ON NEXT PAGE]

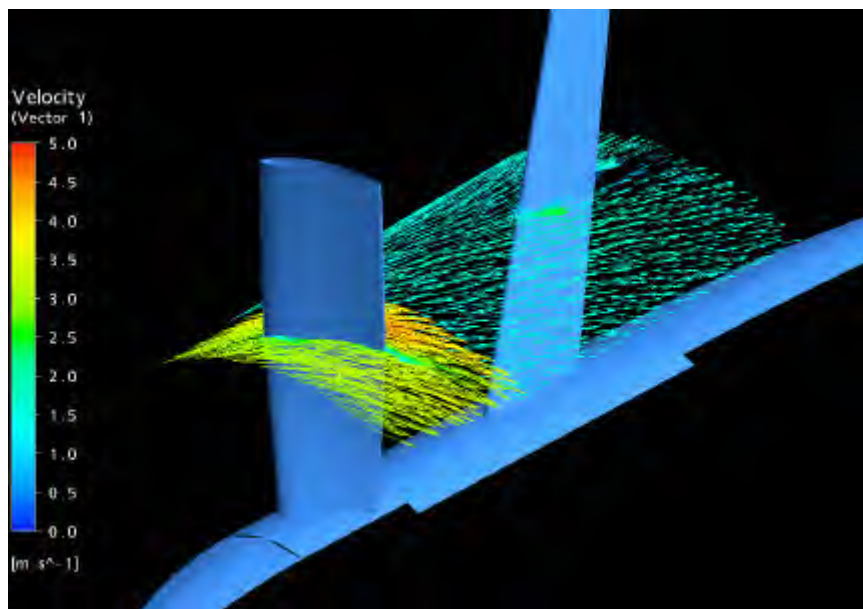


Figure 2.3-2. Details of Blade Geometry and Flow

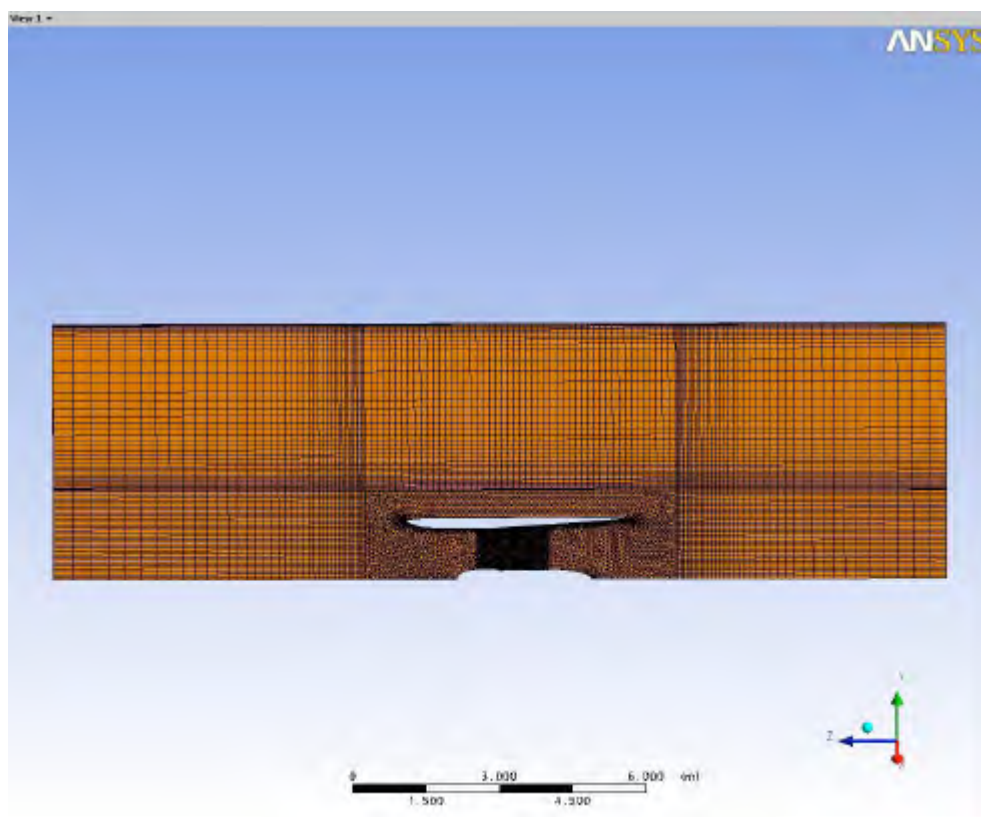


Figure 2.3-3. Flow Domain and Mesh

To create the wake model, FFP added a 300 foot downstream extension to the model and meshed this, with the exit pressure BC moved to the discharge of the extension. The extended mesh is shown in Figure 2.3-4. It maintains the same mesh as the original, but with the extension added to it. Although it is difficult to see the detail in this image, with the extension added, this is over 5 times longer than the original. This 1/7th sector model utilizes 2.3 million elements (2.3 M). The medium is water at 25 °C. Studies were performed using a κ - ϵ turbulence model and an SST turbulence model, with no distinguishable difference in the results. SST combines κ - ϵ with κ - ω and an internal algorithm to determine the preferred model, with the κ - ω model typically being advantageous in adverse pressure gradients and separated flow (Menter).

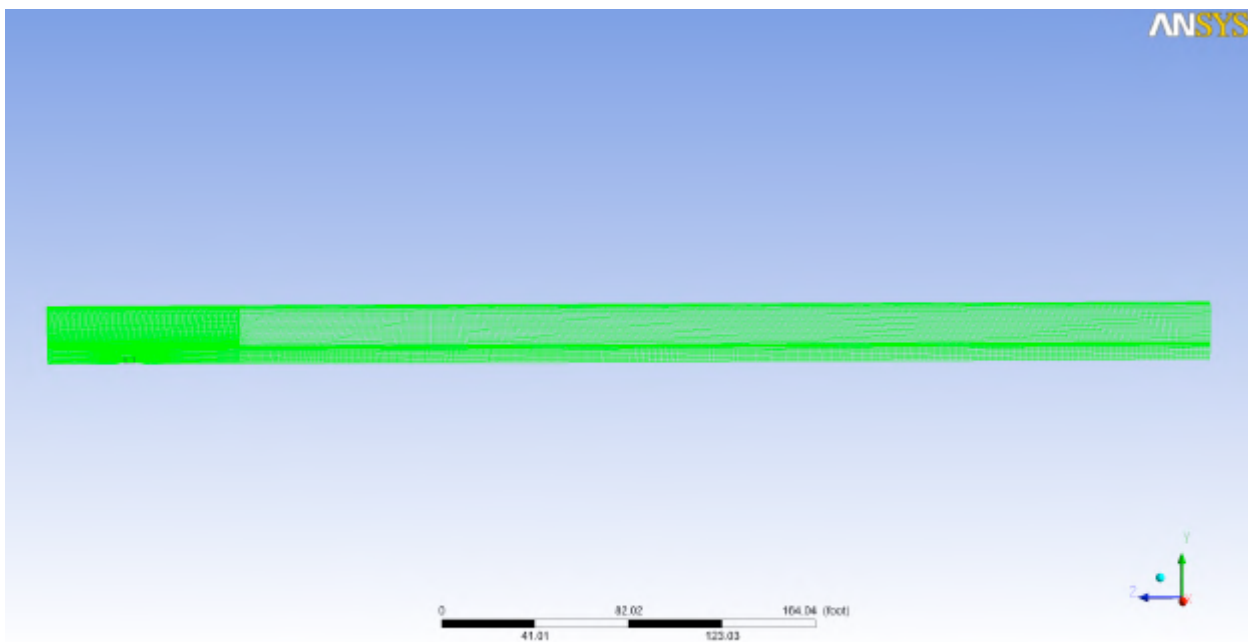


Figure 2.3-4(a). Mesh with Extension

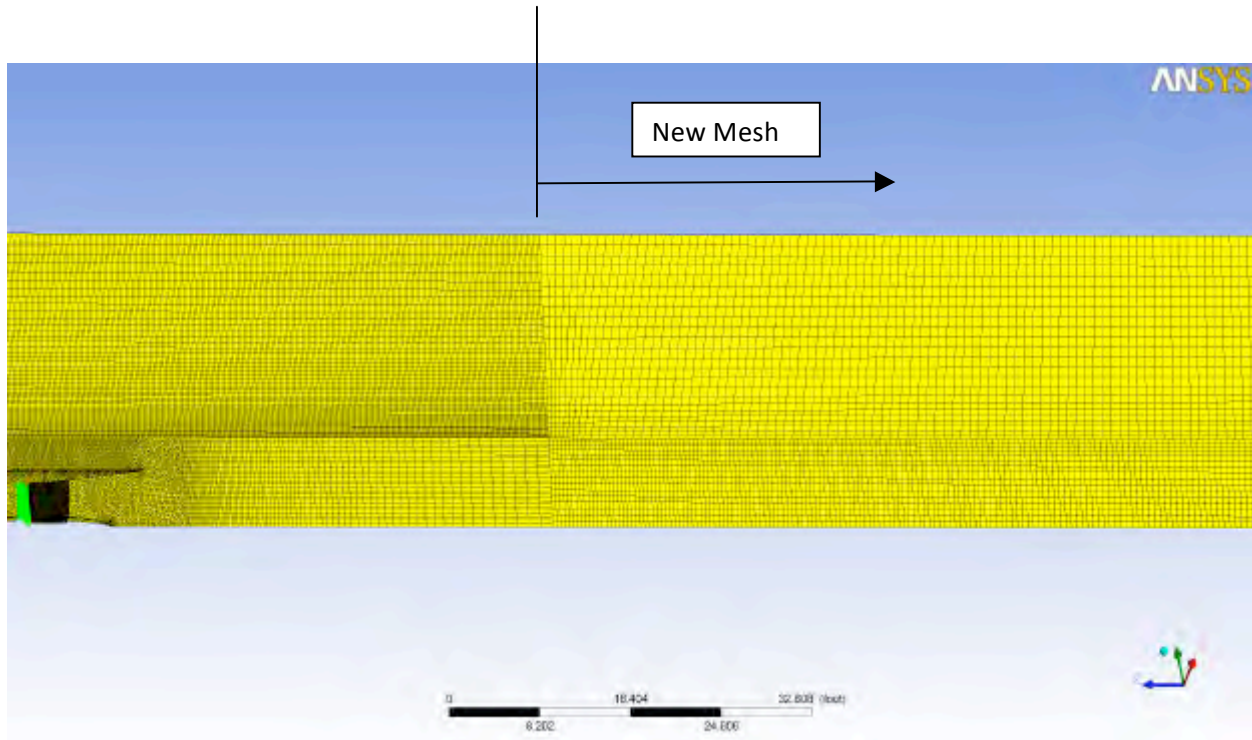


Figure 2.3-4(b). Mesh with Extension – Local Zoom

The model was run at the design condition of 2.25 m/s free stream velocity (inlet BC), 38 RPM, and 10% TKE (Turbulence Kinetic Energy), and showed a wake length of 22 D (Diameters). The wake velocity is plotted in Figure 2.3-5, with the wake length being defined as the mixed region with velocity within 97% of the average value at that location. This is the small region at the very end of the light green contour shown in the image. Note that the turbine is small in this scale, and the easiest manner in which to identify it is to look for the gap at the lower left of the image for the start of the light blue wake just aft of the white gap.

[CONTINUED ON NEXT PAGE]

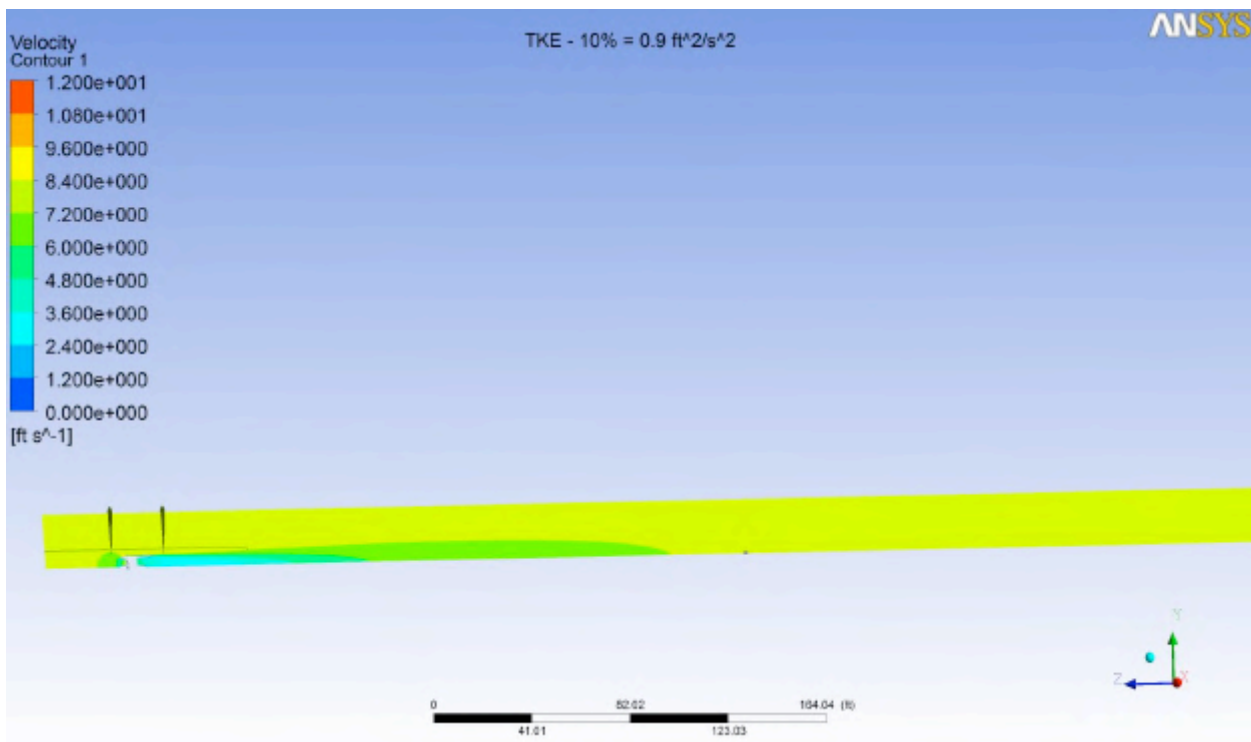


Figure 2.3-5. Turbine Wake Velocity

Although this case was analyzed at 2.25 m/s free stream velocity, these results are general for other flow conditions. The turbine power coefficient, C_p , is constant across varying flows, which is analogous to saying that the drag coefficient is constant. Consequently, as velocity increases, more energy is extracted, but the mixing distance behind the device remains constant due to the higher energy in the wake and the free stream.

Another useful result is the set of pressure contours shown in Figure 2.3-6. Here, the high-pressure region forward of the turbine is clearly visible in red, and the low-pressure region aft of the turbine can be seen in light blue. The pressure loads greatly exceed the friction terms in the total turbine drag, as evaluated from detailed output; this image illustrates the reason that this is the case.

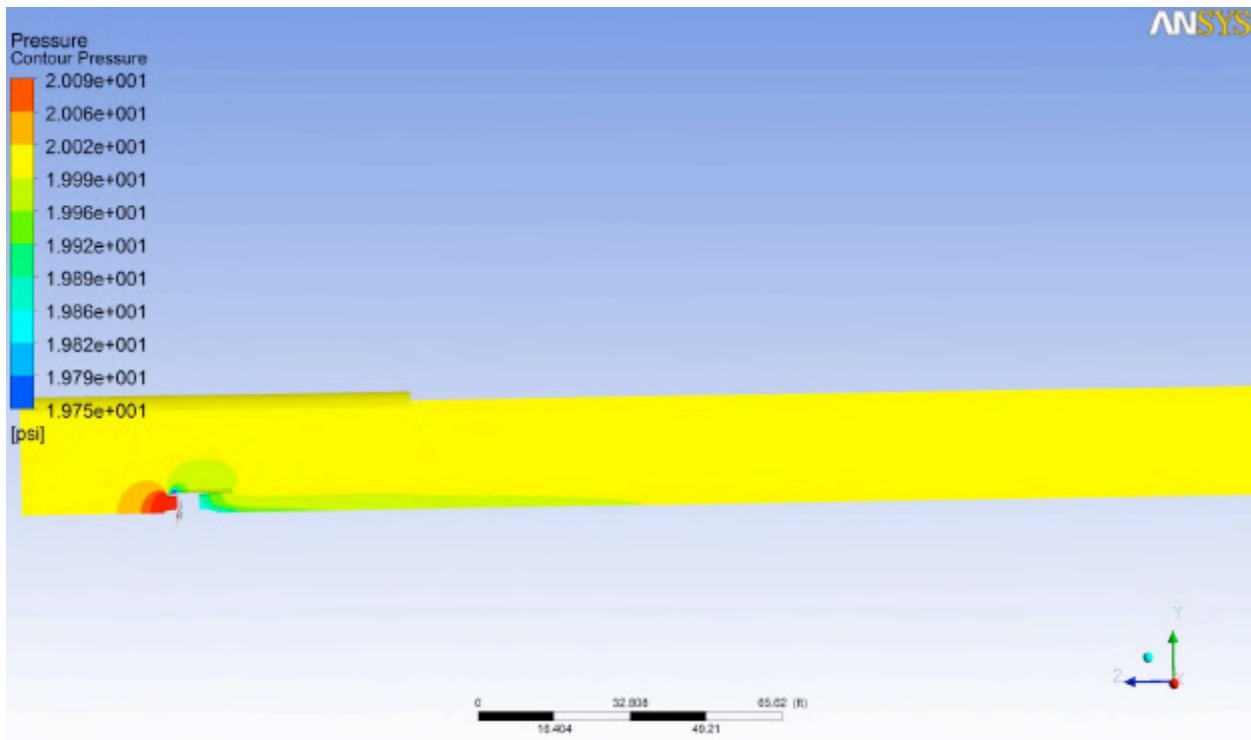


Figure 2.3-6. Pressure

The generally accepted value of turbine wake length is in the range of 15D to 20D, and FFP's turbine has a predicted length of 22D. When adding the extended length, the values of mass flow, torque, and other relevant parameters within the turbine remained unchanged; therefore, this result is effectively a complete near field model. What is lacking, however, is the full 360° model which is needed to perform our analyses with the turbine part of a larger, more complex domain (river and piling mounts).

2.3(b) Equivalent Model - Shrouded

The goal of the turbine model's development is to capture the hydrodynamic effect of the turbine on the flow hydraulics. Its intent is to: (1) capture the correct mass flow through the turbine; (2) extract the proper amount of energy from that mass flow; and (3) capture the flow characteristics in front of, around, and behind the turbine (i.e. the velocities and wake mixing). FFP began the process of generating an equivalent turbine by creating a simplified version of the bladed design and comparing the results of this (17th sector) model to the original. Figure 2.3-7 shows the results of this model in terms of velocity, with the primary focus being on the wake; compared with the original model, (Figure 2.3-5) one can observe that the wakes are similar as is the low velocity (high pressure) region at the turbine inlet. This model retained the shroud of the original design but replaced the internal blade and strut details with a much simpler loss model which is essentially a volume, filling the interior of the turbine that extracts energy based on flow. The quadratic resistance loss model employed defined 3 radial regions (tip, pitch, and hub) and different coefficients of $dP/Length/V^2$ are used for each region, with dP being the pressure

change and V is the velocity. The coefficients were tuned so that the radial velocity distribution was similar to the actual design model, and that the mass flow and the wake were simulated. Figure 2.3-8 shows the velocity profile inside the equivalent turbine (these are “zoomed” to capture only the low velocity values, with everything above 6 ft/s being shown in red).

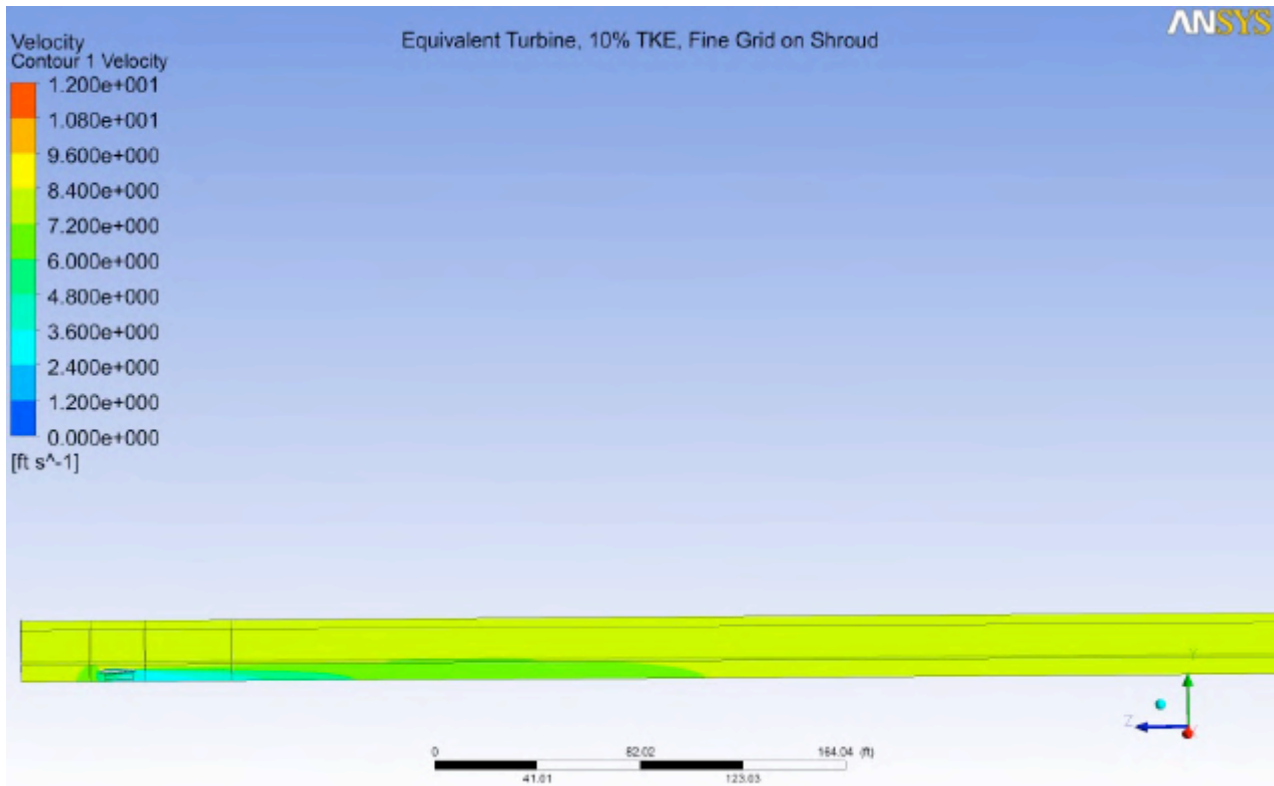


Figure 2.3-7. Equivalent Turbine Wake (sector model)

[CONTINUED ON NEXT PAGE]

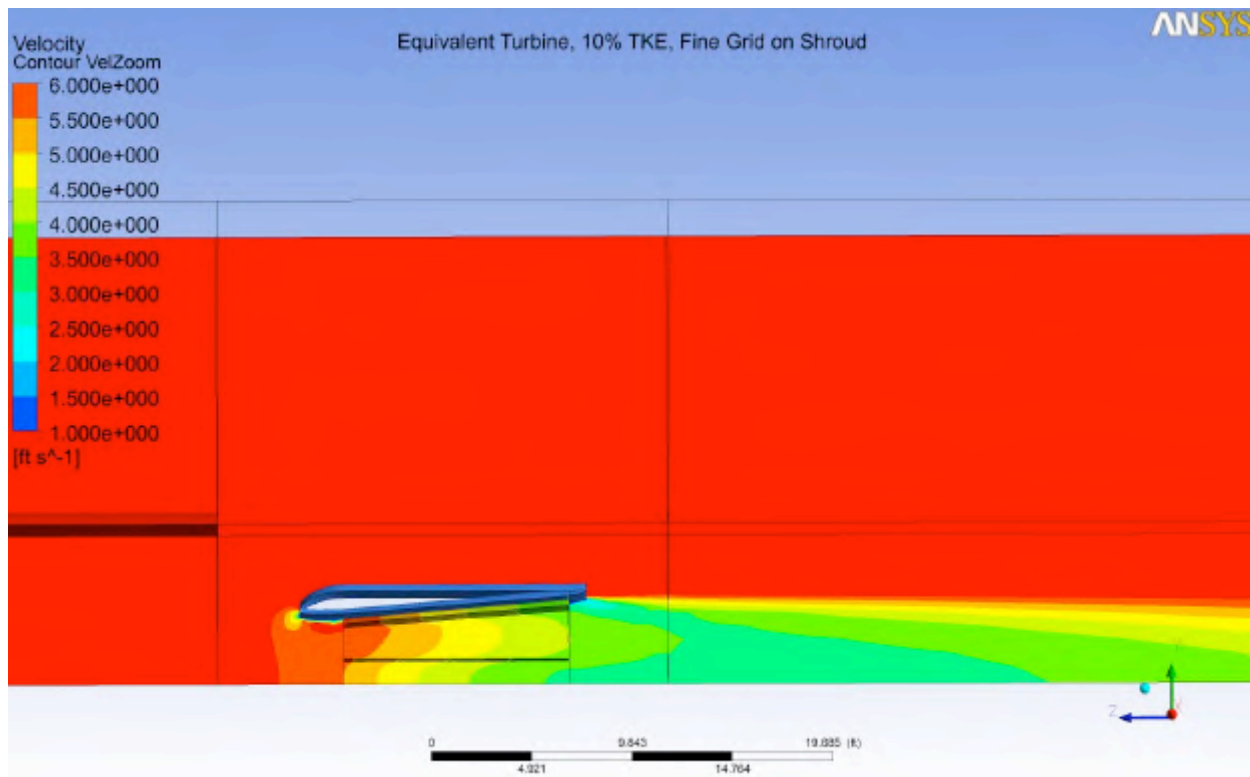


Figure 2.3-8. Velocity Profile on Interior of Equivalent Turbine

Creating this model represented the first step in the process, with the next step the creation of a full 360° model. The values of that model were then compared to the original design model multiplied by 7 for total flow and force. FFP created the full 3D model and the results compare very favorably to the original design scaled to 360°. At the completion of the equivalent turbine model creation and analysis, the flows were within 0.5% of one another.

The design model (scaled to 360 °) results are compared to the full 360° equivalent turbine model in the table below, along with the simplified equivalent turbine discussed later. The similarities in overall performance characteristics are clear. To correlate the flowfield of the equivalent turbine with the detail design results, Figures 2.3-9 and 2.3-10 are useful for comparing the wake and velocity characteristics between the two, and they agree favorably. Consequently, for any river modeling needs which do not require internal turbine flow details, FFP has generated an equivalent turbine which can be used for any near field, near-mid field, or mid field modeling, while fully preserving the external flow fidelity of the more detailed design model.

[CONTINUED ON NEXT PAGE]

	Design (1/7th)	Equiv. Turbine	Equiv. Turbine - Disk Model
FLOW, lbm/s	15,530	15,470	15,440
DRAG, lbf	2,716	2,812	3,101
Drag, Rotor, lbf	1,969	N.A.	N.A.
Drag, Shroud, lbf	710	N.A.	N.A.
Drag, Hub, lbf	37	N.A.	N.A.
Drag, debris, lbf			
Blocked Area, %, for debris			
Ratio to Design Flow	1.000	0.996	0.994

Table 2.3-1. Comparison of Equivalent Turbines to Detail Model

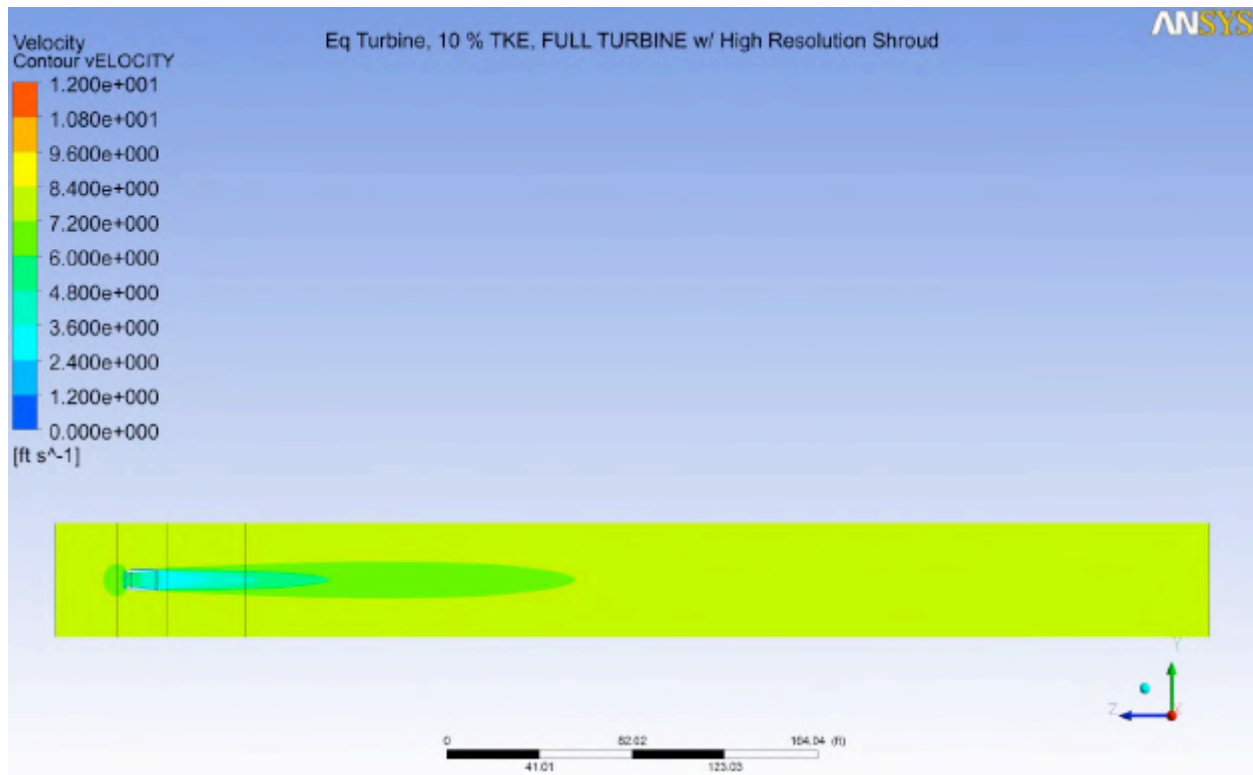


Figure 2.3-9. Velocity Contours, Full Equivalent Turbine – Hi Resolution Shroud

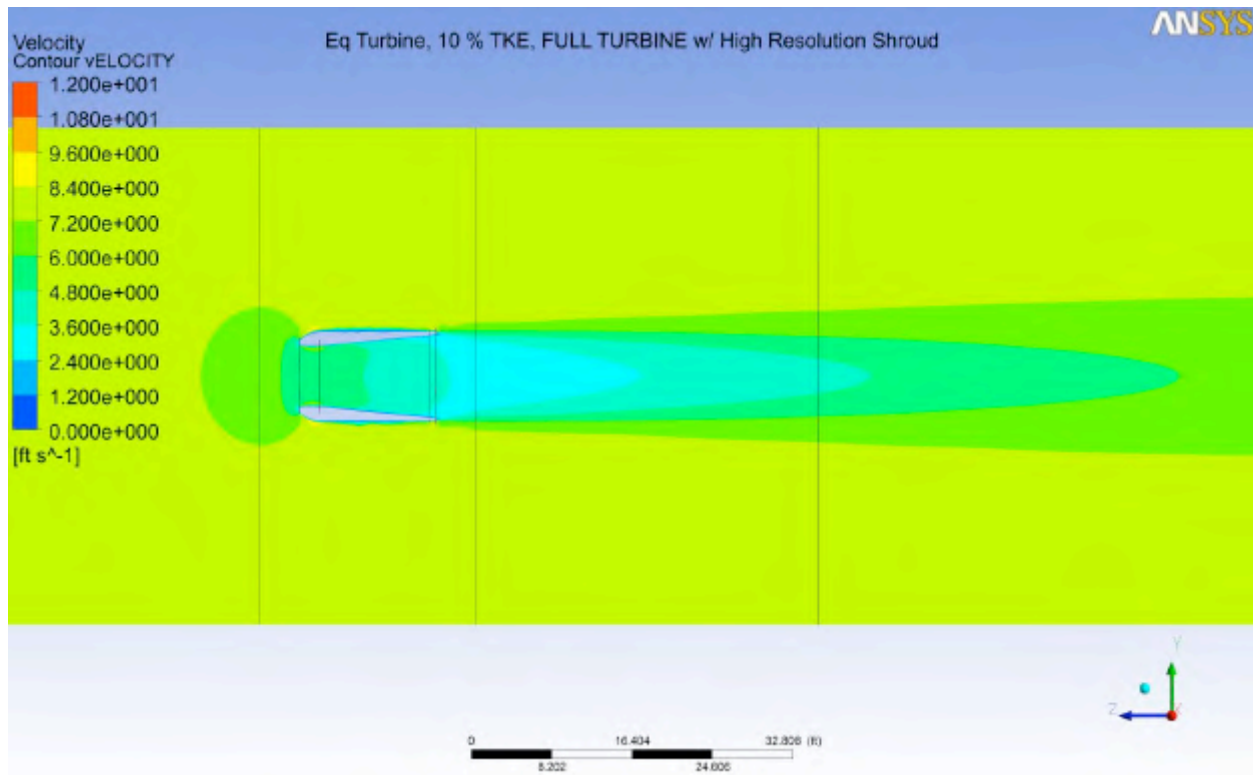


Figure 2.3-10. Close up of Velocity Contours, Full Equivalent Turbine – HiRes Shroud

While this equivalent turbine model is detailed, it is slightly less so than the complete, bladed, turbine model. A total of 3.1 M elements are employed to compare this to the detailed model. Figure 2.3-11 shows a slice of this mesh, with the dark area to the left being the turbine mesh; this is included to convey the details associated with the turbine model, despite its relative aesthetic shortcomings.

[CONTINUED ON NEXT PAGE]

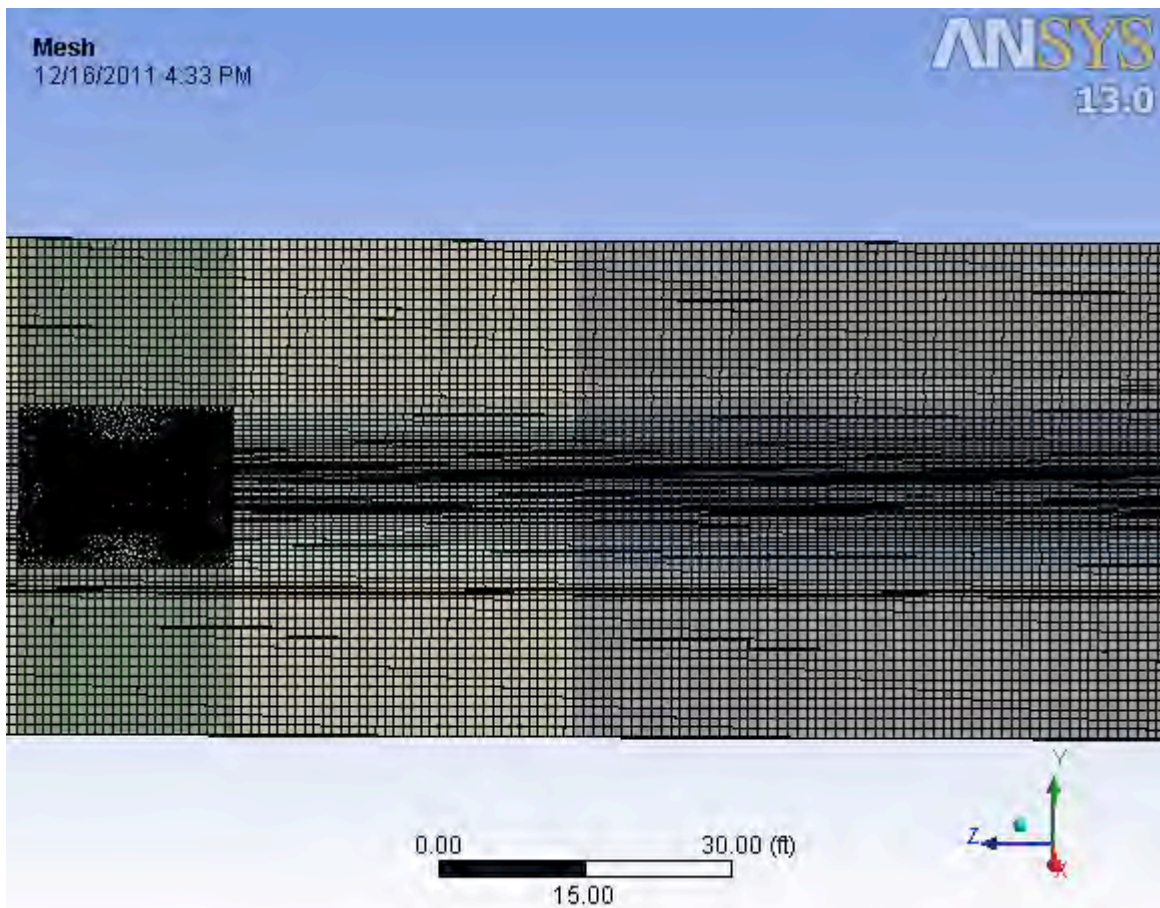


Figure 2.3-11. Equivalent Turbine Model

The characteristic of a reaction turbine is that there is a pressure drop across the rotor induced by the energy removal (loss in total head). Pressure drop, in turn, is what creates drag, which leads to the conclusion that the turbine can be treated as a drag object and the flow field around and behind the device would be nearly similar to the original as long as there is no residual swirl. The fluid resistance of the drag decreases the velocity forward of the device, as the turbine has been observed to do, which causes some of the flow to move around the device. The energy loss in the wake will be the determinant of the wake characteristics and mixing length. As long as these conditions are present, the water will not behave differently.

2.3(c) Equivalent Model – Actuator Disk

The shrouded equivalent turbine is a “universal” model in that it can be used to accurately represent the turbine in any larger model as long as the turbine is operating at its design point (Power Coefficient, C_p , is fixed). The shroud model is detailed enough that its interaction with and effect on the river will be realistic. However, there are still many mesh elements used to define it, primarily in the shroud details. For larger models, where some very localized flow

characteristics can be given up while maintaining essential operating affects, such as mass flow, energy extraction, and wake characteristics, the shroud can simply be eliminated and the internal fluid resistance model can be changed to achieve this result. The goal is a 3 meter fluid resistance model which captures the parameters just described, with a small number of CFD elements to allow dedicating more elements to the river details. Two primary approach options exist: (1) a very short actuator disk; and (2) a longer version that will incorporate some of the length effects. The actuator disk is simpler, but some of the flow in the localized tip region may be artificially abrupt. The longer version will have a smoother integration with the flow field, as the shroud would. It can be argued that, for models that span orders of a magnitude of greater volume than the turbine alone, the difference in very localized affects around the turbine are inconsequential. Therefore, the simplest, lowest mesh element solution is preferable. This assumption will be adopted for large models.

On the other hand, if it is determined that proximity effects of multiple turbines are significantly different between the short and the long “disks,” the longer version (cylinder) could be employed, or the fully shrouded equivalent model will be used, depending on level of detail and mesh elements desired. Proximity effects would likely be only for two turbines mounted near one other, or for capturing interaction with the pilings. In this situation, the shrouded equivalent turbine would be used for near-mid field models that include the pilings and high resolution is desired.

At this time, FFP will present results for the short turbine only, fully recognizing that a similar, but longer model can be implemented should the results show a need for it.

Figure 2.3-12 shows the results of the equivalent disk model, and the results are similar to those shown in Figures 2.3-5 and 2.3-9 for the detail turbine, and the equivalent shrouded turbine. Table 2.3-1 compares the detailed design results to the equivalent shrouded turbine, and the disk turbine, with quite good agreement between the model parameters of flow and drag.

A measure of the benefit of using the reduced turbine may be obtained by comparing the number of elements in the solution and the number of elements for the turbine model. The entire simulation required 458,000 elements (turbine + fluid) compared to 3,100,000 for the shrouded equivalent turbine. The image of the meshed equivalent disk turbine, shown in Figure 2.3-13, illustrates the model’s simplicity.

[CONTINUED ON NEXT PAGE]

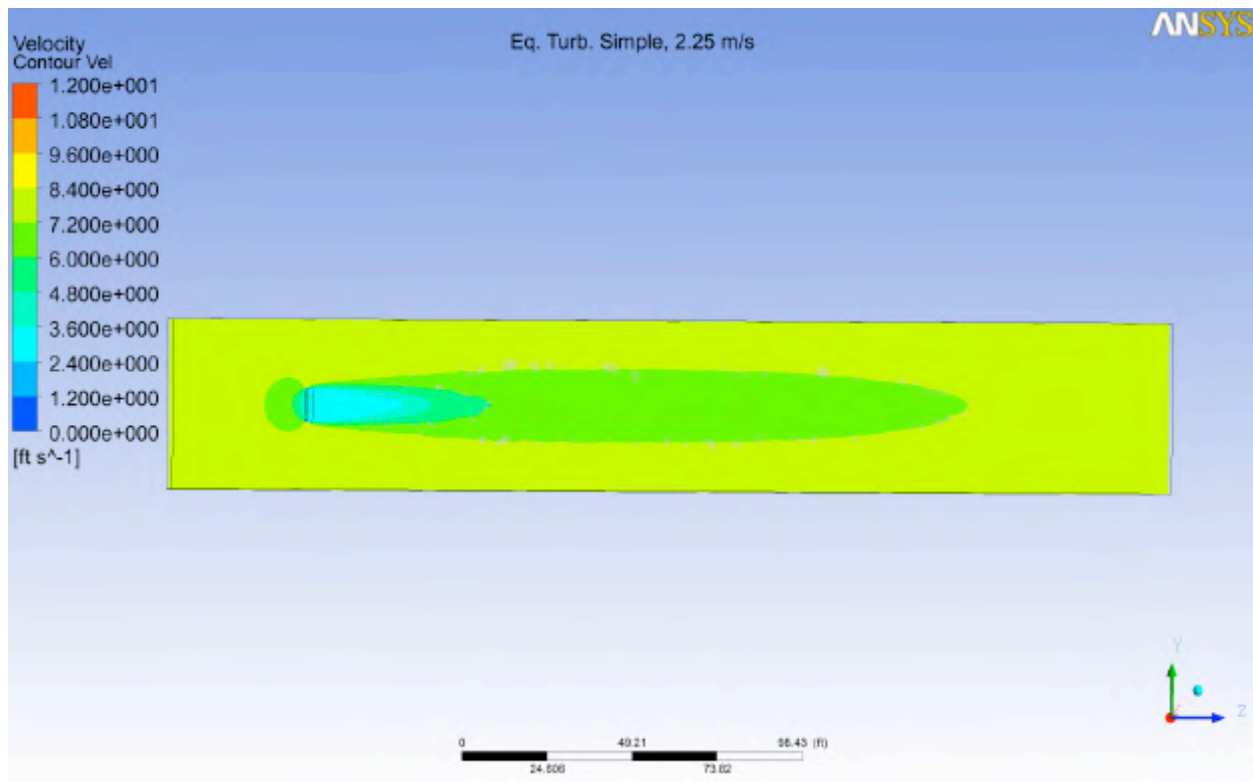


Figure 2.3-12. Equivalent Turbine – Disk Model

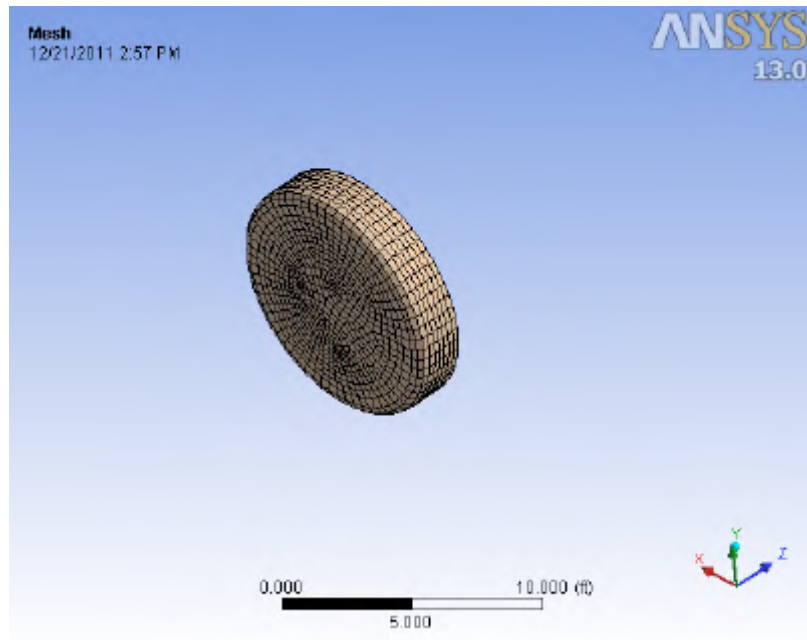


Figure 2.3-13. Equivalent Turbine – Disk Model

2.4 Deteriorated Turbine Performance (non acoustic)

There are advantages to coupling the use of CFD methods to assess issues related to operations and in the Damaged Turbine Studies. Presenting the results here for reference in other evaluations has the benefit of allowing all the CFD studies to be reviewed in a single section, and this is the approach adopted by FFP. One of these is the accumulation of contaminants on the turbine blades and flow surfaces, including sediment and bio-fouling, which may affect the turbine's efficiency or drag force. As part of this analysis, FFP continues to evaluate various surface coatings that minimize accretion of surface contaminants and resist abrasion, but having predictions of the potential for these affects is useful for long term operation and maintenance.

FFP performed CFD analysis with the ANSYS CFX program to make an evaluation and to quantify the sensitivity of changes to surface roughness. The initial design model (blade details and 1/7th sector) was the basis for comparison, and two variations were analyzed from this starting point. The first case added roughness to the turbine blades only and the second one added roughness to all of the flow surfaces (interior and exterior).

The results, summarized in Table 2.4-1, show flow increases with the rough rotor surface, and decrease with a higher roughness magnitude and roughness on all surfaces. Rotor drag is unchanged for a small increase in roughness, but decreases at the higher, combined state. Total drag has only small changes. Most interesting is the rotor torque, which is slightly reduced for mild roughness, and drops further with increasing roughness. Because in the analysis rotor speed is maintained, the torque reduction is directly proportional to change in power. It is therefore clear that the roughness has the expected result that net output power is reduced. The reduction in power extraction is higher than the change in drag, and this explains the reason that the flow is higher through the turbine; the energy extraction process creates higher resistance than the friction, so as the turbine efficiency decreases, the resistance also decreases and more flow can pass through the device. Relative to the roughened turbine, however, when all the flow surfaces are roughened there is additional frictional loss in the device and the flow is less than for the rough blade only (but still higher than the smooth case).

FFP has the capability to capture the effects of surface roughness on the turbine and flow surfaces, but the effect of these changes to the bulk flow is of minimal difference than the design flow conditions. Less electrical power can be extracted (7.2% less in the worst case shown), but that is more of an operational consideration than a flow consideration (i.e. determining surface protection coatings or cleaning intervals).

[CONTINUED ON NEXT PAGE]

	SMOOTH	ROUGH ROTOR	ROUGH ON ALL SURFACES
Roughness, mm	0	0.25	0.5
FLOW, kg/s	7033	7201	7160
Rotor Drag, N	8750	8750	8400
Rotor Friction Drag, N	57.5	98	108.5
Viscous Force / Total Force	0.007	0.011	0.013
Rotor Torque, Nm	3206	3157	2975
Change in Rotor Drag to baseline	1.000	1.000	0.960
Change in Torque to Baseline	1.000	0.985	0.928
Change in Flow to Baseline	1.000	1.024	1.018
Total Drag, N	12080	12369	12298
Total Drag, lbf	2,716	2,781	2,765
Change in Drag, lbf	0	65	49

Table 2.4-1

2.5 Off Design: Locked Rotor and Blocked Inlet Performance

Another operational aspect which CFD can be used for is evaluating the influence of debris on the turbine. Although the amount of debris which could build up at a turbine inlet is unknown at present (ongoing effort, including in situ testing), predicting deterioration in performance from blockage, or the effect on turbine component forces should the debris inhibit operation, is a useful study. FFP has created two CFD models to quantify these results. One is a locked turbine, which uses the design model (17th sector) at 0 blade RPM, and the other is to place obstructions at the turbine inlet to simulate situations such as an accumulation of branches or other debris. For the latter FFP used a complete equivalent turbine model since this better captures the effects of arbitrary upstream geometry on a full diameter.

2.5(a) Locked Rotor

Figure 2.5-1 shows a result of velocity contours at 2.25 m/s river flow with a locked rotor. The effect of resistance can be seen by the lower velocity upstream of the turbine inlet where the back-pressure slows the free stream and causes flow to go around the device. On the downstream side, there is a high loss near the hub (ID) manifested as low velocity flow in that region. The total flow is only slightly different than of the operational turbine, 15,610 lb/s versus

15, 530 for the operational version, but drag is only 57% of the design value, measuring 1,545 lbf. versus 2,716 lbf. The lower drag with a locked rotor can be explained. Although there are high losses near the hub, most of the flow near the higher area region of the tip have low loss. This is due to the very close blade spacing in the region, and all of the flow hits the blades at a normal angle; velocity vectors are based on 0 RPM for the locked rotor. Meanwhile, the tip has large blade spacing. Although it has been stated that high drag is indicative of high resistance (less flow through the turbine), FFP believes that the reason for that is one of static pressure profiles versus total pressure versions. The operational turbine will remove total pressure (energy), but this case presents low pressure behind the turbine due to high velocity from the hub pushing flow outwards. As the wake mixes, the average velocity (energy) will be higher because there is more total pressure, and the wake deficit is therefore less in this case. In parallel, the wake behind the blades is severe but localized as shown in Figure 2.5-2, again indicating regions of high total pressure between the blades (an operational turbine will “smear” the total pressure loss across the passage).

This result completes the locked rotor analysis, and proves that drag is less for a locked rotor than for a normally operating turbine.

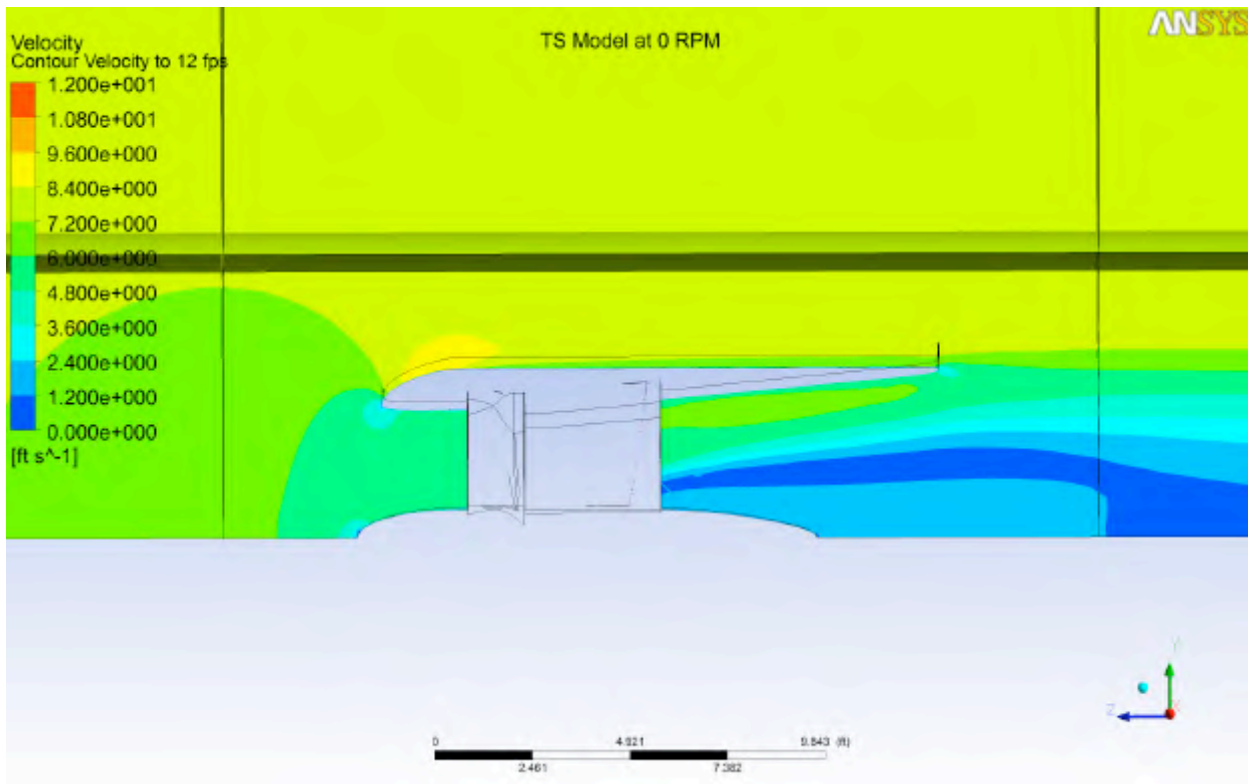


Figure 2.5-1. Velocity Contours, Cross Section, Locked Turbine at 2.25 m/s free stream velocity

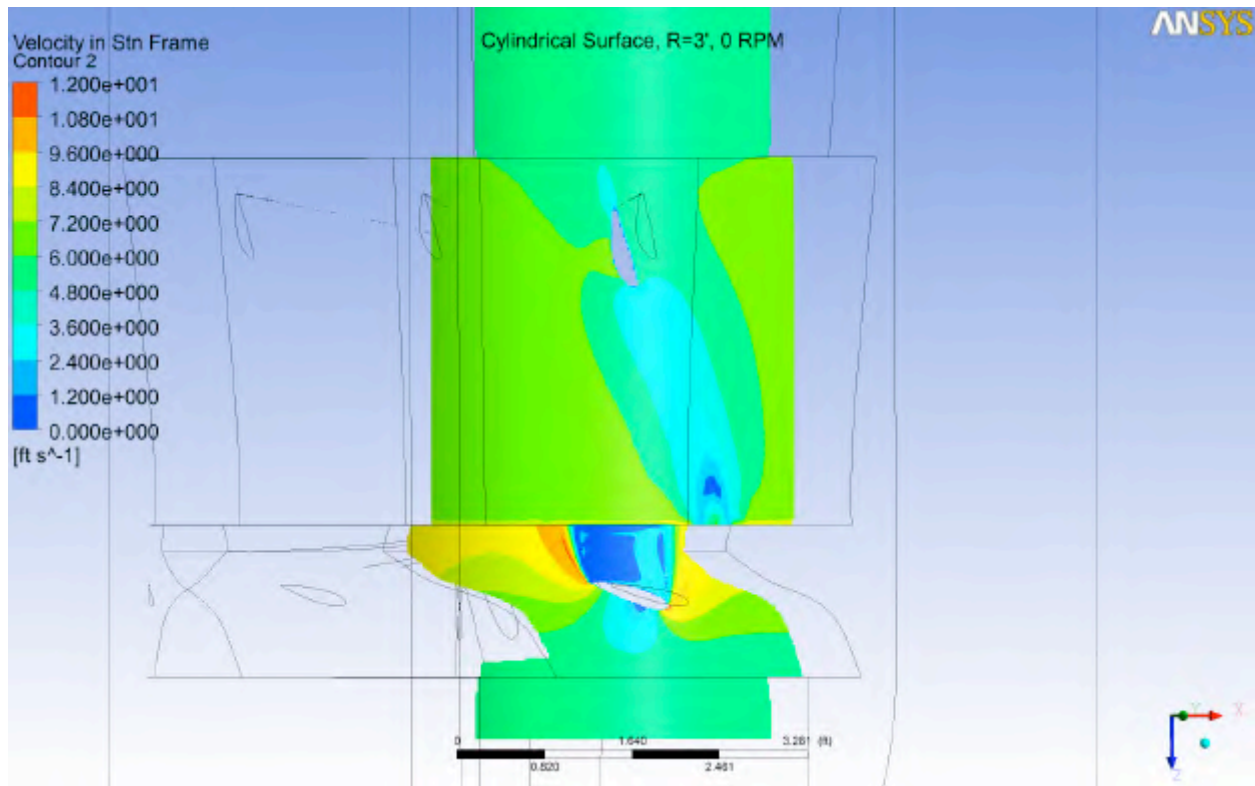


Figure 2.5-2. Velocity Contours, Blade View, Locked Turbine at 2.25 m/s free stream velocity

2.5(b) Blocked Inlet

Thus far the CFD results have shown that there is little effect from external influences (roughness or even a locked turbine) on the amount of flow passing through the turbine, and that the design case has the largest wake deficit. The results are combined in Table 2.6.1 below, but first FFP presents a discussion of the effect of a blocked inlet.

FFP created a blocked inlet CFD model by creating an equivalent shrouded turbine model, and compared the CFD result of that to the same model with simulated debris blocking the inlet. The blocked inlet model is shown in Figure 2.5-3, and the reference case is the same model without the debris. In this case, the debris is modeled as 9 2.5 m long cylinders of 3 inches diameter each. This combination was chosen for reference only, as debris size and distribution can be totally random; the goal is to calculate a sensitivity analysis. The shape of the duct can play a major part in affecting the flow on the debris, and through the turbine, hence a ducted case, rather than a disk actuator, was used for the model.

The analysis showed that the reference case had a flow of 15,180 lb/s and a drag of 3,792 lbf, versus 13,530 lb/s and 3,918 lbf for the blocked case. The drag of the blocked turbine is only slightly more than the open one, and this is a sensible result. The blockage from the debris will

force more flow around the turbine, and that which passes through the turbine will have less velocity (due to the wake of the debris), resulting in a lower device drag. On the other hand, the drag of the debris is additive to the drag of the device. In this case, the debris drag is predicted to be 672 lbf versus 971 lbf based on theoretical drag predictions for a smooth cylinder (see Appendix 2-1). This is an expected result because the turbine flow resistance also lowers the velocity impinging on the debris (a mutually beneficial interference drag). This case uses more than 28% of the inlet area blocked by debris, a significant blockage.

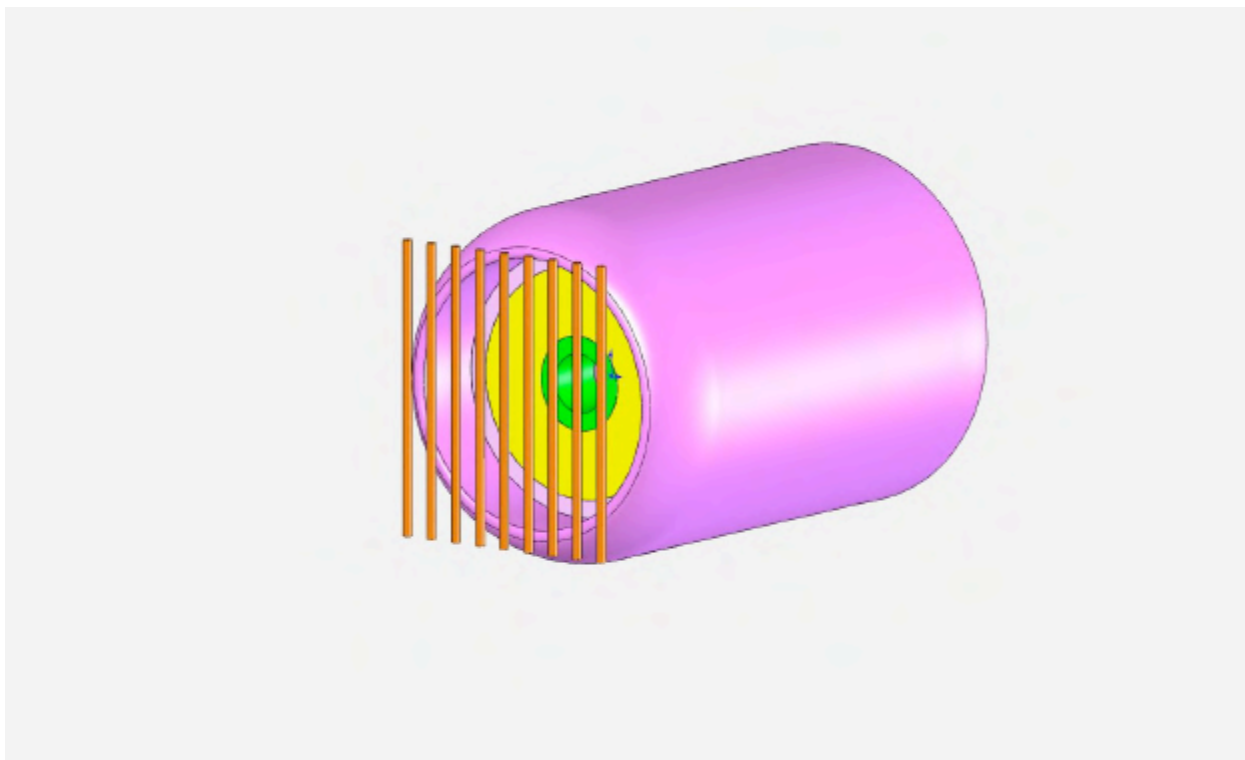


Figure 2.5-3. Equivalent Turbine with Blocked Inlet

Although the drag change due to debris is small in this sensitivity analysis, the effect on flow through the turbine is large. The reduced turbine flow implies that more flow now goes around the device, thus there will be locally higher velocities near the sides of the turbine. The high external velocities are good for wake mixing, and will have a broader influence on items near the inlet.

The results of all the various turbine operating models and conditions are summarized below in Table 2.5-1. The drag models discussed in this section are consistent with one another, and the relative changes due to debris should be accurate for trend indicators. The level of drag on the base case equivalent turbine for drag is higher than it should be, and this implies that more “tuning” of the model is required to get better alignment with the other models. FFP will perform this refinement at a later time, when it is critical to do this. Note that the value of 3,918 lbf. at

2.25 m/s free stream velocity implies a drag coefficient of under 0.5 for the worst case analyzed. In the Damaged Turbine Study Plans, FFP has used values of 0.75 and over 1.0 for operational and blocked turbines respectively, and consequently most of our load cases are extremely conservative as they have a high safety factor built in to them, thus there is little need to spend more time tuning the drag study model.

	2.25 m/s				
	Design (1/7th)	Equiv. Turbine	Equiv. Turbine - Disk Model	Equiv. Turbine, for drag	Equiv. Turbine, for drag, blocked inlet
FLOW, lbm/s	15,530	15,470	15,440	15,180	13,530
DRAG, lbf	2,716	2,812	3,101	3,792	3,918
Drag, Rotor, lbf	1,969	N.A.	N.A.	3,281	2,875
Drag, Shroud, lbf	710	N.A.	N.A.	436	313
Drag, Hub, lbf	37	N.A.	N.A.	75	58
Drag, debris, lbf					672
Blocked Area, %, for debris					
Ratio to Design Flow	1.000	0.996	0.994	0.977	0.871
Ratio of Flow for blocked inlet				1.000	0.891
Ratio of Drag for blocked inlet				1.000	1.033

Table 2.5-1

2.6 Prediction of Turbine Shear Stress

In the SPD Section 5. Fish Entrainment, Movement, Behavior, Habitat Use, and Population Effect Estimation, FFP was assigned the task of predicting, “Results of CFD analysis of shear stress, pressure changes, turbulence, and cavitation in turbine passageways, including an assessment of the rate of injury from these parameters for juvenile and adult fish, fish eggs and larvae, phytoplankton, zooplankton and aquatic macroinvertebrates.”

This section reviews the shear stresses, pressure changes, turbulence, and cavitation in FFP’s turbine at 38 RPM and 54 RPM. These results can be utilized in the Fish Entrainment Reports to perform the calculations defined.

2.6(a) Shear Stress, Pressure Changes, Turbulence, and Cavitation at 38 RPM

In this section, the shear stresses, pressure changes, turbulence, and cavitation are modeled for later use in fish passage calculations, specifically at the design point of 38 RPM and 2.25 m/s river velocity. The program used is the ANSYS CFX CFD program and the model is the identical to that described in Section 2.3(a). The next section will show similar results for higher river and rotational speed.

Figures 2.6-1 through 2.6-6 map the Shear Strain Rate and Eddy Viscosity near the ID of the turbine (hub), the radial centerline (pitch), and the OD of the blade (tip). These are illustrated on cylindrical slices at the tip, pitch, and hub, with two turbine blades shown for reference.

Viscosity is defined as:

$$\text{Eq. 2.6.1} \quad \mu = \tau / d\varepsilon/dt$$

Where τ is the shear stress (psi), ε is the strain (in/in), and $d\varepsilon/dt$ is the strain rate (1/s). A better approach to consider strain rate as v/L , where v is the relative velocity of two particles in the direction of flow, and L is the distance apart in a direction perpendicular to the flow. Alternatively, dv/dy may be used, where y is in the vertical direction.

Equation 2.6.1 can be rearranged to calculate shear stress as:

$$\text{Eq. 2.6.2} \quad \tau = \mu * d\varepsilon/dt = \mu * \dot{\varepsilon}$$

Where $\dot{\varepsilon}$ is the shear strain rate.

Cada defines shear stress as:

$$\text{Eq. 2.6.3} \quad \tau = (\mu + \mu_t) * \dot{\varepsilon}$$

With the terms μ_t being the eddy viscosity, so that the shear stress is the sum of the material viscosity and the eddy viscosity. Eddy viscosity is defined as:

$$\text{Eq. 2.6.4} \quad \mu_t = \rho * k / \omega$$

Where ρ is the density (lbm/ft³), k is the turbulence kinetic energy (TKE, ft²/s²), and ω is the specific dissipation rate (1/s). Important to this equation is that the eddy viscosity is defined through the turbulence (TKE).

To calculate shear stress as defined in Figure 2.6-3, the terms for shear strain rate and eddy viscosity (turbulence) must be defined separately. At the hub, the predominant value is at or below a strain rate of 20/s, with values up to 60/s except for the immediate region near the blades where the value exceeds 200/s. At the pitch the majority of the flow is less than 39/s, with values up to 97/s across the passage, and a peak in excess of 300/s close to the blade surfaces. The tip region has values similar to the pitch, but with a larger percentage of the passage at the lower value due to the larger blade spacing. The values very close to the blades will be ignored for the first level of calculation, since these are such a small percentage of the passage area.

Behind the turbine, in the bulk flow, the values of shear strain rate are very low, in the range of 5 – 10/s as shown in Figure 2.6-7.

The other term used for calculating the shear stress is the eddy viscosity, μ_t . The blade passage distribution of eddy viscosity is shown in Figures 2.6-4 through 2.6-6, and, similar to the shear strain rate, the values away from the blades are low. Values at the hub are predominantly under 0.010 lb/(ft * s), with the bulk of the wake being 0.040 lb/(ft * s) or less. For the pitch the values are predominantly under 0.015 lb/(ft * s), with the bulk of the wake being 0.060 lb/(ft * s) or less. For the tip the values are predominantly under 0.010 lb/(ft * s), with the bulk of the wake being 0.060 lb/(ft * s) or less.

Table 2.6-3 in Section 2.6(b) of this report summarizes the values at 38 RPM and 54 RPM.

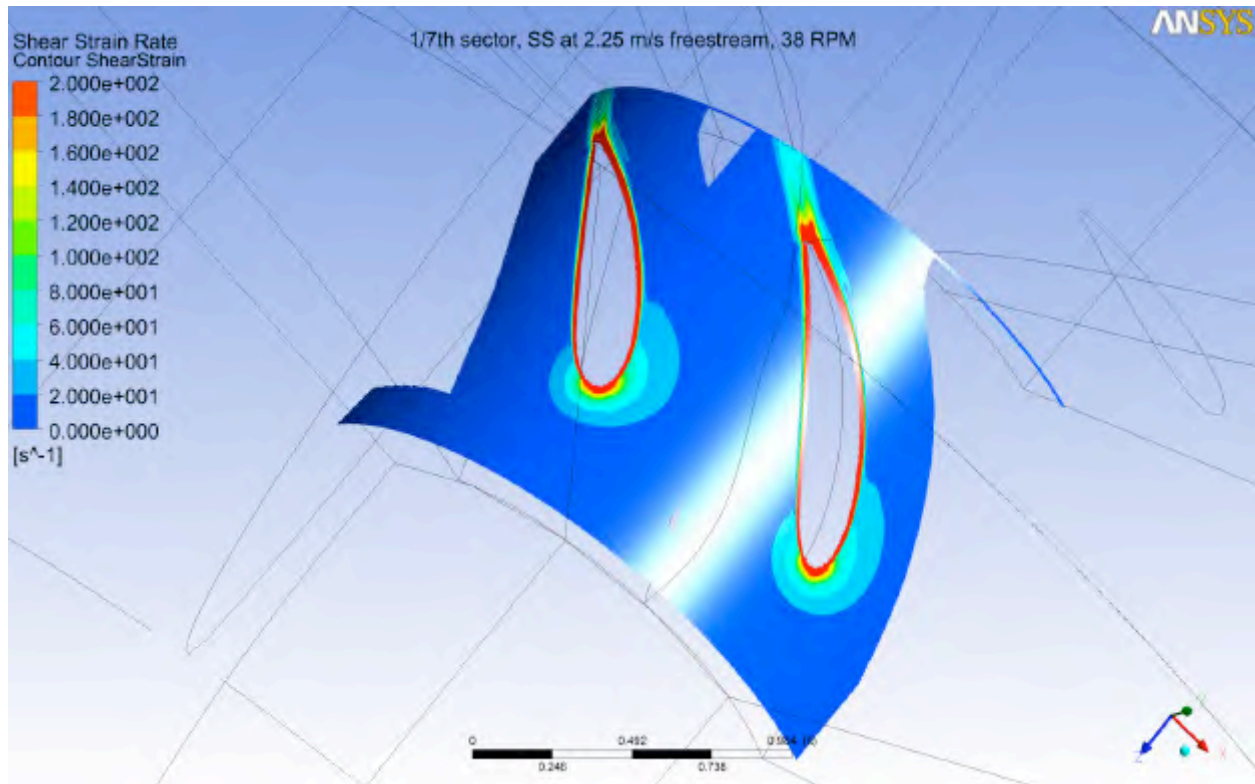


Figure 2.6-1. Shear Strain Rate at Rotor Hub

[CONTINUED ON NEXT PAGE]

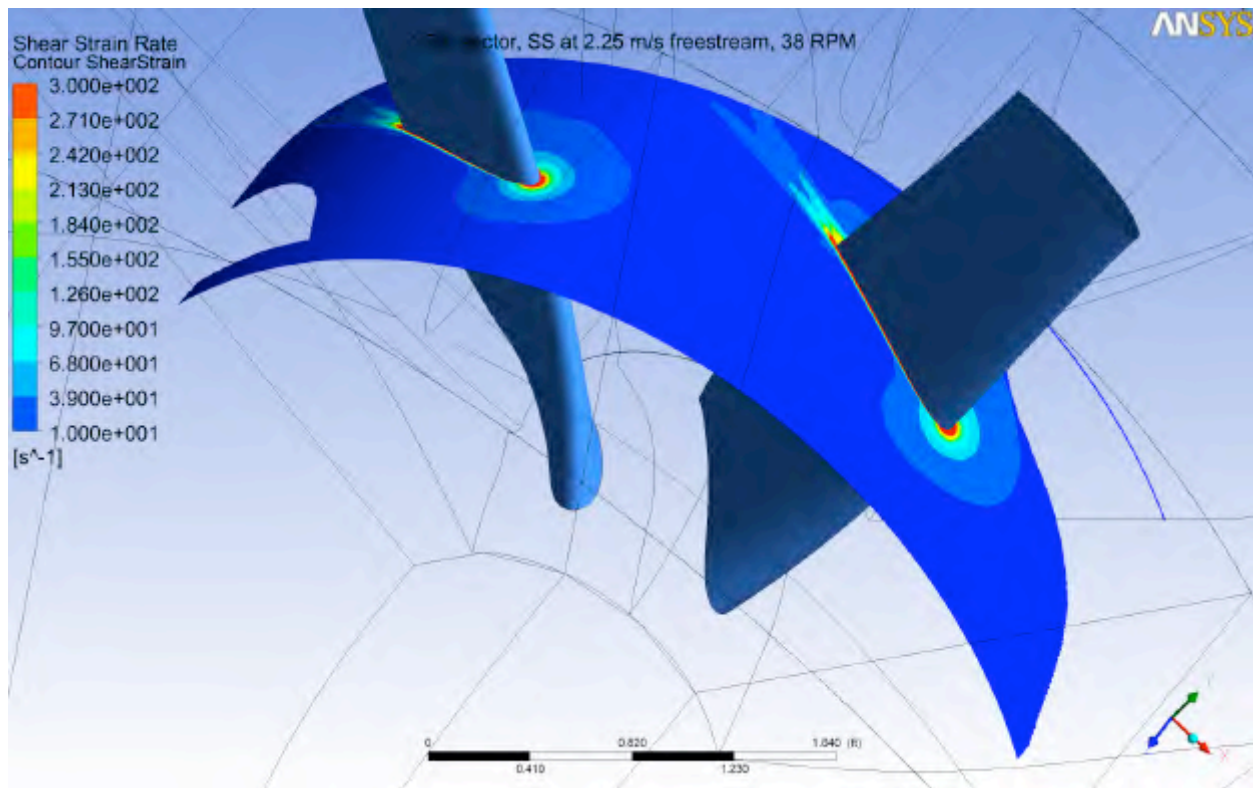


Figure 2.6-2. Shear Strain Rate at Rotor Pitch

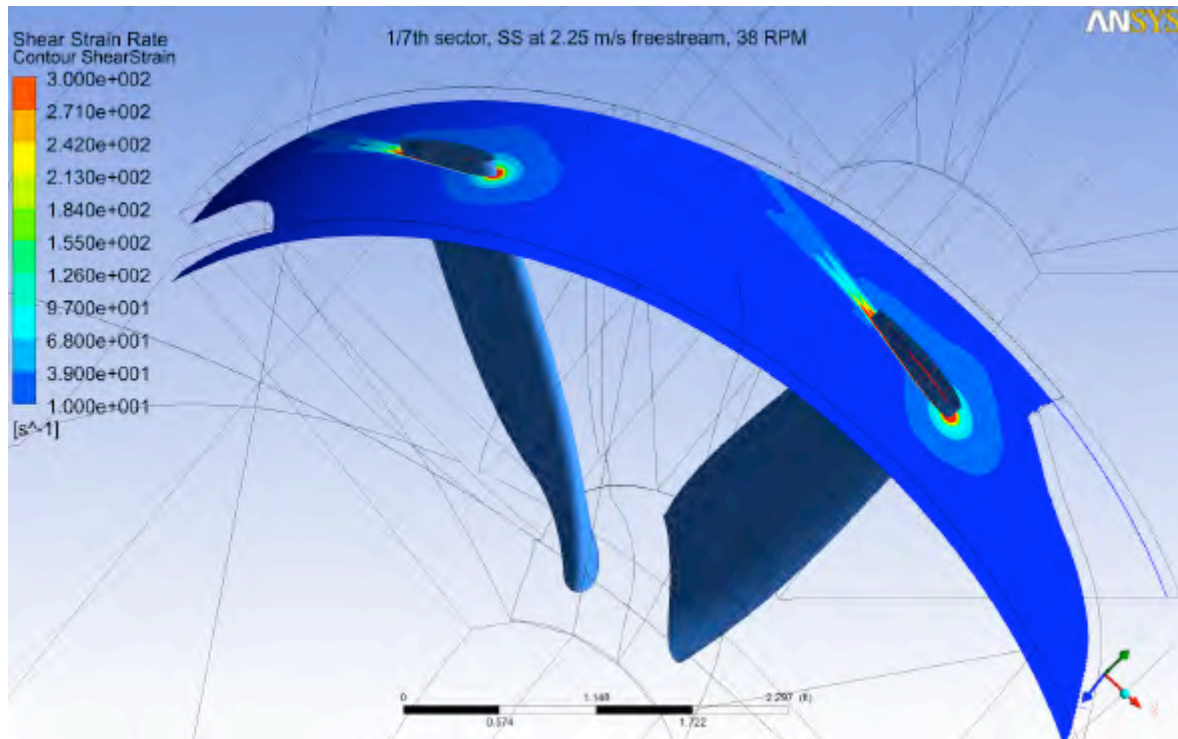
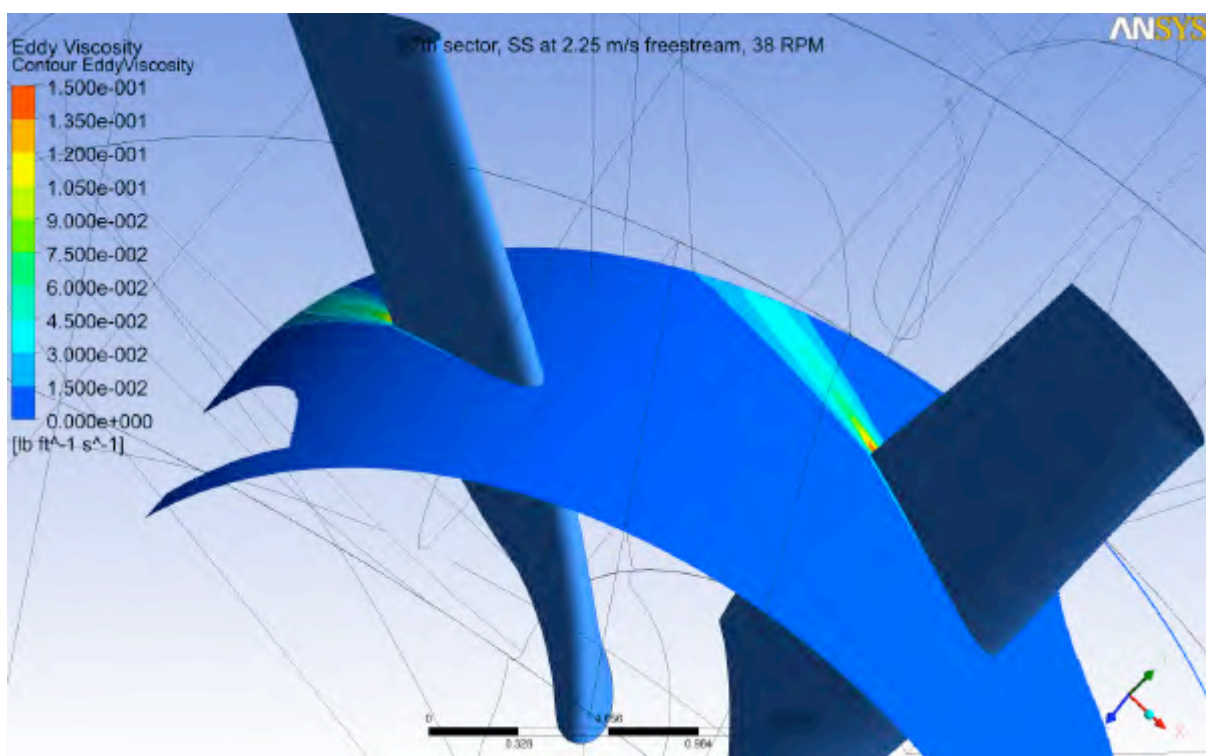
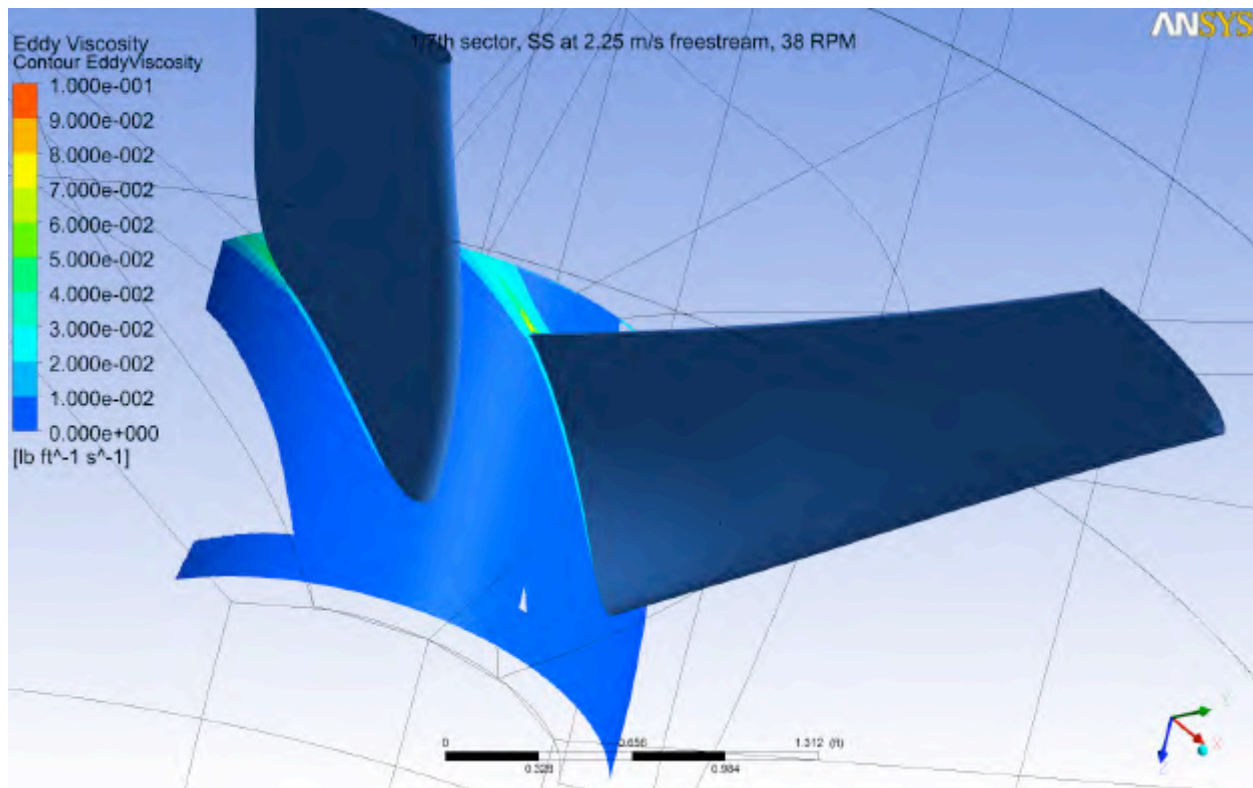


Figure 2.6-3. Shear Strain Rate at Rotor Tip



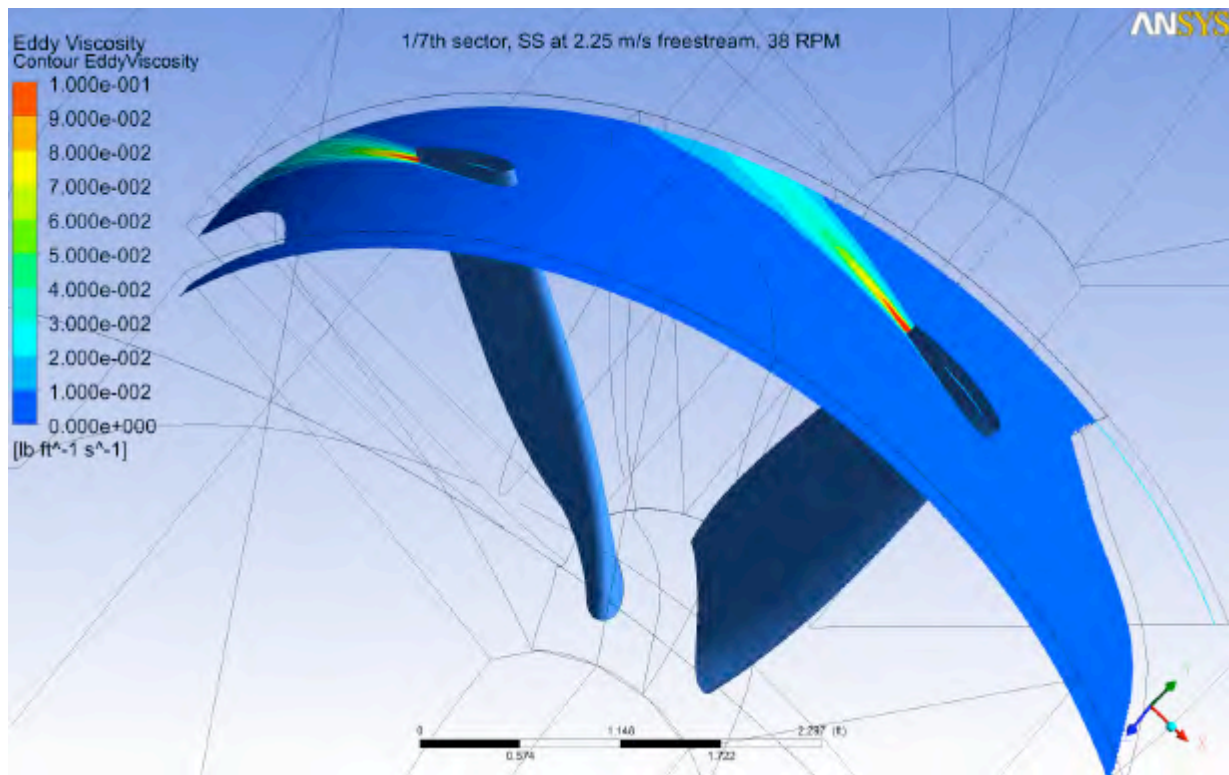


Figure 2.6-6. Eddy Viscosity at Rotor Tip

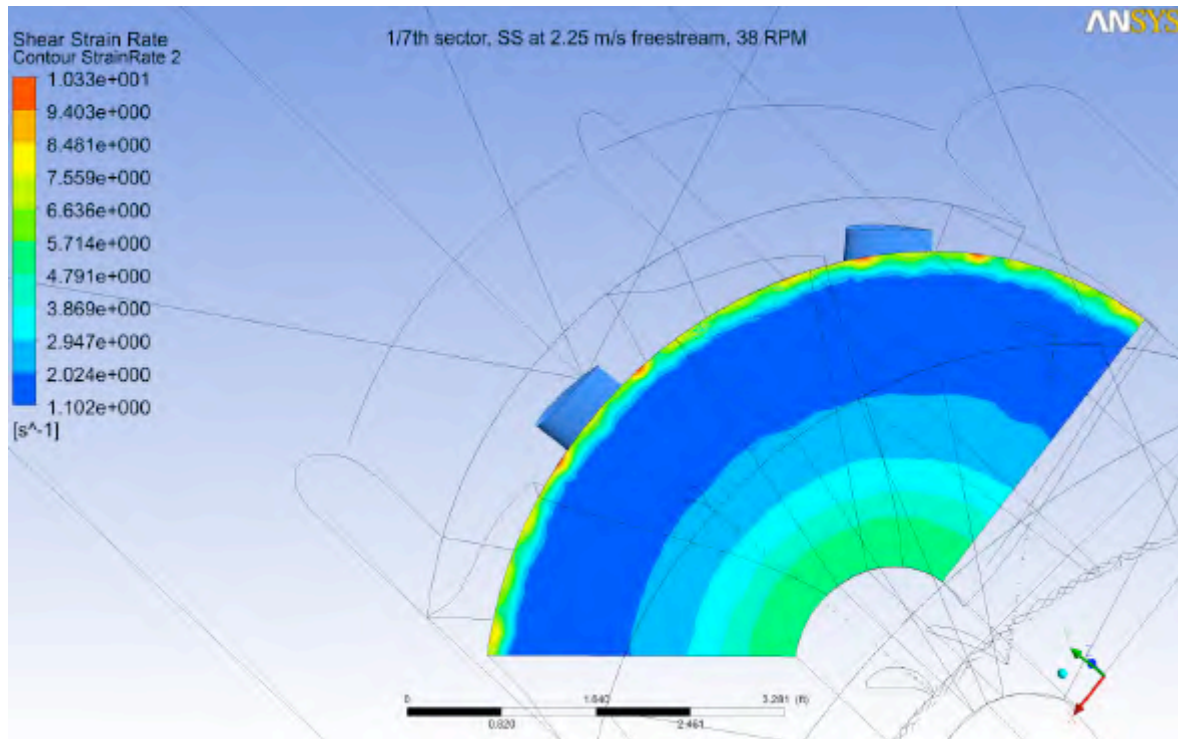


Figure 2.6-7. Distribution of Shear Strain Rate aft of Rotor

For cavitation to occur on the blades, the local pressure must be below the cavitation pressure of water. This number is typically 2.3kPa, but has variation with temperature as shown in Table 2.6-2. Cavitation will be briefly discussed, but the key point to make is that without a vapor, no cavitation exists. Consequently, if we select the highest threshold where vapor can form, and we exceed that value, then no cavitation can occur. Looking at Table 2.6.2, we will assume a maximum temperature of 100 °F and read the value of vapor pressure as 2.2 feet of H₂O, or 6.6 kPa (0.95 psia). Therefore, as long as no pressures below 0.95 psia, then we will not generate cavitation bubbles. As a note, the bubbles themselves are benign, the real damage from the bubbles comes when they collapse, as would happen when they encounter pressures above the vapor pressure, with higher values of pressure creating a faster, and more energetic collapse. The rate of collapse can create localized values of very high pressure, almost a local shock wave, which can be quite damaging at high collapse rates. Again, without generating the vapor bubble, there is no cavitation.

Elevation In Feet	Atmospheric Pressure In Feet of H ₂ O	H ₂ O Temperature In °F	Vapor Pressure In Feet of H ₂ O
0	34.0	50	0.41
500	33.3	60	0.59
1000	32.8	70	0.84
1500	32.2	80	1.17
2000	31.6	90	1.62
2500	31.0	100	2.20
3000	30.5	110	2.96
3500	29.8	120	3.95
4000	29.4	130	5.20
4500	28.7	140	6.78
5000	28.2	150	8.74
5500	27.8	160	11.20
6000	27.3	170	14.20
6500	26.6	180	17.85
7000	26.2	190	22.30
7500	25.7	200	27.60
8000	25.2	210	34.00
8500	24.8	220	41.45
9000	24.3	230	50.35
10000	23.4	240	60.75

Table 2.6-2. Vapor Pressure of Water

Figures 2.6-8 through 2.6-11 show the static pressure at 38 RPM at the tip, pitch, and hub of the device. There are very small, localized pressure pockets as high as 22 psig (36.7 psia STP) and as low as 12 psig in close proximity to the blade surfaces. In no case are we within an order of magnitude of 0.95 psia, therefore no cavitation will exist on the FFP 3 meter turbine at this operating condition.

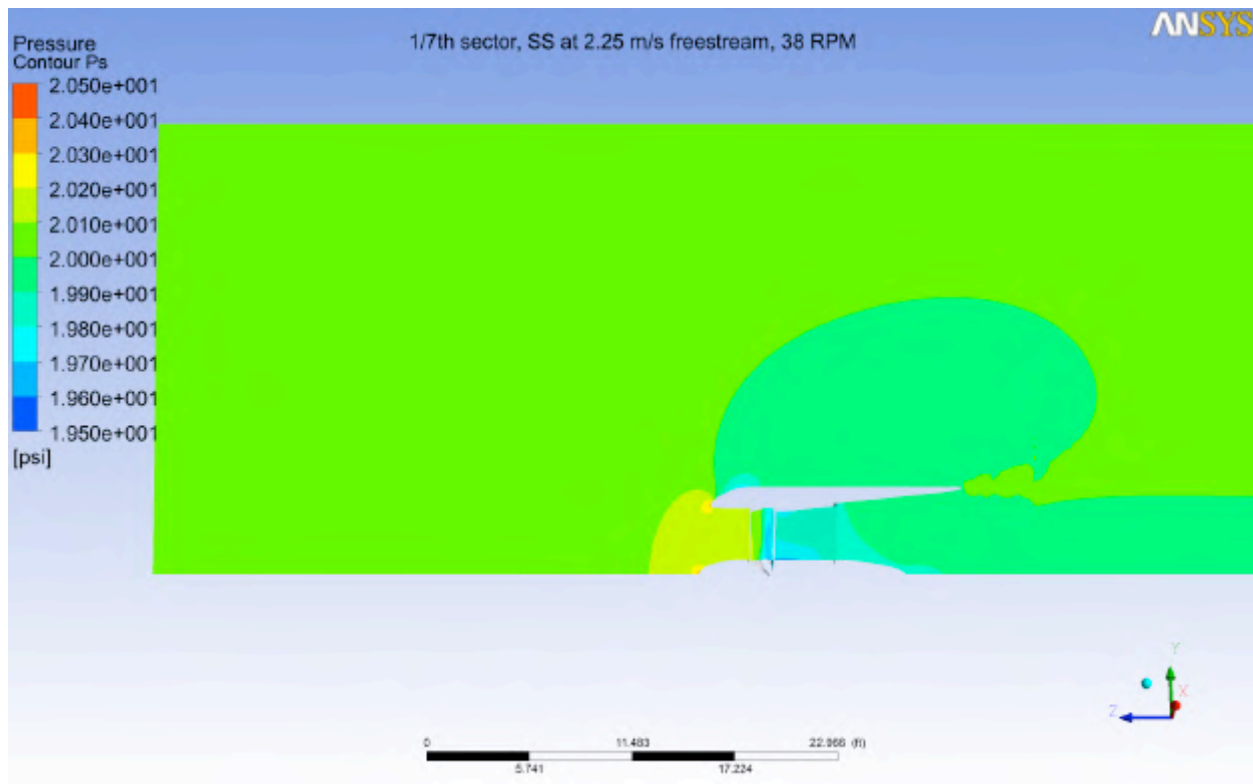


Figure 2.6-8. Static Pressure

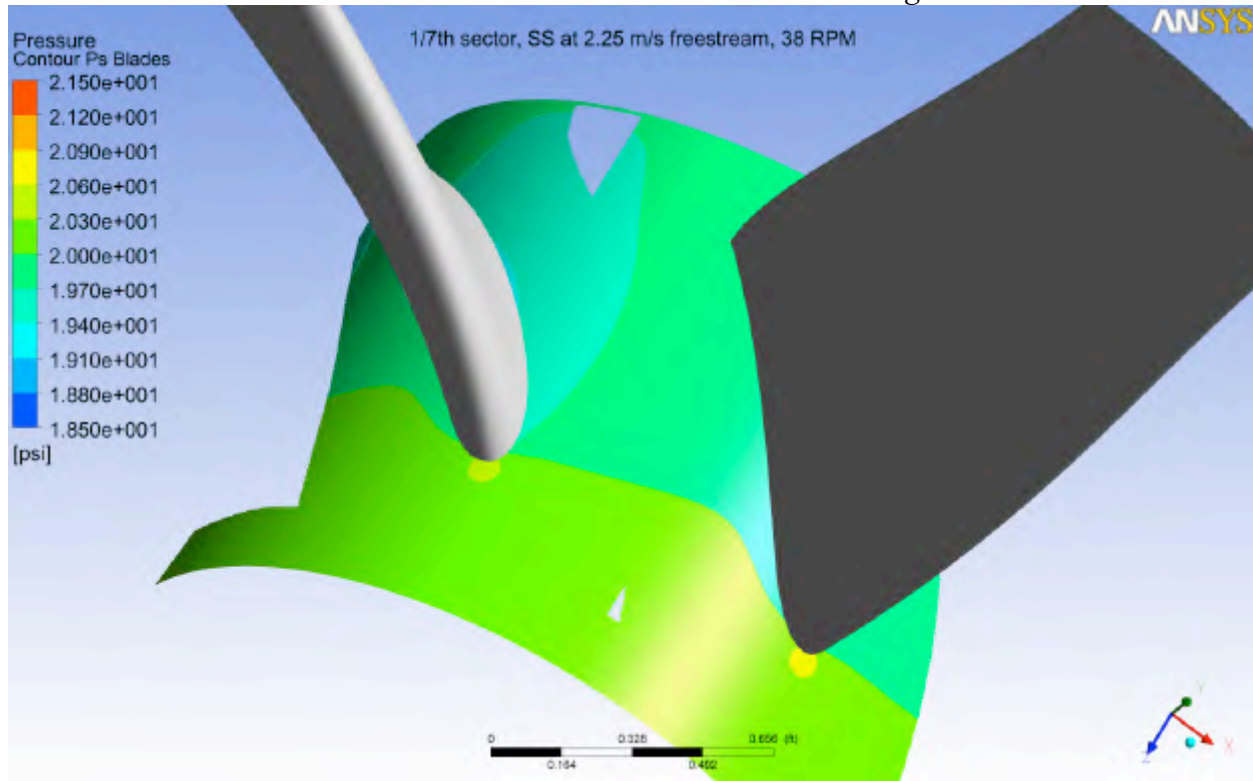


Figure 2.6-9. Pressure Contours, Hub

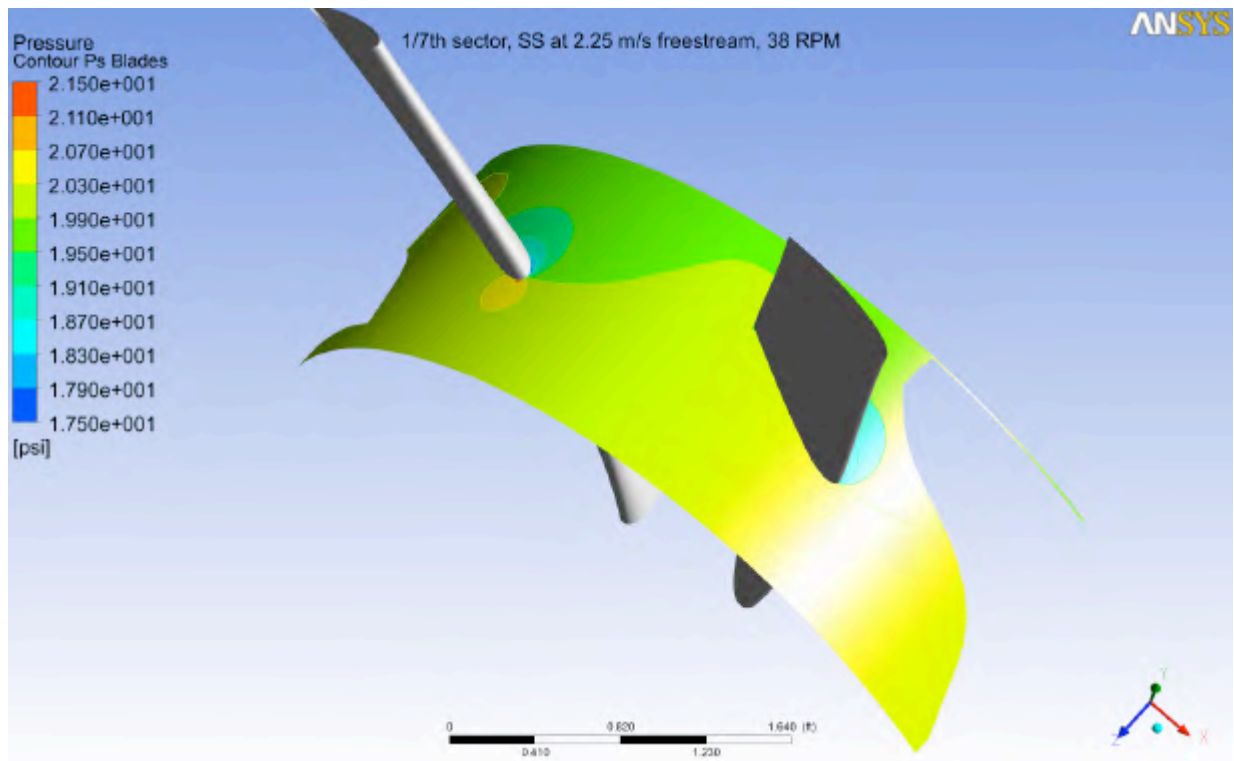


Figure 2.6-10. Pressure Contours, Pitch

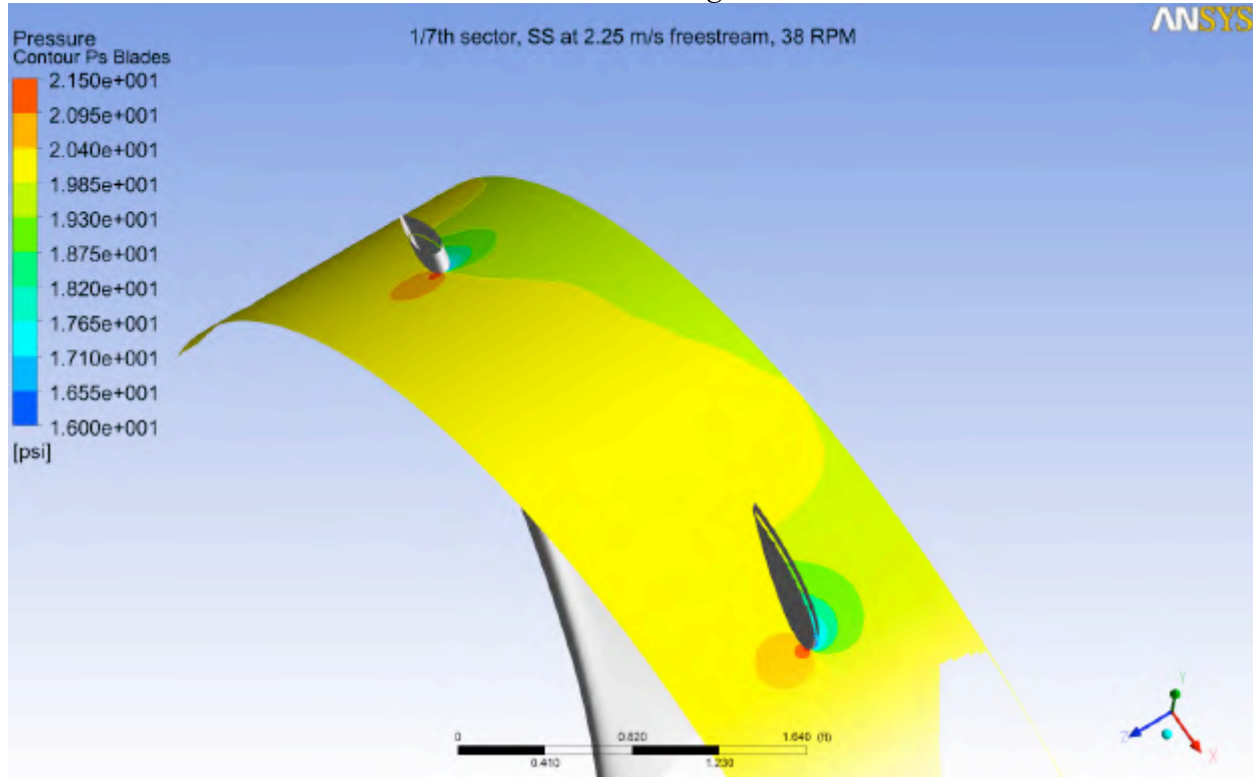


Figure 2.6-11. Pressure Contours, Tip

2.6(b) Shear Stress, Pressure Changes, Turbulence, and Cavitation at 54 RPM

This section reviews the results shown in Section 2.6(a), but at the higher speed of 54 RPM.

Figures 2.6-12 through 2.6-18 map the Shear Strain Rate and Eddy Viscosity near the ID of the turbine (hub), the radial centerline (pitch), and the OD of the blade (tip). These are illustrated on cylindrical slices at the tip, pitch, and hub, with two turbine blades shown for reference. The values very close to the blades will be ignored for the first level of calculation, because these are such a small percentage of the passage area.

To calculate shear stress as defined in Eq. 2.6.3, the terms for shear strain rate and eddy viscosity (turbulence) must be defined separately. At the hub, the predominant value is at or below a strain rate of 88/s, except for the immediate region near the blades where the value ranges from 166 – 400/s; the trailing edge (TE) wake has some isolated values of 127/s. At the pitch the majority of the flow is less than 88/s, with values up to 166 – 205/s in the LE (Leading Edge) vicinity, and a peak in excess of 400/s close to the blade surfaces; the TE wake is predominantly 88/s, but has some isolated values of 127/s. The tip region has values similar to the pitch, but with a larger percentage of the passage at the lower value due to the larger blade spacing.

Behind the turbine, in the bulk flow, the values of shear strain rate are very low, under 9/s as shown in Figure 2.6-18.

The other term used for calculating the shear stress is the eddy viscosity, μ_t . The blade passage distribution of eddy viscosity is shown in Figures 2.7.x – 2.7.x, and, similar to the shear strain rate, the values away from the blades are low. Values at the hub are predominantly under 0.010 lb/(ft * s), with the bulk of the (small) wake being 0.03 lb/(ft * s) or less. For the pitch, the values are predominantly under 0.010 lb/(ft * s), with the bulk of the wake being 0.03 lb/(ft * s) or less. For the tip the values are predominantly under 0.01 lb/(ft * s), with the bulk of the wake being 0.03 lb/(ft * s) or less.

[CONTINUED ON NEXT PAGE]

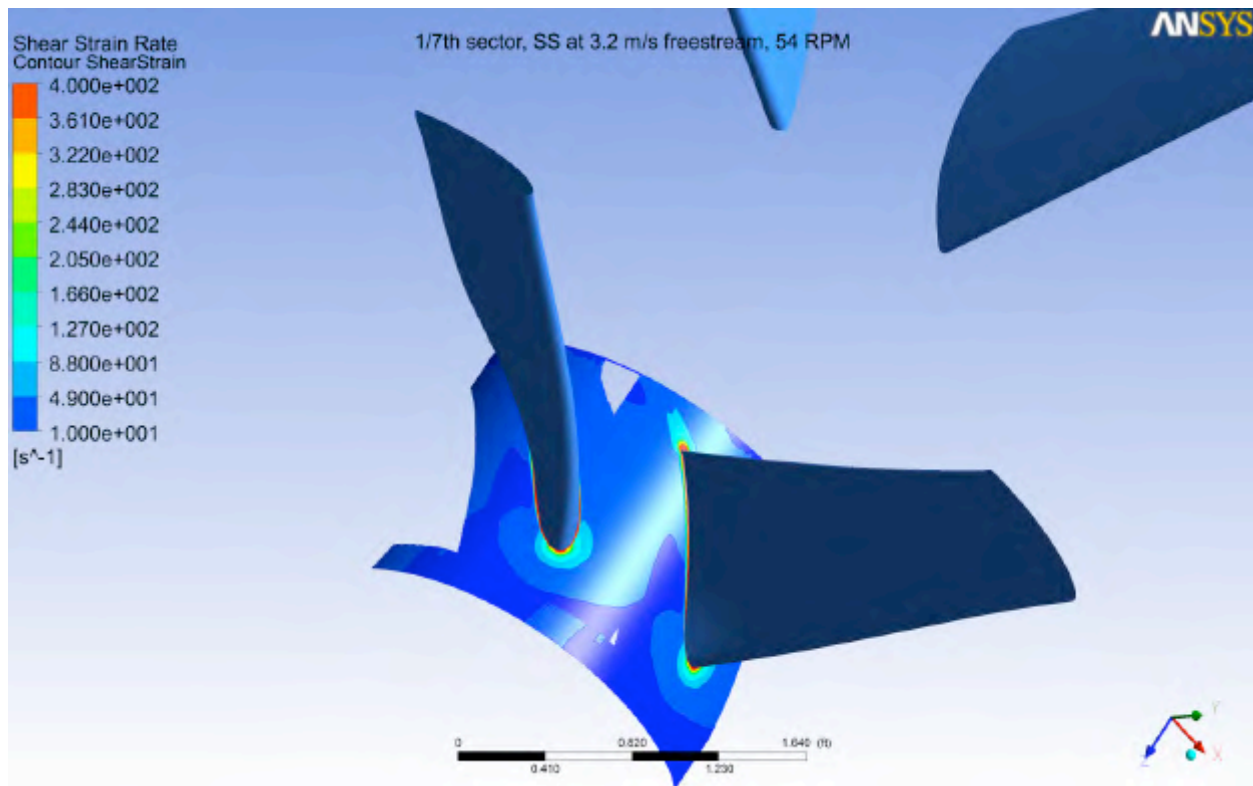


Figure 2.6-12. Shear Strain Rate at Rotor Hub

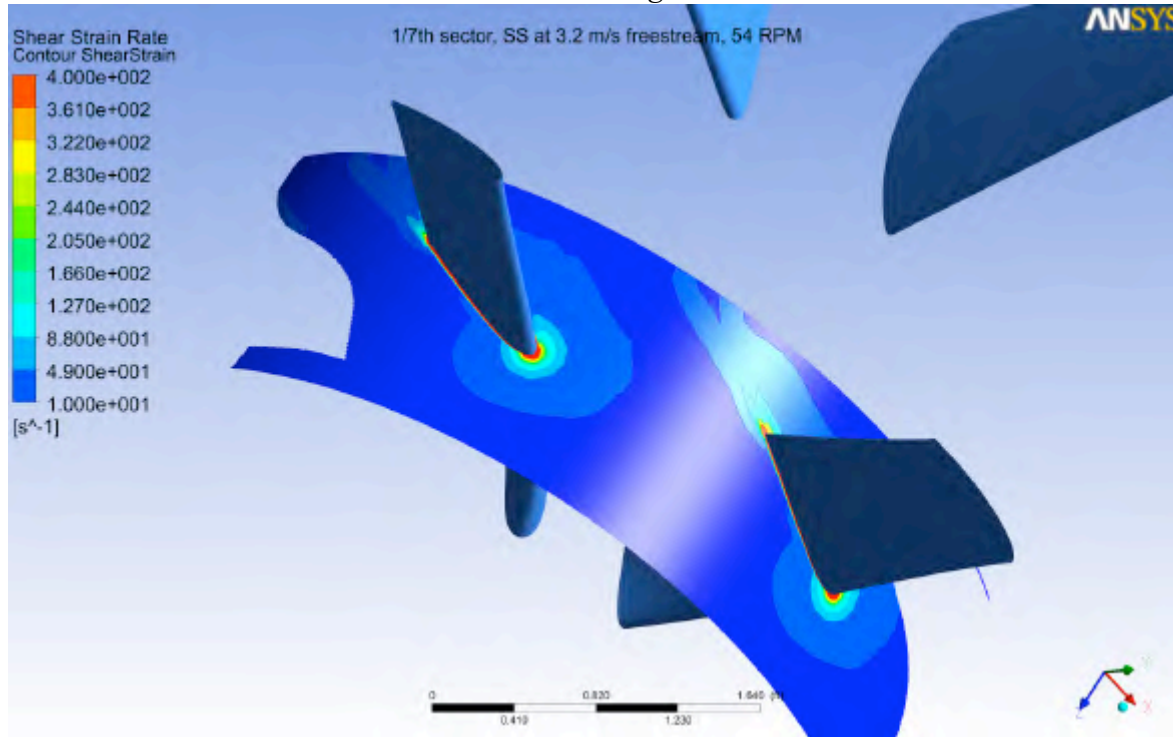


Figure 2.6-13. Shear Strain Rate at Rotor Pitch

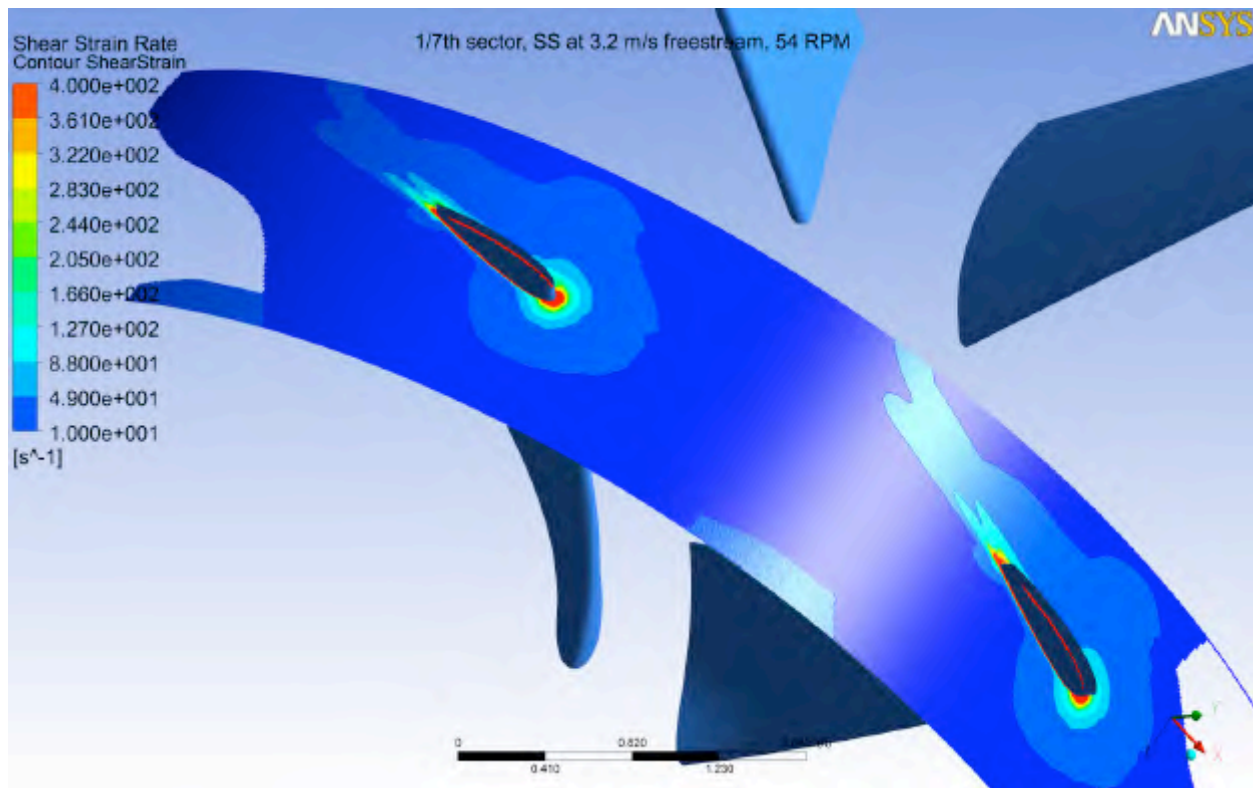


Figure 2.6-14. Shear Strain Rate at Rotor Tip

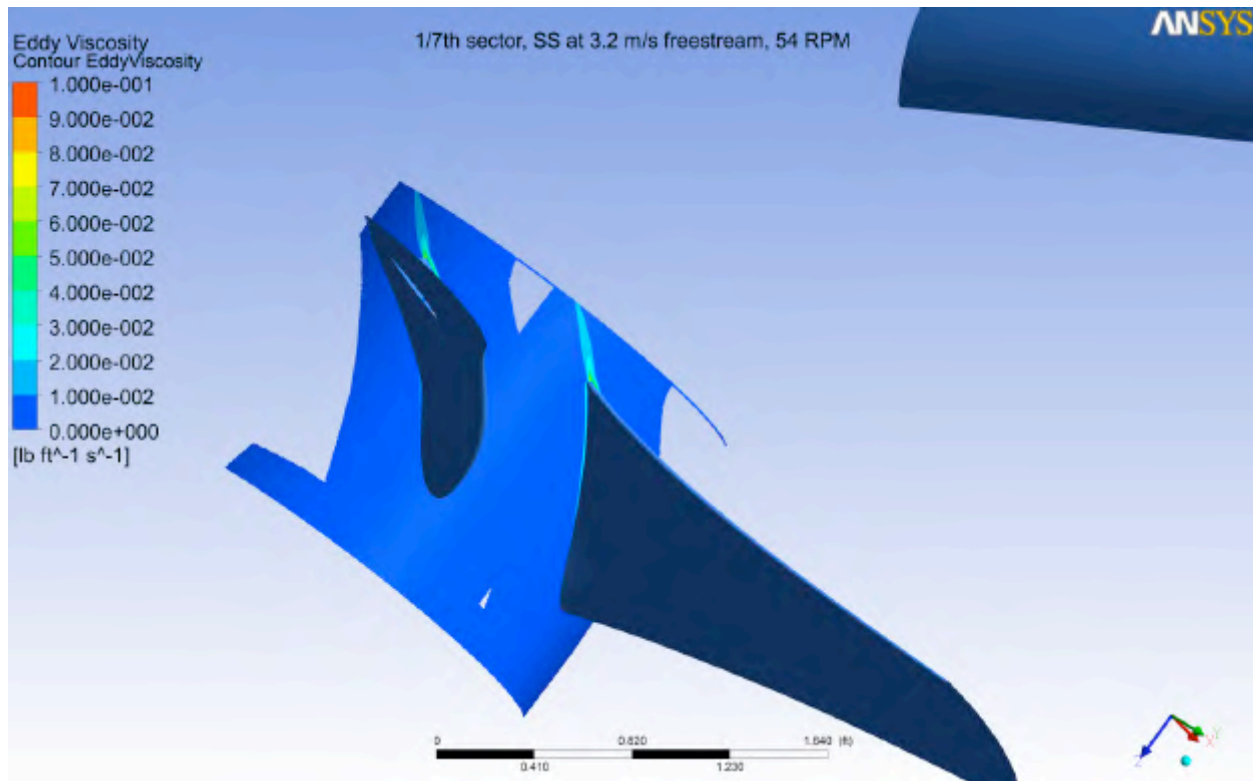


Figure 2.6-15. Eddy Viscosity at Rotor Hub

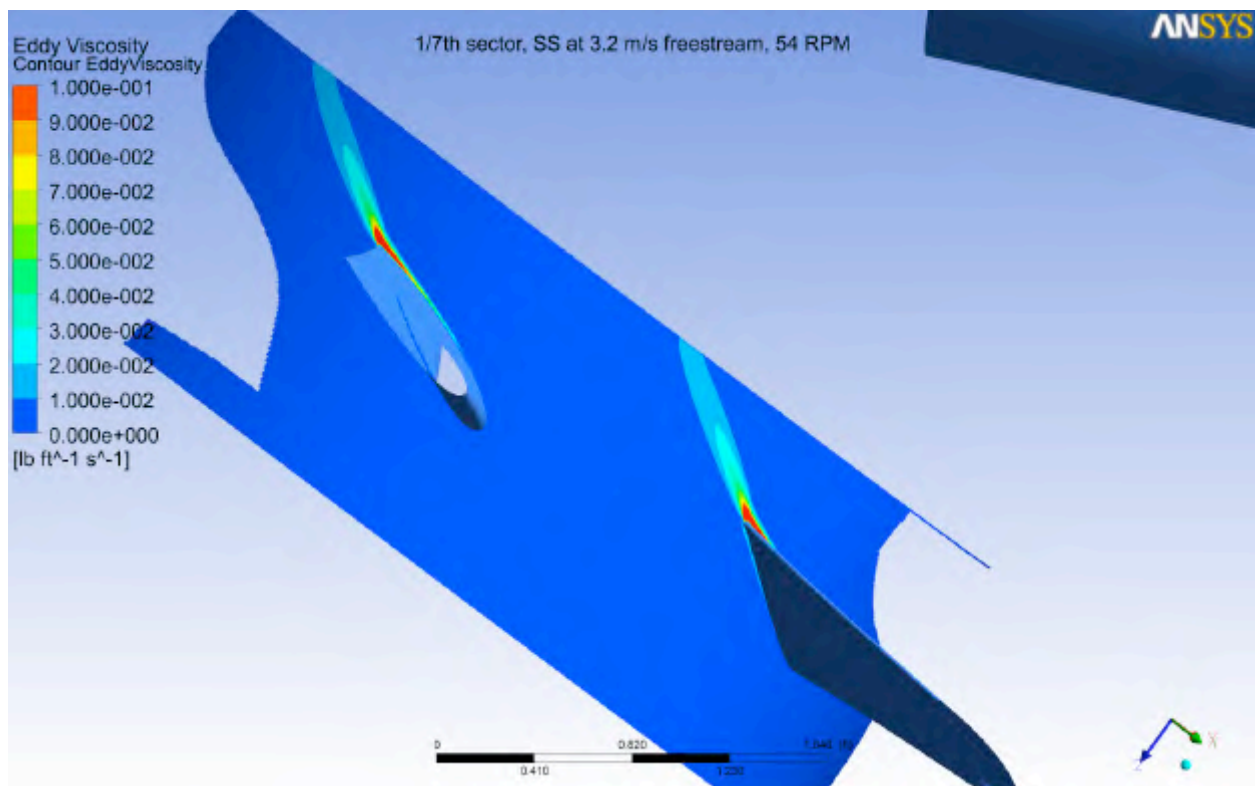


Figure 2.6-16. Eddy Viscosity at Rotor Pitch

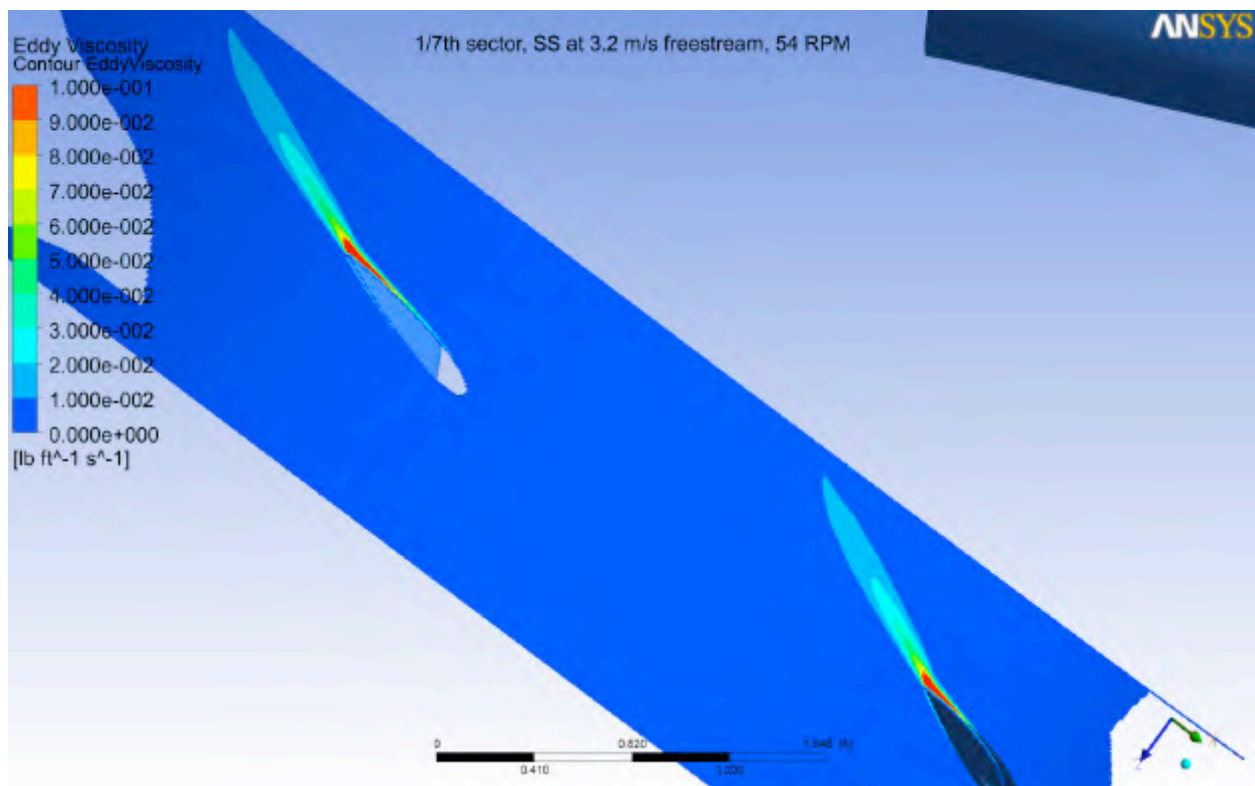


Figure 2.6-17. Eddy Viscosity at Rotor Tip

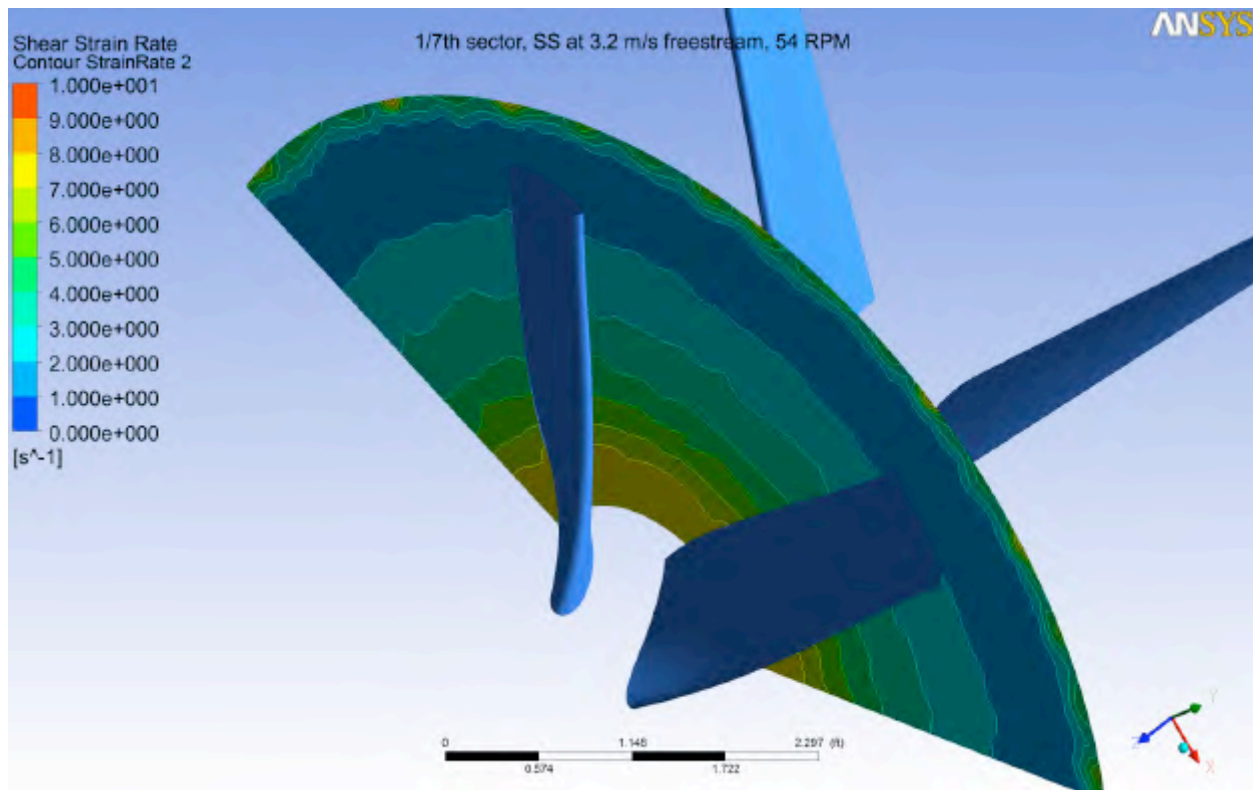


Figure 2.6-18. Distribution of Shear Strain Rate aft of Rotor

Summarizing the average and peak shear stresses at both 38 RPM and 54 RPM, as shown in Table 2.6-3, we see average shear stresses under 10 Pa (N/m^2), with peaks in very small regions of 30 – 45 Pa. This information will be provided as reference in Fish Passage Studies.

[CONTINUED ON NEXT PAGE]

38 RPM, 2.25 m/s				54 RPM, 3.3 m/s			
	Epsdot, 1/s	mut, lbm/(ft*s)	Tau, psi		Epsdot, 1/s	mut, lbm/(ft*s)	Tau, psi
HUB							
Inlet, Avg.	20	0.01	4.606E-05	0.32	88	0.01	2.027E-04
Inlet, High	60	0.01	1.382E-04	0.95	166	0.01	3.823E-04
Wake	80	0.04	7.022E-04	4.84	127	0.03	8.406E-04
Peak	200	0.07	3.050E-03	21.03	400	0.03	2.648E-03
Aft, bulk	10	-----	1.450E-06	0.01	9	-----	1.305E-06
PITCH							
Inlet, Avg.	39	0.015	1.319E-04	0.91	88	0.01	2.027E-04
Inlet, High	97	0.015	3.281E-04	2.26	205	0.01	4.721E-04
Wake	97	0.06	1.270E-03	8.76	127	0.03	8.406E-04
Peak	300	0.1	6.518E-03	44.94	400	0.05	4.374E-03
Aft, bulk	10	-----	1.450E-06	0.01	9	-----	1.305E-06
TIP							
Inlet, Avg.	39	0.01	8.982E-05	0.62	88	0.01	2.027E-04
Inlet, High	97	0.01	2.234E-04	1.54	205	0.01	4.721E-04
Wake	97	0.06	1.270E-03	8.76	127	0.03	8.406E-04
Peak	300	0.1	6.518E-03	44.94	400	0.05	4.374E-03
Aft, bulk	10	-----	1.450E-06	0.01	9	-----	1.305E-06

Table 2.6-3. Summary of Shear Stress

Figures 2.6-19 through 2.6-22 show the static pressure at 54 RPM at the tip, pitch, and hub of the device. There are very small, localized pressure pockets as high as 24 psig (38.7 psia STP) and as low as 11.5 psig in close proximity to the blade surfaces. In no case are we within an order of magnitude of 0.95 psia, so no cavitation will exist on the FFP 3 meter turbine at this operating condition.

[CONTINUED ON NEXT PAGE]

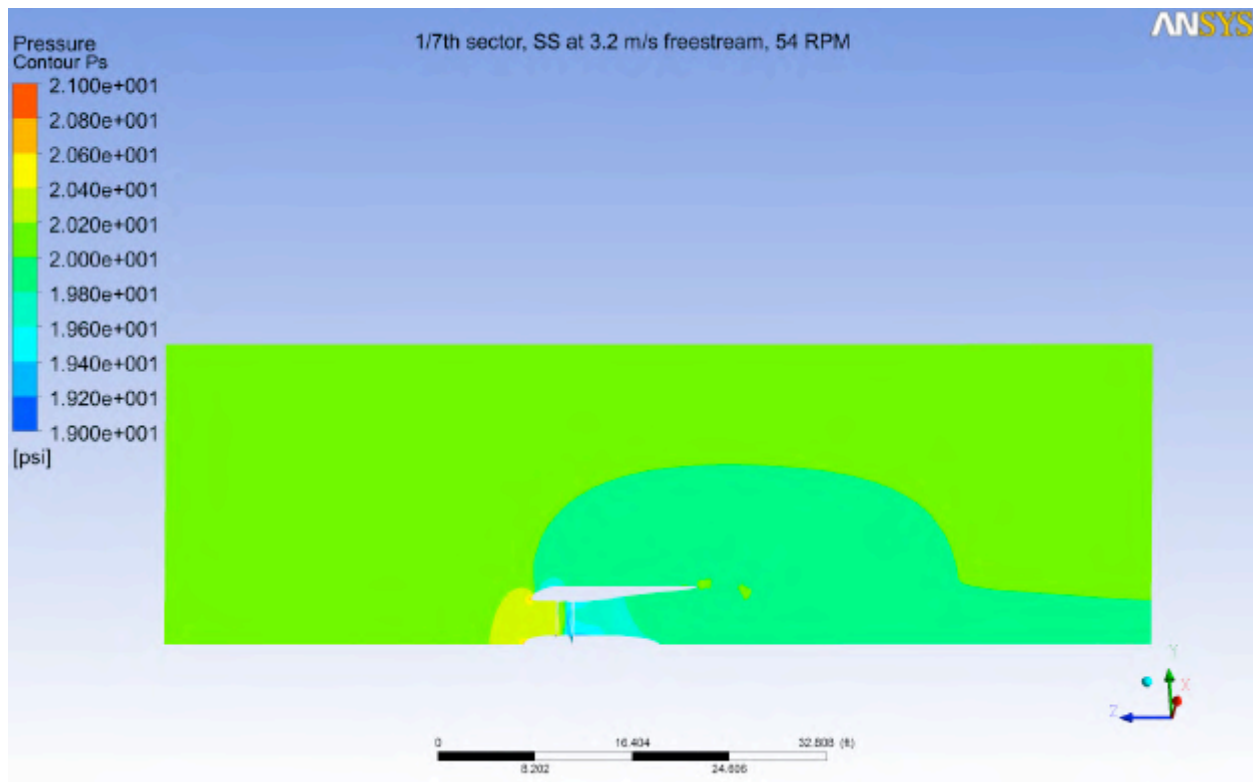


Figure 2.6-19. Static Pressure

[CONTINUED ON NEXT PAGE]

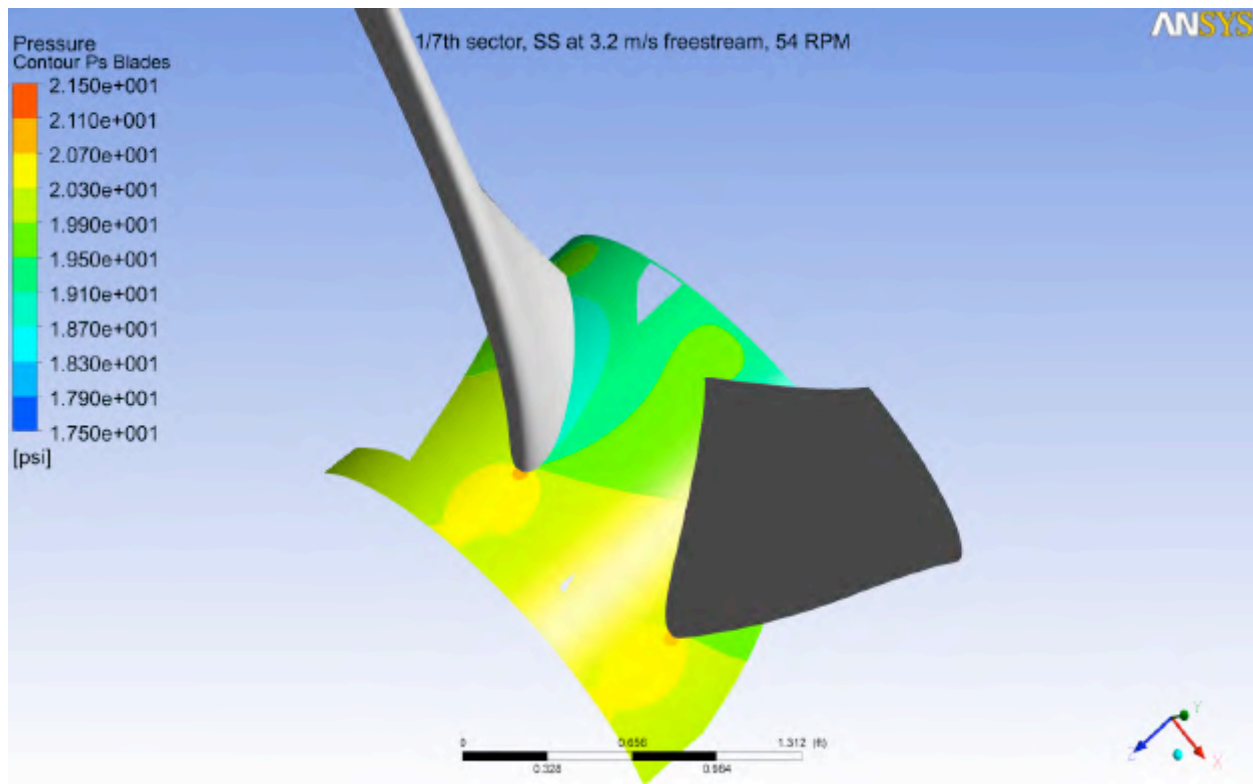


Figure 2.6-20. Pressure Contours, Hub

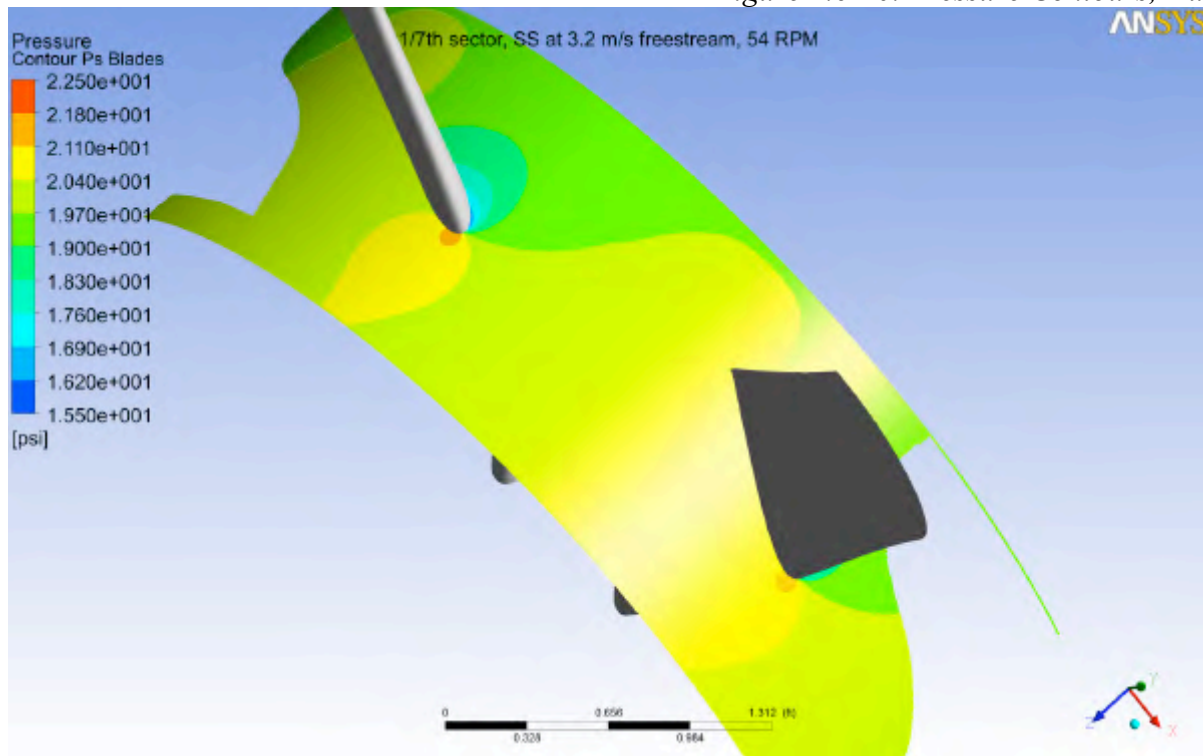


Figure 2.6-21. Pressure Contours, Pitch

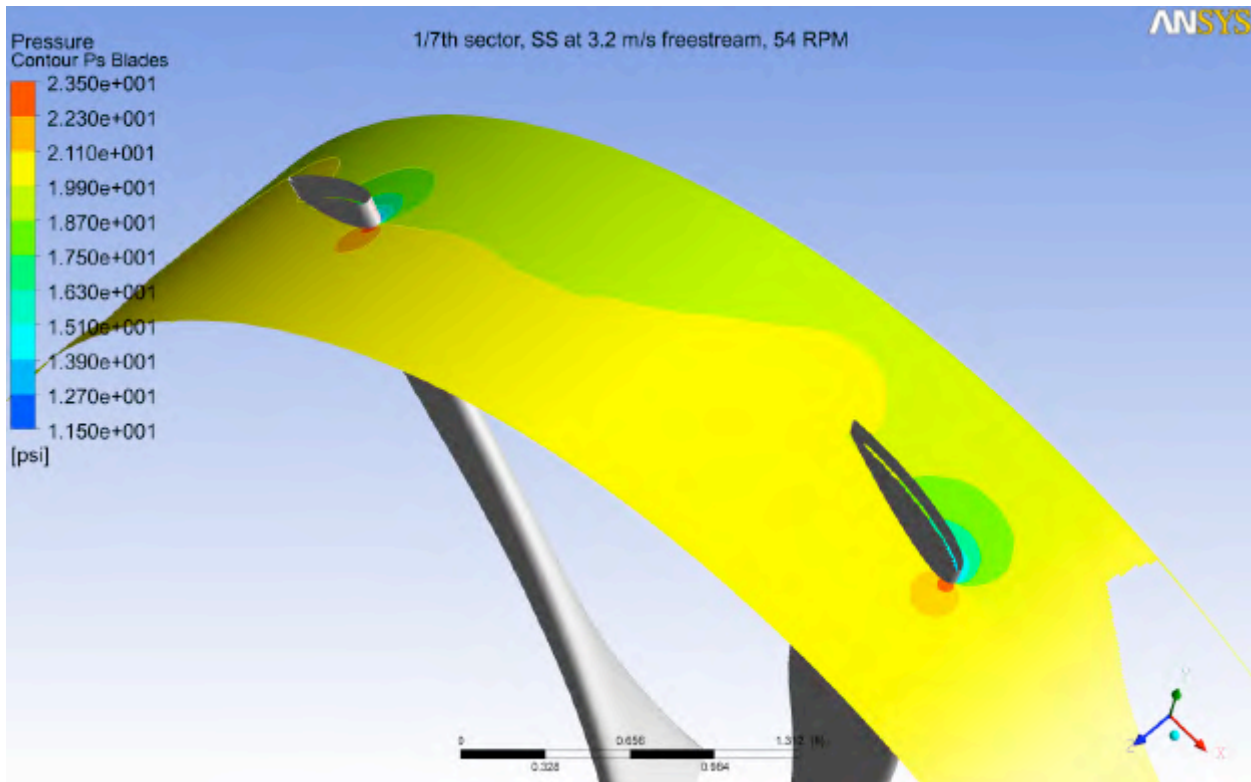


Figure 2.6-22. Pressure Contours, Tip

2.7 Comparison of River Testing Results to CFD Modeling

During the summer of 2011, FFP deployed the 3 meter turbine on the Mississippi River on our floating mount (FM), with the details supplied in Section 4.1 Damaged Turbine and Debris Risk Study, of the July 29, 2011 Fourth Study Report. Some of the data is presented in normalized corrected form in Figure 2.7-1 as Normalized Power versus River Velocity. The raw field data includes generator losses, frictional losses, power transmission losses, and cooling flow losses. Hydrodynamic Power predicted by the CFD modeling is the sum of the electrical output power and the losses within the generator. Using 90% efficiency as a reasonable correction factor for the measured data, Figure 2.7-1 results.

FFP has concluded that the Hydrodynamic Power calculated from test data is at least as good as the value predicted by the CFD model, and more importantly further validates the CFD model for use in the Hydraulic Study and shear pressure predictions for the Fish Entrainment Study.

[CONTINUED ON NEXT PAGE]

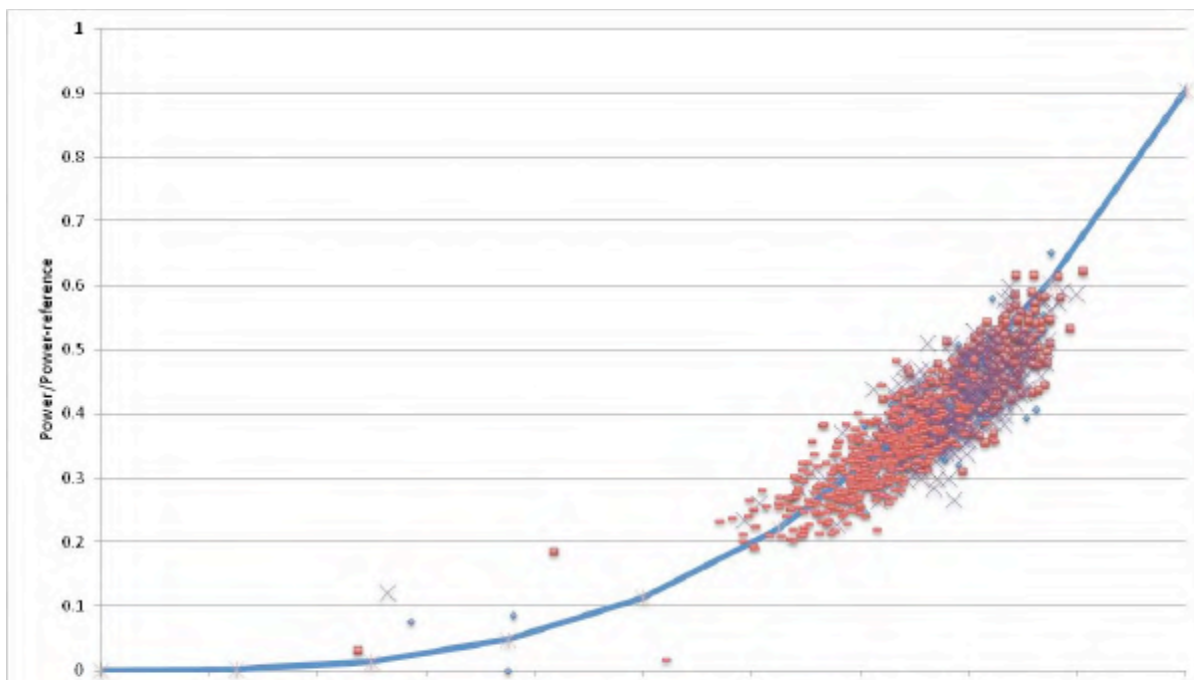


Figure 2.7-1, Normalized Hydraulic Power from Floating Mount Corrected to 90% Efficiency versus the CFD model prediction.

2.8 Update on National Efforts in Hydrokinetic Modeling

In FFP's Second Quarterly Report, dated August 2, 2010, Section 2.1 of the Hydraulic Study outlined the U.S. Department of Energy (DoE) funding provided to the National Labs for technology and market acceleration in the field of marine hydrokinetics. Below are updates on some of the progress and approaches under development.

2.8(a) Sandia National Laboratory

Sandia National Laboratories (SNL) was funded to study extractable energy, overall energy extraction impacts, near and far field flow field changes, and sediment transport with respect to evaluating environmental impacts for marine hydrokinetic (MHK) development in the United States. Some of their efforts encompass hydrokinetic (HK) modeling on the Mississippi River as a case study, and this includes use of site and river data supplied by FFP. A potential benefit to the DoE and to FFP is the ability to compare and share modeling and test results.

One of SNL's efforts was to develop HK modeling capability in an existing modeling tool. SNL employs the Environmental Fluid Dynamics Code (EFDC) used by the United States Environmental Protection Agency (EPA) as the basis of the modeling code and modified this for incorporating HK turbines in any desired installation configuration. EFDC is a quasi-3D modeling tool. References for EFDC and EFDC-SNL modeling results are included in the Literature References at the end of this Section, and efforts are ongoing with hydraulic and sedimentation modeling within EFDC-SNL, including environmental impact prediction, turbine

array optimization, and energy extraction. In August 2011, FFP attended a two-day training class on EFDC-SNL, and believes that this tool will be beneficial for FFP's inclusion in our modeling efforts. Because this is a quasi-3D code, it fits between the 2D models (hydraulic and sedimentation) and the highly detailed 3D ANSYS CFX models (hydraulic). With the 3D capabilities of EFDC-SNL, FFP can evaluate vertical placement optimization of many turbines without the averaging of 2D codes without the high number of elements required in ANSYS CFX. It also demonstrates attention to wake physics and verifying the wake modeling employed in the code, and successful capture of this important flow highly influences turbine placement and river hydraulics. FFP welcomes stakeholder responses to our proposal for including EFDC-SNL as another hydraulic and sedimentation modeling tool in all of FFP's hydraulic studies.

2.8(b) Pacific Northwest National Laboratory

Pacific Northwest National Laboratory (PNNL) is funded with a particular emphasis on tidal hydrokinetics. In its Fiscal Year 2011 Progress Report summary, Yang and Wang describe the use of the 3D FVCOM (Finite Volume Coastal Ocean Manual) for tidal HK modeling. FVCOM was developed by the University of Massachusetts, Dartmouth and the Woods Hole Oceanographic Institute.

With the particular emphasis of these studies on tidal applications in bays and sounds, there was a focus on the drag effects of a large number of turbines inhibiting flow and flushing time, none of which is pertinent to a constant flow river HK system. However, tidal and riverine systems both deal with extracting maximum energy per device, and determining an optimum combination of turbine placement and turbine quantity to achieve the desired tradeoffs in flow through the turbines (energy) and excessive turbine density causing near-field velocity reduction.

Of particular interest to FFP were the studies examining energy extraction versus turbine number using 1D, 2D, and 3D modeling. FFP's hydraulic modeling studies will require performing similar calculations and comparisons, but the results presented in the paper referenced provide optimism for the synergy between the tools. The 2D models used represent two methods, one a frictional loss on the bottom to simulate turbine energy extraction, and the other a more direct momentum deficit approach. Because both are depth averaged models, the results are similar (extractable power versus volume flux ratio), but comparing both methods is a useful validation, and does show that the momentum term can be applied to 2D codes in a more direct and intuitive way than converting to frictional equivalent values.

The 3D to 2D comparison concluded with the 3D analysis predicting less flow inhibition because the water has more flow options when encountering a turbine. In conjunction with lower flow restriction there was also less maximum power capacity, but the goal is not to remove maximum power at the expense of power per turbine. At the more representative conditions of high power per turbine, it appears that the 3D results still showed better power per unit of flow restriction, but agreement is reasonable between 3D and 2D. Understanding that 2D codes may over-predict the flow impact from turbines is a useful perspective to keep in mind. FFP will perform similar 3D to 2D result comparisons using our modeling tools, but having another reference is helpful.

Appendix 2-1

Induced Propeller Velocity Calculations

APPENDIX, Section 2, HYDRAULIC STUDY

2.1 Response to FERC's November 10, 2011 questions and requests – Appendix A, Comments on Responses to Additional Information Requested in our July 14, 2009 Letter

Induced Propeller Velocity Calculation

Propeller_Velocity.xmcd

November 14, 2011

Calculate induced velocity from ship propellers. Simplified, first order calcualtion only.

NOTES and ASSUMPTIONS:

This set of calculations is to determine first order wake velocity from a shallow draft ship on the Mississippi River. The vessels are flat bottom with an abrupt upturn at the rear for the propellers - regulations stipulate that the craft sit no lower than 9 ft below the water line (including the prop) {although it is not uncommon to have them be as low as 12 ft}. With the props sitting close to the surface (large plumes of wake in the air are common) and with the sharp upturn in front of the props, it is likely that they are operating inefficiently, but the level of efficiency can only be guessed at.

We will also assume that:

- Peak power is only used going upstream {fast travel or fighting a fast river current}.
- **Calculations are only valid for the power input** . Peak power is unlikely at low speeds and will thus give erroneous answers. The power input MUST be the one used at the given velocity (for example, high thrust at low V is not at peak power) - for low velocity use actual, not rated, power.
- Efficiency includes unrecovered swirl in the wake.
- Results below are for one propeller - assume that twin screw effects will be no different from approaching the results for one prop at a time.
- Prop exit velocity is averaged - i.e. assumes constant radial velocity distribution.

NOTES:

- On-line data indicates that typical thrust values for tugs are 20 - 32 lbf / HP (stationary bollard test).

$$\text{Thrust_factor} := 20 \frac{\text{lbf}}{\text{hp}} \quad \text{Assumed value of thrust per HP (including transmission losses and propeller efficiency).}$$

$$V_{\text{river}} := 3.5 \frac{\text{m}}{\text{s}} \quad \text{Velocity near the surface of the river. + is downstream direction.}$$

$$V_{\text{river}} = 7.8 \text{ mph}$$

$$V_{\text{ship}} := 12 \text{ mph} \quad \text{Ship velocity relative to water. (+ is against river flow direction; should be larger than } V_{\text{river}} \text{ if going upstream)}$$

$$V_{\text{ship}} = 5.36 \frac{\text{m}}{\text{s}}$$

$$V_{\text{abs}} := V_{\text{ship}} - V_{\text{river}} = 1.9 \frac{\text{m}}{\text{s}} \quad \text{Calculate Velocity relative to shore.}$$

$$V_{\text{abs}} = 4.2 \text{ mph}$$

$$D_{\text{prop}} := 6 \text{ ft} \quad \text{Prop diameter.}$$

$$HP_{\text{prop}} := 2000 \text{ hp} \quad \text{Shaft power to prop at speed of ship relative to water used. See NOTES, peak power will only be at peak velocity or with a very large drag (huge tow for example, which is not likely due to manoueverability concerns).}$$

$$RPM_{\text{prop}} := 500 \text{ rpm} \quad \text{Not used - reference only.}$$

$$\eta_{\text{prop}} := 0.4 \quad \text{Assumed prop efficiency at operating condition selected}$$

$$\rho_{\text{water}} := 62.4 \frac{\text{lb}}{\text{ft}^3}$$

$$A_{\text{prop}} := \frac{\pi}{4} \cdot D_{\text{prop}}^2 = 2.627 \text{ m}^2$$

$$C_t := \frac{1}{4} \cdot \frac{D_{\text{prop}}}{V_{\text{abs}}} \cdot \frac{V_{\text{abs}}^2}{\eta_{\text{prop}} \cdot \rho_{\text{water}}} = 4.24 \text{ m}^2 \text{ N}^{-1}$$

Increase in water speed across prop to get thrust value. (i.e. $A_{\text{prop}} \cdot C_t \cdot V_{\text{abs}}^2$ speed increase to ship). This approach assumes A_{prop} is constant (constant C_t at low V_{abs}).

CALCULATE:

$$dV_{prop_adjust} := \frac{\text{Thrust}}{\rho_{\text{water}} A_{\text{prop}} \cdot (V_{\text{ship}} + \text{Mod_value} \cdot dV_{\text{prop}})}$$

Increase in water speed across prop to get thrust value. (i.e. relative speed $\frac{V_{\text{prop}}}{V_{\text{ship}}}$ increase to ship). This approach assumes ALL mass flow is at propeller diameter (conservative).

$dV_{prop_adjust} = 11.8 \text{ mph}$

Check above - :

$$\text{error1} := \text{Thrust} - \left[\text{RHO}_{\text{wat}} \cdot \text{Aprop} \cdot \left(\text{V}_{\text{ship}} + \frac{dV_{\text{prop_adjust}}}{2} \right) \cdot dV_{\text{prop_adjust}} \right] = 12.534 \text{ N}$$

$$dV_{\text{prop_adjust_1}} := \frac{\text{Thrust_1}}{\text{RHO}_{\text{wat}} \cdot \text{Aprop} \cdot (\text{V}_{\text{ship}} + \text{Mod_value_1} \cdot dV_{\text{prop_1}})} = 7 \frac{\text{m}}{\text{s}}$$

$$dV_{\text{prop_adjust_1}} = 16.7 \text{ mph}$$

Check above - :

$$\text{error1_1} := \text{Thrust_1} - \left[\text{RHO}_{\text{wat}} \cdot \text{Aprop} \cdot \left(\text{V}_{\text{ship}} + \frac{dV_{\text{prop_adjust_1}}}{2} \right) \cdot dV_{\text{prop_adjust_1}} \right] = -10 \text{ N}$$

$$V_{\text{jet_rel}} := dV_{\text{prop_adjust}} = 5.29 \frac{\text{m}}{\text{s}}$$

Velocity of jet relative to river velocity.

$$V_{\text{jet_rel}} = 11.8 \text{ mph}$$

$$V_{\text{jet_rel_1}} := dV_{\text{prop_adjust_1}} = 7.45 \frac{\text{m}}{\text{s}}$$

Velocity of jet relative to river velocity.

$$V_{\text{jet_rel_1}} = 16.7 \text{ mph}$$

$$M_{\text{dotprop}} := \text{Aprop} \cdot (\text{V}_{\text{ship}} + dV_{\text{prop}}) \cdot \text{RHO}_{\text{wat}} = 3.481 \times 10^4 \frac{\text{kg}}{\text{s}}$$

$$M_{\text{dotprop}} = 7.675 \times 10^4 \frac{\text{lb}}{\text{s}}$$

$$M_{\text{dotprop_1}} := \text{Aprop} \cdot (\text{V}_{\text{ship}} + dV_{\text{prop_1}}) \cdot \text{RHO}_{\text{wat}} = 4.725 \times 10^4 \frac{\text{kg}}{\text{s}}$$

$$M_{\text{dotprop_1}} = 1.042 \times 10^5 \frac{\text{lb}}{\text{s}}$$

$$V_{\text{jet_abs}} := V_{\text{jet_rel}} + V_{\text{river}} = 8.8 \frac{\text{m}}{\text{s}}$$

$$V_{\text{jet_abs}} = 19.7 \text{ mph}$$

December 14, 2011
FILE: Drag_Blocked_turb_inlet.xmcd

Assumes room temperature H₂O

INPUT

Input reference water velocity desired for calculation.

$$V_{\text{wat}} = \frac{2.25 \text{ m}}{\text{s}} \quad V_{\text{wat}} = 5.033 \text{ m/s} \quad V_{\text{wat}} = \frac{7.382 \text{ ft}}{\text{s}}$$

Input expected Cd for rough cylindrical body (i.e. debris) at Red (use Red below).

N_debris = 9 Number of pieces of debris (or equivalent debris) at effective length and diameter of reference body.

Cd_debris = 1.0 up to about 2×10^5 , but changes with roughness.

Dout = 3 in

Length = 2.5 m For 1 piece of debris - multiply results later for # of pieces.

$$A_{\text{front}} = (D_{\text{out}}) \text{Length} = 0.19 \text{ m}^2$$

$$A_{\text{front}} = 0.19 \text{ m}^2 \quad A_{\text{front}} = 2.051 \text{ ft}^2 \quad A_{\text{front}} = 295.276 \text{ in}^2$$

$$A_{\text{front_turb}} = \frac{\pi}{4} (2.35 \text{ m})^2 = 4.337 \text{ m}^2 \quad A_{\text{front_turb}} = 6.723 \times 10^3 \text{ in}^2$$

$$A_{\text{all_debris}} = 1937 \text{ in}^2 \quad \text{Area of debris across turbine inlet (from SolidWorks)}$$

PROPERTIES

$$C_{\text{Pwat}} = 1.00 \frac{\text{BTU}}{\text{lb R}}$$

$$\rho_{\text{H2O}} = 62.1 \frac{\text{lb}}{\text{ft}^3} \quad \rho_{\text{H2O}} = 0.036 \frac{\text{lb}}{\text{in}^3}$$

$$\mu_{\text{wat}} = 1.0 \times 10^{-3} \text{ Pa s} \quad \mu_{\text{wat}} = 2.089 \times 10^{-5} \frac{\text{lbf}}{\text{ft}^2 \text{ s}}$$

CALCULATE:

$$q = 0.5 \rho_{\text{H2O}} V_{\text{wat}}^2 \quad \text{For actual water velocity.}$$

$$q = 0.365 \text{ psi}$$

$$Re = \frac{\rho_{\text{H2O}} V_{\text{wat}} D_{\text{out}}}{\mu_{\text{wat}}} = 1.705 \times 10^5$$

$$\text{Drag_frontal_debris_1} = A_{\text{front}} q C_d \text{debris} \quad \text{Drag from 1 piece of debris}$$

$$\text{Drag_frontal_debris_1} = 107.834 \text{ lb} \quad \text{Drag_frontal_debris_1} = 479.67 \text{ N}$$

$$\text{Drag_debris_all} = \text{Drag_frontal_debris_1} N_{\text{debris}} = 971 \text{ lbf}$$

$$\text{Area_ratio_blocked} = \frac{A_{\text{all_debris}}}{A_{\text{front_turb}}} = 0.288$$

Literature References

Theodorsen, T., 1959. *The Theory of Propellers, IV, Thrust, energy, and efficiency formulas for single and dual-rotating propellers with ideal circulation distribution*, NACA Report L4J12, 1944.

US Army Corps of Engineers, US Army Engineering District, *New Orleans, FILE NO: H-5-55630, Mississippi River Low Water Reference Plane and 1950, 1973, 1983, 1997 High Water, Black Hawk, LA to Head of Passes, LA*. (Published Graphs)

Cada, G., Carlson, T., et. al., *Exploring the Role of Shear Stress and Severe Turbulence in Downstream Fish Passage*, Voith Hydro, Inc., 1997, Report No. 2677-0141, ORNL/CP-101532

Menter, F., Kuntz, M., Langtry, R., *Ten Years of Industrial Experience with the SST Turbulence Model*, Turbulence, Heat and Mass Transfer 4, 2003 Begell House, Inc.

Evans, J., Cavitation – A Largely Misunderstood Phenomenon, <http://pump-flo.com/pump-library/pump-library-archive/joe-evans,-phd/cavitation---a-largely-misunderstood-phenomenon.aspx>, Pump-Flo.

Tetra Tech, Inc., *The Environmental Fluid Dynamics Code User Manual*, US EPA Version 1.01, 2007.

James, Scott C.; Lefantzi, Sophia; Barco, Janet; Johnson, Erick; Roberts, Jesse D.; *Verifying marine-hydro-kinetic energy generation simulations using SNL-EFDC*, Oceans 2011 Conference Paper

S. C. James; J. D. Roberts; C. Jones, *Predictive Simulations of Near- and Far-field Influence of MHK Devices*, Ocean Science, 2010.

James, S.C., Shreshta, P.L., Roberts, J.D., *Noncohesive Sediment Transport Modeling with Multiple Size Classes*, ASCE Conf. Proc. doi:10.1061/40792(173)429 Impacts of Global Climate Change Proceedings of World Water and Environmental Resources Congress 2005

Yang, T., Wang, T., *Assessment of Energy Removal Impacts on Physical Systems: Development of MHK Module and Analysis of Effects on Hydrodynamics*, PNNL-20804 FY2011 Progress Report.

Chen, C., G. Cowles, and RC Beardsley, . *An unstructured grid, finite volume coastal ocean model: FVCOM User Manual, Second Edition*. SMAST/UMASSD Technical Report-06-0602, pp. 315, 2006.

APPENDIX 5

HYDRAULIC MODELING REPORT

HYDROKINETIC PROJECT – SITE 42



PREPARED BY:

FREE FLOW POWER CORPORATION

239 CAUSEWAY STREET, SUITE 300

BOSTON, MA 02114

SUBMITTED:

JULY 2012

HYDRAULIC MODELING REPORT

HYDROKINETIC PROJECT – SITE 42

TABLE OF CONTENTS

Section 1	Introduction	3
1.1	Purpose	3
Section 2	Data Collection	5
2.1	River Flow	5
2.2	Water Levels	5
2.3	Bathymetry	6
2.4	Velocity	7
2.4	Substrate	7
2.5	Digital Elevation Model (DEM)	8
Section 3	Modeling Approach	10
3.1	Overview	10
3.2	AdH Two-Dimensional Model	10
3.2(a)	Model Background	10
3.2(b)	Bed Topography	10
3.2(c)	Manning Roughness and Eddy Viscosity	11
3.2(d)	Boundary Conditions	12
3.2(e)	Computational Mesh	12
Section 4	Results	15
4.1	Flow Duration Analysis	15
4.2	Rating Curve	16
4.3	Flood Frequency Analysis	17
4.5	Water Surface Elevation	18
4.6	Depth-Averaged Velocity	21
	Upstream of River Mile 732	21
	Between River Miles 727-732	24
	Downstream of River Mile 727	26
Section 5	Literature Cited	29

LIST OF TABLES

Table 2-1. LWRP Elevations at Site 42	6
Table 3-1. Manning Roughness Used for Each Model Portion	11
Table 3-2. Boundary Conditions.....	12
Table 4-1. Maximum Velocities within Site 42.....	24

LIST OF FIGURES

Figure 1-1. Mississippi River Hydrokinetic Project, Site 42	4
Figure 2-1. Location of USGS Gauge at Site 42	5
Figure 2-2. Location of transect measurements at Site 42.....	7
Figure 2-3. Substrate Size Classes	8
Figure 2-4. Digital Elevation Model around Site 42.....	9
Figure 3-1. Distribution of Material Types at Site 42.....	11
Figure 3-2. Computational Mesh for Site 42	13
Figure 3-3. Closer View of the Computational Mesh for Site 42.....	14
Figure 4-1. Flow Duration Curve, Site 42	16
Figure 4-2. Rating Curve, Mississippi River Site 42	17
Figure 4-3. Peak Flood Flows at Site 42.....	18
Figure 4-4. Water Surface Profile of Mississippi River at Site 42	19
Figure 4-5. Water Depth Map of Mississippi River at Site 42, Q=155,300cfs	20
Figure 4-6. Water Depth Map of Mississippi River at Site 42, Q=400,000cfs	20
Figure 4-7. Water Depth Map of Mississippi River at Site 42, Q=800,000cfs	21
Figure 4-8. Velocities at Site 42 Upstream of River Mile 732, Q=155,300cfs	22
Figure 4-9. Velocities at Site 42 Upstream of River Mile 732, Q=400,000cfs	23
Figure 4-10. Velocities at Site 42 Upstream of River Mile 732, Q=800,000cfs	23
Figure 4-11. Velocities at Site 42 between River Mile 727-732, Q=155,300cfs	25
Figure 4-12. Velocities at Site 42 between River Mile 727-732, Q=400,000cfs	25
Figure 4-13. Velocities at Site 42 between River Mile 727-732, Q=800,000cfs	26
Figure 4-14. Velocities at Site 42 Downstream of River Mile 727, Q=155,300cfs	27
Figure 4-15. Velocities at Site 42 Downstream of River Mile 727, Q=400,000cfs	27
Figure 4-16. Velocities at Site 42 Downstream of River Mile 727, Q=800,000cfs	28

Section 1 Introduction

1.1 Purpose

Hydraulic modeling was conducted in support of the Federal Energy Regulatory Commission (FERC) licensing study plan for FFP's hydrokinetic projects on the Mississippi River. The hydrokinetic turbines need to be located at places with reliable higher velocities to optimize the utilization of the energy potential of the waterway. Part of the study plan is to estimate potential localized changes in velocity magnitude, direction, and water surface elevations due to the hydrokinetic projects, and determine the significance, or insignificance, of likely impacts to navigation, flood levels, sediment transport, and other resource issues. Figure 1-1 shows the outline of Site 42 near Memphis, TN. The contents of this report pertaining to Site 42 may also be informative to other sites with similar geometric and flow characteristics.

The specific objectives of the study were to:

- Develop a model for baseline (existing) conditions without turbines
- Calibrate the baseline model to known water surface elevations
- Determine the locations in the waterway within the boundary of Site 42 that are likely to have higher velocities



*Figure 1-1. Mississippi River Hydrokinetic Project, Site 42
(Source: FFP)*

Section 2 Data Collection

2.1 River Flow

The gauge USGS 07032000 Mississippi River at Memphis, TN reports peak stream flow and gage height from 1872 to 1994. There is no daily or real time flow or gage height information currently being recorded at this location. Measurements of peak flow are less frequent, spread far in between and only account for the river at high stages. Figure 2-1 shows the location of USGS gauge at Site 42.



*Figure 2-1. Location of USGS Gauge at Site 42
(Source: FFP)*

2.2 Water Levels

Water level data under low flow condition was obtained from a publicly available document created by the Memphis District of the US Army Corps of Engineers. This document contains the tabulated values of Low Water Reference Plane (LWRP) revised

in 2007 and published in 2008 in the North American Vertical Datum of 1988. Table 2-1 gives the elevation of LWRP at each River Mile within the boundary of Site 42. These elevations will serve to calibrate the numerical model by adjusting the roughness parameter until reasonable agreement is achieved between computed water surface elevation at low flow and LWRP.

River Mile	Elevation LWRP (ft NAVD88)
726	174.80
727	174.99
728	175.00
729	175.10
730	175.30
731	175.60
732	175.80
733	176.11
734	176.80
735	176.91
736	177.20

*Table 2-1. LWRP Elevations at Site 42
(Source: USACE)*

2.3 Bathymetry

Bathymetry information at Site 42 was obtained from hydrographic surveys conducted by the Memphis District of the US Army Corps of Engineers between November 2007 and February 2008, a period typically characterized by flows below the mean annual discharge.

Data received in different ASCII formats were checked and processed to ensure consistency in Geographic and Projected Coordinate Systems as well in Vertical Datum. River bed elevations in feet NAVD88 were recorded on 1 foot intervals along transects spaced approximately 1,000 ft. Due to the low water levels occurring at the time of survey, some shallow areas in the river could not be measured. Figure 2-2 shows the location of transects taken at Site 42.

Longitudinal measurements of river bed elevation along the banks and channel centerline are to be conducted in the near future to better define the profile of the river bottom between consecutive transects.



*Figure 2-2. Location of transect measurements at Site 42
(Source: FFP)*

2.4 Velocity

One-dimensional models are usually calibrated when good agreement is found between computed and measure water surface elevation. Two-dimensional models, on the other hand, have more degrees of freedom (more unknown variables to be solved) and therefore need of not only water surface elevation but also of additional calibration and verification against velocity measurements. At the time the hydraulic analysis of Site 42 was performed no velocity information was available. ADCP surveys taken prior to piling siting will improved calibration of the hydraulic model.

2.4 Substrate

Knowledge of substrate type and size is of great importance for analyzing open channel flows. The interaction between particle size, flow dynamics and bedforms is well established and documented in the literature, e.g., Best (2005). Figure 2-3 displays some typical substrate types and their respective sizes. Based upon observations from a site

visit in February 2010 the predominant substrate material was estimated to be silt and sand.

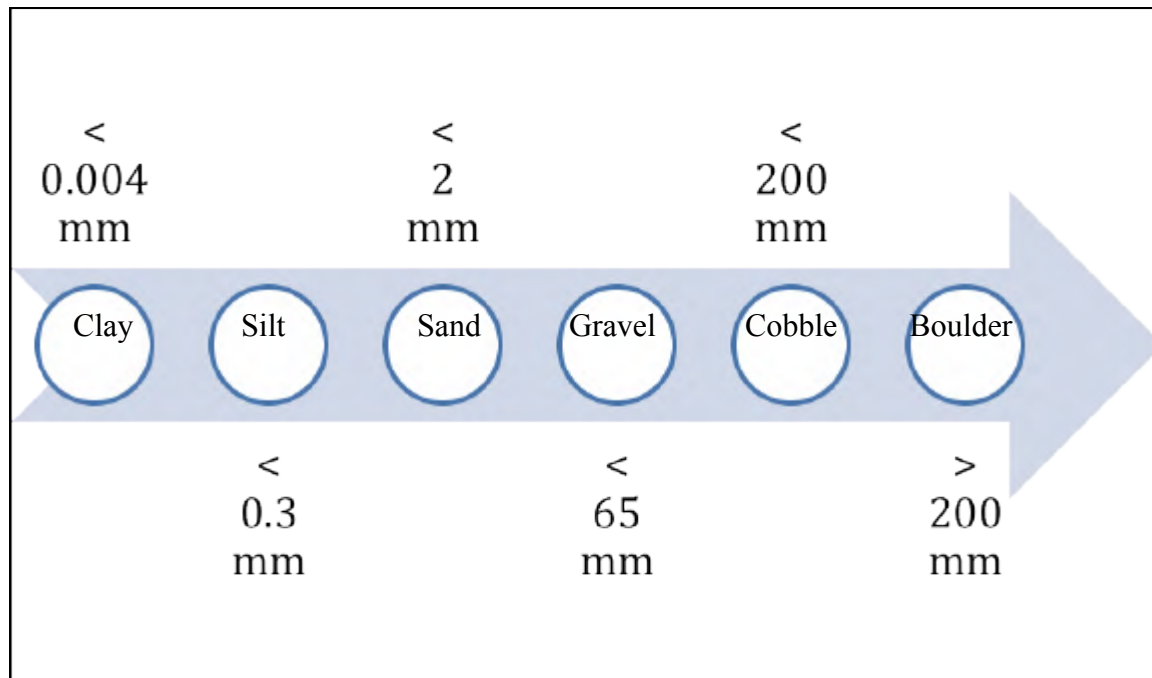


Figure 2-3. Substrate Size Classes
(Source: FFP)

2.5 Digital Elevation Model (DEM)

The USGS Digital Elevation Model (DEM) is a compilation of elevation data from the contiguous United States, Alaska, Hawaii, and territorial islands. These elevation data are publicly available on the internet and can be accessed via the National Elevation Dataset (NED) website (<http://seamless.usgs.gov/ned13.php>) maintained and updated by the USGS. NED data are available in resolutions (pixel size) of 30 meters, 10 meters, and 3 meters. Very few areas have data with 3 meters resolution. Approximately 95% of the contiguous United States is covered with a resolution of 10 meters.

For the purpose of this study a DEM with a resolution of approximately 10 meters was obtained from the USGS, encompassing the entire portion of the Mississippi River at Site 42. The DEM is very accurate in areas not covered by water, and less accurate under the water. Data from the bathymetry measurements were merged into the DEM from USGS to enhance its accuracy and resolution within the river channel. Figure 2-4 show the

DEM produced around Site 42.

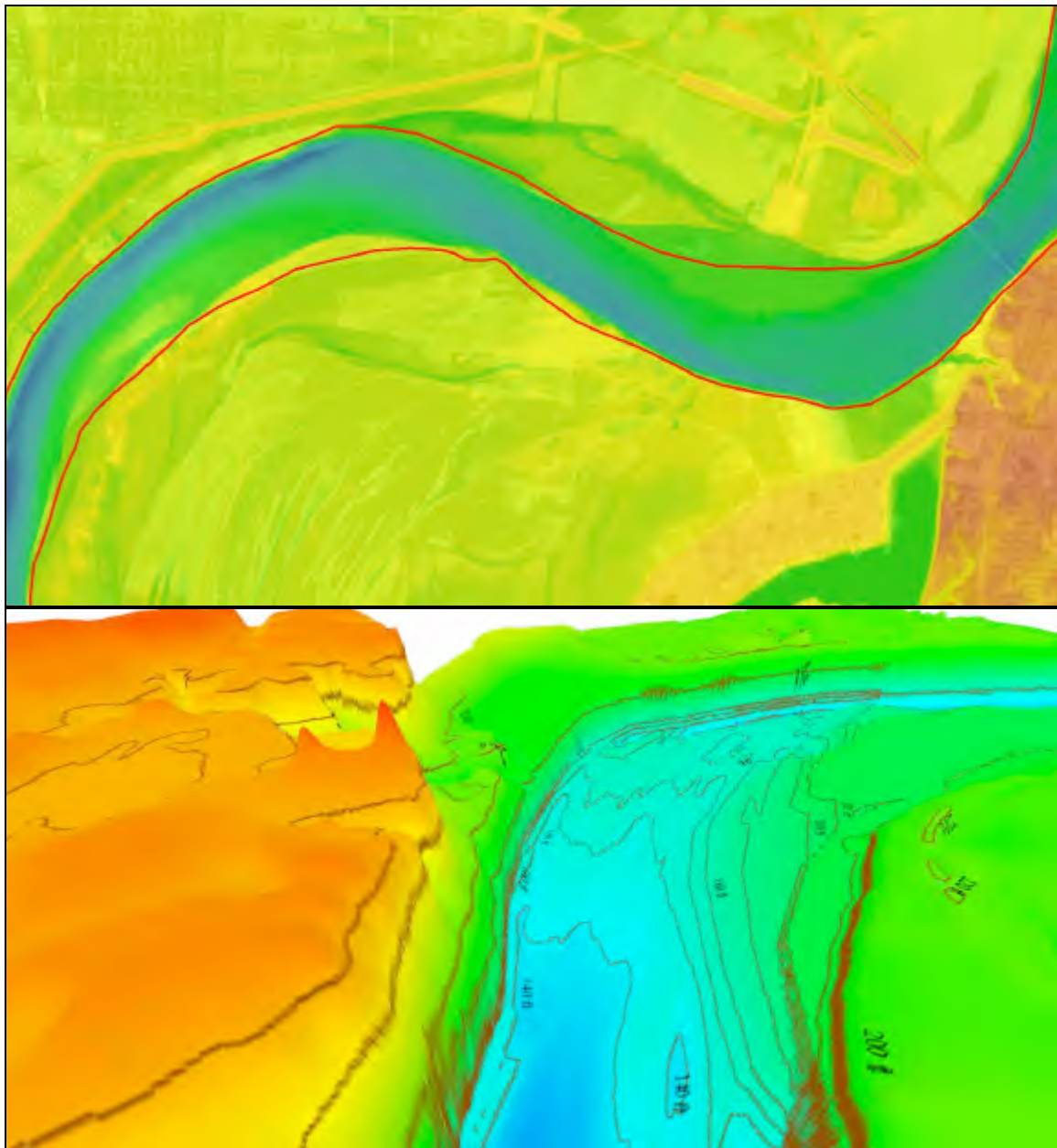


*Figure 2-4. Digital Elevation Model around Site 42
(Source: FFP)*

Section 3 Modeling Approach

3.1 Overview

Two-dimensional numerical models were used during the course of this hydraulic study to analyze different variables under various conditions, i.e., low, mid and high flows. AdH two-dimensional model was used for the purposes of estimating mid-channel water surface profile, velocity magnitude and bed shear stress. The use of the SMS package also enabled the visualization of results.

3.2 AdH Two-Dimensional Model

3.2(a) Model Background

AdH uses the 2D shallow water equations to model open channel flow environments such as rivers, estuaries, reservoirs, and coastal regions. AdH can calculate in 2D velocity, depth, and concentrations describing their horizontal distribution in the area of interest. In the vertical direction, parameters such as concentration and velocity have an assumed vertical distribution. This is adequate for most riverine applications (Berger, et al., 2010). AdH in 2D can simulate flow as well as sediment transport and bed morphology. Both cohesive (clays) and noncohesive (sands and gravels) may be represented. Additionally, AdH includes a correction for the 3D effects of a bendway upon flow and sediment transport. With this correction, the 2D model can be used to reasonably characterize meandering rivers. AdH in 2D is calculated on an unstructured mesh composed of triangular elements. AdH can adapt by refining or unrefining the mesh based upon user-defined parameters. Adaption generates an accurate result while using the least computational effort necessary.

3.2(b) Bed Topography

The foundation for the 2D modeling is the topography. The topography used in the model was taken from the Digital Elevation Model described in Section 2.5. The model developed in this study only depicts existing conditions; therefore, no additional modification was made to the geometry extracted from the DEM. A bed mesh consisting

of nodes ranging in spacing from 500 feet in the floodplain away from the river channel down to approximately 150 feet inside the river channel.

3.2(c) Manning Roughness and Eddy Viscosity

A Manning roughness value was assigned to each triangular element in the computational mesh. Since substrate maps were not available at Site 42, the Manning roughness coefficients in the different areas in the river channel were estimated so as to match the water surface elevations from the LWRP table. Table 3-2 shows the average roughness height used for each model reach, and Figure 3-1 displays the spatial location of the different material types. Values of eddy viscosity were also assigned to each element. The AdH estimated eddy viscosity option was used with its default weighting factor of 0.5 and the isotropic formulation.

Model Portion	Manning Roughness, n
Channel Downstream	0.019
Channel Middle	0.039
Channel Upstream	0.030
Floodplain	0.065

Table 3-1. Manning Roughness Used for Each Model Portion
(Source: FFP)

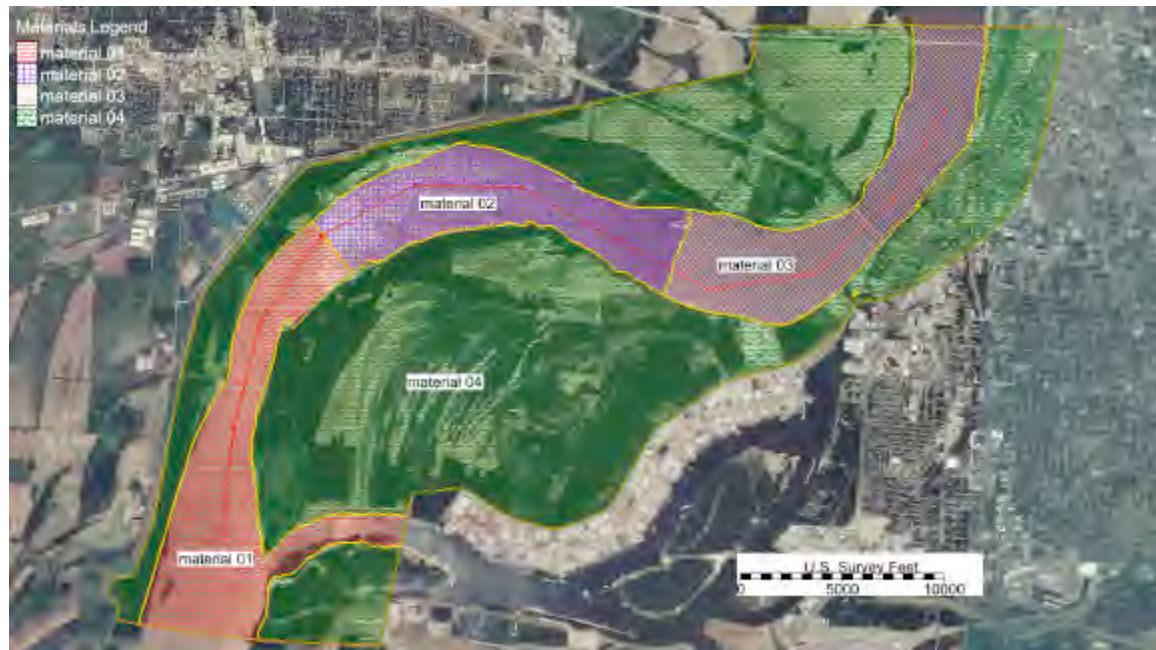


Figure 3-1. Distribution of Material Types at Site 42
(Source: FFP)

3.2(d) Boundary Conditions

The numerical model is setup such that the upstream boundary condition contains the inflow discharge value and the downstream boundary condition contains the elevation of the water surface at the outflow. The boundary conditions used in the model were calculated from measured stage and discharge data.

The discharge for low flow was obtained from the LWRP tables developed by the USACE. The mid flow in the model was selected to represent the median annual flow, i.e., this flow is expected to be exceeded half of the time. The high flow in the model was selected as the value for the 2 year flood obtained from the analysis of historic peak flows recorded at the USGS gauging station.

The downstream water surface elevation for low flow was obtained from the LWRP tables developed by the USACE. For mid and high flow conditions a rating curve developed from data at the gauge USGS 07032000 Mississippi River at Memphis, TN was used. For each flow the downstream boundary condition was selected so that, at the gauge location, a good agreement was obtained between water surface elevations from the rating curve and the numerical model. Table 3-2 summarizes the boundary conditions used in the numerical model for each flow.

Mississippi River	High Flow		Mid Flow		Low Flow	
	Q (cfs)	D/S WSEL (ft NAVD 88)	Q (cfs)	D/S WSEL (ft NAVD 88)	Q (cfs)	D/S WSEL (ft NAVD 88)
Site 42	800,000	583.99	400,000	580.71	155,300	580.38

Table 3-2. Boundary Conditions
(Source: FFP)

The flows used in the model were also determined based on exceedence. The low flow (155,300 cfs) represents the 97% exceedence level, the mid flow (400,000 cfs) represents the 50% exceedence point, and the high flow (800,000 cfs) represents approximately a 17% exceedance.

3.2(e) Computational Mesh

A computational mesh comprised of linear triangular finite elements was developed to discretize the domain under analysis. The mesh consists of more than 16,000 nodes and

more than 32,000 elements. Figures 3-2 and 3-3 show details of the computational mesh and the size of its elements.

The mesh contains elements of variable sizes. The size of the triangular elements (also referred to as nodal distance) ranges from 500 feet in the floodplain areas away from the river channel to 150 feet in the region inside the channel. A gradual transition of element sizes was provided so as to reduce undesirable numerical oscillations in the computations. The maximum allowable area change ratio between two neighboring elements was set at 50%.

$$\frac{\text{Area of Smaller Element}}{\text{Area of Larger Element}} \leq 0.50$$

Also, great care was exercised in the process of mesh generation to ensure that the majority of the elements were equilateral and thereby the internal angles were also approximately equal. When geometrically distorted elements could not be avoided, the internal angles were maintained in the range of 20° to 130°.

$$\begin{aligned} \text{Minimum Interior Angle} &\geq 20^\circ \\ \text{Maximum Interior Angle} &\leq 130^\circ \end{aligned}$$



*Figure 3-2. Computational Mesh for Site 42
(Source: FFP)*



*Figure 3-3. Closer View of the Computational Mesh for Site 42
(Source: FFP)*

Section 4 Results

4.1 Flow Duration Analysis

Daily and monthly flow data were not available at Site 42 in the Mississippi River. A flow duration analysis had been previously performed by FFP and presented in an earlier progress report. Such analysis was based on flow information at the gauge USGS 07289000 Mississippi River at Vicksburg, MS. Figure 4-1 displays the flow duration curve at Site 42. Flows at the gage USGS 07289000 were adjusted to Site 42 by using an adjustment factor of 0.82 based on the following equation.

$$Q_{\text{Site 42}} = Q_{\text{Vicksburg}} \times \left(\frac{BA_{\text{Site 42}}}{BA_{\text{Vicksburg}}} \right)$$

where

$Q_{\text{Vicksburg}}$ = flow at USGS gage 07289000,

$Q_{\text{Site 42}}$ = adjusted flow Site 42 (Memphis, TN),

$BA_{\text{Vicksburg}}$ = basin area USGS gage 07289000(1,144,500 square miles),

$BA_{\text{Site 42}}$ = basin area at Site 42 (932,800.0 square miles).

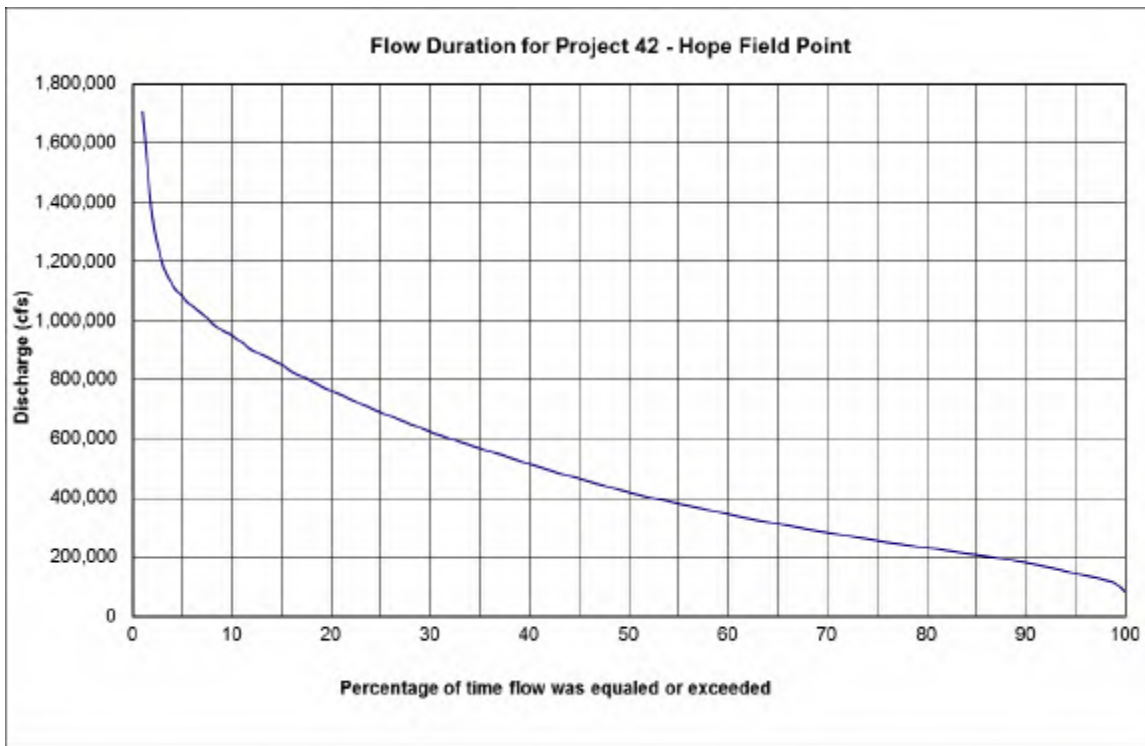


Figure 4-1. Flow Duration Curve, Site 42
(Source: FFP)

4.2 Rating Curve

Although records of daily flow at the gauge USGS 07032000 Mississippi River at Memphis, TN were not available, there were available some records of historic peak flows paired with their corresponding gage heights allowing the development of an approximate rating curve at the gauge location. The rating curve obtained in this manner is an approximation of the expected behavior of water surface elevation versus total discharge. Figure 4-2 shows the Rating Curve developed for Site 42.

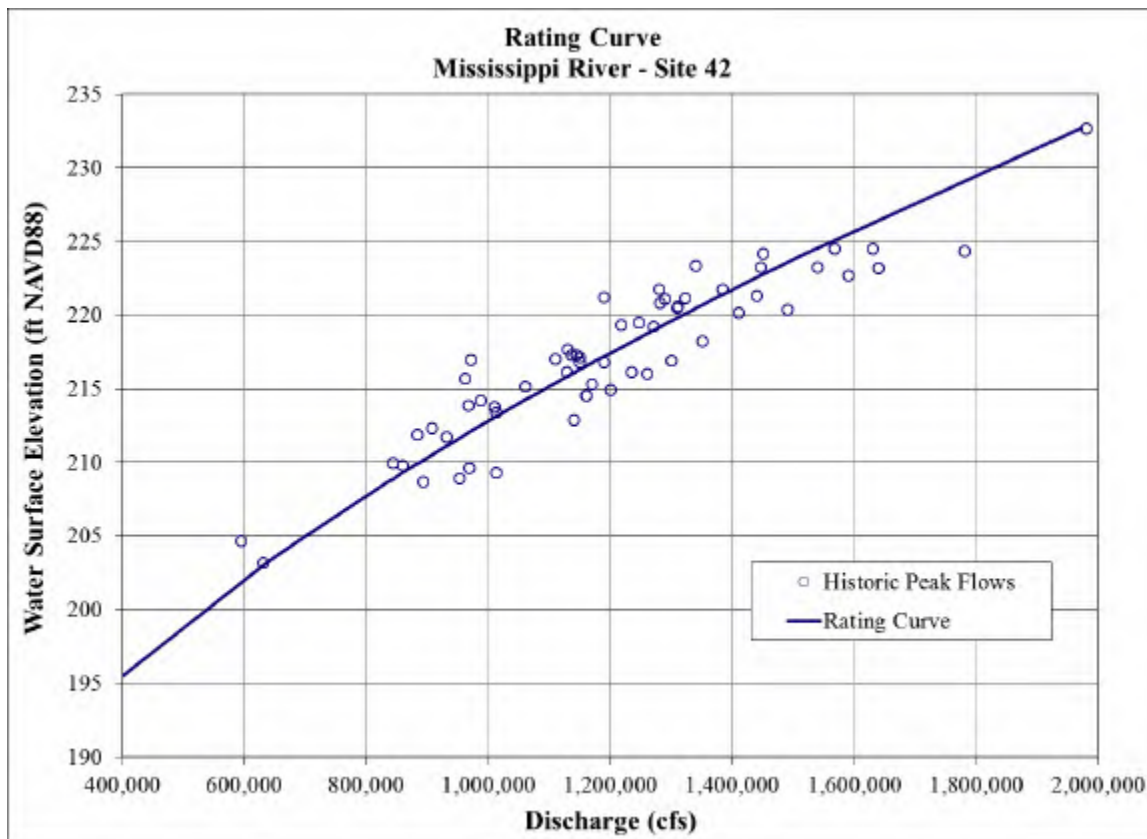


Figure 4-2. Rating Curve, Mississippi River Site 42
(Source: FFP)

4.3 Flood Frequency Analysis

HEC-SSP was used to develop a flood frequency analysis from peak flow data collected at USGS gauge 07032000 Mississippi River at Memphis, TN. The outcome of the analysis at selected return periods is shown in Figure 4-3. The value of the 2-yr flood at the location of Site 42 is approximately 800,000 cfs.

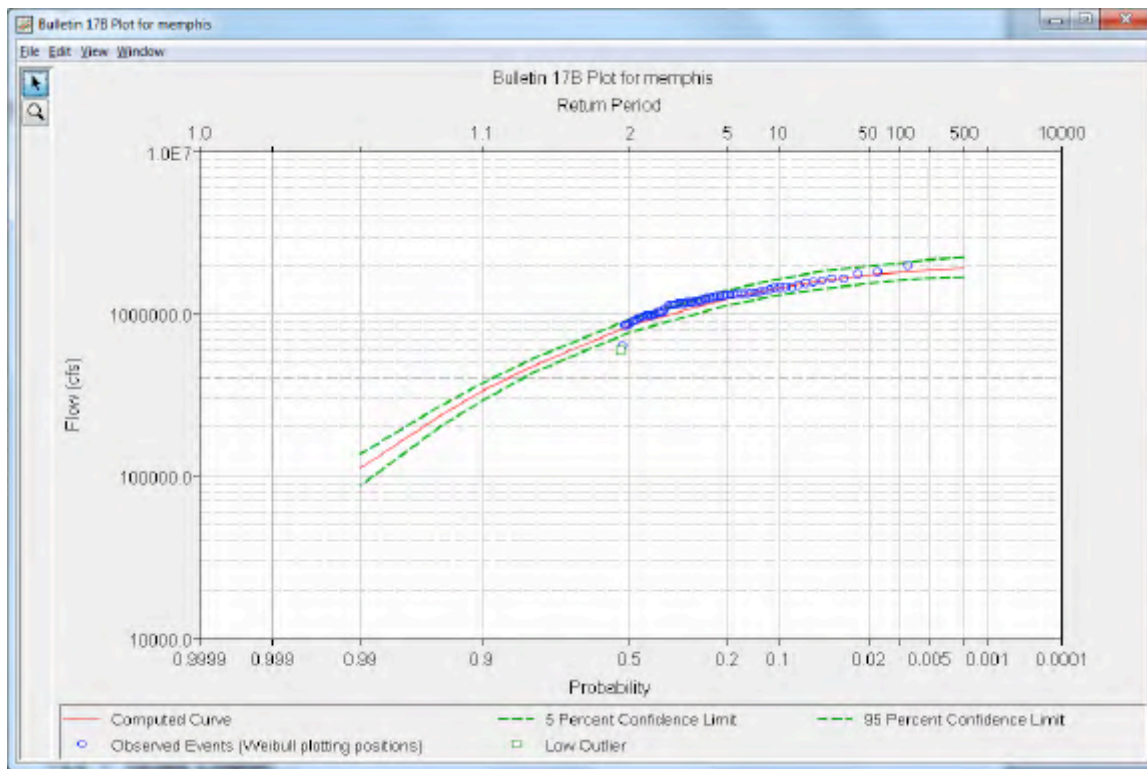


Figure 4-3. Peak Flood Flows at Site 42
(Source: FFP)

Flood levels along the river reach are expected to remain unchanged or vary in a very narrow range as a result of the placement of the hydrokinetic turbine fields (less than 1% of the cross sectional area is to be used by the turbines).

4.5 Water Surface Elevation

The AdH model was used to develop water surface profiles, and water depth maps under low, mid and high flow scenarios. Figure 4-4 displays the water surface profile for the portion of the Mississippi River corresponding to Site 42. The figure shows good agreement between the modeled results and the calibration data at low flow and mid flow. In these scenarios the difference between modeled and calibration data is less than 0.2 ft. At high flow the difference between modeled and calibration data is slightly higher, however, the difference is less than 1 ft. In this manner the numerical model is calibrated to existing conditions. It is observed in Figure 4-4 that the overall difference in water surface elevation between River Mile 726 and River Mile 736 is 2.5 feet.

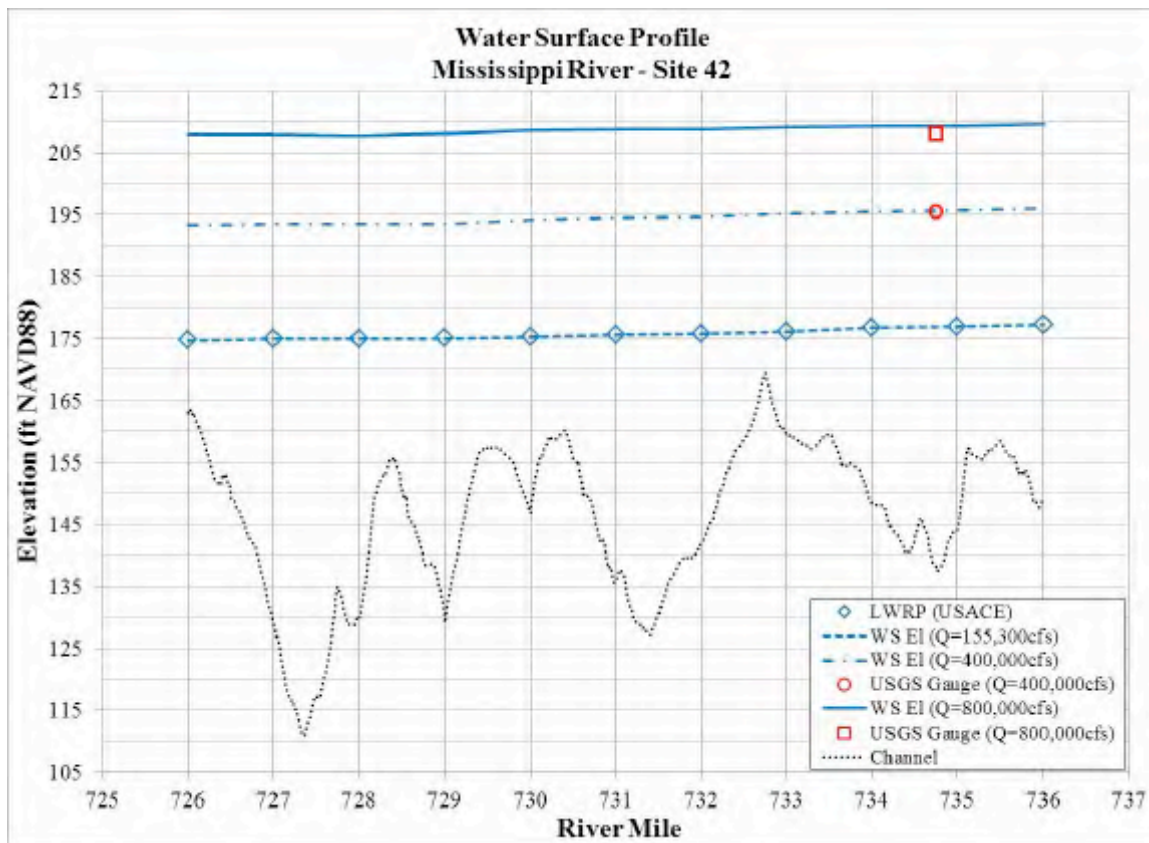


Figure 4-4. Water Surface Profile of Mississippi River at Site 42
(Source: FFP)

Figures 4-5, 4-6, and 4-7 show maps of water depth for low, mid and high flow respectively. These figures show that the deepest areas are located on:

- Near the right hand side of the channel between River Miles 727-730
- Near the left hand side between River Miles 732-733
- On the left hand side in the vicinity of the bridge between River Miles 734-735

The absolute deepest points are located at River Mile 727.4 and River Mile 730 where, even under low flow conditions, there is a depth of at least 85 feet below LWRP. When the flow is 400,000 cfs (50% exceedence point) the water depth at these locations is around 106 feet. When the flow is 800,000 cfs (17% exceedence point) the water depth at these locations is around 120 feet.

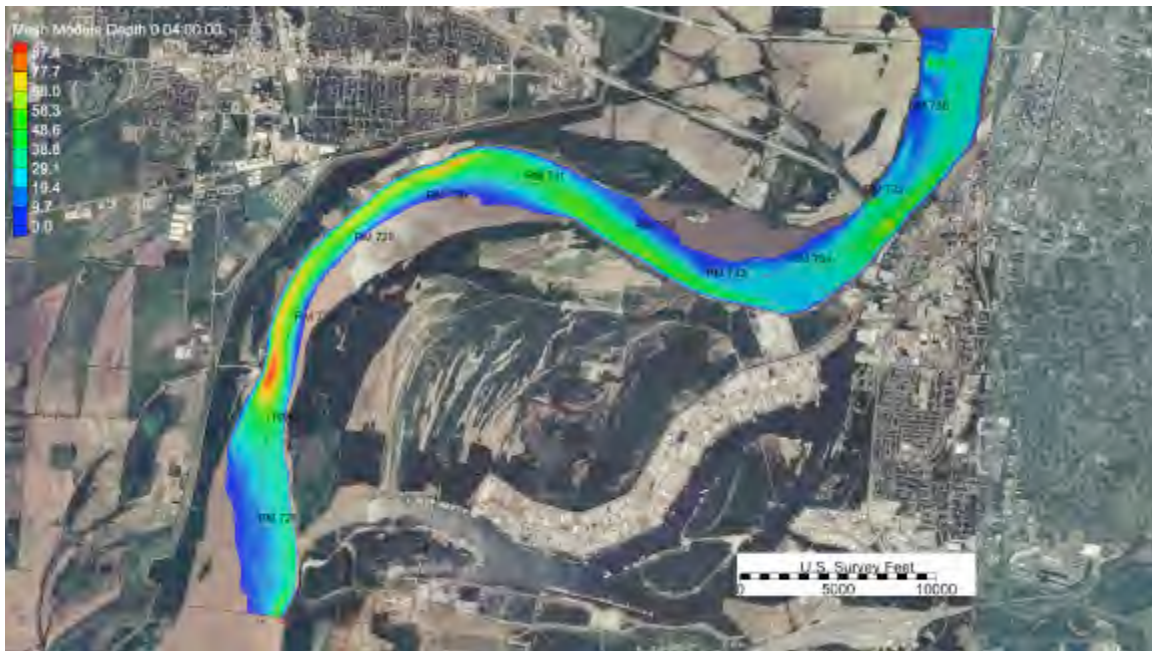


Figure 4-5. Water Depth Map of Mississippi River at Site 42, $Q=155,300 \text{ cfs}$
 (Source: FFP)



Figure 4-6. Water Depth Map of Mississippi River at Site 42, $Q=400,000\text{cfs}$
(Source: FFP)

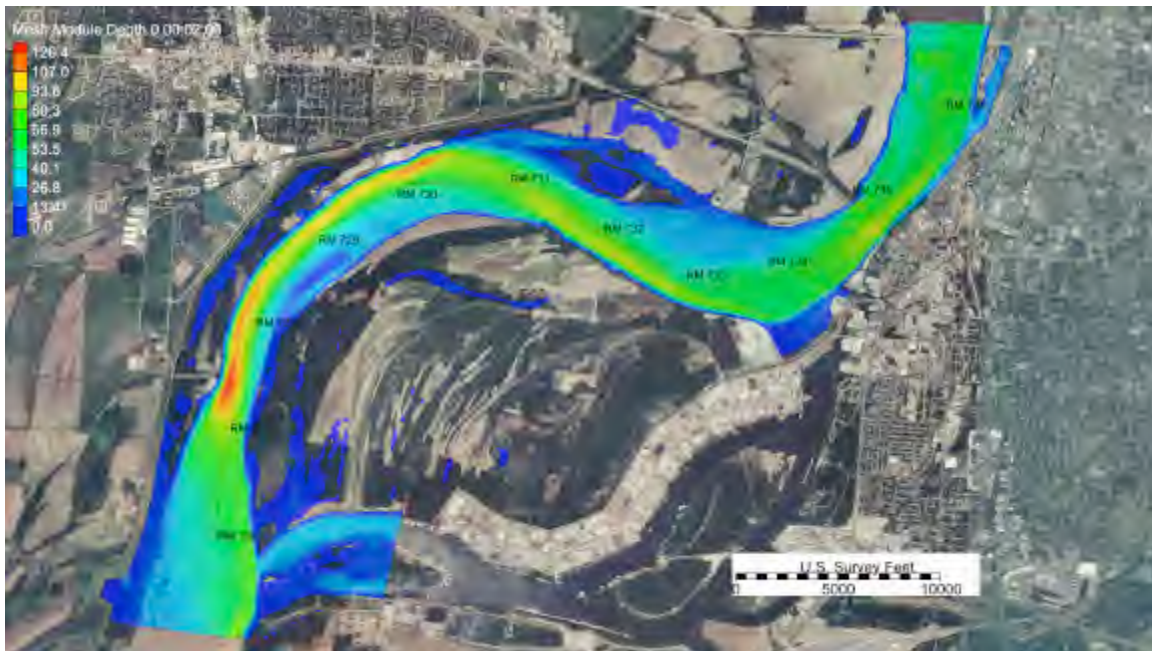


Figure 4-7. Water Depth Map of Mississippi River at Site 42, $Q=800,000\text{cfs}$
 (Source: FFP)

4.6 Depth-Averaged Velocity

This section presents the depth-averaged velocity results from the two-dimensional model described in Section 3.2. The discussion of results is broken down in 3 regions of the model: upstream of River Mile 732, between River Miles 727-732, downstream of River Mile 727. Below is a description of each region.

Upstream of River Mile 732

Figures 4-8, 4-9, and 4-10 show maps of velocity in the region upstream of River Mile 732. This portion of the model contains the upstream boundary condition which is located near River Mile 737. The flow entering the reach goes north to south, passes a contraction through a bridge and takes a sharp turn, almost 90° , to the right. The right side of the channel is shallow and displays lower depth averaged velocities. The left side is deeper and thereby attracts more flow with higher velocities.

Velocities in the right side of the channel are in the range of 1-2 ft/s at low flow conditions. For mid flow, as the flow depths are increased in the entire section, the range of velocity is also increased to 1-3 ft/s. When the flow is high, like the case of the 2-yr

flood, the velocities are increased to the range of 2-5 ft/s.

Velocities in the left side of the channel at low flow conditions are in the range of 2-6 ft/s. With increasing depths at mid flow, velocities are also increased to the range of 4-6 ft/s. In the high flow case velocities are increased to the range of 5-8 ft/s. The highest velocities were found around the bridge contraction in River Mile 734.7 (4-7 ft/s) and around the 90° bend in River Mile 732.7 (6-8 ft/s).

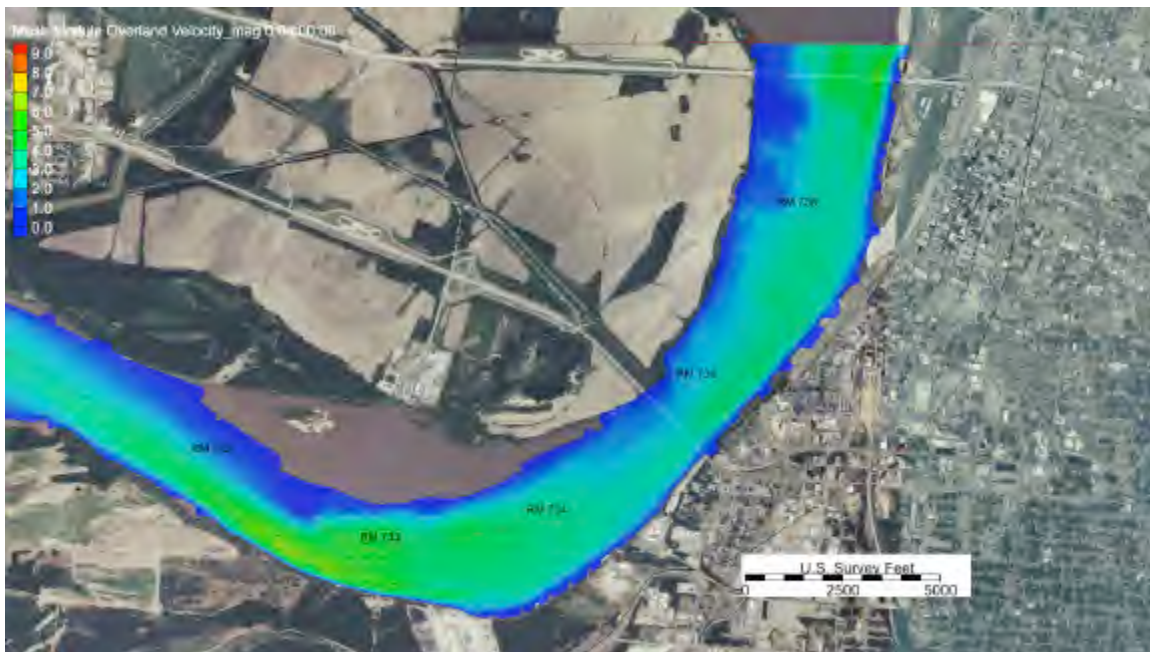


Figure 4-8. Velocities at Site 42 Upstream of River Mile 732, $Q=155,300\text{ cfs}$
(Source: FFP)



Figure 4-9. Velocities at Site 42 Upstream of River Mile 732, $Q=400,000\text{cfs}$
(Source: FFP)

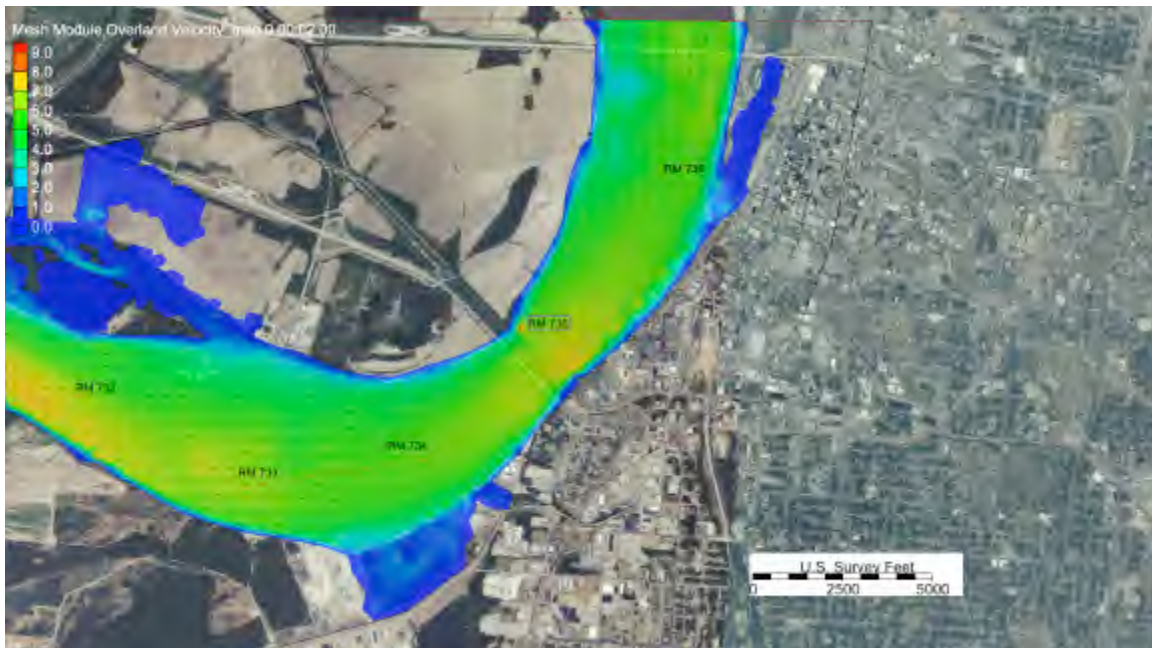


Figure 4-10. Velocities at Site 42 Upstream of River Mile 732, $Q=800,000\text{cfs}$
(Source: FFP)

Between River Miles 727-732

Figures 4-11, 4-12, and 4-13 show maps of velocity in the region between of River Miles 727-732. In this portion of the model the river flows east to west coming out of the 90° bend in River Mile 733 and then takes another sharp turn, almost 90°, to the right, around River Mile 730. Secondary flows are typically found around river bends and are expected to be found in this region. AdH can account for some of the three-dimensional features of the secondary currents, by means of the bendway correction. The location of the deep and shallow areas changes from side to side as the flow makes its way through the reach.

At RM 731-732 the left side is deep and the right side is shallow. Velocities in the deeper left side are in the range of 3-4 ft/s at low flow, 4-5 ft/s at mid flow and, 6-8 ft/s at high flow. Velocities in the shallower right side are in the range of 1-2 ft/s at low flow, 2-3 ft/s at mid flow and, 3-4 ft/s at high flow.

From RM 730-731 there is a transition zone where the center channel is deeper and both sides are shallower. Velocities in the channel center-section are 3 ft/s (low flow), 4 ft/s (mid flow), 6 ft/s (high flow). The sides have velocities around 1 ft/s (low flow), 2 ft/s (mid flow) and, 3 ft/s (high flow).

From RM 727-730 the right side is deep and the left side is shallow. Velocities in the left side are in the range of 1-2 ft/s at low flow, 2-2 ft/s at mid flow and, 3-5 ft/s at high flow. Velocities in the right side are in the range of 3-4 ft/s at low flow, 4-6 ft/s at mid flow and, 6-9 ft/s at high flow.

The highest velocities were found around the left side in River Mile 731.4, around the right side in River Mile 729 and on the right side of River Mile 727.6. Table 4-1 shows the magnitudes of velocity found at these locations for the flows modeled.

Mississippi River (River Mile)	Low Flow 155,300 cfs	Mid Flow 400,000 cfs	High Flow 800,000cfs
	Velocity (ft/s)	Velocity (ft/s)	Velocity (ft/s)
731.4 (left)	3.3	5.1	8.2
729 (right)	3.7	5.9	7.8
727.6 (right)	2.6		

Table 4-1. Maximum Velocities within Site 42
(Source: FFP)

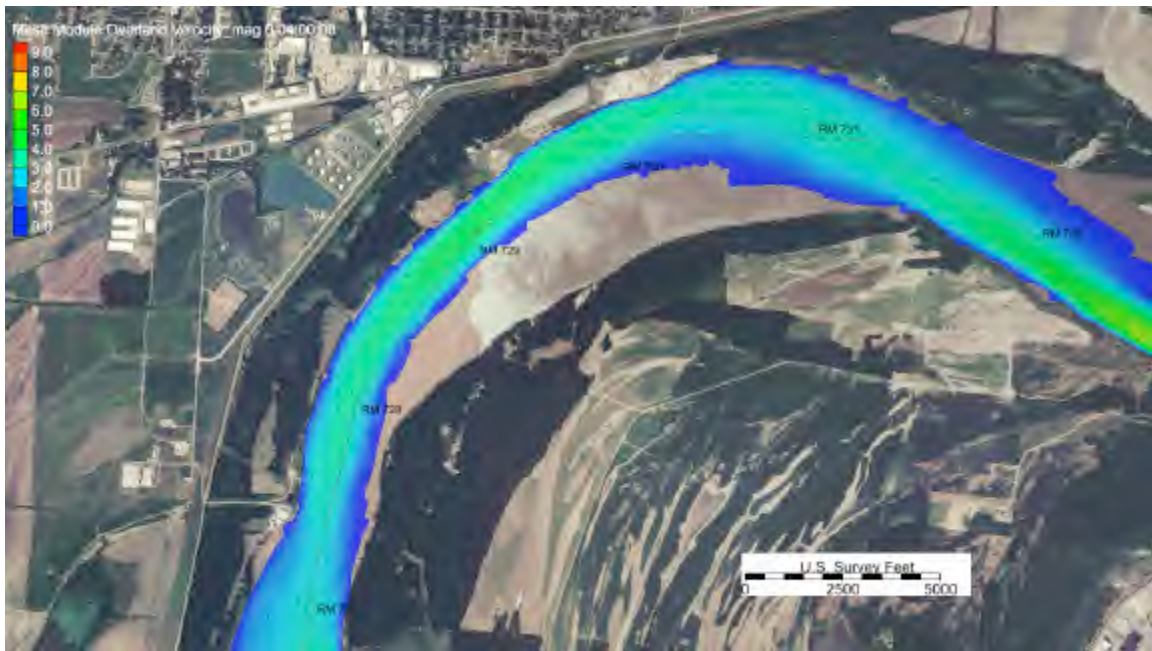


Figure 4-11. Velocities at Site 42 between River Mile 727-732, $Q=155,300\text{cfs}$
(Source: FFP)

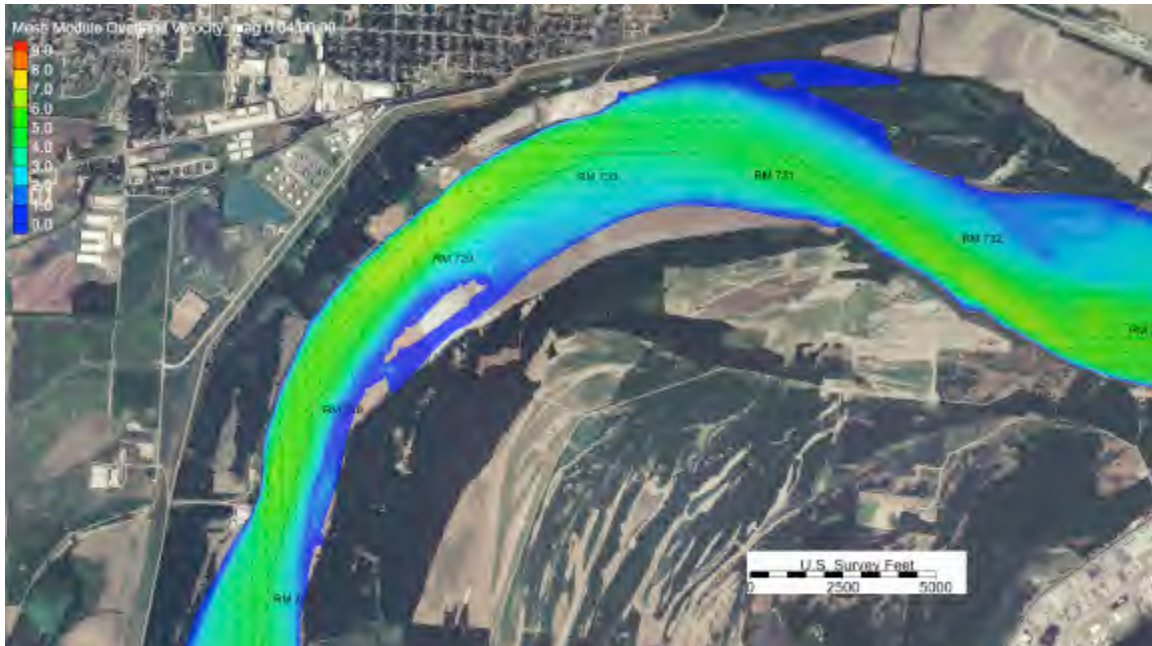


Figure 4-12. Velocities at Site 42 between River Mile 727-732, $Q=400,000\text{cfs}$
(Source: FFP)

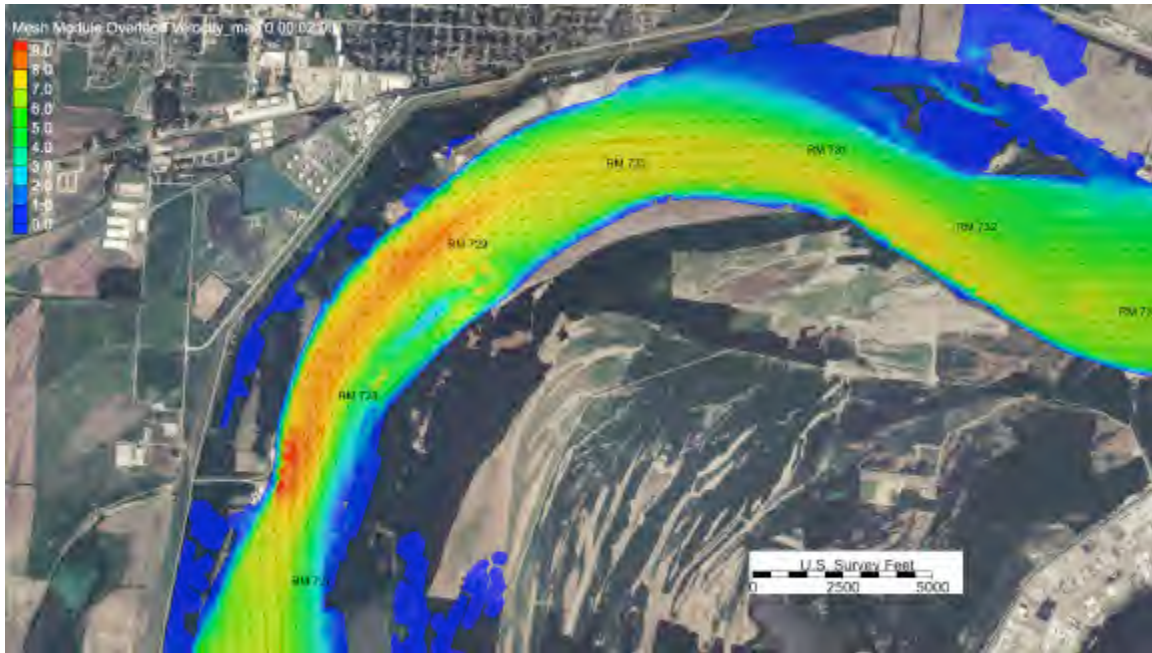


Figure 4-13. Velocities at Site 42 between River Mile 727-732, $Q=800,000\text{ cfs}$
(Source: FFP)

Downstream of River Mile 727

Figures 4-14, 4-15, and 4-16 show maps of velocity in the region downstream of River Mile 727. This portion of the model contains the downstream boundary condition which is located near River Mile 725. The flow leaving the reach flows southward.

Velocities in the right side of the channel are in the range of 2-4 ft/s at low flow conditions. For mid flow, the range of velocity is increased to 3-5 ft/s. When the flow is high, the velocities are increased to the range of 5-6 ft/s.

Velocities in the left side of the channel at low flow conditions are in the range of 1-2 ft/s. With increasing depths at mid flow, velocities are also increased to the range of 2-3 ft/s. In the high flow case velocities are increased to the range of 5-6 ft/s.

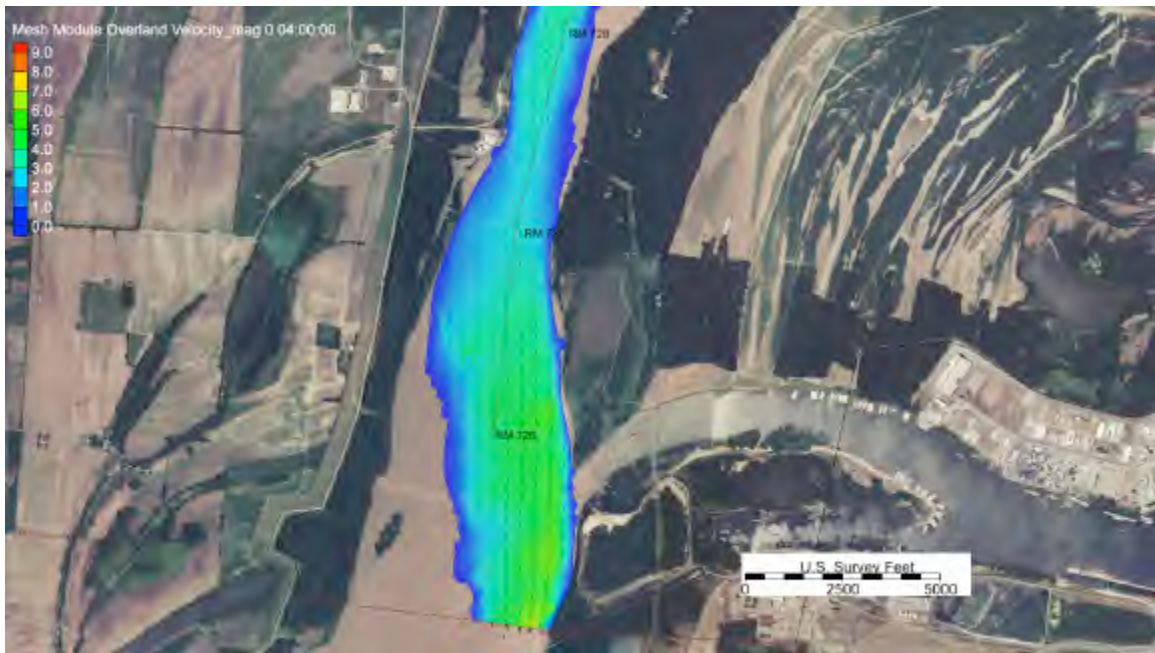


Figure 4-14. Velocities at Site 42 Downstream of River Mile 727, $Q=155,300\text{cfs}$
(Source: FFP)

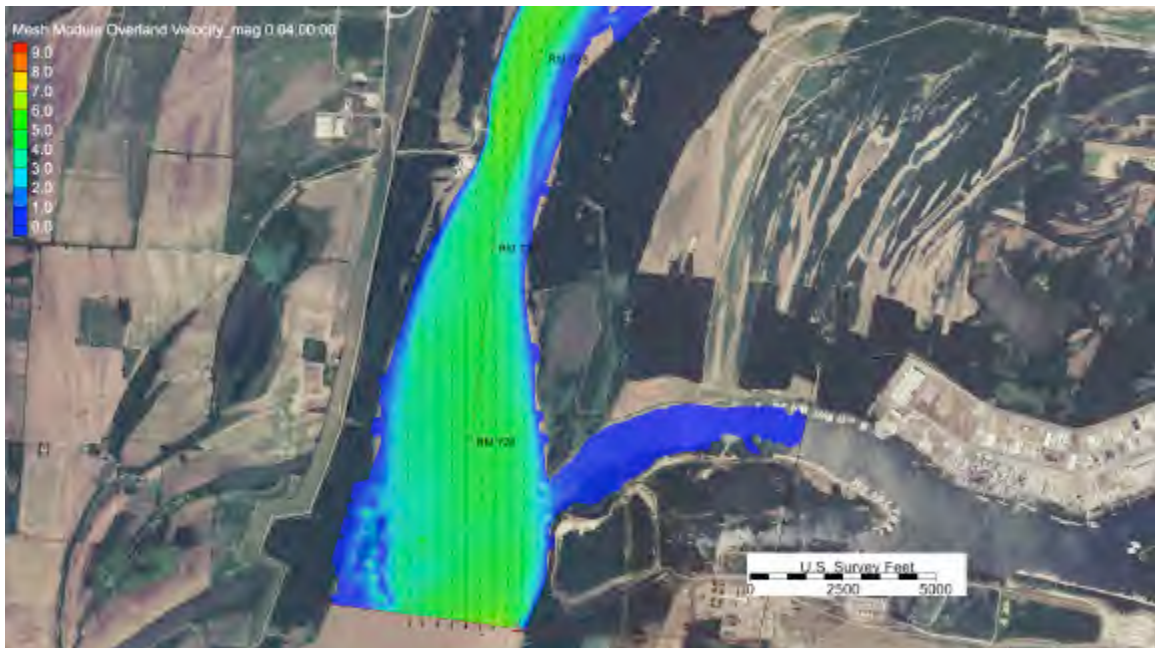


Figure 4-15. Velocities at Site 42 Downstream of River Mile 727, $Q=400,000\text{cfs}$
(Source: FFP)

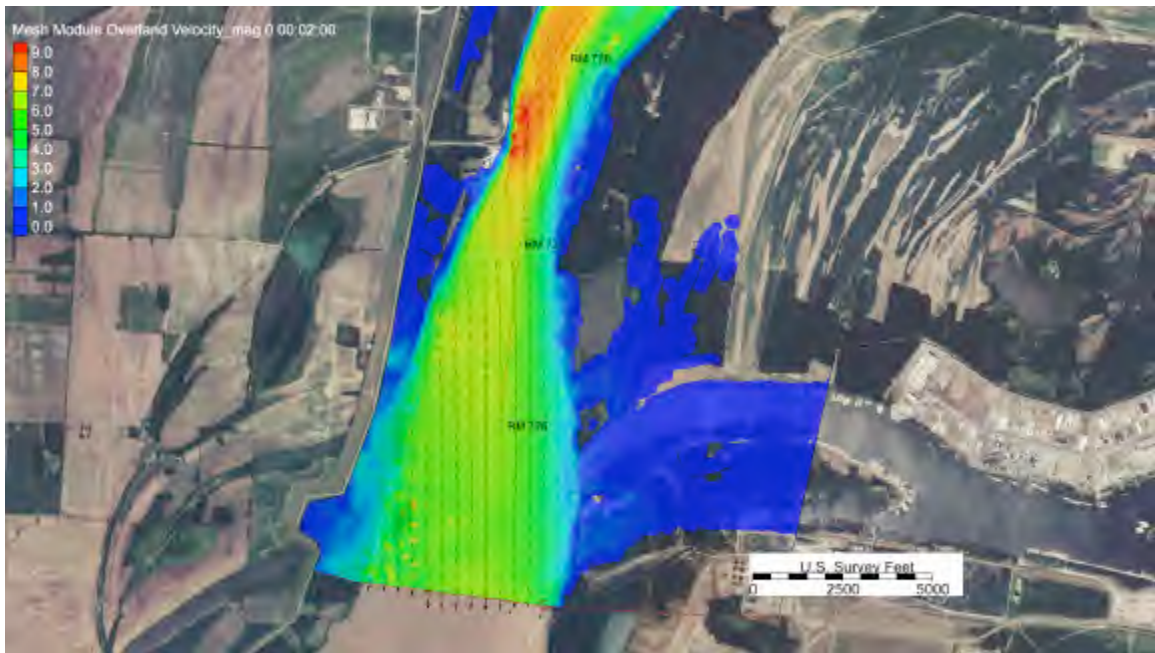


Figure 4-16. Velocities at Site 42 Downstream of River Mile 727, $Q=800,000\text{cfs}$
(Source: FFP)

Section 5 Literature Cited

Berger, R.C., Tate, J.N., Brown, G.L., and Savant, G. (2012). *Adaptive Hydraulics User Manual*. Engineer Research and Development Center, USACE.

Best, J. (2005). *The fluid dynamics of river dunes: A review and some future research directions*. J. Geophys. Res, 110(1).

Chang, H. H. (1988). *Fluvial Processes in River Engineering*. Malabar, Florida: Krieger Publishing Company.

Chow, V.T. (1959). *Open Channel Hydraulics*. New York, USA: McGraw-Hill Book Company.

Fischer, H. B. (1979). *Mixing in Inland and Coastal Waters*. New York: Academic Press.

Jirka, G. H. and Socolofsky, S. A. (2002). *Environmental Fluid Mechanics. Part I: Mass Transfer and Diffusion*. 2nd ed. Karlsruhe: Universitat Karlsruhe.

Melville, B. W., and Coleman, S. E. (2000). *Bridge scour*. Water Resources Publications, Highlands Ranch, Colorado.

National Elevation Dataset (NED) website (<http://seamless.usgs.gov/ned13.php>)

Rubin, H., and Atkinson, J. F. (2001). *Environmental fluid mechanics*. Marcel Dekker, New York.

U.S Army Corps of Engineers, Memphis District. (2008). *2007 Low Water Reference Plane Mississippi River: LWRP Tabulated For Each One-Tenth River Mile*. Office of The District Engineer Memphis, Tennessee.

Appendix 6

HYDRAULIC MONITORING METHODOLOGY



239 Causeway Street
Boston, MA 02114-2103
USA

MAIN: (978) 252-2822
FAX: (617) 367-3372

www.free-flow-power.com

Filename: 2012-06-28_R01_Hydraulic_Insitu_Study_Plan

Subject: In-situ Monitoring Plan for Hydraulic Monitoring

Date	Release Rev	Description
05-04-2012	00	Original
06-28-2012	01	Revisions after initial review

1 Requirements of FERC's Study Plan Determination

- (1) Determine metrics for measuring impact on flows and on sedimentation.
- (2) Determine thresholds for impact.
- (3) Determine the force or “drag” from a single turbine and small groups of turbines and effects on flow energy and behavior.
- (4) Assess the impact of turbine deployment on flow conditions and sedimentation, including effects from fouling and debris loading.
- (5) Use computational fluid dynamics (CFD) methods to evaluate hydraulic impact associated with decreased efficiency of the turbine over time.
- (6) Evaluate effects on navigation, on USACE structures, natural river bank stability, flood water elevations, and aquatic habitat.

From the above requirements, requirements (1), (2), (3), (5) and (6) are not expected to be addressed in the in-situ deployment monitoring as they are not applicable to site test data acquisition. Requirement (4) can be addressed by monitoring flow changes (distribution, direction, and magnitude) and how sedimentation both suspended in the water column and along the river bottom changes with the installation of FFP’s turbines and pilings. Options for measuring requirement (3) will be addressed in this document as well where potential monitoring methods to determine the forcing on the turbines and piling will be described.

2 Methods Executed by Other Companies

1.1 ORPC-Cobscook Bay (P-12711)¹

- The ocean floor that made up the project site was determined by using a single beam sonar with side-scan sonar and a sub bottom profiler. An underwater video survey was done to further characterize the transect data provided by the side-scan sonar over varying length of the transects that the side-scan sonar survey captured.²
- Multi beam surveys were also conducted using 240 kHz RESON 8101 system coupled to a TSS DMS 3-05 Motion Sensor and a Hemisphere GPS VS110 dual antenna differential global. Surveys were done with the positioning system (DGPS) digital compass during the pre deployment phase of the monitoring effort. Surveys were done from November 16-19, 2010 to characterize a one-mile stretch over the potential deployment site.
- Sub tidal video recording from scuba divers was completed around the project site to monitor scouring. Concrete anchors weighing 4,000 lbs were dropped onto the site and steel cables were attached between the anchors to act as a path of travel for the divers. These surveys were done on July 14th and July 15th, 2011 for a total of three hours.
- The underwater camera was a Panasonic Model DMR-T3040 DVD Video Recorder.
- The divers were supplied with surface air so that they could communicate with team members on board the vessel, who were looking into the live video supplied by the diver.
- The timeline for these surveys is as follows:
 - 2012: Monthly dives to monitor the site and the area where cable will be routed to shore.
 - 2013 and afterward: bi-monthly dives to monitor the site and the area where cable will be routed to shore.
- Sediment samples were acquired using an apparatus based around a PVC pipe on the ocean floor as well as samples on the shore where the cabling was placed.
- A 600kHz and 300kHz Teledyne RDI Acoustic Doppler Current Profiler (ADCP) was used to characterize flow through the project site. This unit was deployed at six different locations across the project area for varying periods of time from 7 days up to 58 days to measure the direction and magnitude of the flow over the entire water column. These units were configured with a six-minute ping period and a one meter depth bin. The deployments were also made at different parts of the lunar cycle to see the varying speeds as the moon varied.

¹ Ocean Renewable Power Company, 2011. Safe Guard Plans, Final Pilot License Application Cobscook Bay Tidal Project, FERC Project Number 12711. September 2011.

² University of Maine, 2010. University of Maine Interim Fisheries Report Appendix E Study Reports and Assessments. December 2010.

1.2 Verdant (P-12611)³

- For pre-deployment two surveys were done using side-scan sonar, sub-bottom profiling and a bathymetric survey. The sub bottom profiling was done using a 10kHz SyQwest Stratabox mounted on a boat that conducted the surveys with transects spaced 25ft apart for both studies. The side-scan sonar profiling was done with 500kHz and 100kHz units, the first survey using the 500kHz unit and the latter using the 100kHz unit. The bathymetric survey was done using a single beam sonar device in both studies. These studies were all done before the deployment to characterize the bottom of the water way that the turbines were being deployed in. Due to the rocky nature of the bottom of the water way, it was concluded that scouring would not be an issue once the turbines were deployed and it was therefore not monitored after deployment.
- An ADCP sensor was installed on the bottom of the project site from December 2006-September 2009. Mobile ADCP surveys were also conducted using a RDI 1200kh Rio Grande which was attached to the survey boat on the port gunnel with a specialized mounting clamp. The sensor was placed 1 foot below the water's surface and data was recorded using WinRiver software from RDI which also interfaced with a Trimble Pro XRS GPS for sub meter tracking.

1.3 SnoPud-Hydroelectric (P-2157)⁴

- Aerial surveys of the site up and down stream of the dam were conducted to roughly characterize the site bathymetry.

1.4 SnoPud-Tidal (P-12690)⁵

- Bathymetric, geophysical, and geological hazard site surveys were performed from June 25th-June 30th 2009. This included high-resolution multi-beam bathymetry, sub bottom profiling, side-scan sonar, and bottom grab.
- Bottom grabs were done using a Van Veen system to characterize the ocean floor of the project site.

³ Verdant Power, Inc. 2010. Pilot License Application Roosevelt Island Energy Project, Volume 2, Exhibit E Environmental Report, FERC Project Number 12611. December 2010.

⁴ Snohomish County Public Utility District 1, 2010. Henry M. Jackson Hydroelectric Project, Fisheries and Habitat Monitoring Plan, FERC Project Number 2157. September 2, 2011.

⁵ Snohomish County Public Utility District 1, 2012. Admiralty Inlet Tidal Project, Application for a New Pilot Project License (Minor Water Power Project), Volume 2 Exhibit E, FERC Project Number 12690. February 29, 2012.



Figure 1 - Van Veen Bottom Grab System

- Conducted Remotely Operated Vehicle (ROV) to characterize sea floor in April 2009 and in the months of August, September, and October 2010. The ROV deployments provided video of the project site both before the units were installed. Further ROV surveys are planned after deployment to monitor the operation of the turbines.
- High resolution multi-beam echo sounders (MBES) were used to determine the depth of the area as well as side scan sonar with back scatter imaging to provide a visual of the project site. This was done with a Reson SeaBat 8101 MBES. This data was recorded to the Hypack/Hysweep data acquisitioning program which connected directly to the MBES.
- The side-scan sonar that was used over the project site was from a Klein 3000 sonar tow fish.
- Sub bottom profiling was done using a Edgetech full spectrum system (CHIRP) which includes: SB-216S tow fish, the Model 3200 topside processor, EdgeTech's Discover acquisition software and an EPC 1086 NT thermal printer for printing out the images produced by the software. The system has a pulse rate between 4-8 Hz and a sweep range frequency between 2 to 15 kHz.
- Mobile ADCP surveys were conducted in April, May, August, and November in 2009, February and May in 2010, and August in 2011.
- Additionally, stationary ADCP instruments on the seabed were made. This unit was deployed in April 2009 and will be deployed until December 2013. Multiple ADCPs were deployed on Seaspiders around the locations that were most likely to be the site of where the turbines were to be installed. Data was retrieved four times to date, though a specific methodology for its retrieval is not specified.

1.5 MCT-SeaGen⁶

- Pre-deployment work included mobile acoustic surveys coupled with divers and drop down video surveys.
- Post-deployment surveying included diver video and still images to monitor scouring.

2 Monitoring Options

In the prior examples from different companies it should be noted that some of the hydraulic study work was done to initially characterize the site. Below are multiple plans that have been proposed to monitor the hydraulic conditions of FFP's *in situ* site for the pre- and post-deployment periods of the *in situ* installation.

2.1 Mobile Single Beam Bathymetry Surveys

Conduct periodic acoustic single-beam bathymetry surveys of the in-situ site area (around the project site and 500m downstream of the project site). This would be done at the same rate for pre- and post-deployment of the turbines.

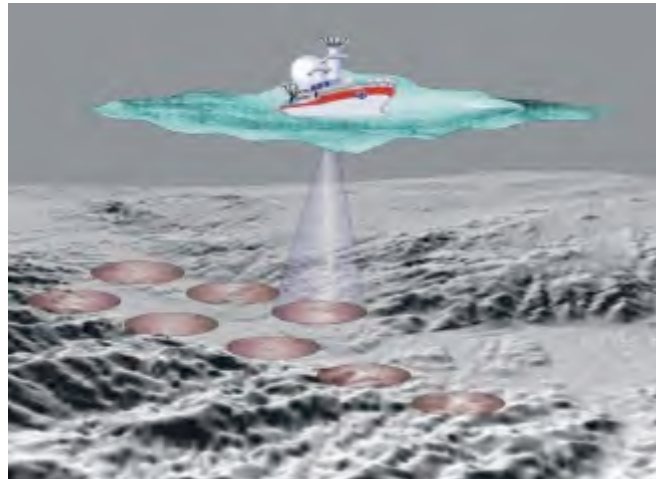


Figure 1 - Example of a Single-Beam Bathymetry Survey

Pros

- No permanent installations to the project site accompany this survey.
- The equipment that would be used in this survey is the same equipment as the mobile surveying for the Fish Entrainment study.

Cons

- With this method it will be impossible to know the elevation of the entire river bottom.
- The river height will have to be factored into the measurements taken from the vessel survey to account for seasonal variation of the river's height.

⁶ Marine Current Turbines, 2011. SeaGen Environmental Monitoring Programme, Final Report. January 16, 2011.

- It will be impossible to detect any scouring near the turbines as the scanner will detect the turbines and will be unable to detect the river bottom beneath the turbines. Typical single beam sensors have a resolution to .1ft/.1m, with an accuracy of .5% of the measured value, but since the turbines will be on top of the river bottom where scouring will be taking place then the single beam sensor will only pick up the turbine and not the river bottom beneath it.

Cost

- A single beam acoustic monitoring system from Vendor 16 (the same system that could be used to monitor fish populations through a mobile survey) costs \$40,000 for the Echosounder, cabling, a transducer, and all of the necessary software to run the system. Additional costs of hiring someone to drive a boat over the site must also be factored in.
- A similar product from Vendor 22 costs a little over \$34,000. The system would need to be mounted to a boom (as shown below) or some other rigid structure to ensure that the unit stays at a fixed height which otherwise would throw off the measurements.
- A day rate was provided by Vendor 2 for conducting a single beam bathymetric survey over FFP's project site. The pricing for a full day's work on FFP's project site is \$3,450.
- A system from Vendor 20 (ES70) which costs a little over \$48,000 would serve the same as the system from Vendor 16 as it could be used to monitor both fish population as well as to collect bathymetric data from the river bottom.



Figure 2 - Stratabox 3510 Installed on a Boom Mount

2.2 Dive Team Video Monitoring

Once the turbine array has been deployed a diver would be sent down to provide video and images of the bases of the pilings to identify any scouring effects. Anchors with steel cables would also have to be deployed to be used as a guide for the divers.



Figure 3 - Diver Filming Underwater

Pros

- A diver provides a wide field of view of the bases of the pilings.

Cons

- With the visibility level of the water in Mississippi River, this method is impractical.
- Installation of the anchors needed to provide anchoring for the divers could interfere with river traffic and affect the deployment habitat.
- Images produced could provide relative information as to how much scouring there is around FFP's pilings but it would not be able to provide quantifiable data.

Cost

- Due to the impracticality of this option, a cost estimate was not determined.

2.3 Install Scour Detection Units

- Install 4 of Vendor 23's new scour units on the downstream faces of FFP's pilings to monitor scour around the pilings and one unit on the forward face of one piling. For a direct comparison of pre-deployment vs. post deployment near field bathymetry data the GPS coordinates of the data would be recorded and then the surveyed data would be compared to the GPS coordinates that the scour unit would be detecting once the pilings and turbines have been installed.

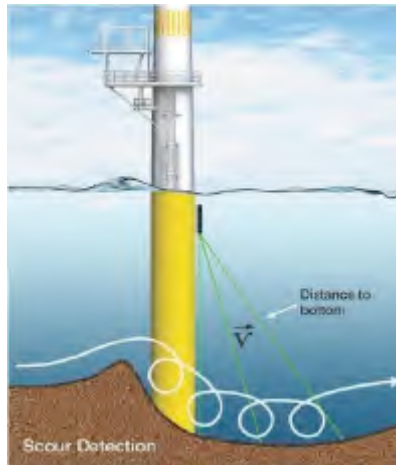


Figure 4 - Scour Detection Unit on an Offshore Wind Turbine

Pros

- These instruments would provide concrete data to quantify scouring.
- Installed unit would have little effect on the in-situ site environment.

Cons

- The range of the device would be limited and it would be impossible to characterize the whole project area.

Cost

Vendor 23 has two different kinds of scour units, a 1MHz unit and a 2MHz unit. Both of these units are in their developmental stages, the beam angles for both systems from the vertical are 10° , 20° , 30° , and 45° . The 1MHz system has a longer range but a more coarse resolution and the 2MHz system is naturally just the opposite. The 1MHz system has a range of 30m and measures accurately to within 3cm, while the 2MHz system has a range of 10m and measures accurately to within 1.5 cm. The ballpark cost for one scour unit is \$15,000. A precise cost is not available as this product is still in development.

2.4 Install River Height and Current Instrumentation (Option 1)

Install a river velocity sensor and a river height sensor in front of a turbine piling. A rough sketch of the proposed fixture can be seen below.

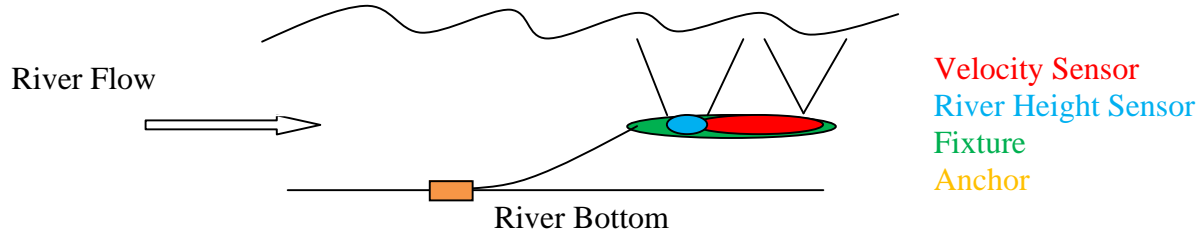


Figure 5 - Diagram of Proposed Flow and Height Monitoring System

Pros

- This sensor configuration would lead to minimal environmental impact.

Cons

- Measurements (especially with river height) may vary as the system's height relative to the river bed fluctuates as currents become stronger/weaker. A weaker current will allow the device to float up to the surface higher, while a stronger current, with the increased drag force, will lower the unit.
- Deployment of an anchored system could disrupt river traffic.

Cost

The AquaDopp system, which was previously purchased by FFP for the floating mount, costs \$8,780. The AWAC records wave height, so for purposes of the study FFP could take the recorded wave heights and average them over the course of a day for river height. The ballpark pricing on an AWAC unit is \$24,000. Data is recorded internally and would need to be retrieved in order to acquire the data. In lieu of the AWAC sensor, a pole could be drilled onto the top side of a riverbank where a yard stick or some other measurement device could be mounted to record the change in river height.

2.5 Install River Height and Current Instrumentation (Option 2)

Install a Vendor 24 deployment unit in front of a turbine piling with the ADCP and river height monitoring equipment installed.



Figure 6 - Seaspider System with Attached Sensors

Pros

- The Seaspider can take on many different sensors as it has a variety of mounting brackets.
- The Seaspider will be fixed on the river bed and thus measurements will not fluctuate with river flow as in the previous example.

Cons

- River sediment may cover the Seaspider and thus make the measurements useless.
- Deploying an anchored system in the middle of the river could disrupt river traffic.

Cost

A Seaspider costs \$2,880 though this does not include any additional mounts that may need to be installed in order to accompany the sensors. The AWAC records wave height, so for FFP's study we could take the recorded wave heights and average them over the course of a day for river height. Data is recorded internally and would need to be retrieved in order to acquire the data. The ballpark pricing on an AWAC unit is \$24,000. The AquaDopp was previously purchased by FFP for the floating mount for \$8,780. In lieu of the AWAC sensor, a pole could be drilled onto the top side of a riverbank where a yard stick or some other measurement device could be mounted to record the change in river height.

2.6 Install River Height and Current Instrumentation (Option 3)

Install the ADCP sensor directly above the turbine using the mounting arms as a base. The sensor would be secured in a metal container that would connect directly with the top most mounting bar on the turbine. For the river height monitoring a pole would be mounted on shore with a meter stick or other measurement device attached to it. A remote camera would monitor the river height with a live video feed.

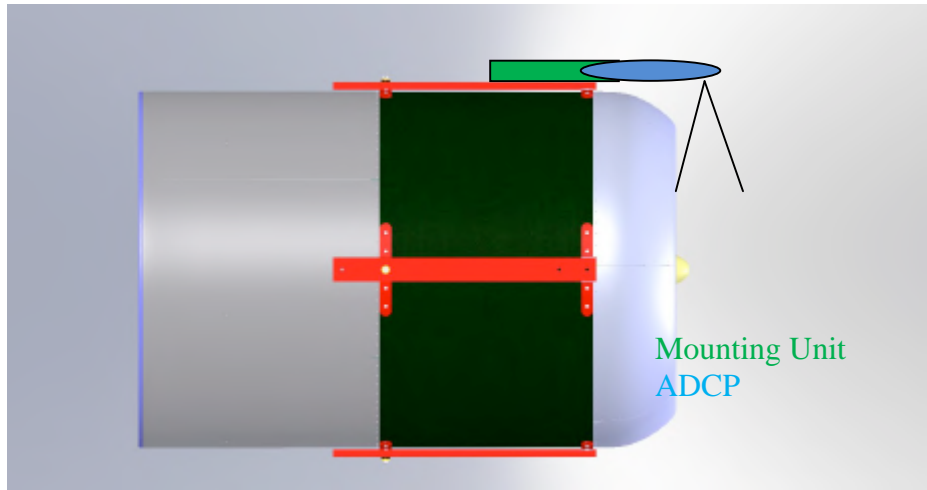


Figure 7 - Depiction of ADCP Mounted to the Turbine

Pros

- The flow going directly into the blades of the turbine can be characterized by this methodology.
- The ADCP is stabilized by the turbine so its positioning relative to the turbine will not change.

Cons

- In this configuration the ADCP is only going to be retrievable by divers.
- The placement of the ADCP would affect the flow of water over the turbine, though this can be assumed to be a trivial effect.

Cost

- The cost of an ADCP unit from Vendor 23 as previously stated is \$8,780. The price of a mounting unit to hold the ADCP in place would be roughly \$300. The cost of possibly drilling additional tapped holes into the mounting bar must also be factored in, which would be roughly \$50 per hole. A wireless camera to monitor the river height would be approximately \$100 and a metal pole, meter stick, and a means to secure the two together would cost approximately \$50 dollars. A total estimate for this effort would be \$9,330.

2.7 Mobile Side-Sonar Scans

Conduct periodic side sonar scans to get a visual image of the river bottom before and after deployment.

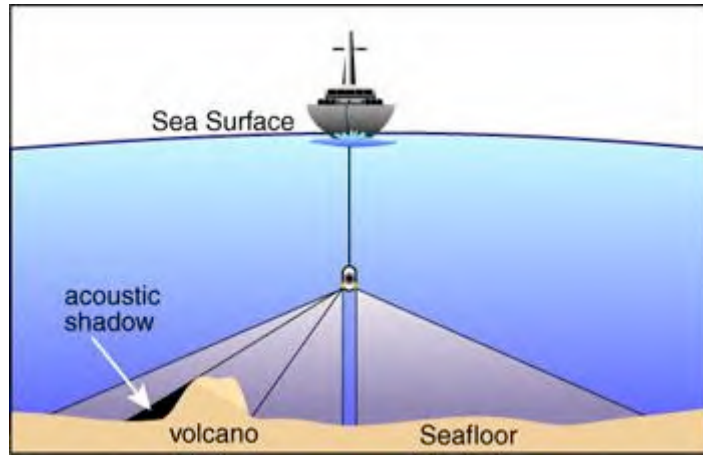


Figure 8 - Side-Scan Sonar System

Pros

- With a side-scan sonar it is possible to get a more complete look at the bottom of the river.

Cons

- The depth data gathered is an average over a wider field of view thus it is less accurate than the previously mentioned hydro acoustic survey.
- The system is more favorable if you are interested in looking at the images of a river bottom than trying to determine the depth of the river as a whole.

Cost

- Vendor 22 has an AquaScan system that has a retail cost of \$7,875. The cost for renting a boat to tow this device must also be factored in. Based on day rates from Vendor 2 this would be \$1,580 for a 10-hour day of monitoring.

2.8 Mobile ADCP Surveys

Conduct periodic mobile surveys to profile the river velocity both upstream and downstream of the project site.



Figure 9 - Boat Conducting ADCP Survey

Pros

- With a mobile survey it is possible to classify a broad range of areas along the project site.

Cons

- With periodic scans only small snap shots of characteristic flow are taken which makes it difficult to see the gradual change of flow over time.

Cost

- The system from Vendor 24 costs \$23,690, which does not include the cost of an accompanying GPS system that costs \$1,775. The cost of someone driving a boat with this unit installed over the project site as well as the cost of a mounting device for the sensors must be incorporated. Based on day rates from Vendor 2 this would be \$1,580 for a 10 hour day of monitoring.

2.9 Renting a Multi-Beam Sonar System for Mobile Surveys

Survey the project area with a multi-beam sonar system for increased resolution and a wider field of view than the single beam system.

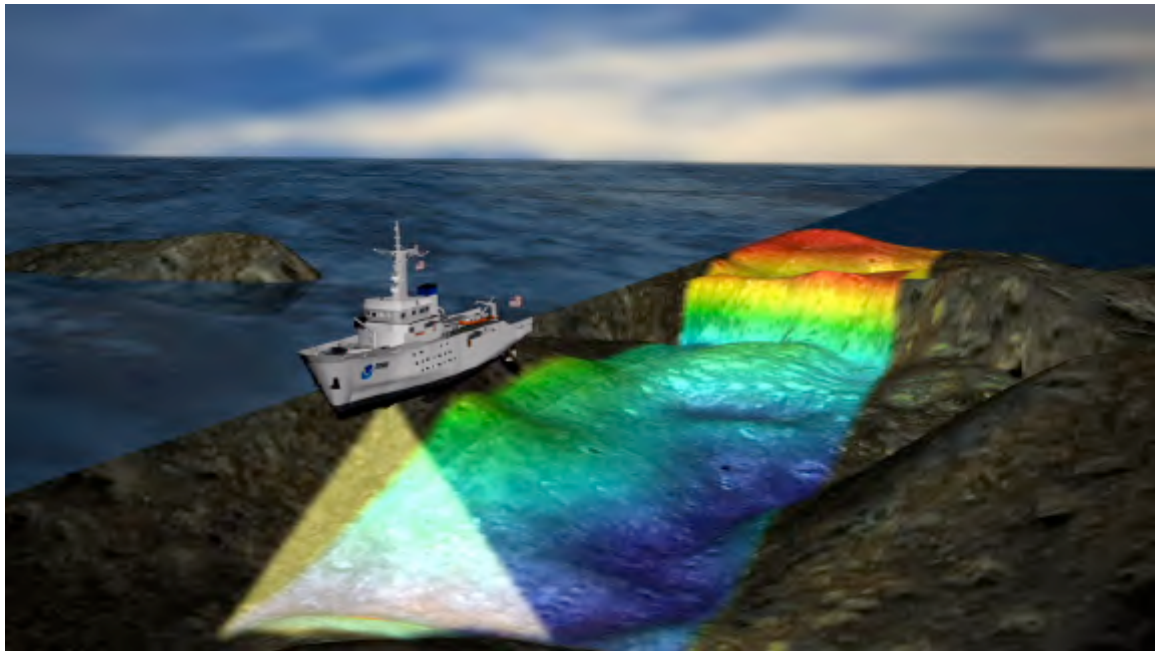


Figure 10 - Ship Conducting a Multi-Beam Sonar Survey

Pros

- A multi-beam survey has a higher resolution than a single beam survey.
- The width of the beams from a multi-beam survey is far greater than a single beam survey which cuts down on survey time.

Cost

- A system could be rented through Vendor 5 for \$1,000/day.

2.10 Perform Suspended Sediment Surveys

Perform periodic suspended sediment surveys to characterize the levels of suspended sediment over the project area. This would involve a boat and two workers on board to drive the boat and to perform the river sample collection. In talking to a representative of the USGS – Vickburg, the USGS does suspended sediment surveys as follows: surveys are conducted once a month at Natchez, MS, Vicksburg, MS, and Arkansas City, AR. Sediment samples are taken at four depths, 84% of the total depth, 57% of the total depth, 32.3% of the total depth, and 10.7% of the total depth. Six different sampling points are chosen along the river based on the cumulative discharge. The process for determining the points along the river is done by starting at one bank and going across the river until 8% of the total discharge of the river is in-between the surveying boat and the bank. This marks one point and the same process is used for points that mark 25%, 42%, 58%, 75%, and 92% of the total discharge. The sampler used is a P61 sampler or an equivalently sized isokinetic device. Lastly two different sieves are used to characterize the sediment, a total sands sieve and a total seines sieve. The differentiation between being categorized as a sand or a seine is having an average diameter greater than or less than .0625cm (for sands it is greater .0625cm, for scenes less).



Figure 11 - Suspended Sediment Surveying on the Colorado River

Pros

- Characterization of the level of suspended sediment around the project site is feasible.
- The surveying is quick and relatively inexpensive.

Cons

- Levels of suspended sediment will vary as you move away from the riverbed so the results of this survey are not indicative of the entire river column.

Cost

A day rate for a suspended sedimentation survey from Vendor 2 would cost \$1,650 to retrieve the samples. Vendor 2 also contacted a lab in the Memphis District which was willing to perform the data analysis of the samples. The lab would charge a rate of \$10 for every sieve used per sample. A small fee would be added from Vendor 2 for use of their containers. After talking to the chief river engineer at USGS-Vicksburg the typical suspended sediment survey is conducted where four different vertical samples are taken at six different points on the river for a total of twenty four different samples. USGS-Vicksburg also uses two different sieves for each sample to break down and characterize the samples. This brings the rough total cost of a suspended sediment survey to \$2,130.

2.11 Install Optical Backscattering Systems Near the Project Site

Optical backscattering sensors would be installed on mounts on the piling to record the turbidity of the water flow.



Figure 12 - Optical Backscattering Sensor

Pros

- Suspended sediment in the river could be continuously monitored.
- The sensor has the built in ability to remove the effects of bio fouling.

Cons

- This sensor detects the turbidity of the water column and converts that recorded value to suspended particle concentration. There are two major short comings with this methodology⁷:
 - The turbidity to suspended sediment concentration calibration is dependent on particle size.
 - The turbidity to suspended sediment concentration calibration is dependent on particle color.
- The sensor would have to be retrieved in order to acquire the data as it logs the data internally.
- The harsh conditions of the Mississippi River may degrade the accuracy of this sensor if it is placed in the river for prolonged periods of time.

Cost

- Vendor 25 has a single beam sensor that with internal recording and battery capabilities costs \$5,890. Vendor 25 also has a triple beam sensor which is more accurate that was roughly estimated to cost \$16,000 with an internal battery and recording ability.

⁷ Agrawal, Y.. "Sediment Monitoring Technology for Turbine Erosion and Reservoir Siltation Applications." *Sedinet*. Sedinet, 2011. Web. 15 Jun 2012. <http://www.sedinet.info/pdf/Agrawal_Prague_Paper.pdf>.

2.12 Install Laser Diffraction System to Monitor Suspended Sediment



Figure 13 - Laser Diffraction System

Pros

- With this unit it is possible to determine the mass concentration of particles in the water column.
- The system outputs volume concentration of particle size ranges in different size ranges over an overall measurement range of 2.5-500 microns.
- These instruments would be something that could either be sold at the end of FFP's monitoring effort or they could be used again when monitoring another site.

Cons

- An array of these instruments would need to be used to characterize the sediment in all vertical transects of the river.
- Fouling from a long deployment period may disable the unit.

Cost

- The cost of a laser diffraction system from Vendor 26 that can be submerged in the water is \$35,300.

2.13 Install Vendor 23Scour Units on Mounts Near the Piling to Characterize Suspended Sediment.

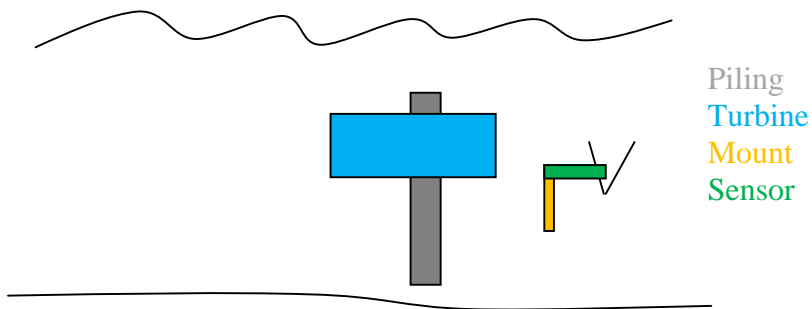


Figure 14 - Scour Unit Measuring Backscatter from Suspended Sediment

Pros

- Suspended sediment in the river could be continuously monitored.
- A fixture could potentially be made to change the orientation of the units on the piling monitoring scouring so that the sensor could monitor suspended sediment periodically.

Cons

- The sensor would only be able to measure backscatter and would not be able to characterize particle size of the suspended sediment. The useful output data from an acoustic instrument such as the scour unit would be the relative change in sediment concentration though it will not tell you why the concentration has changed. You will therefore not know if it is more numerous small particles that have come into the flow or fewer, larger particles that are no occupying the flow.

Cost

- The cost for a scour unit from Vendor 23 is \$15,000. The pricing for a mounting fixture would also have to be factored into the cost and can be estimated to be \$300.

2.14 Install Accelerometers and Strain Gauges to the Piling to Monitor Vibration and Forcing on the Installed System. Each piling will have one accelerometer and one strain gauge.

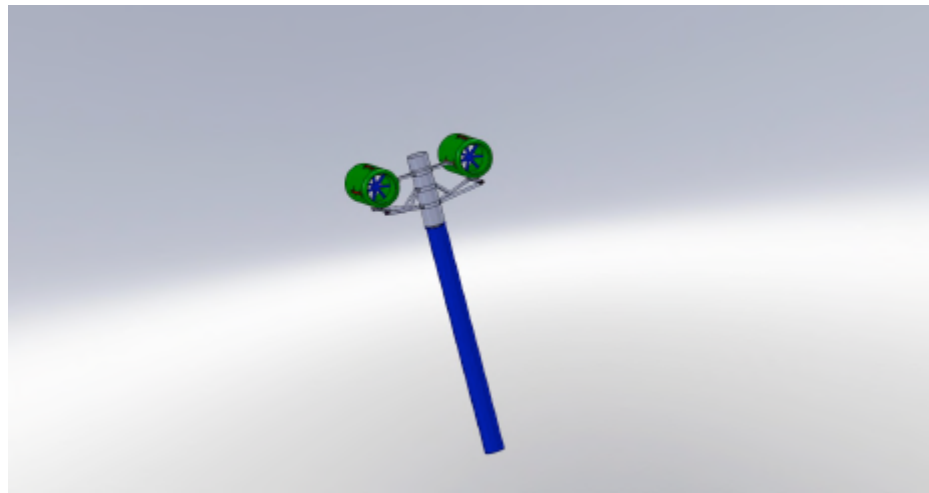


Figure 15 - A Simplified Version of Our Piling and Turbines

Pros

- This monitoring method will deliver real time data on the forces on the piling as well as the vibration caused by the turbines as they rotate on the piling.

Cons

- The determination of these forces could be modeled out using ANSYS and other modeling software so this monitoring effort may not be necessary.

Cost

- Vendor 27 sells water proof accelerometers for \$185/unit with a \$160 50 ft. cable, a \$125 magnetic mount, and a \$525 dollar power supply. A total cost for all accelerometers and associated equipment on FFP's four pilings would be \$3,980. Strain gauges cost \$9,800 a piece and each need an amplifier which costs \$2,720 (pricing for both from Vendor 28), and lastly \$180 for a 100ft. cable. A total cost for all strain gauges and associated equipment on four pilings would be \$50,800. Vendor 29 sells underwater DAQ systems for \$4,750. Five would be needed for FFP's project site each with 100ft of cabling (estimated) at \$3/foot for a total combined price of \$25,250.

3 Recommendation

The following table summarizes the options reviewed.

River Sediment Monitoring						
	Vendor 23 Scour Scanners - Scour	Suspended Sediment Surveys	Optical Backscattering System	Laser Diffraction Monitoring System	Vendor 23 Scour Scanners - Suspended Sediment	Comments
Is this method practical for FFP's deployment?	Yes	Yes	Yes	Yes	Yes	
Far or near field installation bathymetry monitoring?	Near	Far	Near	Near	Near	
Can it quantify sediment data?	Yes	Yes	Yes	Yes	Yes	
Will this data be available over a live feed?	No	No	No	No	No	
Is this method harmful to the river environment?	No	No	No	No	No	
Relative cost?	High	Moderate	Low	Moderate	Low	
Relative risk of not achieving a useful result?	Low	Low	Moderate-High	High	Moderate-High	The optical backscatter system and the Vendor 23 scour monitors (for S.S.) can calculate suspended sediment concentration but a lot of assumptions need to be made in order to make the proper calculation. A laser diffraction system would have a high likelihood of becoming fouled for a long deployment period.

River Velocity Monitoring Methods					
	River Condition Monitoring Option #1	River Condition Monitoring Option #2	River Condition Monitoring Option #3	Mobile ADCP Survey	Comments
Is this method practical for FFP's deployment?	Yes	Yes	Yes	Yes	
Can the devices be retrieved from the river bottom after it has been deployed?	Yes	Yes	No	N/A	Retrieval would have to be done with either divers or more likely a deployable air balloon released from the units.
Will the data be available in a live feed?	No	No	No	Yes	Data could be run through a cable to shore though it does not seem necessary.
Is this method harmful to the river environment?	Yes	Yes	Yes	No	All methods harm the river in a trivial manner.
Relative cost?	Moderate	Moderate	Moderate	High	
Relative risk of not achieving a useful result?	Moderate	Moderate-High	Low	Low	Option #1 will not be reliable in monitoring river height (if a river height sensor is installed) as the height of the sensor in the water will fluctuate with flow rate. Option #2 will be less reliable as sand and sediment has a high probability of covering the sensors and making measurements useless.

River Bathymetry Monitoring Methods					
	Mobile Acoustic Surveys	Dive Team Video Monitoring	Mobile Side-Scan Sonar	Multi-Beam Survey	Comments
Is this method practical for FFP's deployment?	Yes	No	Yes	Yes	
Far or near field installation bathymetry monitoring?	Far	Near	Far	Far	
Can it quantify bathymetric data?	Yes	No	No	Yes	
Is this method harmful to the river environment?	No	Yes	No	No	All methods have minimal environmental impact.
Relative cost?	Moderate	High	Moderate	Moderate	
Relative risk of not achieving a useful result?	Low	High	High	Low	A dive team would not be able to see anything due to the murky waters in FFP's project site. A side-scan sonar would not be able to provide quantifiable data for FFP's project site.

3.1 River Sediment Transport

It will be useful to monitor the effects of FFP's turbine array down river even though the likelihood of FFP's turbines interfering with the natural sediment movement downriver is low. To monitor, this mobile acoustic bathymetry surveys could be conducted once a month in the deployment region for both the pre and post deployment period. For pre-deployment surveys will be done in close proximity to the intended locations of the pilings so that scour data can be coupled with the mobile surveys during the pre-deployment stage to gauge near field scour change.

3.2 Pile Scouring

For close proximity monitoring for scouring effects the Vendor 23 instrumentation should suit FFP's study needs. Though the risk of scouring at the base of the piling is low, without the instrumentation from Vendor 23 there is no way to prove that scouring at the base of FFP's pilings is not occurring. It is likely that more scouring will take place behind the pilings than in front of them, which is why four units should be placed behind the piling while one unit should be placed in front of one piling to monitor the effects of scouring in front of a piling.

3.3 Velocity and Suspended Sediment

Flow up and down stream of FFP's project site must also be characterized and that can be done with mobile ADCP surveys to monitor any change in the characteristic flow of the river for pre and post deployment. Option 3 presented above provides a slightly more reliable option than choices 1 and 2 given how much sedimentation is moving through the river and the risk that a Seaspider mount may get buried in the river bed over the course of the monitoring period. To further monitor the ever-changing river conditions suspended sediment surveys will be conducted, on average, every two weeks to characterize suspended sediment in different flow conditions. Surveys may be done at times when flow has significantly changed to characterize suspended sediment levels at different rates of flow. USGS does monthly surveys, but were surveys to be done at a higher frequency the seasonal variations of river flow over the course of a year could be captured in a six-month period.

3.4 Piling Force and Vibration

Installing accelerometers and strain gauges to FFP's pilings is another potential facet of FFP's monitoring effort to characterize the forcing and vibrations on FFP's systems.

4 Cost Analysis

For the far field monitoring FFP has received a quote from Vendor 2 on a day rate for the cost of conducting a mobile survey that would acquire bathymetric data, river flow data, and suspended sediment data. This service comes at the rate of \$3,450 per survey; which propagates to a cost of \$20,700 for the pre deployment phase, a cost of \$41,400 for the deployment phase, and a total cost of \$62,100 for both.

For the near field monitoring effort, the cost of the five scour units from Vendor 23 can be estimated to be \$75,000 in total (\$15,000 per unit).

Vendor 27 sells water proof accelerometers for \$185/unit with a \$160 50 ft. cable, a \$125 magnetic mount, and a \$525 dollar power supply. A total of four of these instruments would be needed (one per piling) which would cost a total of \$3,980. Strain gauges from Vendor 28 cost \$9,800 for a submersible unit, which also needs an amplifier that costs \$2,720. The cost of cabling which would be \$180 for a 100ft for the strain gauge. The combined cost for all four pilings for the strain gauges and their accessories would be \$50,800.

Activity	Cost	Comments
(Pre-deployment) Bi-weekly mobile surveys to with a mobile ADCP sensor and a single beam acoustic sensor to monitor river flow velocity and bathymetry respectively. The pre-deployment surveys will also involve taking suspended sediment samples over the project site.	\$47,160*	<p>-This pricing is from a quote received by FFP from Vendor 2 for a day's work of surveying and data analysis (\$3,450/day).</p> <p>-For suspended sediment specific costs, a lab in Memphis quoted the price of \$10 for every sieve used in the analysis per sample, with 24 samples and 2 sieves for each sample that brings the total cost to \$480 per survey.</p>
(Post Deployment) Bi-weekly mobile surveys to with a mobile ADCP sensor and a single beam acoustic sensor to monitor river flow velocity and bathymetry respectively.	\$82,800*	<p>-This pricing is from a quote received by FFP from Vendor 2 for a day's work of surveying and data analysis (\$3,450/day).</p>
(Post Deployment) Install accelerometers and strain gauges to the pilings to characterize piling vibration and forcing respectively.	\$80,030	<p>Accelerometer -\$185 (Vendor 27 ACC786 accelerometer) -\$160 (50ft. cable) -\$125 (magnetic mount base) -\$525 (power supply)</p> <p>Strain Gauge -\$180 (cost of 100 ft. of polyurethane cabling) -\$9,800 (cost of a submersible unit from Vendor 28) -\$2,720 (cost of an amplifier from Vendor 28).</p> <p>Data Acquisition System -\$23,750 (cost of five DAQs from Vendor 29 at \$4,750/DAQ) -\$1,500 (price of cabling for DAQs at \$3/ft for 500 total feet (100ft/DAQ))</p>
(Post Deployment) Install five scour units on the pilings of FFP's turbines, four looking leeward of the flow and one looking up river.	\$75,000	Pricing is from Vendor 23 (the scour unit is still in its developmental stages and pricing now is estimated between \$12,000-\$15,000 per unit).

(Post Deployment) Install an ADCP sensor on top of the turbine pointing down into the flow going into the turbine.	\$9,230	-\$8,780 for an AquaDopp sensor from Vendor 23. -\$300 for a mounting fixture to the turbine mounting arm. -\$100 for drilling holes into the mounting arm. -\$50 for mounting a measuring device to the river bank.
Total Cost	\$294,220	

*Note on the total cost matrix, the cost for the mobile surveys for the hydraulic surveys and the fish population surveys are split between the two, since the same survey boat will be doing the hydraulic and fish population surveys." The cost on the cost matrix reflects the actual cost, the cost in this document reflects the cost ONLY associated with the mentioned surveying.

Appendix 7

NAVIGATION MONITORING METHODOLOGY



239 Causeway Street
Boston, MA 02114-2103
USA

MAIN: (978) 252-2822
FAX: (617) 367-3372

www.free-flow-power.com

Filename: 2012-06-28_R01_Navigation_Insitu_Study_Plan

Subject: In-situ Monitoring Plan for River Traffic

Date	Release Rev	Description
05-04-2012	00	Original
06-28-2012	01	Revisions after initial review

1 Requirements of FERC's Study Plan Determination

- (1) Assess existing river navigation patterns relevant to the Free Flow Power projects
- (2) Determine construction and maintenance practices that would minimize impacts to river navigation and risks to public safety.

Requirement (1) is not relevant to the in-situ monitoring plan and will be addressed elsewhere. Requirement (2) will be addressed by the in-situ monitoring plan and will be the basis of this document.

2 Methods Executed by Other Companies

2.1 ORPC-Cobscook Bay (P-12711)¹

- The studies conducted showed that commercial and recreational navigation would not be a significant factor in their project area.
- Local dredgers, commercial fishing boats, and commercial shipping via radio broadcasts were contacted so as to give the coordinates of the project site.
- An exclusion zone that surrounded the project site was installed that utilized lighted buoys to mark off the project area to shipping.

¹ Ocean Renewable Power Company, 2011. Safe Guard Plans, Final Pilot License Application Cobscook Bay Tidal Project, FERC Project Number 12711. September 2011.

2.2 Verdant (P-12611)²

- A video camera monitoring system was installed with a live feed over the project site, mostly to monitor recreational boat traffic.
- Places around their project site where recreational boats could be rented were contacted to explain their project and how it may affect recreational travel over the project site.
- The initial project site was marked off so that boats could not travel inside of it.

2.3 SnoPud-Hydroelectric (P-2157)³

- Navigation of commercial or recreational boats was not relevant to their project thus no research was initiated.

2.4 SnoPud-Tidal (P-12690)⁴

- The deployment area was monitored by Vessel Tracking Service (VTS), which mapped out the number of minutes vessels were in a certain spot over a year.
- Coordination with the Coast Guard was done to make the project site a Marine Exclusion zone so that no anchoring occurs at the project site.

2.5 MCT-SeaGen⁵

- Through all of the SeaGen documentation there was no mention of monitoring traffic at any of their projects sites including the site that is currently operational.
- It should be noted that some documents on their website were forbidden from public viewing and that only a portion of their documents were available.

3 Monitoring Options

The ultimate goal of this plan is to determine the financial impact that FFP's deployments will have on the commercial shipping traffic that uses the Mississippi River, specifically the section of river that is part of FFP's *in situ* deployment site.

² Verdant Power, Inc. 2010. Pilot License Application Roosevelt Island Energy Project, Volume 2, Exhibit E Environmental Report, FERC Project Number 12611. December 2010.

³ Snohomish County Public Utility District 1, 2010. Henry M. Jackson Hydroelectric Project, Fisheries and Habitat Monitoring Plan, FERC Project Number 2157. September 2, 2011.

⁴ Snohomish County Public Utility District 1, 2012. Admiralty Inlet Tidal Project, Application for a New Pilot Project License (Minor Water Power Project), Volume 2 Exhibit E, FERC Project Number 12690. February 29, 2012.

⁵ Marine Current Turbines, 2011. SeaGen Environmental Monitoring Programme, Final Report. January 16, 2011.

3.1 Free Online Ship Monitoring

Utilize the website <http://www.marinetraffic.com/ais> to monitor FFP's *in situ* deployment site on the Mississippi River.

3.1.1 Pros

- This website can be used free of charge and is readily accessible.
- With this service it is possible to monitor FFP's site with no investment in permanent equipment.

3.1.2 Cons

- This website may not be able to provide adequate service for monitoring a specific section of the Mississippi River as it has no data recording abilities or any archived data.
- With this website it will not be possible to monitor recreational vehicle traffic over FFP's project site.

3.1.3 Cost

- There is no cost associated with this system.

3.2 Using a AIS Monitoring Company

Pay a monthly fee to monitor river traffic over FFP's *in situ* site through a company with installed AIS systems.

3.2.1 Pros

- Through these means it is possible to monitor FFP's site with no investment in permanent equipment.
- Vendor 12, a web based AIS monitoring company, has the ability to create a custom monitoring zone on a location on the river.
- Vendor 12 will coordinate with Free Flow Power if one of FFP's sites falls out of Vendor 12's monitoring area to lower the cost for FFP's ability to monitor in that area.

3.2.2 Cons

- It will not be possible to monitor recreational vehicles through Vendor 12 or an equivalent service.
- An AIS unit may not be stationed near one of FFP's project sites, therefore we will not be able to monitor certain sites with one of these companies.

3.2.3 Cost

Through Vendor 12 the price for using their services is \$2,000/year. If we have a deployment site where Vendor 12 does not have coverage we have the option of renting an AIS receiver through Vendor 12. An AIS receiver needs an electrical and internet connection in order to function.

Vendor 12 has two services, the Plus service and the Advantage service. The Advantage service caters to data analysis while the Plus Service will provide us all of the monitoring needs that we would need for FFP's study. Vendor 12 confirmed that they had monitoring capabilities over all of FFP's project sites.

3.3 Purchase an AIS Sensor

Purchase an AIS sensor to monitor the project site directly.

3.3.1 Pros

- Isolated site monitoring would provide all of the information we would need for each site.

3.3.2 Cons

- The installed AIS sensor could be stolen as it will be left unattended.
- An AIS receiver depends on AIS transmitters to monitor river traffic and small recreational vessels will not have an AIS transmitter and will therefore not be monitored.

3.3.3 Cost

The cost for a AIS unit from Vendor 13 is \$4,000. This does not include installation of a mounting fixture and the necessary cabling to accompany this sensor.

3.4 Live Video Monitoring

Install cameras on the shore to monitor the in-situ site for both commercial and recreational traffic with live feeds and event counters.

3.4.1 Pros

- With live video monitoring it is possible to monitor both commercial and recreational river traffic.

3.4.2 Cons

- The cameras may get stolen as they will be left unattended to monitor the site
- Event counters installed and integrated into the system may mistakenly detect birds or other objects in the river and mistake them for boat traffic.

3.4.3 Cost

Lots of systems from various suppliers that cost around \$500 for multiple cameras and cabling. A mount to secure the cameras would have to be factored into the cost.

3.5 Acoustic Sensor

Use acoustic sensors to detect ship traffic by noting spikes in readings.

3.5.1 Pros

- Instrumentation for this monitoring effort will already be deployed to monitor the noise generated by the turbine array.

3.5.2 Cons

- It will be impossible to differentiate between two boats if two boats pass the test area simultaneously.
- Other noises in the river could be mistaken for boat traffic, such as factory operation, river bank construction, ect.

3.5.3 Cost

The cost of an acoustic sensor from Vendor 14 that would be ideal for this deployment is \$5,900.

4 Recommendation

	Marine Traffic	Vendor 12	Purchase AIS Sensor(s)	Live Video Monitoring	Acoustic Sensor	Comments
Can the project site specifically be monitored?	No	Yes	Yes	Yes	No	
Can the number of commercial boats passing over the site be monitored specifically?	No	Yes	Yes	Yes*	No**	*Event counter may be triggered by non-marine traffic **Acoustic sensor may not pick up multiple boats if multiple boats pass over the site simultaneously
Is installation of onsite equipment required?	No	No	Yes	Yes	Yes	
Can recreational traffic be monitored?	No	No	No	Yes*	No	*Event counter may be triggered by non-marine traffic
Relative cost?	Free	Low	High	Low	High	
Relative risk of not	High	Low	Low	Moderate	High	Marinetraffic.com will not be able to

achieving a useful result?						log vessel history at open points on the river. A live video monitoring system may not be triggered every time a ship travels through FFP's project site. An acoustic sensor will not be able to characterize or quantify the traffic that passes over the project site.
----------------------------	--	--	--	--	--	--

5 Analysis

Though live monitoring and historical monitoring will make up a big part of the navigation study, coordination with shipping companies on the river is still going to be very important during the installation of the pilings, turbines, and necessary monitoring instrumentation.

6 Total Cost Analysis

Vendor 12's system will cost \$2,000 for a year's subscription, resulting in a total payment of \$4,000 for the 18-month period of monitoring of the *in situ* deployment site.

Activity	Pricing	Comments
(Pre-deployment) Monitor commercial traffic with a one year subscription to Vendor 12.	\$2,000	Priced in the event that it is not possible to buy a six month subscription to Vendor 12.
(Post-deployment) Monitor commercial traffic with a one year subscription to Vendor 12.	\$2,000	
Total Cost	\$4,000	

Appendix 8

DAMAGED TURBINE AND DEBRIS RISK STUDY FIFTH REPORT

SECTION 4**Damaged Turbine and Debris Risk Study**

The goals of Free Flow Power's (FFP) Damaged Turbine Recovery and Debris Risk Study (Damaged Turbine Study) are as follows:

- To assess the risk of damage to turbines or other infrastructure as a result of debris or other foreseeable conditions, including the probabilities of occurrence of such damage;
- To determine any adverse impacts associated with damaged turbine features, including abandoned pilings, broken turbine housings or blades and, if necessary, to determine how damaged turbines would be recovered from the river.

In the First Quarterly Study Report (1Q Report), FFP provided information regarding recovery requirements and constraints by agencies; a preliminary design of support structures and proposed installation approaches; and information regarding the presence and characteristics of neutrally-buoyant or floating debris transported by the river.

In the Second Quarterly Study Report (2Q Report), FFP supplied information and analysis regarding responses to comments received from the Commission regarding the 1Q Report; preliminary assessment of risk to turbines; evaluation of recovery approach options, available salvage resources, and recovery operation feasibility and constraints; a plan for analysis of potential effects of debris on turbines and piling mounting systems, focusing on structural factors and risk of turbine damage; synthesis of hydraulic data on debris; and preliminary design of piling turbine mounting structures and analysis of loads and vibrations, including potential effects on U.S. Army Corps of Engineers (USACE) structures.

In the Initial Study Report, FFP provided information consisting of: responses to comments received from the Commission and the U.S. Coast Guard (USCG) regarding the 2Q Report; a photographic record of observations of large neutral-buoyancy debris and accumulations of floating debris transported by the river, including accumulated trees, root wads, and other large debris that can be observed at low water at some locations; and a detailed plan for analysis of potential effects of debris on barge-mounting systems focusing on structural factors and risk of turbine damage and barge breakaway.

In the Fourth Study Report, FFP provided additional information for: A narrative description of FFP's in-river deployment of its three-meter hydrokinetic turbine (3M01) on a newly fabricated floating mount (FM) and the results of that deployment that FFP has recorded to date. Observations regarding in-river debris, fish, and navigation traffic, and its effect on both the FM and the 3M01 turbine.

In this Fifth Study Report, FFP provides information regarding:

- A summary of consultation conducted regarding the 4SR, including responses to comments received from the Commission and USACE – Section 4.1; and
- A presentation of studies of damage to the turbine caused by debris, with a focus on the forward shroud – Section 4.2.

4.1 Consultation Summary and Outreach

4.1(a) Commission's Comments on 4SR

In the Fourth Interim Report, you describe your deployment of a barge-mounted 3-meter (diameter) turbine at a private dock for testing. Figure 4.1 of the report shows the Baton Rouge River gage timeline with a red dashed line labeled “Mooring threshold (<40-ft).” Please describe the meaning of this line as it relates to future planned deployments. What actions will be required if the water level is predicted to exceed 40 feet at this (or other) locations?

The mooring threshold described was required by the owner of the dock structure to which FFP's floating mount (FM) was attached. The owner preferred to wait until the water level receded beneath 40 feet before mooring the FFP equipment, so that the FFP equipment would not impede its pier work at that time in conjunction with high water levels in May 2011. There is therefore no particular reason that a barge based system deployment would be inhibited deployment at or above a 40 foot depth, or at an equivalent high river level at a different location

Please provide table 4.9 referenced on page 4-9 of the Fourth Interim Report; it appears to have been omitted from the report.

FFP apologizes for this misstatement. The reference to a Table 4-9 was unintentional, and no such table was intended to be included in the 4SR.

In its comments on the Initial Study Report, USCG comments that your response/recovery plan should address the risk management standards specifically identified in NVIC No. 02-07. On page 1-11 of your response to comments on the Initial Study Report filed on April 15, 2011, you state that you will expand your study to “address environmental and navigation safety issues...in the context of USCG’s risk management standards as requested.” Please ensure that your response/recovery plan addresses the specific risk management standards that are identified in NVIC No. 02-07.

FFP will ensure that NVIC No. 02-07 is consulted throughout the planning on all aspects of these Projects.

In table 4.8 in the Second Interim Report, you provided estimated probabilities and magnitude of damage to or failure of the turbine system from a variety of likely sources. Table 4.8 did not address potential effects from seismic loading or propeller wash loads, and some probabilities are shown as “to be determined.” Please provide estimates of these probabilities, as well as those shown for turbine component damage from debris in table 4.12 of the Second Interim Report.

Please see Section AIR 4 for a discussion of the potential effects of seismic loading and propeller wash loads, and Hydraulic Study Section 2.1 for the completion of estimates from Table 4.12.

As stated in our March 18, 2011, letter, this study should consider: (1) the potential effects on navigation and the cost of recovery; (2) the effects of unrecovered damaged turbine parts and

other hydrokinetic infrastructure on aquatic habitat, including habitat for rare, threatened, and endangered (RTE), and candidate species, as well as submerged cultural resources potentially occurring in the proposed project sites; and (3) the potential for seismic activity associated with the New Madrid Seismic Zone. As noted in our letter, you should be developing information to support proactive planning for response and recovery to a damaged turbine incident as called for in the Study Plan Determination and in anticipation of emergency action planning and risk management under the Commission's Part 12 requirements and under USCG's NVIC No. 02-07. In identifying damaged turbine recovery approach options, we recommend you provide a discussion of the operational limits for each option, including acoustic visualization, diving, or crane lift limitations, if any, in high current or other restrictive river conditions.

Should a part or system fail, the first analysis will be a determination of the appropriate time to attend to the failure. If a response for a failure can be deferred until an optimal time, such as a scheduled maintenance, or a low flow situation, then it would defer until that time. For example, if a part is failed and poses no risk of breaking away, then a request would be made to defer the recovery until lower flow conditions exist, although this would exclude a condition posing a threat to aquatic habitat or cultural resources. Another possibility is that a part breaks and remains stationary but must be removed immediately, even in high flow conditions. An example of this would be a turbine-piling being washed against a pier. This could occur during the day or at night, but in actual terms is fundamentally similar to recovering a sunken ship or barge. Barge cranes are frequently used for that type of recovery, and the weight and drag of a piling and turbines would be far less than a sunken barge or tug.

The Mississippi River has high turbidity, and lines of sight, even with lighting, are quite limited. Acoustic (including ultrasonic) methods, however, have virtually unlimited visualization capabilities in the depths and turbidity encountered in the Mississippi River, from side scanning commercial sonar (including “fish finders”) to high-resolution multi-beam equipment. With the high resolution available from these devices, they can also be used in conjunction with divers to aid in visualizing details before a dive, or, with handheld versions, to aid in seeing through the turbidity. In short, visualization is not a restriction in any condition expected in the Mississippi River.

This discussion is preliminary, and is intended to provide an initial evaluation of expected operations in these scenarios; it should be possible to recover any major system component regardless of river conditions. FFP will enlist the aid of salvage and recovery companies to gather their feedback and comments, and use these as the basis for a more formal inclusion of recovery restrictions in the recovery report.

Please describe your proposal for handling transmission cables if a site is decommissioned.

FFP is continuing to analyze the standard and most common practices for handling decommissioned cables in the Mississippi River and will provide a proposal in a future Study Report.

4.1(b) USACE Comments on 4SR

Table 4.9 is referenced but not found in the report.

FFP apologizes for this misstatement. The reference to a Table 4-9 was unintentional, and no such table was intended to be included in the 4SR.

4.2 Turbine Impact Damage

Although there are no quantitative values for the size of and amount of neutrally buoyant debris that might impact a turbine, it is still possible to calculate the amount of damage that could occur due to any arbitrary strike from such an impact. FFP's approach is to use energy methods and to evaluate how much energy a component could sustain, and how much the system (turbine and mounts) could reliably absorb. Ultimately, the impact model will be a set of springs and masses in series, with each component being modeled as a spring with the associated inertia (mass). As a strike occurs, first contact with the turbine will be either on the shroud, the nose cone, or the rotor.

The following analysis focuses on the shroud and explains the propagation and energy absorption path.

Beginning with the shroud and a debris strike on this component, forces will build up on the shroud causing it to deflect, while the force will simultaneously be transmitted to the primary turbine structure and the turbine mounts. The turbine and mounts will be displaced due to the forces, and will also absorb energy during this process. Resisting the displacement is the inertia and stiffness of the components. However, they still absorb some portion of the energy, with the result that the component with the initial contact (shroud in this case) does not have to absorb all of the kinetic energy from the debris.

Energy absorbed (E) can be defined as shown in Equations 4.2.1 and 4.2.2 below as the summation (integral) of Force (F) times distance (x), which becomes equation 4.2.2 for a linear spring with a fixed spring constant of k (F/x units).

$$\text{Eq. 4.2.1 } E = \int F dx$$

$$\text{Eq 4.2.2 } E_{\text{lin}} = 0.5 \cdot k \cdot x^2$$

The debris will have kinetic energy as defined below in equation 4.2.3, where m is the mass and v is the velocity. So long as the value of kinetic energy is below that of energy absorption, the part will not fail (the definition of failure will be discussed shortly).

$$\text{Eq. 4.2.3 } E_{\text{KE}} = 0.5 * m * v^2$$

A time-stepping model shows that the forces increase on the shroud with each time step, and this force both slows down the debris by absorbing energy and causes the rest of the turbine/mount

structure to move in relation to this force, further slowing the debris. If the shroud fails completely and the debris punches a hole in it, the debris can continue, albeit with reduced velocity and energy, to impact the next piece, which will absorb additional energy. At some point, unless the mass and velocity of the debris is high, the debris will have lost all its energy and the device will either continue to operate or fail structurally in some manner. The model can capture these effects during each small time increment as the series of springs and masses described earlier, but we have to account for any non-linearity's or failure of a part. This simply means that the spring constants of each part will be nonlinear and that once a part has reached its energy absorption threshold, it is removed from the model (spring constant set to 0).

Specialized commercial codes (DYNA3D, MARC, for example) are capable of complete dynamic impact analysis and operate as described above. FFP's approach is simpler but effective for conservative failure analysis using our existing commercial codes. FFP will use the SolidWorks Simulation Premium FEA package (previously COSMOS) with its non-linear capabilities, and a simple series of springs-masses to approximate results, with individual component analysis providing the equivalent spring constant and energy absorption for that part. A distinct limitation of this method is that the software stops when the first failure point is reached, which occurs when the first crack is initiated; non-negative stress-stain slopes are another restriction. Since a significant amount of energy will be absorbed beyond the crack initiation, this is a very conservative approach. Approximations and simplifications can be used to estimate total strain energy to failure of that part, and FFP will apply those methods in developing the series spring-mass models. Knowing what level of impact might create the start of a crack is conservative, but also provides a threshold below which no damage is expected. The primary focus of this analysis is the regulatory component, specifically to estimate if an entire turbine could break away, and for predicting the size and type of shards that may break off.

Equation 4.2.3 defines the kinetic energy of an object and shows the relationship of energy to mass and velocity squared. Figure 4.2-1 plots the mass of a log by size, and Figure 4.2-2 plots kinetic energy against mass for various values of velocity. The goal of the FEA analysis will be to overlay the energy absorption capability of the various parts, and then the entire turbine system on this chart.

[CONTINUED ON NEXT PAGE]

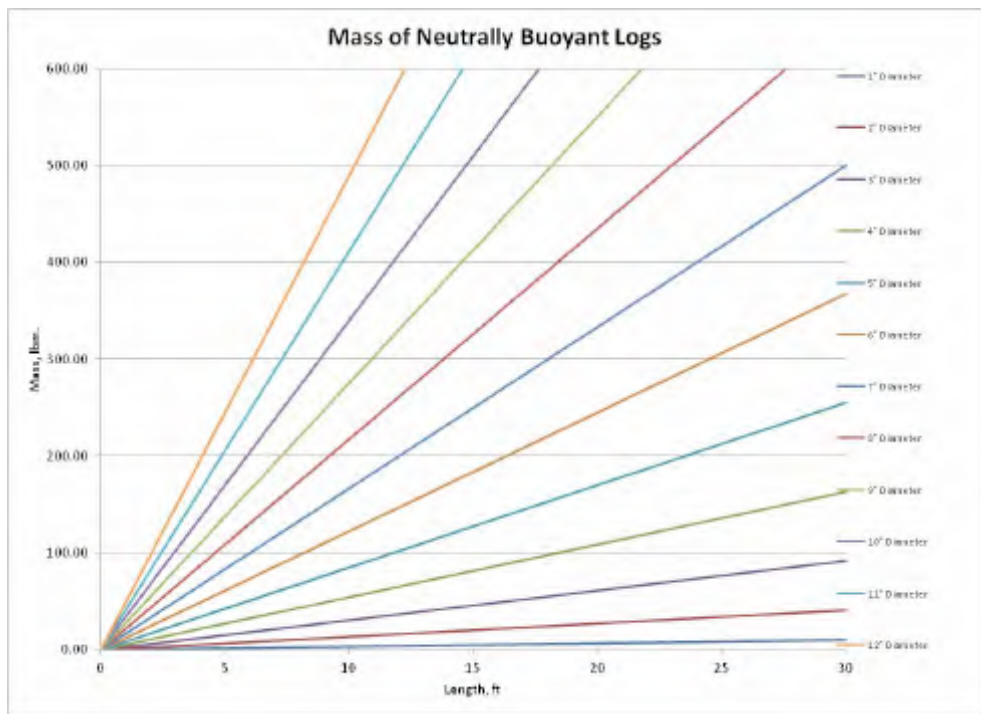


Figure 4.2-1. Mass of log by size

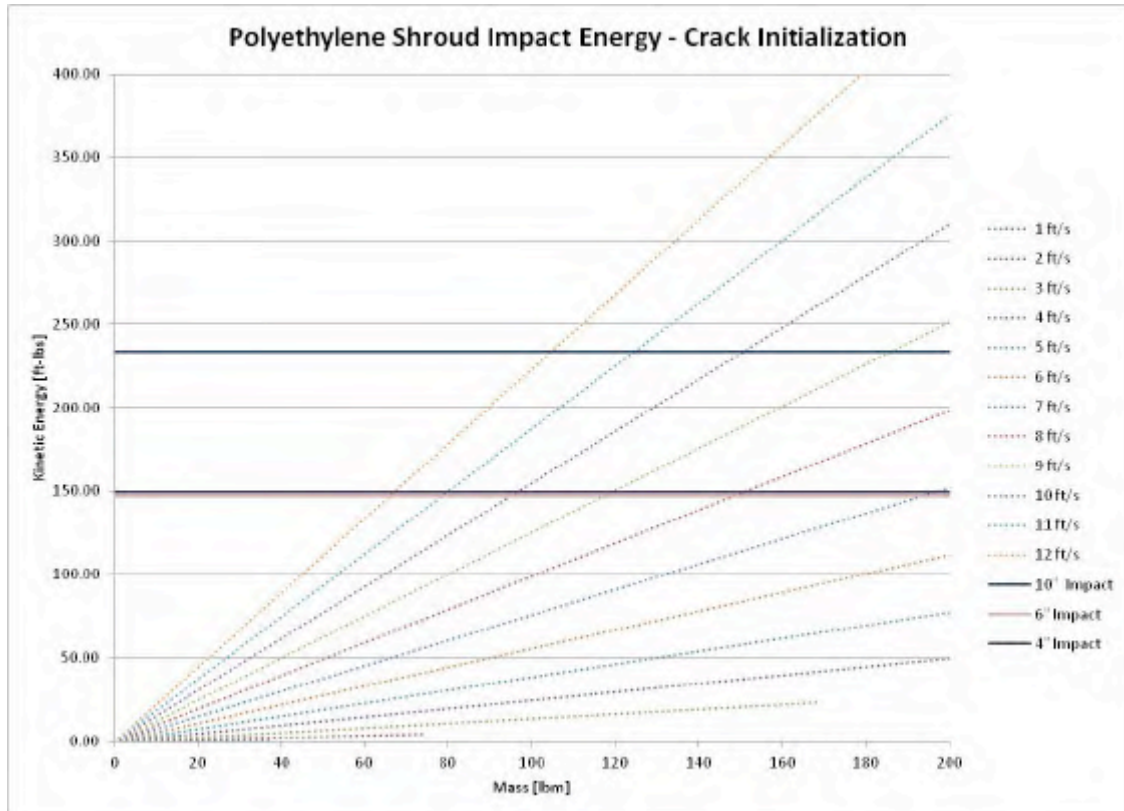


Figure 4.2-2. Kinetic Energy versus Mass

4.2.1 Shroud

The shroud is a UHMWPE (Ultra High Molecular Weight Polyethylene) part with a 3-m OD and a 2.25-m ID having a wall thickness of 0.3". Its primary purpose is twofold: (1) to provide a smooth hydrodynamic face; and (2) to behave as a "bumper" similar to that on an automobile and absorb small to medium impacts. To analyze the part FFP chose 3 diameters to represent a range of small to medium debris, and applied incremental loads to the nose of the shroud at the diameters selected. The diameters were 4", 6", and 10" respectively. The analysis is a non-linear static FEA with the loads defined as acting on an elliptical contact area of the nose, with that area geometry being the diameter of the striking medium (debris) as the major axis and a minor axis representing the final displaced position when projected on the undistorted shroud lip. The aft displacement distance is approximately 0.4" and the resulting ellipse is shown in magenta in Figure 4.2-3. The fixed load/fixed face is the crudest but fastest analytical method, with the full dynamic impact analysis being the most accurate, but it is time consuming and requiring much more costly software. The intermediate approach is to perform a contact analysis, and FFP will present the results of this methodology in a subsequent report. However, the methods applied here provide reasonable results and are useful for determining the first order load capability for impact studies.

Figure 4.2-4 shows the equivalent stress from forces on the three representative areas, with the 2:30 location being the 4" contact area, the 8:00 location being the 6" contact area, and the 10:00 position being used for the 10" contact area. The respective loads are 3,600 lbf., 4,200 lbf., and 4,900 lbf., applied in the direction of the machines axis (flow direction). This analysis was performed in 5 steps, with the loads applied in steps of 20%, giving results at 20%, 40%, 60%, 80%, and 100% of the full load to capture the non-linear behavior at each increment. The forces used were iterated to approach the ultimate strength of the material. However the high stress regions were typically very localized in very small portions of the affected area; this would indicate crack initiation only and not propagation. The amount of residual energy from crack initiation to breakage is expected to be large on this tough material, and the FEA results are therefore relatively conservative. To calculate the energy absorbed in the analysis, we return to the definition of Energy, which is the integral of Force * Distance. Therefore, FFP calculated the area under the Force-Displacement curve absorbed in every load step, then summed the energy of each step to get the final energy at full load. The results are provided later in this Section.

To provide a sense of the deflection associated with the loads listed, Figure 4.2-5 shows a 1:1 plot of the shroud, while Figure 4.2-6 shows the deflections magnified to 5:1 scale (this plot is rotated approximately 30 degrees clockwise from Figure 4.2-4). The three contact areas (ellipses), used to simulate the contact with different log diameters show fairly uniform stress and deflections across the faces, and as these faces are displaced inward, they pull the shroud material around them and push on and deflect material aft of them. This is precisely what is desired for good impact absorption.

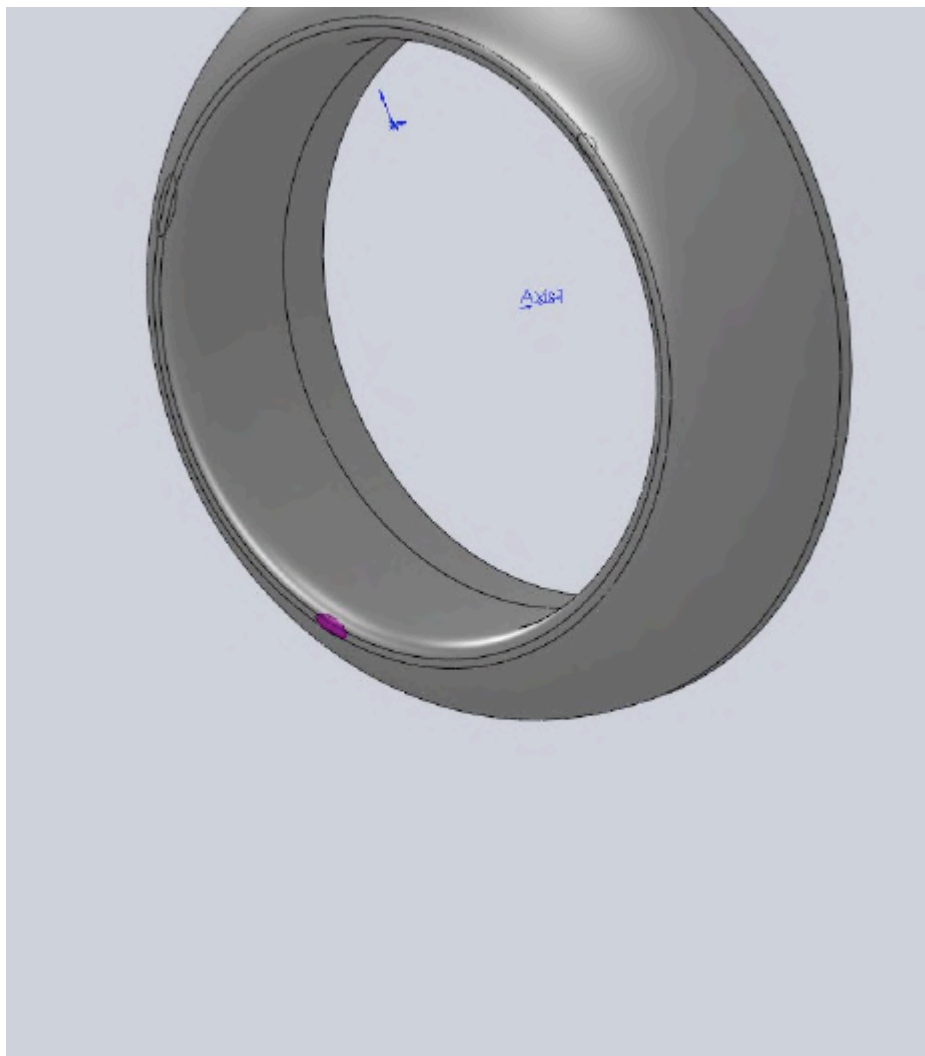


Figure 4.2-3. Shroud with Location Ellipse

[CONTINUED ON NEXT PAGE]

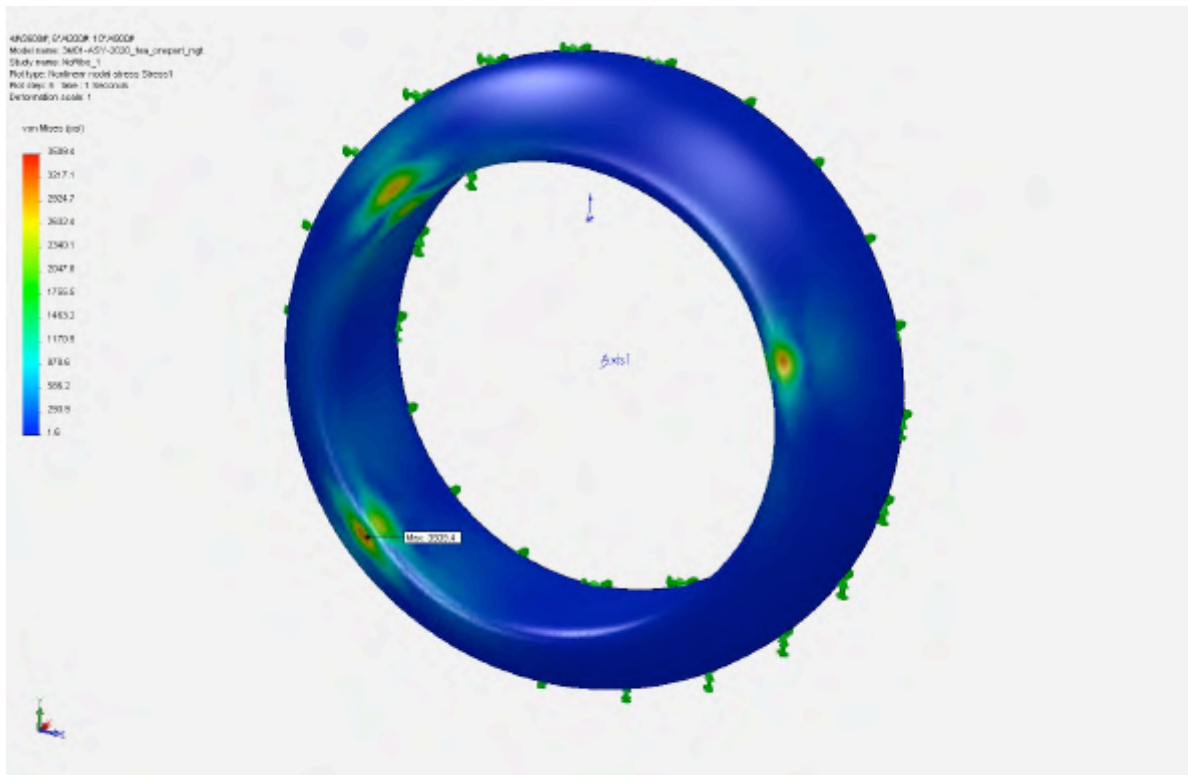


Figure 4.2-4. Shroud FEA Model

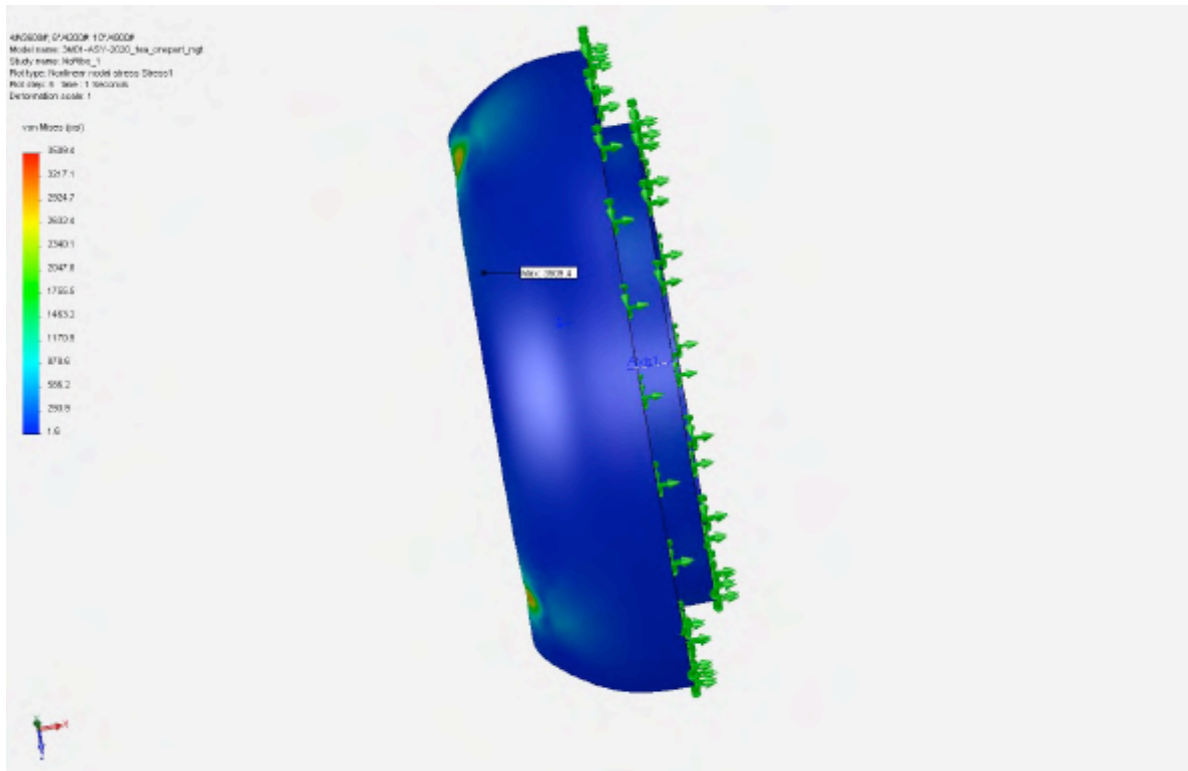


Figure 4.2-5. Shroud FEA Model – Actual Scale Deflections

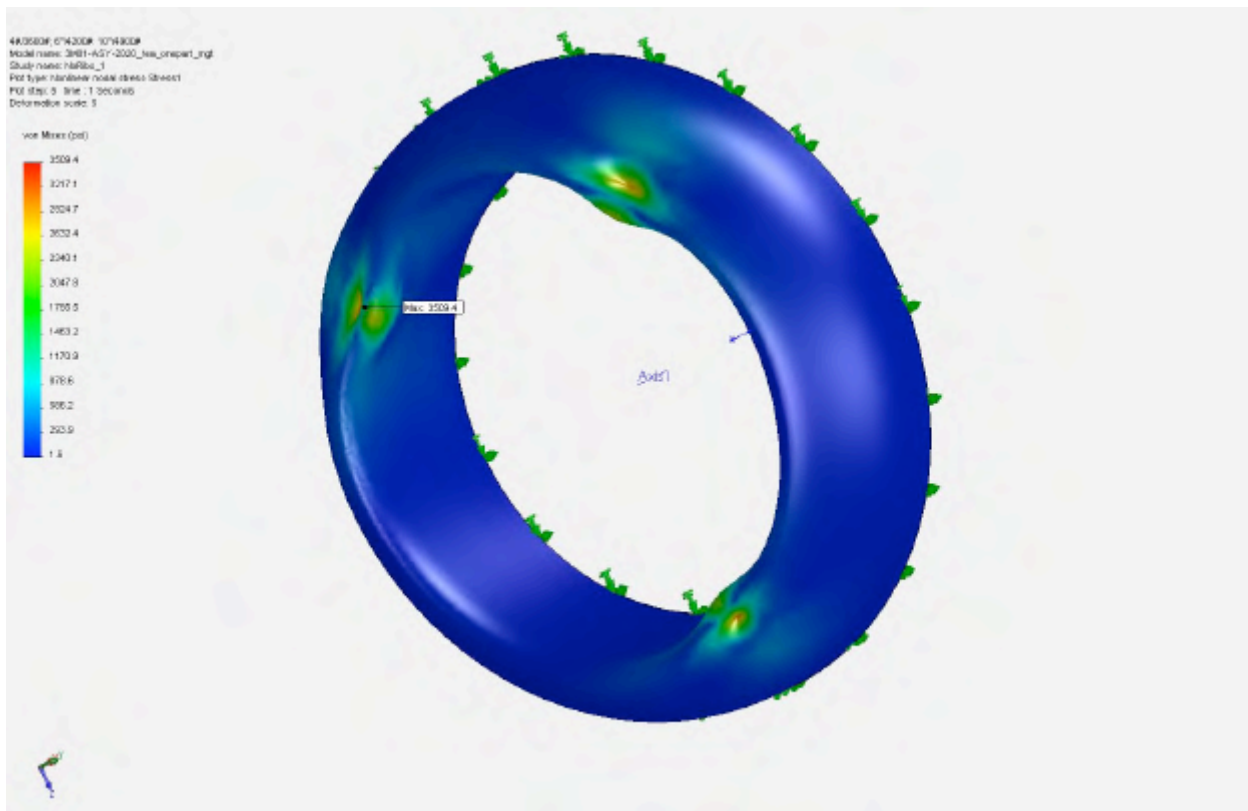


Figure 4.2-6. Shroud FEA Model – Deflections at 5X Scale

Because the analysis is taken to failure, it is non-linear and the actual stress strain curve is used in the FEA. Figure 4.2-7 shows the stress-strain curve used for this analysis. For UHMWPE there will be a temperature effect on the 20 °C studied here, but this will be accounted for at a later time (if relevant).

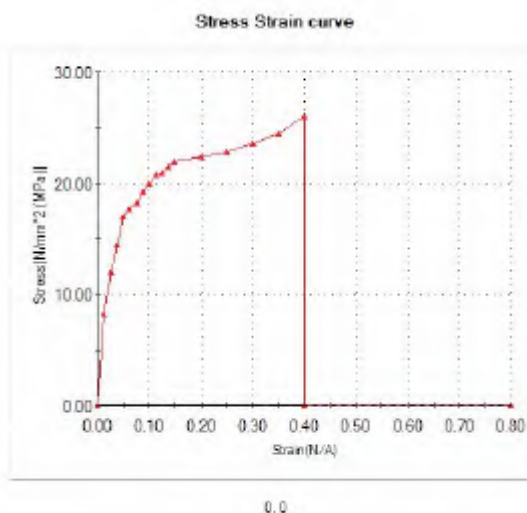


Figure 4.2-7. Non-Linear Stress-Strain Curve for UHMWPE

Table 4.4.1 summarizes the results for the non-linear FEA with the total displacement and total energy highlighted in yellow for each case. The final stresses and strains do not all reach the same peak, likely indicating that more energy absorption is available for the 6" and the 10" diameter cases, but the code struggled to reach convergence at higher values than listed below.

4-inch										
Timestep	Failure?	Full Force, [s]	Force lbf	Delta Force [lbf]	Max Stress [psi]	Max Strain	Δ Displacem [in]	Δ Displacement [in]	k lbf/ft	Energy [ft-lbs]
0.2	N	3600	720	720	840	0.007	0.077	0.077	112208	2.3
0.4	N	3600	1440	720	1500	0.017	0.16	0.083	104096	7.5
0.6	N	3600	2160	720	2060	0.034	0.27	0.11	78545	16.5
0.8	N	3600	2880	720	2600	0.06	0.42	0.15	57600	31.5
1	N	3600	3600	720	3690	0.14	0.76	0.34	25412	91.8
								0.76		149.6

6-inch										
Timestep	Failure?	Full Force, [s]	Force lbf	Delta Force [lbf]	Max Stress [psi]	Max Strain	Δ Displacem [in]	Δ Displacement [in]	k lbf/ft	Energy [ft-lbs]
0.2	N	4200	840	840	770	0.007	0.08	0.08	126000	2.8
0.4	N	4200	1680	840	1500	0.016	0.175	0.095	115200	10.3
0.6	N	4200	2520	840	2000	0.032	0.29	0.115	104276	20.9
0.8	N	4200	3360	840	2640	0.057	0.45	0.16	89600	41.6
1	N	4200	4200	840	3200	0.144	0.87	0.42	57931	153.1
								0.87		228.6

10-inch										
Timestep	Failure?	Full Force, [s]	Force lbf	Delta Force [lbf]	Max Stress [psi]	Max Strain	Δ Displacem [in]	Δ Displacement [in]	k lbf/ft	Energy [ft-lbs]
0.2	N	4900	980	980	580	0.008	0.09	0.09	130667	3.7
0.4	N	4900	1960	980	1290	0.02	0.2	0.11	58800	11.5
0.6	N	4900	2940	980	1860	0.04	0.34	0.14	34588	25.2
0.8	N	4900	3920	980	2260	0.04	0.54	0.2	21778	52.0
1	C	4900	4900	980	2800	0.08	0.95	0.41	12379	141.2
								0.95		233.5

Table 4.2-1 (a, b, c). FEA Summary for 4", 6", and 10" Diameter Impacts

Figure 4.2-8 below plots the results of force and displacement at each step, and Figure 4.2-9 plots the total energy.

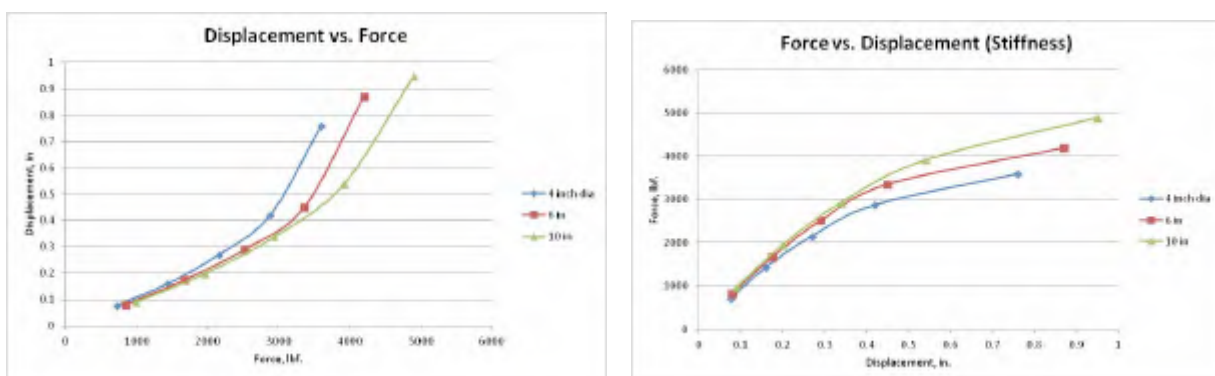


Figure 4.2-8. Displacement-Force and Force-Displacement Results

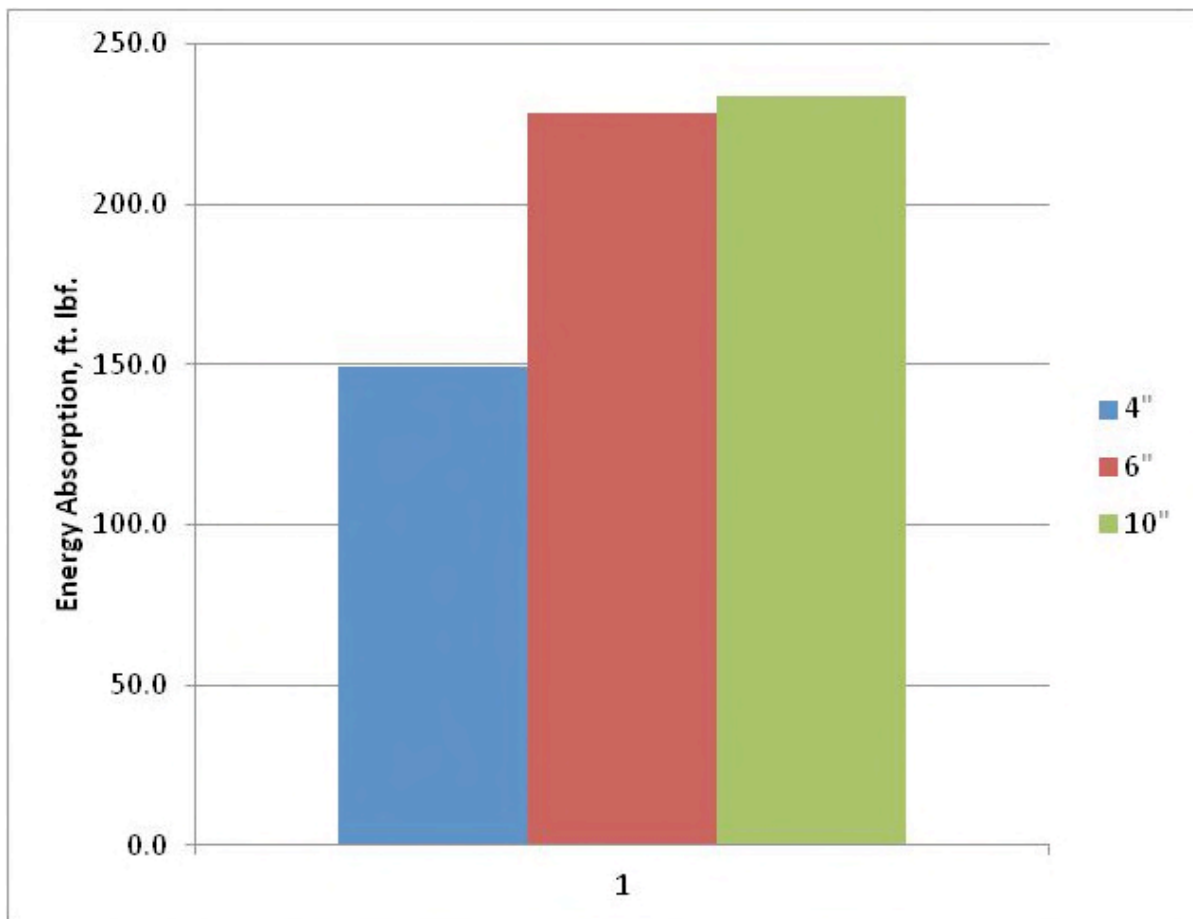


Figure 4.2-9. Energy Absorbed

A more relevant way to display the energy plotted in Figure 4.2-9 is shown in Figure 4.2-10, where energy capacity of the shroud is shown as horizontal lines for each case, overlaid on the kinetic energy contained in combinations of mass and velocity. As long as the kinetic energy is less than the shroud energy, there will be no crack initialization of the shroud.

[CONTINUED ON NEXT PAGE]

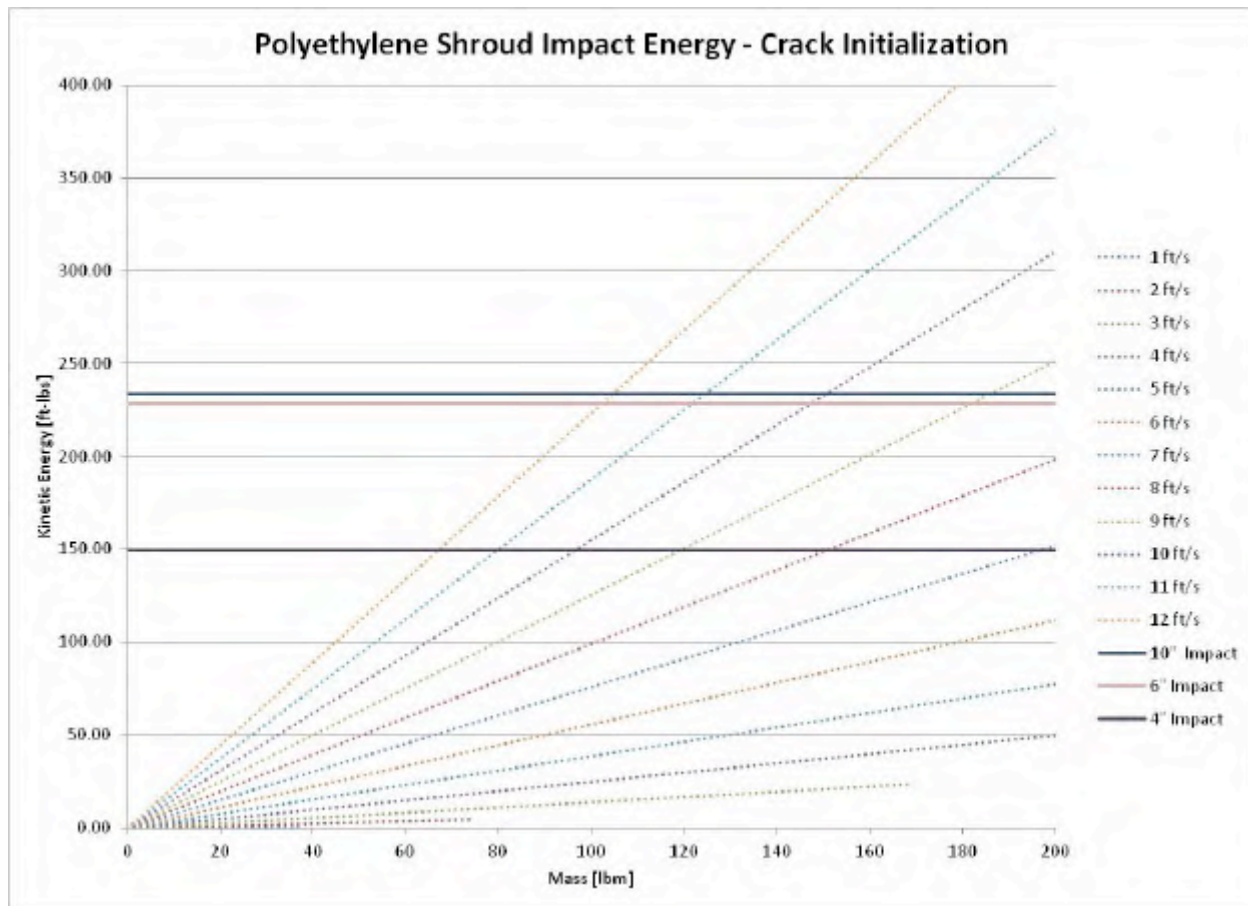


Figure 4.2-10. Shroud Impact Energy Capacity

The analyses presented represent a head-on impact with a log, directly on the nose of the shroud. Other scenarios are an offset impact on the side of the shroud (outward of the nose), inside of the nose, and a non head-on impact. For an offset hit on the outer portion of the shroud, we will defer deciding whether this case needs to be run and what would be representative; many conditions would deflect the debris, and contact point and angle are difficult to estimate. If debris hits inward of the nose, it would contact the rotor or the nose cone, and it is therefore a case which we can ignore for the shroud. Finally, there is the condition where the debris is possibly angled relative to the direction of flow. The bounds of this from an analytical perspective are: (1) a log that is totally perpendicular to the flow and contacts the shroud in two locations simultaneously; and (2) the direct impact previously discussed. Other conditions will be between these results, and will likely involve less energy transfer because the debris will likely be deflected (not brought to a complete stop, hence there is residual kinetic energy). The log that is perpendicular to the flow will distribute its kinetic energy over two contact areas and, would imply that the energy lines in Figure 4.2-10 would be twice the value plotted. The contact area would be a cylindrical face rather than the flat face assumed for a head-on impact, which would change the stress distribution. A study would be necessary to quantify the effects of this, but an estimation based on the toughness and pliability of the PE material is that it would be a less critical case than that presented here; consideration of how quickly the cylindrical contact area would grow with the time-deflection process and spread the load out is another factor.

4.2.2 Composite Material Characterization

FFP tested numerous fiberglass coupons in 2010 to characterize the composite system we are using and for validating predictive capabilities. Much of the information is FFP proprietary, but FFP will be creating a final report from which results will be inserted into the damaged turbine report, particularly for energy absorption capacity. After that data is synthesized, FFP will be able to predict the damage levels on the nose cone, rotor, strut assembly, and housing with good fidelity.

4.2.3 Rotor

FFP will perform non-linear FEA analyses on the rotor similar to what was done on the housing, but using the final material properties from a composite evaluation. Similar to the forward shroud, FFP will then derive a spring model of the rotor for incorporation into the system model.

4.2.4 Remainder of Turbine

Similar to the shroud and rotor, load analysis will be completed for the nose cone, strut assembly and the housing. The nose cone is in the path of potential debris impact, but housing and struts are going to be more affected by impact loads on the shroud, rotor, and nose cone, and the load path through these parts than by an impact directly.

As discussed previously, each component will be analyzed and then simplified into an equivalent spring model, so that ultimately FFP can construct a series spring-mass model to capture force-deflection-energy distributions of the entire turbine.

4.2.5 Piling and Turbine Mounts

In previous reports, FFP stated that impact analysis can be performed for the piling, and has provided some quantified stresses induced by static debris captured by the base of the piling. FFP will perform the non-linear impact analysis of debris strikes on the piling similar to what was done on the shroud. The proposed method will entail two debris sizes and two cases: one near the top and one near the bottom. FFP will perform a contact analysis to determine forces and displacements that result in failure of the metal based on a head-on impact. The top impact case will include the local forces and deflections on the pilings cylindrical face, but will also deflect the entire piling thus absorbing energy in the process. On the other hand, the impact force will create a large bending moment at the base, rendering it critical to evaluate the stress at the base as well.

The impact at the base will be treated as a fixed section of piling and all the impact loads will be converted to deflection and stress of the piling-debris interface.

Finally, the turbine mounting structure will be evaluated on a force-deflection-energy basis to determine its equivalent spring model. We will assume that the forces are transmitted by the turbine during an impact and quantify the stress margin on the mounting arms for the loads applied. During the load-deflection study, FFP will calculate the energy absorbed by the mounts similar to what was performed for the shroud. Because the turbine and mounts are offset from the pilings, there will be a torsional component of loading and energy absorption to the piling induced by turbine impact, and these values will be calculated and integrated into a final model.

After all of the component load-deflection analyses are completed, FFP will have the equivalent spring models of each component, and can integrate these into a system impact model such that the loads and energy absorption path can be calculated. The expected result will be that FFP can quantify on a percentage basis how much of the debris' kinetic energy will be absorbed by each component. For a hypothetical result showing that the distribution from a shroud impact would be 85% shroud, 10% turbine, 3% turbine mount, and 2% piling, it then becomes possible to recreate Figure 4.2-10 with the system curve showing that the lowest system threshold is higher than any single component. For example, if the shroud is the limiting factor for permanent damage, then the curves would be 17% higher than shown.

4.3 Literature References

Gerard, G., Becker, H., *Handbook of Structural Stability Part I - buckling of Curved Plates and Shells*, NACA, technical note 3783, 1957.

NAVFAC Criteria Office (Code 15C), *Interim Technical Guidance - Wire Rope and Strand*, 11460, 15C/rdc, 20 NOV 95, http://www.wbdg.org/ccb/NAVFAC/INTCRIT/fy96_01.pdf

Southwest Wire Rope Catalog, wire rope cp05.pdf.

Latorre, C., Wakeley, L., *Guideline for Installation of Utilities Beneath COE Levees using Horizontal Directional Drilling*, USACE, ERDC/BSL TR_02_09, June 2002.

Sauls, D., Sparks, A., Ramos, M., *Over or Under Geotechnical Considerations for Pipeline Levee Crossings*, ASCE Pipelines 2011.

USACE – CELMN-ED-F, *Guidelines for Permit Review - Installing Pipelines by Nearsurface Directional Drilling Under Levees*, New Orleans District HDD General Criteria - January 2010.

Specifications for Structural Steel Buildings, AISC, March 9, 2005.

Introduction to COSMOSWorks, Users Guide, SolidWorks Corporation, 2004. (now called SolidWorks Simulation)

AISC 303-05, *Code of Standard Practice for Steel Buildings and Bridges*, American Institute of Steel Construction, Inc. 2005.

USACE EM 1110-2-2906, *Design of Pile Foundations*, US Army Corps of Engineers, 1991.

Appendix 9

FISH STUDY FIFTH REPORT

SECTION 5 Fish Entrainment, Population Sampling, Habitat Use, and Movement

The goals of Free Flow Power's (FFP) Fish Entrainment, Movement, Behavior, Habitat Use, and Population Effect Estimation Study (Fish Study) are as follows:

- To quantify the blade rotation rate, rotor blade tip speed, shear stress, pressure changes, turbulence, and cavitation associated with the turbine generator using CFD modeling techniques;
- To determine the range of fish species in the Mississippi River that may be affected by turbine deployment, based on literature review and assessment of fish distribution data collected by the U.S. Army Corps of Engineers (USACE);
- To assess the probability of strike-related injuries and mortality for representative species, based on a laboratory-based or *in situ* testing program (with an expressed preference for a laboratory-based program, if feasible);
- To develop risk-based projections of population effects for several fish species.

In the First Quarterly Study Report (1Q Report), FFP provided a proposal of fish species, age classes, and sizes to be used in controlled entrainment testing; a list of literature for review on the sensitive of aquatic biota; a proposed methodology for conducting controlled entrainment testing in a laboratory or *in situ* setting; a proposal for fish sampling and observation methodologies at the *in situ* test deployment; a discussion of available data from the USACE Engineer Research and Development Center, Environmental Laboratory (ERDC-EL) for information regarding fish populations in the Mississippi River; and a proposed methodology for analyzing the effects of blade strike on zooplankton, aquatic macroinvertebrates, fish eggs, and fish larvae.

In the Second Quarterly Study Report (2Q Report), FFP provided a literature review on the parameters that are likely to cause injury or mortality to juvenile and adult fish, fish eggs and larvae, phytoplankton, zooplankton, and aquatic macroinvertebrates; a revised methodology for a controlled test of entrainment injury and mortality in a laboratory setting; and minutes from a consultation meeting that discussed the various testing alternatives presented in the 1Q Report.

In the Initial Study Report (ISR), FFP provided information regarding responses to comments received from the Commission regarding the 2Q Report; a discussion of data contained in the ERDC-EL data set and a proposed methodology for estimating population-level effects; and a revised proposed methodology for controlled entrainment testing in a laboratory-based setting at Conte Anadromous Fish Research Laboratory (Conte).

In the Fourth Study Report (4SR), FFP provided information regarding conclusions drawn from an analysis of the ERDC-EL dataset. Several of the specific objectives stated in the Commission's Study Plan Determination (SPD) involve determining the range of fish species in the Mississippi River that may be affected by turbine deployment, with this determination based on literature review and assessment of data from ERDC-EL. From the results to be generated in the laboratory-based Fish Entrainment Study proposed at Conte, and in conjunction with data on fish population estimates from the ERDC-EL dataset, FFP proposed to develop a probability-

based approach to providing risk-based projections of population trends for three to four species for which reliable data on fish abundance is available.

In this Fifth Study Report (5SR), FFP is providing information on the following aspects of the Fish Study, most notably a report highlighting the uniformity of the FFP Project Sites and other stretches of the Lower Mississippi River in their fish distributions:

- A summary of consultation conducted regarding the 4SR, including responses to comments received from the Commission – Section 5.1;
- A detailed biostatistical analysis of the ERDC-EL dataset focused on the effects of depth on fish distributions from data collected with trotlines and otter trawls – Section 5.2; and
- An expert report on fish distribution in the LMR written on FFP’s behalf by fish biologist Dr. Steve Miranda, with the conclusion that there is no difference between the FFP project sites and other stretches of the river in fish distribution – Section 5.2(a).

5.1 Consultation Summary and Outreach

5.1(a) Commission’s Comments on 4SR

In the Fourth Interim Report (pages 5-4 and 5-5), you explain that the U.S. Fish and Wildlife Service (FWS)/USGS research team is proposing to increase its ongoing pallid sturgeon telemetry monitoring efforts in the Mississippi River. We recommend that you consult with the FWS/USGS research team to determine whether the telemetry program can be adapted or modified to provide information on the position of sturgeon within the water column relative to the river bed. It may be possible to obtain this type of information using depth-sensitive transmitters in combination with detailed bathymetry information at sites that are frequented by pallid sturgeon. This information would help in assessing the potential exposure of benthic species, including the endangered pallid sturgeon, to entrainment-related injuries and the potential for population-level effects.

FFP is appreciative of this insight, and FFP intends to conduct this outreach and to present the results of that consultation in a future Study Report.

The Conte Anadromous Fish Research Laboratory’s proposal for controlled entrainment testing included in appendix 5-2 of the Initial Study Report describes the species, sizes, and number of fish that are planned to be tested. We request clarification on the following elements of this proposal:

- *Will tests be conducted at velocities 2.25 and 3.0 meters per second as proposed in First Interim Report and the Second Interim Report?*
- *How many fish of each species and size class will be used during test and control releases at each velocity?*
- *Will individual fish be used in more than one test, and if so, will the results for those fish be used to evaluate the potential effects of multiple turbine passage events?*

- *Why is the number of hatchery trout potentially available limited to “up to 500,” given that hatchery trout can be obtained in large numbers from many different sources?*

FFP’s plan is to test at both 2.25 and 3.0 m/s river equivalent speeds corresponding to 38 and 56 rpm at the turbine rotor. This is stated as a river equivalent velocity because the flow distribution in a water flume is different than it is in an open river.

The number of replicants for each species for test and control cannot be provided *a priori* for two reasons. Firstly, Conte cannot predict with certainty how many of each species will be available at the time the testing is planned. Second, in the 2Q Report, on page 5-36, FFP stated in list item #4 “Locked Rotor Control Test Setup” that a modified control strategy would be used for those species where limited replicants were available by determining that tagged fish that were observed not to strike a blade would be considered control replicants.

There is no plan to re-introduce fish for multiple tests, as this would add to the uncertainty regarding control handling and harm to the fish not caused by the turbine. The Conte program management is conservative in its estimates of trout. Every reasonable effort to maximize the number of trout species will be made within restrictions of the Massachusetts state regulators and availability at the time of testing.

The testing program described in the Conte Anadromous Fish Laboratory’s proposal includes testing with multiple species and sizes of fish that would be obtained from different sources, and each species and size class may be subject to different forms of stress or injury during collection, transport, holding, and experimental procedures. We note that if sufficient care is not taken to ensure that fish handling and experimental procedures do not contribute to injury or mortality of fish used during testing, procedures may need to be modified and additional testing performed to obtain valid estimates of injury and mortality. Please define the maximum percentage of mortality of control fish that would be considered acceptable to provide valid results, above which test procedures would need to be modified and testing repeated.

Most testing would be valid, but with increasing uncertainty. It is already expected that both mortality and control results will be near zero and would be for almost any number of replicants at these extremely low tip speeds and tip speed ratio. All previous literature studied and reported on suggests this. As noted, uncertainty increases with decreasing replicants. The most applicable reference study to-date that includes models of certainty has been analyzed and reported on in the previous FFP reports. FFP and Conte will follow similar statistical analysis standards.

Our Study Plan Determination requires that you develop a detailed proposed methodology for conducting a focused fish sampling and observation plan at test deployments of piling-mounted and barge-mounted turbines to: (1) validate the controlled entrainment study; (2) assess local-scale behavior around the turbines and mounting structures; and (3) assess reach-scale behavior around the turbines and mounting structures. In the First Interim Report (pages 5-15 through 5-16), you provide a very general description of how you propose to monitor changes in fish distribution and habitat use during the in situ test deployment. However, the detailed methodology for assessing habitat use pre-and post-deployment at the in situ test deployment

site(s) required by the Study Plan Determination has not been presented. This gap was noted by FWS in its comments on the Initial Study Report (filed on March 17, 2011). A site-specific plan and schedule for assessing fish habitat use, pre- and post-development, must be developed and provided to stakeholders for review so that their input can be incorporated into the plan before pre-deployment monitoring commences. The plan should include a detailed description of the sampling methods, equipment, locations, and sampling schedule for assessing the local and reach-scale behavior of fish at the *in situ* test deployment site. Please develop a detailed plan and provide it to the agencies and other stakeholders for comment, allowing at least 30 days for comments to be provided, and file a revised plan with any comments received on the plan, indicating how those comments have been addressed.

Based on the literature review on the effects of construction noise on fish that you provided on pages 6-1 through 6-15 of the First Interim Report, there appears to be potential for causing mortality to fish that are exposed to high acoustic energy levels during pile-driving. Your plan should include a proposed approach for assessing this potential source of mortality during installation of the *in situ* test deployment.

The reported plan for fish turbine entrainment monitoring at the *in-situ* test deployment site was very specific. FFP deferred a more detailed fish distribution and habitat monitoring (outside of the *in-situ* turbine entrainment plan) until after our Mississippi River system wide fish population study, which is included in this report, had been reported and reviewed. The results of that study are informative in terms of what discriminating and significant data is likely to be observed at the *in-situ* site.

5.2 Biostatistical Analysis of the ERDC-EL Dataset

Within the SPD, FFP proposed to conduct a fish entrainment study and to forecast population level effects on certain fish species. FFP identified four objectives including determination of the range and distribution of fish species in the Lower Mississippi River (LMR) that may be affected by turbine deployment based on literature review and assessment of fish distribution data collected by the USACE. To estimate population effects, FFP determined that an effective approach was through a biostatistical analysis of the ERDC-EL dataset developed by USACE. The ERDC-EL dataset contains fish collects between 1997 and 2011 using various sampling gears, and should be considered as the most comprehensive and best information available on fish survey data throughout the entire Lower Mississippi River (LMR).

In review of the ERDC-EL dataset, depth was selected for the biostatistical analysis because FFP's hydrokinetic turbine locations must conform to depth restrictions established by USACE to avoid interference with navigation. These parameters included a minimum depth of 20 feet below a surface Low Water Reference Plane (LWRP) north of Baton Rouge, LA in the shallow-draft region of the LMR, and minimum depth of 65 feet below surface LWRP south of Baton Rouge, LA in the deep draft sections of the LMR. As result, sufficient depth at LWRP from the bottom in the shallow-draft region of the river to accommodate the height of one turbine is 40 feet, accounting for a distance of at least 10 feet above the riverbed to establish sufficient

clearance, and approximately 10 feet (3 meters) for the outside diameter of the FFP's turbine design. The sufficient depth at LWRP from the bottom in the deep-draft region of the river to accommodate the height of one turbine is 85 feet, similarly accounting for a distance of least 10 feet above the riverbed to establish sufficient clearance, and approximately 10 feet (3 meters) for the outside diameter of the FFP's turbine design.

Furthermore, depth was selected because it can be measured easily and accurately, and it has been confirmed to index a variety of other environmental characteristics relevant to fish distribution such as current velocity, light availability, substrate, distance from shore, various water quality descriptors, and biotic factors including competition, predation risk, and food availability. As result, knowledge on depth distribution of fish populations in the LMR is important to understand species and community habitat needs. To the best of FFP's knowledge, no study has formally analyzed depth-distributions of fish in the Mississippi River. As result, FFP contracted with Dr. Steve Miranda of Mississippi State University to investigate fish species distribution and fish assemblage composition along depth gradients in the LMR through a biostatistical analysis of the ERDC-EL dataset. Specific objectives included examining if depth affected seasonal patterns in fish species distributions, richness, and size structures. Additional objectives included analysis of the fish assemblages and depth distributions between the shallow and deep drafts regions, between FFP and non-FFP Project Sites reaches throughout the LMR, and whether depth profiles were influenced by the size of fish. This analysis is expected to help support assessment of potential population effects from hydrokinetic turbine fish entrainment within the SPD.

The biostatistical analysis of the ERDC-EL focused on the effects of depth on fish distributions from data collected with trotlines and otter trawls. Other gear types including electrofishing, gill nets, and hoop nets were used in the dataset but were mostly limited to shallow depths and low velocity habitat areas. Therefore, trotlines and trawls should be considered appropriate gear types for long-term monitoring in the diversity of currents, depths, and habitats encountered in the LMR. Fish distribution relative to depth was investigated primarily in the 703-miles reach above RM 250 in the shallow-draft region of the LMR. Fish collection data was limited below RM 250 in the deep-draft region of the LMR. While the deep-draft region represents 26% of the LMR, it included less than 16% of all fish collected throughout the entire LMR in the ERDC-EL dataset.

A total of 1,096 trotline samples and 612 trawl samples were collected in the study reach between 1997 and 2011. The trotline effort produced 9,821 fish of 19 species, and the trawling effort produced 42,138 fish of 62 species. The most common species collected by trotlines were blue catfish (47.3% of total catch), shovelnose sturgeon (37.2%), channel catfish (7.3%), freshwater drum (18.0%), flathead catfish (2.1%), and pallid sturgeon (1.7%). The most common species collected by trawls were blue catfish (25.8), freshwater drum (21.0%), channel catfish (16.5), speckled chub (13.2), channel shiner (8.7), shovelnose sturgeon (5.7), silver chub (2.2), silverband shiner (1.8), paddlefish (1.3), and gizzard shad (1.2).

Cumulative fish species richness was examined with the trawl dataset only, because the trotline dataset included a reduced number of species. Combined cumulative fish species distributions were examined with the trawl and trotline datasets for all, and for selected species when large

enough sample sizes (> 100 specimens) were collected and multiple samples (> 20 sets or tows) were sufficient for the analyses. Species were cumulated over depths based on the shallowest depth at which they were collected (i.e., first appearance), and based on the deepest depth at which they were collected (i.e., last appearance). Six species collected with trotlines and 13 species collected with trawls met the sample size requirements for cumulative-frequency analyses.

Cumulative species richness and cumulative frequency distributions were found to exhibit a sigmoid response relative to depth that varied over the low- and high-water periods. Catch rates increased with depth, peaked, and decreased at greater depths. Depth of first appearance was generally shallow with 50% of the species first collected by a depth of 5 ft. Conversely, about 50% of the species were no longer collected below 25 ft. In the low water period, about 20% of the cumulative species remained in water deeper than 40 ft. In the high water period, about 15% of the cumulative species remained in water deeper than 52 ft. As expected, the low-water period concentrated species in relatively shallow water, but species became more dispersed over depths in high water. The maximum number of species occurred at 15-20 ft in the low- or high-water periods. Overall, the number of species present near the bottom at depths beyond 40 ft was reduced to about 20% of all species collected.

Depth-distribution curve analysis estimated the percentage of time fish populations occupied water deeper than 40 ft during low water and deeper than 52 ft during high water. For all species combined, trotlines estimated these percentages at 37.7 and 27.1, respectively. For trawl samples these percentages were 33.3 and 6.6, respectively. For individual species, estimates ranged from 0.1 to 39.7%, and averaged 14.0% during low water. During high water, estimates ranged from 0% to 27.1%, with an average 6.8% for the populations studied. Distribution of fish shifted towards deeper water during high water for trotlines, but towards shallower water for trawls, potentially reflecting differences in fish sizes and life stages collected by the two gears. But most often depth distribution of all species decreased rather than increased during high water. This observation suggests that fish more or less do not stay at a fixed position on the riverbed possibly associated with a certain habitat type. Instead, fish exhibit seasonal changes in depth distributions that may be attributed to a multiplicity of environmental and behavioral factors, such as when water velocity changes with depth where fish may move to shallower or deeper water to avoid fast or slow currents, and when increases in depth due to higher river stages flood riparian habitats associated with fish feeding or reproductive behaviors.

A comparative analysis was conducted to assess whether fish depth distributions and species richness differed between the lower (deep) and upper (shallow) segments of the LMR. FFP has 67 Project Site reaches throughout the LMR. 43 reaches or 64% of the total occur in the upper region of the LMR between RM 250 and RM 953. In all, 66 fish species were collected with trotlines and trawls in the lower region, and 62 fish species were collected in the upper region. No statistically significant differences between the two regions were found relative to depth distribution of catch rates of trotlines or of trawls. Similarly, depth distribution of species richness as measured with trawls did not differ significantly between segments.

A comparative analysis of the FFP Project Site reaches with the non-FFP reaches produced minimal differences in fish depth distributions. No comparisons were made in the lower segment because sufficient fish collection data was not available from the deep reaches where FFP's Project Sites are located. No differences in distribution over depths between FFP and non-FFP reaches were evident for either the trotlines or the trawls data set during the low or the high water periods. As expected, fish depth distribution are intrinsic to their habitat preferences, and probably do not change greatly as long as a wide range of depths is available.

A comparative analysis of species richness cumulative curves computed based on the depth at which species first appeared were not significantly different between the FFP Project Site reaches and non-FFP reaches during the low-water period or high-water periods. Conversely, species richness cumulative curves computed based on the depth at which species last appeared were not significantly different between FFP and non-FFP reaches during high water, but were significantly different during low water. These results suggested that when differences did occur, species richness in the FFP Project Site reaches increased more steeply, with lesser richness in shallow water than non-FFP reaches, and with more species disappearing sooner than in non-FFP reaches. Given that species richness and fish density was found to decrease with depth, and FFP's Project Sites will be located in the deeper waters of the main river channel, species richness and fish abundance are expected to be even less within this area. Furthermore, while no population size estimates were available to quantify this inference, species richness in the FFP reaches were found to be lower than in non-FFP reaches.

Lastly, and considering all species combined, larger fish tended to occur in deeper water during the high-water period, but no correlation was evident during the low-water period. Less than half of the species included in these analyses exhibited statistically significant correlations between body size and water depth. No parabolic-shaped relationships were evident by examining scatter plots. Species exhibited various direct and inverse correlations with depth, in low- and high-water periods. Some species exhibited a correlation in one season but not in the other, and some exhibited a direct correlation in one season and an inverse correlation in the other. Overall, the statistically significant correlation coefficients were not large. Thus, patterns in depth distribution relative to body size were evident, but were not strong.

In conclusion, the occurrence of fish frequency diminishes in deep water. The biostatistical analysis of the ERDC-EL dataset suggests that fish in the LMR exhibit non-random depth distributions that vary seasonally and according to species. In terms of species counts, trawls estimated that in the low water period only 20% of the species collected remained in water deeper than 40 ft. In terms of fish counts, trotlines and trawls estimated that during the low-water months 38% and 33% of all fish, respectively, occupied depths deeper than 40 ft. However, these estimates varied among species with individuals of some species frequent in deep water, others frequent in shallow water, and some switching from deep water to shallow water depending on time of year. Estimates differed between the low-water and high-water periods, with fewer species and generally fewer individuals of a species occupying depths deeper than 52 ft during high water (equivalent to 40 ft during low water).

These estimates reflect the fraction of time that fish species occupy various depths. Because these estimates do not consider depth availability, they do not reflect the fraction of an entire population or community occupying various depths. The latter can be estimated by considering depth distributions in the LMR. For instance, the distribution of depths in the LMR above RM 250 indicates that depths over 40 ft occur in 12% of the river. If fish exhibited no depth preferences and were uniformly distributed over all depths, then 12% of the fish community would occupy depths over 40 ft. However, because the data show that fish are not randomly distributed relative to depth and that fewer fish occur in deeper water, the percentage of the population present below 40 ft should be less. As a conservative assumption, this percentage may be estimated as the product of the probability of finding water deeper than 40 ft, and the probability of fish occupying water deeper than 40 ft, as the low water threshold from data collected by multiple gear types. In all cases, the probability of finding fish in low water (40 ft) was found to be greater than in high water (52 ft). For example, if the probability of finding shovelnose sturgeons during low water at depths over 40 ft is 35.3% from the trotline data and from 3.1% from the trawl data (see Table 3 in Miranda 2012 study), and depths over 40 ft occur in 12% of the upper river region (see Figure 1 in Miranda Study), then between 4.2% (i.e., 0.353 X 0.12) for the trotline data and 0.37% (i.e., 0.031 X 0.12) for the trawl data of the shovelnose sturgeon population, is estimated to occur in depths over 40 ft at any one time and would be at risk of encountering a turbine. While this is an estimated range for this population that may be exposed to FFP turbines installed in water deeper than 40 ft, the actual percentage at risk of being impacted by a turbine would be less considering the fraction of the river volume that a fish species and its population could encounter the turbine throughout a multi-dimensional representation of river at the project locations. These estimates when averaged for shovelnose sturgeon and other species in the LMR with sufficient trotline and trawl data are presented in Table 5-1 as follows.

Species	Trotline P @ $\geq 40'$	Trawl P @ $\geq 40'$	AVG. P @ $\geq 40'$	% of Depths $\geq 40'$ in upper LMR	Adjusted P
Blue Catfish	39.7%	29.9%	34.8%	12.0%	4.2%
Freshwater Drum	16.5%	26.9%	21.7%	12.0%	2.6%
Shovelnose Sturgeon	35.3%	3.1%	19.2%	12.0%	2.3%
Channel Catfish	14.5%	12.1%	13.3%	12.0%	1.6%
Flathead Catfish	24.1%	0.5%	12.3%	12.0%	1.5%

Table 5-1. Probability (P) of Time That Select Species Occupy Water Deeper Than 40 Feet
Source: FFP

While the overall results suggest that most fish avoid excessive depths reducing the risk of encountering FFP's turbines at greater depths, fish depth distribution curves will shift seasonally with river stage, and slightly greater risk of encountering FFP's turbines during the low water period, or approximately over half of a year.

Perhaps the most interesting conclusion of the analysis is that the stretches of the LMR in which FFP sites are located are no different than other stretches of river in their fish distributions. The LMR is fairly uniform in its distribution, providing the result that there are no differences between the FFP Project Sties and other lengths of the river in terms of fish distribution.

5.1(a) Miranda 2012 Study

Please find the Report in its entirety beginning on the next page.

Fish Depth Distribution in the Lower Mississippi River with Implications for Free Flow Power Installations

Report submitted to

Free Flow Power

by Steve Miranda, Ph.D., Fish Ecology Analysts

January 2012

Depth is a key characteristic of aquatic ecosystems and an important factor shaping fish assemblages (Hynes et al. 1999; Lorance et al. 2002; Brokovich et al. 2008; Miranda 2011). Aquatic systems with broad depth range often exhibit large differences in physicochemical attributes and habitat structure (Friedlander and Parrish 1998; Lara and Gonzalez 1998; Nanami and Nishihira 2002; Madenjian and Bunnell 2008). Decreased light levels associated with depth gradients may curtail plant growth (Russ 2003) and hinder the ability of fish to forage (Rickel and Genin 2005). Patterns of species distributions along depth gradients may represent simple trends in response to single environmental variables, such as light and temperature, or potentially more complex trends in response to other variables, such as water velocity, physical heterogeneity, and species interactions.

Patterns of species distributions are often described by hump-shaped curves, so that peak abundances occur at some intermediate level (Lomolino 2001; Austin 2007). Hump-shaped patterns may be due to single or multiple abiotic and biotic gradients that provide optimal conditions for a population or a community near the middle of the gradient. Fish use habitats within a water body that are physiologically convenient mainly in terms of oxygen concentration and water temperature (Brandt 1980; Brosse and Lek 2002; Matthews et al. 2004). Biotic factors such as food availability, predation risk, and competition also play a role in depth selection (Eckmann and Imbrock 1996; Mous et al. 2004). For each ontogenetic stage of fish, biotic and abiotic conditions cross at an equilibrium that represents an optimum for depth occurrence within a specific water body. Moreover, location of the hump along a gradient may shift seasonally or with ontogenetic stage. Clear exceptions to hump-shaped patterns sometimes occur, especially in cases where densities decrease continuously from a peak at shallow depth (Day and Pearcy 1968).

Species body-size distributions are an important component of community structure (Blackburn and Gaston 1994). Early studies in the deep sea revealed a shift toward smaller average size with increasing depth. Later studies revealed variable and conflicting results. Studies on benthic marine fishes have reported positive, negative or no relationship between body size and depth (Jensen 1988; Rex and Etter 1998). It remains unclear if there are general trends in body size with depth.

Whereas a substantial body of literature exists about depth distribution of fish in oceans, lakes, and reservoirs (e.g., McKaye and Stauffer 1986; Smith and Brown 2002; Prchalová et al. 2009), only few studies have examined depth distribution of fish in large rivers (e.g., Kubecka and Duncan 1998) and no study has formally analyzed depth-distributions of fish in the Lower Mississippi River. Instead, most of the emphasis on fish distributions in rivers has focused on longitudinal and latitudinal spatial distributions (Vannote et al. 1980; Junk et al. 1989). Knowledge on depth distribution is necessary to understand species and community habitat needs. Such understanding is particularly important in heavily impacted rivers, where anthropogenic modifications have altered discharge, depth, and associated habitat characteristics, and periodic human intervention is needed to restore or maintain riverine environments. Additionally, large rivers often serve industrial uses, such as navigation (Gutreuter et al. 2003; Killgore et al. 2011) and free-flow kinetic hydropower (Cada et al. 2007), and other needs that require knowledge about the depth distribution of fish to minimize impact.

With respect to free-flow kinetic hydropower, Free Flow Power Corporation (FFP) is seeking approval from regulatory agencies to install turbines at sites in the Lower Mississippi River (LMR). To obtain approval FFP is required to produce information about the potential interaction between fish assemblages in the river and power installations. Such installations are to be positioned in at least 40 ft of mean low water level depth below the water surface to avoid interference with other industrial uses of the river. Thus, species depth distributions are of central concern to installation of free-flow kinetic hydropower. Knowledge about species depth distributions and the likelihood that species occupy depths below 40 ft are necessary to evaluate the potential effect free-flow kinetic hydropower installations may have on fish assemblages. Nevertheless, as stated earlier, information about fish depth distributions in major rivers is inadequate at best.

Considering this void in understanding, the goal of this research was to investigate fish species distribution and fish assemblage composition along depth gradients in the LMR. Specific objectives included examining if depth affected seasonal patterns in fish species distributions, richness, and size structures. This information is expected to help support decisions about development of free-flow kinetic hydropower in the LMR. Additional objectives to inform these decisions included testing if reaches identified as potential development reaches exhibited depth distributions that were similar to other reaches in the river, and interpreting results of these analyses in terms of the possible interactions between fish assemblages and free-flow kinetic hydropower development. This assessment focuses on species that occupy the bottom at least part time because fish collections were made with gears that target benthic environments.

Methods

Study Area

The LMR extends 953 miles from its mouth in the Gulf of Mexico upstream to the mouth of the Ohio River. Along the length of this stretch, the river shows two distinct depth distribution patterns (Figure 1). Over its first 250 miles segment the river has been engineered to maintain

deep water to support navigation of large container vessels. Minimum navigation depths established by the USACE in most of this segment are 35-45 ft; however, channel depths are normally deeper with mean depths of about 65 ft and maximum depths of about 120 ft. In this segment variability in depths is reduced as the river becomes a relatively homogeneous navigation channel. Above river mile (RM) 250, minimum navigation depth is 12 ft, but mean depths hover around 25 ft and maximum depths around 60 ft. Variability in depths in this upper segment of the river is higher than in the first 250 miles, with coefficients of variability (CV, computed as 100 X standard deviation/mean) around 60 (Figure 1).

Fish distribution relative to depth was investigated primarily in the 703-miles reach above RM 250. The lower 250-miles segment was not completely integrated into these analyses for several reasons. First, the deep water in the lower segment is restricted to the navigation channel, and no sampling could be conducted in this channel. Sampling with trawls is not possible in deep water (more below), and sampling with trotlines was not feasible in the navigation channel because marker floats would be in the pass of vessels. Therefore, the range of depths sampled in the deeper lower segment was equivalent to that sampled in the shallower upper segment. Second, the lower 250-miles segment is largely an artificial aquatic environment, and the fish assemblage is somewhat different from that upstream because it includes occasional estuarine fish species. Lastly, while the lower section represented 26% of the LMR, it included less than 16% of all fish collections. Consequently, the number of samples available for analyses was small, particularly once samples are partitioned according to time periods and species. Nevertheless, a test was conducted to determine if the depth distribution of fish in the upper segment differed from that of the lower segment. The comparison of lower and upper segments does not consider extensive reaches with depths over 100 ft in the lower segment, as these depths were not sampled. Fish distribution in depths >100 ft remains unknown.

Discharge and water temperature vary widely in the study reach over an annual cycle. Both variables tend to reach higher values in the lower parts of the study reach, but the annual trend is similar throughout the LMR. Discharge typically ranges from 250,000 ft³/s or less in autumn to nearly 1 million ft³/s in spring (Baker et al. 1991). Mean monthly stages fluctuate 20-25 ft, peaking in April and plummeting in September (Figure 2). Water temperature also exhibit seasonal trends. Temperatures during winter in the study area average about 45°F and approach freezing, increase rapidly from February to June to a summer high of nearly 85°F, and rapidly fall during autumn (Figure 3).

Fish Collections

Fish were collected with trotlines and otter trawls over the length of the study area. These gears were chosen because they target different aspects of the fish community and can be used over a broad spectrum of habitats. Other gears (e.g., electrofishing, gill nets, hoop nets) have been used to sample selected habitats in the LMR (Pugh and Schramm 1998; Phelps et al. 2009), but are mostly limited to shallower, low velocity habitats. However, trotlines and trawls provide the safety and economy necessary for long-term monitoring in the diversity of currents, depths, and habitats encountered in the LMR.

Trotlines.-- Trotlines were fished throughout all months of the year over a 14-year period ranging from 1997 to 2011, and excluding 1999. Trotlines are typically used to target benthic fishes such as catfishes and sturgeons. Trotlines can be deployed in a variety of habitats such as the deep and swift waters encountered in reaches of the Mississippi River (White 1956; Hubert 1996). Trotlines were 200-ft long, had 60 dropper lines spaced every 3 ft and tied to 2/0 hooks baited with worms (Canadian night-crawlers); were fished overnight and retrieved the following morning after approximately 16 h; and with few exceptions were set parallel to shore. Trotlines were reefed into a “jump box” typically used by commercial fishers. A buoy and anchor were deployed at the upstream position of the line; the box was slowly rotated as the boat drifted downstream, thus allowing the line to be deployed within minutes without tangling. Small weights attached to the line every 25 ft maintained bottom position. Catch rates according to all fish and individual species were expressed as the number of fish caught per overnight trotline set.

Trawls.-- Fish were collected with trawls throughout all months of the year over an 11-year period ranging from 2001 to 2011. A Missouri-type otter trawl similar to that described by Herzog and Barko (2005) was used. The foot-rope of the trawl was 10-ft wide and fitted with a tickler chain to maintain bottom contact. The trawl was fitted with 1 x 3 ft otter boards to keep it open while towed along the bottom. When in operation, the gape size was assumed to be 10-ft wide and 3-ft tall. The trawl had two mesh sizes. The exterior mesh size was 1.5-in stretch to retain small fish and the interior mesh was 2-in stretch. The length of the trawl warps were about three times the water depth to ensure that the trawl mouth maintained contact with the bottom at a proper opening. The trawl was deployed from the bow while the boat was backing downstream. This approach provided a margin of safety and greater maneuverability in case the trawl became entangled on underwater objects. When the trawl did become entangled, a trailer boat grabbed the cod-end float and backed upstream until the trawl was lifted off the underwater obstruction.

Target tow distance was 0.5-1 mile. Boat speed varied because it had to be adjusted to ambient water velocity so that the trawl travelled slightly faster than water velocity. Catch rate according to species was expressed on an area basis, estimated as the number of fish caught per trawl tow divided by the product of the width of the net's mouth and the distance trawled, the latter being determined from the latitude and longitude coordinates. Coordinates and water depth were recorded along the trawl's pass with a Magellan GPS and a boat-mounted Garmin depth sounder, respectively.

Sampling reaches.-- Sampling reaches were selected systematically along the length of the river, but selection was influenced by access to the river. Generally, sufficient habitat diversity existed in relatively short river reaches a few miles long, but occasionally homogeneous river reaches were encountered requiring deployment of gear over longer spans. Six trotlines were normally deployed over a 1-mile river reach, aiming to maximize variation in habitat types over the reach, including slack and swift water habitats. Similarly, five tows of the trawl were made over a 3-mile river reach, in a downstream direction, aiming to target a constant depth with a single tow but a diversity of depths over multiple tows. However, the number of trotlines and trawls fished,

as well as the size of the reach sampled varied depending on multiple factors such as habitat availability, weather and river conditions, and gear loss.

Gear limitations.-- Use of bait associated with fishing trotlines generates sampling biases (Løkkeborg and Bjordal 1992). First, by their nature, trotlines target fish feeding near the bottom and, in particular those species most attracted to Canadian night crawlers. Second, if bait is lost or a fish is captured, that hook is no longer an effective unit of effort, except when the captured fish becomes bait for a larger fish or in the remote chance that a fish is snagged by a bare hook. This reduction in number of effective hooks biases catch rates, and extent of the bias increases when catch rates are high. No attempt was made to adjust catch rates by the reduction of effective hooks because it was unknown when during the soak period a hook became ineffective.

Otter trawls select for fish present on or near the bottom, whether feeding or otherwise. Otter trawls sweep an area through the bottom equivalent to the area of the trawl's mouth, but do not catch all the fish in their path because area of the mouth is flexible (Walsh 1996), and because fish have behavioral avoidance responses. Mouth area can be highly variable within and among tows as angle of the towing cable changes due to changes in bottom topography or depth (Hovgård and Riget 1992). This variability allows fish escapement under and over the trawl. Swimming speed and endurance of the target species plays a key role in capture success. Moreover, fish may sense the trawl visually or otherwise, resulting in a herding response (Ramm and Xiao 1995). Herding may be reduced in turbid waters, and in general gear avoidance may vary with light availability. In the study area use of trawls was limited to daytime and was further limited by depth, as trawling was rarely conducted in waters deeper than 50 ft because it required too much rope to maintain the 3:1 rope:depth ratio to achieve a proper net mouth opening (Hayes 1983). Also, areas with rip-rap and high amounts of instream structures and debris were avoided for fear the trawl would hang up.

The limitations of employing catch-rate data for indexing fish population abundance have long been acknowledged (e.g., Marr 1953). Equating catch rates with abundance involves the assumptions that vulnerability of fish to the fishing gear is constant over time and space, and that fish, fishing effort, or both, are randomly distributed. Comparing catch rates across species requires the additional assumption that species are equally vulnerable. These requirements are rarely met (Fréon and Misund 1999). Therefore, relative abundance estimates may not adequately reflect factual abundance and may be useful only for spatial and temporal comparisons if vulnerability to fishing gear remains relatively constant over them.

Data Analyses

Data analyses focused on isolating the effects of depth on fish distributions. Potential variability attributable to time was considered by adding season as a factor. Season was coded as high water (January-June) and low water (July-August) as suggested by long-term empirical stage data from the LMR (Figure 2). Average difference in depth between these two periods is 11-14 ft at four locations surveyed (Figure 2). Potentially additional temporal (e.g., lifestage, temperature annual cycle, inter-annual) and spatial (habitat type, smaller river stretches)

partitioning could account for more variability in fish depth distributions, and facilitate isolation of depth effects. Although the dataset was extensive, it could not support finer partitioning and still satisfy the sample size and missing values constraints imposed by available statistical models. Longitudinal differences in species composition along the study reach have been reported (Killgore et al. 2007; Miranda and Killgore 2011). To avoid partitioning the available samples into small subsets, thus loosing statistical power in estimating the effect of depth, longitudinal differences were not considered. Nevertheless, whereas species composition and abundance may change longitudinally, depth patterns in the study reach were relatively uniform (Figure 1), and a species relationship to depth is unlikely to change greatly as long as the same range of depths are available. Given that longitudinal differences if they exist were not considered, any depth trends identified by the analyses are conservative.

Fish depth distributions.-- Species richness (i.e., species counts) and fish depth distributions were examined with cumulative frequencies relative to depth according to season in the 703-mile upper segment. A cumulative frequency represents the sum of all the frequencies of the y-variable up to a given depth. Cumulative species richness was examined with the trawl dataset only, because the trotline dataset included a reduced number of species. Species were cumulated over depths based on the shallowest depth at which they were collected (i.e., first appearance), and based on the deepest depth at which they were collected (i.e., last appearance). Cumulative fish distributions were examined with the trawl and trotline datasets for species combined and for selected species. Only species with large sample sizes (≥ 100 specimens) collected over multiple samples (≥ 20 sets or tows) were considered for analyses. Because neither trawl nor trotline efforts were distributed equally over all depths, prior to estimating cumulative frequencies the catches were averaged according to 3-ft depth increments so that the variable cumulated was the mean catch per depth.

Cumulative species richness and cumulative frequency distributions often exhibit a sigmoid response relative to depth. At very shallow depths, cumulative values may increase slowly, increase more rapidly at intermediate depths, and rate of increase may diminish in deep water as few additional species and individuals are added. This sigmoid pattern was modeled with a Gompertz logistic-type curve that differs from the logistic model in that the former can be asymmetrical about its point of inflection, and therefore is more broadly applicable (Berger 1981). The Gompertz model summarized cumulative species richness and cumulative frequency distributions of single and combined species relative to depth as:

$$Q = 100e^{-e^{a(depth - b)}} \quad (1)$$

where,

Q = cumulative catch or species richness,

a = coefficient controlling slope of the relationship (a smaller a suggest a steeper curve),

b = coefficient indicator of depth at which the curve inflects (i.e, depth where slope changes from accelerating to decelerating).

The model was implemented with the NLIN procedure (SAS 2011) that fits nonlinear regression models and estimates the parameters iteratively (Gauss method) by nonlinear least squares. Goodness of fit was assessed with a pseudo- R^2 computed as 1 - sum of squares of error of the fitted curve / sum of squares of error of a horizontal line fitted through the mean Q .

Lower versus upper segment.-- As stated above, the study of fish distributions relative to depth focused on the upper 703-mile segment. In this segment the entire range of depths was sampled, depth distributions were less artificial than in the lower segment, and the segment included more trotline and trawl samples than the lower 250-mile segment. However, a test was conducted to assess if fish depth distributions differed between the lower and upper segments. This test considered the first 100 ft of depth for trotlines and 75 ft for trawls, as deeper water was not sampled despite extensive deeper water in the lower 250-mile segment. This analysis tested if the cumulative frequency distribution curves differed between the lower and upper segments. To this end, equation 1 was expanded to include segment designation as a dummy variable, and the interaction of segment and depth as:

$$Q = 100e^{-e^{a(depth-b)+c(segment)+d(depth \times segment)}} \quad (2)$$

where,

Q = cumulative catch or species richness,

a = coefficient controlling slope of the relationship (a smaller a suggest a steeper curve),

b = coefficient indicator of depth at which the curve inflects (i.e., depth where slope changes from accelerating to decelerating).

c = coefficient indicator of the effect of segment designation (i.e., 0=lower 250-miles segment; 1=upper 703-mile segment) on the position of the curve along the depth axis,

d = coefficient indicative of a change in curve slope in the upper segment.

When reach designation is 0 (lower segment), the last two terms drop out of the equation. When reach designation is 1 (upper segment), the slope of the relationship becomes $a + d$ and the position of the curve along the depth axis becomes $b + c$. Thus, d indicates how much steeper (or gentler) is a in the upper segment than in the lower segment, and c indicates how much greater (or smaller) is b . The 95% confidence limits around c and d were computed to test if Q differed between segments. Differences were considered statistically significant if the confidence limits around c or d did not overlap zero.

FFP versus non-FFP reaches.-- The depth distribution of fish was compared between reaches identified as suitable for installation of free-flow kinetic hydropower and other reaches in the upper segment. No comparisons were made in the lower segment because fish collections were not available from deep reaches where FFP may be installed. In all, 67 reaches were identified by FFP as potential development sites in the LMR; 43 of these reaches occurred between RM 250 and RM 953 and were included in this analysis (Table 1). The 43 FFP reaches ranged in length from 1.7 to 16.4 miles. This analysis tested if the cumulative frequency distribution curves differed between FFP reaches and non-FFP reaches. To this end, equation 2 was modified to

include reach designation as a dummy variable, and the interaction of reach designation and depth as:

$$Q = 100e^{-a(depth - b) + c(reach) + d(depth \times reach)} \quad (3)$$

where,

Q = cumulative catch or species richness,

a = coefficient controlling slope of the relationship (a smaller a suggest a steeper curve),

b = coefficient indicator of depth at which the curve inflects (i.e., depth where slope changes from accelerating to decelerating).

c = coefficient indicator of the effect of reach designation (i.e., 1=FFP reach, 0=non-FFP reach) on the position of the curve along the depth axis,

d = coefficient indicative of a change in slope at FFP reaches.

When reach designation is 0 (non-FFP reach), the last two terms drop out of the equation. When reach designation is 1 (FFP reach), the slope of the relationship becomes $a + d$ and the position of the curve along the depth axis becomes $b + c$. Thus, d indicates how much steeper (or gentler) is a in FFP reaches than in non-FFP reaches, and c indicates how much greater (or smaller) is b . The 95% confidence limits around c and d were computed to test if Q differed between FFP and non-FFP reaches. Differences were considered statistically significant if the confidence limits around c or d did not overlap zero.

Fish size distributions.-- Distributions of fish sizes relative to depth were examined through correlation analyses. Lengths were averaged by 3-ft depth increments and these means correlated with depth using Spearman rank correlation. Rank correlation was applied to avoid assumptions of data normality and to account for potential increasing or decreasing curvilinear trends. Potential parabolic-shaped relationships were considered by examining scatter plots of mean lengths plotted against depth. This analysis was limited to species with large sample sizes (≥ 100 specimens) collected over multiple samples (≥ 20 sets or tows). Fork lengths were used for sturgeon species and total lengths for all others. Analyses were conducted separately for the trotline and trawl data sets.

Results

A total of 1,096 trotline samples and 612 trawl samples were collected in the study reach between 1997 and 2011. Depths sampled with trotlines ranged from 2 to 89 ft ($N=157 \geq 40$ ft), and those sampled by the trawls ranged from 3 to 74 ft ($N=30 \geq 40$ ft). Sample distribution by depths <25 ft, 25-49.9 ft, and ≥ 50 ft were 548, 499, and 49 trotlines, and 461, 142, and 9 trawl tows. In all, 59% of the trotline samples and 43% of the trawl samples were taken during the high-water period and the remainder during the low-water period. Up to 18 trotlines (mean = 6.4) were deployed over a river segment. The trotlines were deployed over segments that 75% of the time encompassed no more than 0.7 miles, although extended up to 5.8 miles. Trawl tows

averaged 0.6 miles (SD = 0.37) and ranged from 0.1 to 3.9 miles; vessel speed averaged 2.9 miles/h (SD = 0.81) and ranged from 0.5 to 5.1 miles/h. Up to 11 trawls (mean = 3.8) were towed over different depths in a river segment. The trawls were towed over segments that 75% of the time encompassed no more than 4 miles, although extended up to 8.8 miles.

The trotline effort produced 9,821 fish of 19 species, and the trawling effort produced 42,138 fish of 62 species (Table 2). In all, 70% of the fish collected by trotlines and 45% of the fish collected by trawls were taken during the high-water period, although species percentage frequency of occurrence varied between low water and high water (Table 2). The most common species collected by trotlines were blue catfish (47.3% of total catch), shovelnose sturgeon (37.2%), channel catfish (7.3%), freshwater drum (18.0%), flathead catfish (2.1%), and pallid sturgeon (1.7%). The most common species collected by trawls were blue catfish (25.8), freshwater drum (21.0%), channel catfish (16.5), speckled chub (13.2), channel shiner (8.7), shovelnose sturgeon (5.7), silver chub (2.2), silverband shiner (1.8), paddlefish (1.3), and gizzard shad (1.2). The most commonly collected fish species exhibited broad depth distributions; occasionally species showed narrow depth ranges but these were usually associated with small sample sizes.

Distribution of fish lengths collected differed between the two gears, although there was considerable overlap. Trawls collected smaller species and smaller specimens of large species than trotlines. The median length of fish collected with trotlines was 18.1 in (range 2.1-42.2) and that of trawls was 2.1 in (range 0.4-49.7). Moreover, 99% of the fish collected by trotlines were larger than 4 in, and 73% of the total catch of fish in trawls was composed of fish smaller than 4 in. Thus, while lengths overlapped because trawls occasionally collected large specimens, large fish were atypical in trawl samples resulting in a strongly right-skewed size distribution.

Species Richness Relative to Depth

Cumulative species richness exhibited a sigmoid pattern along depth gradients that varied over low- and high-water periods. Depth of first appearance was generally shallow with 50% of the species first collected by a depth of 5 ft (Figure 4); conversely, about 50% of the species were no longer collected below 25 ft. The inflection points for the first collection curves were 4.9 ft (i.e., b ; Figure 4) for low water and 4.2 ft for high water. The inflection points for the last collection curves were 23.6 ft for low water and 21.4 ft for high water. The pseudo- r^2 for the curves were 0.98 for low water and 0.92 for high water. In the low water period 20% of the species remained in water deeper than 40 ft; in high water 15% of the species remained in water deeper than 52 ft. Thus, as expected low-water concentrated species in relatively shallow water but species became more dispersed over depths in high water. However, the maximum number of species occurred at 15-20 ft (maximum vertical distance between curves in Figure 4) in the low- or high-water periods. Moreover, the number of species present near the bottom at depths beyond 40 ft was reduced to about 20% of all species collected.

Species Depth Distribution

Overall, catch rates increased with depth, peaked, and decreased at greater depths. For trotlines, catch rates ranged from 0 to 52 fish/trotline, with some of the highest catches at intermediate depths (Figure 5). When cumulated over 3-ft intervals, and according to low- and high-water period, cumulative percentage catch distribution of all species combined showed sigmoid curves that inflected at 27.5 ft in low water and 29.4 ft in high water. For trawls, catch rates ranged from 0 to 1,087 fish/ac, with the highest catches also at intermediate depths (Figure 5). When cumulated over 3-ft intervals, and according to low- and high-water periods, cumulative percentage catch was sigmoidal inflecting at 22.8 ft in low water and 14.3 ft in high water. Percentage frequency distribution curves were log-normal in appearance, ascending rapidly at shallow depths, peaking at inflection points noted above (i.e., b), and descending more slowly than they rose. Distribution of fish shifted towards deeper water during high water for trotlines, but towards shallower water for trawls, potentially reflecting differences in fish sizes and life stages collected by the two gears. The pseudo- r^2 for the curves ranged 0.97-0.98 (Table 3).

Six species collected with trotlines and 13 species collected with trawls met the sample size requirements for cumulative-frequency analyses (≥ 100 specimens collected over ≥ 20 sets or tows), with five of the species analyzed collected by both gears (Table 3). With few exceptions, values of a (equation 1) ranged from -0.213 to -0.052, suggesting gently ascending cumulative percentage curves and log-normal percentage curves similar to those illustrated for all species combined (Figure 5) and for selected species (Appendix 1a for trotlines and Appendix 1b for trawls). The exceptions, all collected in the low-water period with trawls, included species with a values ranging -1.354 to -0.623, suggesting sharply rising cumulative percentage curves, leptokurtic percentage log-normal curves, and narrow depth distributions. Values of b ranged -0.7 to 32.0 ft, and were mostly larger for trotlines than trawls, but no seasonal trend was evident. A comparison of estimates made for the five species collected with trotlines and trawls (i.e., shovelnose sturgeon, flathead catfish blue catfish, channel catfish, freshwater drum) showed gear-related differences, with estimated depth at curve inflection (b) differing by 1-18 ft (mean 6.9) between gears for the same species. The pseudo- r^2 for the curves ranged 0.85-0.99 (Table 3).

Depth-distribution curves also estimated the percentage of time populations occupied water deeper than 40 ft during low water and deeper than 52 ft during high water. For all species combined, trotlines estimated these percentages at 37.7 and 27.1, respectively (Table 3). For trawl samples these percentages were 33.3 and 6.6, respectively. For individual species, during low water, estimates ranged from 0.1 to 39.7%, and averaged 14.0%. During high water, estimates ranged 0 to 27.1%, with an average 6.8% for the populations studied.

Lower versus Upper Segment

The depth of the LMR up to RM 250 averages 46.3 ft, with 53.63% of the river deeper than 40 ft and 5.60% deeper than 100 ft. Upstream of RM 250 through RM 953 depth averages 22.0 ft, with 11.53% of the river deeper than 40 ft and 0.05% deeper than 100 ft. The trotline

data set included 192 trotline sets in the lower segment, and 1,096 sets in the upper segment. Similarly, the trawl data set included 131 tows in the lower segment and 612 tows in the upper segment. In all, 66 fish species were collected with trotlines and trawls in the lower segment, and 62 fish species in the upper segment. Overall, maximum depth sampled with trotlines was 89 ft and with trawls was 74 ft. No statistically significant differences between the two segments were evident relative to depth distribution of catch rates of trotlines or of trawls (Table 4). Similarly, depth distribution of species richness as measured with trawls did not differ significantly between segments.

FFP versus Non-FFP Reaches

The 43 FFP reaches between RM 250 and RM 953 averaged 23.8 ft (max 245) in mean depth. The mean depth of the LMR within the 703-miles segment is 22.0 ft, and the mean in this segment excluding the FFP reaches is 20.5 ft (max 142). The trotline data set included 507 trotline sets within the 43 FFP reaches, and 589 sets outside the FFP reaches. Similarly, the trawl data set included 349 tows within the FFP reaches and 263 tows outside these reaches. In all, 42 fish species were collected with trotlines and trawls in the FFP reaches, and 47 fish species in the non-FFP reaches.

The comparison of cumulative catch distributions over depth identified few statistically significant differences between the FFP reaches and the non-FFP reaches (Table 5). Species richness cumulative curves computed based on the depth at which species first appeared were not significantly different between FFP and non-FFP reaches during the low-water period or high-water period. Conversely, species richness cumulative curves computed based on the depth at which species last appeared were not significantly different between FFP and non-FFP reaches during high water, but were significantly different during low water. These results suggested that when differences did occur, richness in FFP reaches increased more steeply, with lesser richness in shallow water than non-FFP reaches, and with more species disappearing sooner than in non-FFP reaches (Figure 6). No differences in distribution over depths between FFP and non-FFP reaches were evident for either the trotlines or the trawls data set, during the low or the high water periods. Differences in depth profiles between FFP and non-FFP reaches could likely cause differences in species depth distributions. However, the observed differences between FFP and non-FFP sites were small, even if some were statistically significant.

Fish Size Relative to Depth

Considering all species combined, larger fish tended to occur in deeper water during the high-water period, but no correlation was evident during the low-water period (Table 6). Less than half of the species included in these analyses exhibited statistically significant ($P \leq 0.05$) correlations between body size and water depth, with correlation coefficients as high as 0.64. No parabolic-shaped relationships were evident by examining scatter plots. Species exhibited various direct and inverse correlations with depth, in low- and high-water periods. Some species

exhibited a correlation in one season but not in the other, and some exhibited a direct correlation in one season and an inverse correlation in the other. Overall, the statistically significant correlation coefficients were not large. Thus, patterns in depth distribution relative to body size were evident, but were not strong.

Discussion

During 1997-2011 fish were collected with trotlines in depths up to 89 ft, and with trawls in depths up to 74 ft. These collections suggested that fish in the LMR exhibit non-random depth distributions that vary seasonally and according to species. In general, fish frequency of occurrence diminishes in deep water. In terms of species counts, trawls estimated that in the low water period only 20% of the species collected remained in water deeper than 40 ft. In terms of fish counts, trotlines and trawls estimated that during the low-water months 38% and 33% of all fish, respectively, occupied depths deeper than 40 ft and may be exposed to FFP turbine installations. However, these estimates varied among species with individuals of some species frequent in deep water, others frequent in shallow water, and some switching from deep water to shallow water depending on time of year. Also, estimates differed between the low-water and high-water periods, with fewer species and generally fewer individuals of a species occupying depths deeper than 52 ft during high water (equivalent to 40 ft during low water). Overall species combined, fish collected in deep water tended to be larger than those collected in shallow water during the high-water period, but no such relationship was evident during low water. Depth distribution of fish in reaches identified as candidates for FFP were not different from those in other reaches.

These estimates reflect the fraction of time that fish species occupy various depths. Because these estimates do not consider depth availability, they do not reflect the fraction of an entire population or community occupying various depths. The latter can be estimated by considering depth distributions in the LMR. For instance, the distribution of depths in the LMR above RM 250 indicates that depths over 40 ft occur in 12% of the river (Figure 1, table inset). If fish exhibited no depth preferences and were uniformly distributed over all depths (i.e., in Figure 5 cumulative percentage curves were straight rather than s-shaped, and the percentage increment curves were a horizontal line rather than a dome-shaped line), then 12% of the fish community would occupy depths over 40 ft. However, because the data show that fish are not randomly distributed relative to depth and that fewer fish occur in deeper water, the percentage of the population present below 40 ft should be less. As a conservative assumption, this percentage may be estimated as the product of the probability of finding water deeper than 40 ft, and the probability of fish occupying water deeper than 40 ft, as the low water threshold from data collected by multiple gear types. In all cases, the probability of finding fish in low water (40 ft) was found to be greater than in high water (52 ft) (Table 3). For example, if the probability of finding shovelnose sturgeons during low water at depths over 40 ft is 35.3% from the trotline data and from 3.1% from the trawl data (Table 3), and depths over 40 ft occur in 12% of the upper river region (Figure 1, table insert), then between 4.2% (i.e., 0.353×0.12) for the trotline data and 0.37% (i.e., 0.031×0.12) for the trawl data, of the shovelnose sturgeon population is estimated to occur in depths over 40 ft at any one time and would be at risk of encountering a

turbine. While this range estimate of this population may be exposed to FFP turbines installed in water deeper than 40 ft, the actual percentage at risk of being impacted by a turbine would be less considering the fraction of the river volume that this species and its population could encounter the turbine throughout a multi-dimensional representation of river at the project locations.

A comparison of proposed FFP sites with non-FFP sites produced minimal differences in fish depth distributions. This result was not unexpected considering depth distributions are intrinsic to species in a habitat, and probably do not change greatly as long as a wide range of depths is available. Whereas the depth distributions did not change greatly, fish densities could have. Given that species richness and fish density decreased with depth, and the FFP sites are deeper, is possible that species richness and fish abundance in FFP sites may be lower. No population size estimates were available to substantiate this inference, but species richness in FFP sites was lower than in non-FFP sites.

Whereas river stage increased by about 12 ft between the low-water and high-water periods, depth distribution of species (Figure 4) and depth distribution of catch rates (Figure 5, Table 4, Appendix 1a, b) did not increase by a corresponding 12 ft. Indeed, the greatest increase was about 6 ft, but more often depth distribution of species decreased rather than increased during high water. This response suggests that fish are not merely staying at a more or less fixed position on the riverbed possibly associated with a certain habitat type, but instead change positions between the low-water and high-water periods. Depth is an indicator for many factors that affect fish depth distribution. For example, water velocity changes with depth and likely influences fish depth distribution as fish move to shallower or deeper water to avoid fast or slow currents. As another example, increases in depth due to higher river stages flood riparian habitats potentially prompting changes in depth distribution associated with feeding or reproductive behaviors. Thus, fish exhibit seasonal changes in depth distributions that may be attributed to a multiplicity of environmental and behavioral factors.

Seasonal shifts in depth distributions were also reflected by the differences in the percentage of fish collected below 40 ft during low water and below 52 ft during high water. The null expectation would be that the percentages would remain relatively stable if fish were staying at a fixed position in the riverbed. When considering all species combined, a higher percentage of fish occurred below 40-ft depth during low water than below 52-ft depth during high water. This trend was apparent for most species, but some species exhibited a reversed trend. Also, some species showed large shifts in depth distribution during low-water and high-water periods whereas some did not, reflecting species-specific seasonal habitat needs, and possibly random variability in the data. Nevertheless, results suggest that most fish avoid excessive depths and thus the risk of encountering an FFP installation will shift seasonally with river stage, and will be highest during low water.

In this study fish distributions were examined relative to depth. Perhaps an equivalent analysis could have been conducted in relation to other environment descriptors such as current velocity, substrate composition, bottom slope, distance from shore, habitat type, and others. Depth was selected because it can be measured easily and accurately, and because it has been

confirmed to index a variety of other environmental characteristics relevant to fish distribution such as current velocity, light availability, substrate, distance from shore, and various water quality descriptors. Depth is also relevant in the context of FFP installations because their location is largely determined by depth. Depth measurements used in this study were made in relation to the water surface, so that to maintain the same depth as the water level changes, location must change. For FFP installations, which have fixed locations, perhaps a more relevant way to look at the effect of depth would have been to compare fish catches at a fixed location as depth changes with water level. This alternative approach was not feasible with the available data because trotlines were not consistently fished in the same location, and trawls are an active capture gear that does not fish at a fixed site.

The sampling gears used in this study target species that occupy benthic habitats part-time or full-time. Species choose these habitats for various reasons, but principally because they provide access to food, safe haven from predators, and refuge from strong currents considering that rigor of the river bottom can be high. Nevertheless, the FFP turbines would be suspended in depths ranging from 10 to 55 ft off the bottom. Thus, depending on depth, turbines may be installed near the bottom or some distance away from the bottom. Most riverine fish travel along the bottom to avoid high-velocity currents, but occasionally may migrate vertically. Shovelnose sturgeons, for example, use the bottom to feed and as refuge from currents, but may occasionally move up in the water column and periodically surface (LeBreton et al. 2004; Allen et al. 2007). Other species uncommonly caught in trotlines and trawls (e.g., temperate basses, gars, herrings) may spend less time on the bottom. Thus, additional survey work is being planned by FFP once turbines are installed during the in-situ deployment to determine if fish in general, and particular species, are found at the installations in mid-water.

Acknowledgments

Data used in these analyses were provided by Dr. Jack Killgore, U.S. Army Corps of Engineers Research and Development Center, Vicksburg, Mississippi.

References

Allen, T.C., Q.E. Phelps, R.D. Davinroy, and D.M. Lamm. 2007. A laboratory examination of substrate, water depth, and light use at two water velocity levels by individual juvenile pallid (*Scaphirhynchus albus*) and shovelnose (*Scaphirhynchus platorynchus*) sturgeon. *Journal of Applied Ichthyology* 23:375-381.

Austin, M. 2007. Species distribution models and ecological theory: A critical assessment and some possible new approaches. *Ecological Modelling* 200(1-2):1-19.

Baker, J.A., K.J. Killgore, and R.L. Kasul. 1991. Aquatic habitats and fish communities in the Lower Mississippi River. *Reviews in Aquatic Sciences* 3:313–356.

Berger, R.D. 1981. Comparison of the Gompertz and logistic equations to describe plant disease progress. *Phytopathology* 71:716-719.

Blackburn, T.M., and K.J. Gaston. 1994. Animal body size distributions: patterns, mechanisms, and implications. *Trends in Ecology and Evolution* 9:471–474.

Brandt, S.B. 1980. Spatial segregation of adult and young-of-the-year alewives across a thermocline in Lake Michigan. *Transactions of the American Fisheries Society* 109:469-478.

Brokovich, E., S. Einbinder, N. Shashar, M. Kiflawi, and S. Kark. 2008. Descending to the twilight-zone: changes in coral reef fish assemblages along a depth gradient down to 65 m. *Marine Ecology Progress Series* 371:253–262.

Brosse, S., and S. Lek. 2002. Relationships between environmental characteristics and the density of age-0 Eurasian perch *Perca fluviatilis* in the littoral zone of a lake: a nonlinear approach. *Transactions of the American Fisheries Society* 131:1033–1043.

Cada, G., J. Ahlgrimm, M. Bahleda, T. Bigford, S. Damiani-Stavrakas, D. Hall, R. Moursund, and M. Sale. 2007. Potential impacts of hydrokinetic and wave energy conversion technologies on aquatic environments. *Fisheries* 32:174-181.

Day, D.S., and W.G. Pearcy. 1968. Species associations of pelagic fishes on the continental shelf and slope off Oregon. *Journal of the Fisheries Research Board of Canada* 25:2665–2675.

Eckmann, R., and F. Imbrock. 1996. Distribution and diel vertical migration of Eurasian perch (*Perca fluviatilis* L.) during winter. *Annales Zoologici Fennici* 33:679–686.

Fréon, P., and O. A. Misund. 1999. Dynamics of pelagic fish distribution and behavior: effects on fisheries and stock assessment. *Fishing News Books*, Blackwell, Oxford, U.K.

Friedlander, A.M., and J.D. Parrish. 1998. Habitat characteristics affecting fish assemblages on a Hawaiian coral reef. *Journal of Experimental Marine Biology and Ecology* 224:1–30.

Gutreuter, S., J.M. Dettmers, and D. H. Wahl. 2003. Estimating mortality rates of adult fish from entrainment through the propellers of river towboats. *Transactions of the American Fisheries Society* 132:646–661.

Hayes, M.I. 1983. Active fish capture methods. Pages 123–145 in L.A. Nielsen and D.L. Johnson, editors. *Fisheries Techniques*. American Fisheries Society, Bethesda, Maryland.

Herzog, D.P., and V.A. Barko. 2005. Efficacy of a benthic trawl for sampling small-bodied fishes in large river systems. *North American Journal of Fisheries Management* 23:594–603.

Hovgård, H., and F.F. Riget. 1992. Comparison of long-line and trawl selectivity in cod surveys off West Greenland. *Fisheries Research* 13:323–333.

Hubert, W.A. 1996. Passive capture techniques. Pages 157–192 in B. Murphy and D. Willis, editors. *Fisheries techniques*, 2nd edition. American Fisheries Society, Bethesda, Maryland.

Hynes, G.A., M.E. Platell, I.C. Potter, and R.C.J. Lenanton. 1999. Does the composition of the demersal fish assemblages in temperate coastal waters change with depth and undergo consistent seasonal changes? *Marine Biology* (Springer-Verlag) 134:335–352.

Jensen, P. 1988. Nematode assemblages in the deep-sea benthos of the Norwegian Sea. *Deep-Sea Research* 35:1173–1184.

Junk, W.J., P.B. Bayley, and R.E. Sparks. 1989. The flood pulse concept in river-floodplain systems. Pages 110–127 in D.P. Dodge, editor. *Proceedings of the International Large River Symposium*. Canadian Special Publication of Fisheries and Aquatic Sciences 106.

Killgore, K.J., J.J. Hoover, S.G. George, B.R. Lewis, C.E. Murphy, and W.E. Lancaster. 2007. Distribution, relative abundance and movements of pallid sturgeon in the free-flowing Mississippi River. *Journal of Applied Ichthyology* 23:476–483.

Killgore, K.J., L.E. Miranda, C.E. Murphy, D.M. Wolff, J.J. Hoover, T.M. Keevin, S.T. Maynard, and M.A. Cornish. 2011. Fish entrainment rates through towboat propellers in the Upper Mississippi and Illinois rivers. *Transactions of the American Fisheries Society* 140:570–581.

Kubecka, J., and A. Duncan. 1998. Diurnal changes of fish behaviour in a lowland river monitored by dual-beam echo sounder. *Fisheries Research* 35:55–63.

Lara, E.N., and E.A. Gonzalez. 1998. The relationship between reef fish community structure and environmental variables in the southern Mexican Caribbean. *Journal of Fish Biology* 53:209–221.

LeBreton, G.T.O. , F.W.H. Beamish, and S.R. McKinley, editors. 2004. Sturgeons and paddlefish of North America. Kluwer, Dordrecht, The Netherlands.

Løkkeborg, S., and Å. Bjordal. 1992. Species and size selectivity in long-line fishing: A review. *Fisheries Research* 13:311–322.

Lomolino, M.V. 2001. Elevational gradients of species diversity: historical and prospective views. *Global Ecology and Biogeography* 10:3–13.

Lorance, P., S. Souissi, and F. Uiblein. 2002. Point, alpha and beta diversity of carnivorous fish along a depth gradient. *Aquatic Living Resources* 15:263-271.

Madenjian, C.P., and D.B. Bunnell. 2008. Depth distribution dynamics of the sculpin community in Lake Michigan. *Transactions of the American Fisheries Society* 137:1346-1357.

Marr, J. C. 1953. On the use of the terms abundance, availability, and apparent abundance in fishery biology. *Copeia* 2:163–169.

Matthews, W.J., K.B. Gido, and F.P. Gelwick. 2004. Fish assemblages of reservoirs, illustrated by Lake Texoma (Oklahoma - Texas, USA) as a representative system. *Lake and Reservoir Management* 20:219–239.

McKaye, K.R. and J.R. Stauffer. 1986. Seasonality, depth and habitat distribution of breeding males of *Oreochromis* spp., ‘chambo’, in Lake Malawi National Park. *Journal of Fish Biology* 33:825–834.

Miranda, L.E. 2011. Depth as an organizer of fish assemblages in floodplain lakes. *Aquatic Sciences* 73:211-221.

Miranda, L.E., and K.J. Killgore. 2011. Catfish spatial distribution in the free-flowing Mississippi River. *American Fisheries Society Symposium* 77:521-534.

Mous, J.P., W.L.T. van Densen, and M.A.M. Machiels. 2004. Vertical distribution patterns of zooplanktivorous fish in a shallow, eutrophic lake, mediated by water transparency. *Ecology of Freshwater Fish* 13:61–69.

Nanami, A., and M. Nishihira. 2002. The structures and dynamics of fish communities in an Okinawan coral reef: effects of coral-based habitat structures at sites with rocky and sandy sea bottoms. *Environmental Biology of Fishes* 63:353–372.

Ramm, D.C., and Y. Xiao. 1995. Herding in groundfish and effective pathwidth of trawls. *Fisheries Research* 24:243–259.

Rex, M.A., and R.J. Etter. 1998. Bathymetric patterns of body size: implications for deep-sea biodiversity. *Deep-Sea Research* 45:103–127.

Phelps, Q.E., D.P. Herzog, R.C. Brooks, V.A. Barko, D.E. Ostendorf, J.W. Ridings, S.J. Tripp, R.E. Columbo, J.E. Garvey, and R. A. Hrabik. 2009. Seasonal comparison of catch rates and size structure using three gear types to sample sturgeon in the middle Mississippi River. *North American Journal of Fisheries Management* 29:1487-1495.

Prchalová, M., J. Kubečka, M. Čech, J. Frouzová , V. Draštík , E. Hohausová, T. Jůza, M. Kratochvíl, J. Matěna, J. Peterka, M. Říha, M. Tušer, and M. Vašek. 2009. The effect of depth, distance from dam and habitat on spatial distribution of fish in an artificial reservoir. *Ecology of Freshwater Fish* 18:247-260.

Pugh, L.L., and H.L. Schramm. 1998. Comparison of electrofishing and hoopnetting in lotic habitats of the lower Mississippi River. *North American Journal of Fisheries Management* 18:649-656.

Rickel, S, and A. Genin. 2005. Twilight transitions in coral reef fish: the input of light-induced changes in foraging behaviour. *Animal Behaviour* 70:133–144.

Russ, G.R. 2003. Grazer biomass correlates more strongly with production than with biomass of algal turfs on a coral reef. *Coral Reefs* 22:63–67.

SAS. 2011. SAS/STAT® 9.2 user's guide. SAS Institute, Inc. Cary, North Carolina.

Smith, K.F., and J.H. Brown. 2002. Patterns of diversity, depth range and body size among pelagic fishes along a gradient of depth. *Global Ecology and Biogeography* 11:313-322.

Vannote R.L. , G.W. Minshall, K.W. Cummins, J.R. Sedell, and C.E. Cushing. 1980. The River Continuum Concept. *Canadian Journal of Fisheries and Aquatic Sciences* 37:130-137.

Walsh, S. J. 1996. Efficiency of bottom-sampling trawls in deriving survey abundance indices. *NAFO Science Council Studies* 28:9-24.

White, C.E., Jr. 1956. Fish catches with various types of commercial fishing gear used in TVA lakes from June, 1954 through January, 1955. *Proceedings of the Annual Conference Southeastern Association of Fish and Wildlife Commissioners* 9(1955):80–86.

Table 1. Location and depth characteristics of 67 reaches identified by FFP as potential development sites in the Lower Mississippi River. Also shown are mean catch per trotline (CPL) and mean catch per acre (CPA). CV = 100 X standard deviation/mean; N = number of sets/tows; and SE = standard error. Blanks indicate no collections were made within a reach.

Name	FFP ID	Reach (mile)		Depth (ft)			Trotlines			Trawls		
		Start	End	Mean	Max	CV	CPL	N	SE	CPA	N	SE
Ironton Light	2038	58.5	61.5	79.1	182.1	49				9.4	2	9.4
Live Oak	2032	67.2	69.0	73.8	134.8	49				218.5	3	107.2
Twelve Mile Point	2037	75.8	86.1	73.2	180.1	42	12.4	21	1.5	250.2	18	95.9
Algiers Light	2036	92.8	95.0	101.4	199.1	42						
Gouldsboro Bend	2035	95.6	98.2	81.4	137.1	38						
Greenville Bend	2033	99.1	102.0	81.0	192.9	44						
Carrollton Bend	2034	103.3	105.2	86.9	171.9	44						
Avondale Bend	2019	108.0	109.8	79.7	142.1	45						
Kenner Bend	2020	111.1	115.5	55.8	138.1	51						
St. Rose Bend	2021	117.0	119.8	68.9	144.0	45	3.1	7	1.6			
Fashion Light	2039	121.5	126.5	59.7	153.9	52	7.6	15	2.2	302.8	2	90.3
Thirty Five Mile Point	2022	128.3	130.9	74.1	157.2	48						
Forty Eight Mile Point	2023	139.5	146.2	59.4	161.1	57	11.3	27	1.0	109.3	25	38.3
Remy Bend	2024	149.8	152.2	68.6	164.0	51						
College Point	2025	155.5	157.8	61.0	150.9	55	4.8	9	0.9			
Brilliant Point	2026	160.8	166.4	61.7	157.2	50				219.2	7	115.0
General Hampton	2027	168.3	174.5	60.0	166.0	57	11.0	32	1.4	86.6	5	48.3
Eighty One Mile Point	2028	175.5	182.0	53.1	178.1	62	21.0	8	7.1			
White Alder	2029	191.2	196.4	40.7	143.0	73	13.9	23	1.2	363.6	7	99.0
Point Pleasant	2030	197.9	201.0	48.6	143.0	67						
Reliance Light	2031	205.7	210.8	37.1	163.1	76						
Duncan Point	2018	219.5	224.0	32.2	123.0	86						
Scotlandville Bend	2017	233.9	236.9	40.7	109.9	56						
Springfield Bend	2042	238.8	246.3	38.4	98.1	62				153.8	3	139.8
Point Menoir	2043	252.5	255.1	42.3	115.2	58						
Sara Bend	2000	262.3	266.2	21.7	82.0	86						
Morgan's Bend	2001	274.9	283.5	33.5	110.9	63						
Raccourci Island	2044	287.2	291.5	24.6	92.8	60						
Raccourci Cut-Off	2064	295.9	305.9	23.0	109.9	68						
Fort Adams	2045	307.3	311.5	32.2	84.0	58	13.0	41	1.2	124.8	1	
Breeze Point	2041	311.5	316.5	23.3	82.0	60	3.8	4	1.2			
Palmetto Point	2046	316.5	322.0	35.8	111.9	65	6.0	5	1.3	114.2	1	
Jackson Point	2047	326.5	334.0	29.5	108.9	78						
Saint Catherine Bend	2048	341.8	349.6	36.7	99.1	63						
Vidal Island	2067	360.7	371.1	29.2	96.1	53	8.0	3	1.7	424.9	1	

Kempe Bend	2002	381.1	386.5	28.2	104.0	73						
Bondurant Chute	2049	395.4	400.9	31.8	95.1	62	12.6	22	1.7	206.4	1	
Davis Island Bend	2050	411.9	417.7	33.8	109.9	68	7.1	75	0.8	281.6	20	103.3
Newton Bend	2003	417.8	427.4	24.9	76.1	64	5.5	40	1.1	144.4	12	38.1
Vicksburg Bend	2066	427.3	442.5	30.2	94.2	65	8.1	107	0.7	214.8	59	50.6
Cat Island	2004	493.6	500.0	26.2	84.0	66						
Matthews Bend	2051	510.8	516.9	31.8	89.9	69						
Anconia Point	2005	530.1	531.8	34.1	67.9	39						
Miller Bend	2052	543.5	547.5	15.7	63.0	81						
Georgetown Bend	2053	550.8	556.3	39.4	84.0	49				316.9	3	124.0
Malone Field Light	2006	582.1	591.5	25.3	86.9	74	7.0	54	1.0	148.0	2	146.1
Burke Landing	2055	631.0	636.3	22.0	78.1	78	21.5	2	0.5			
Old Town Bend	2054	642.0	645.4	30.5	100.1	71	50.0	1		274.9	4	208.9
Helena Reach	2007	662.4	669.0	20.3	74.1	62	11.0	2	0.0			
Ashley Point	2008	679.1	695.5	20.7	88.9	76	9.0	82	0.9	269.7	228	28.9
Cow Island Bend	2056	711.6	717.8	21.0	86.9	70						
Hope Field Point	2009	725.0	736.9	24.3	92.8	63	11.3	10	4.5	421.4	3	11.5
Island 35 Bend	2057	761.6	772.6	23.0	245.1	82	5.6	15	0.5			
Plum Point	2040	776.5	788.9	22.0	130.9	68	11.9	14	2.0			
Barfield Point	2058	800.1	804.4	32.2	80.1	59						
Bar Field Bend	2014	804.7	814.5	23.3	103.0	69						
Huffman Light	2010	822.8	826.5	25.9	68.9	54						
Linwood Bend	2059	837.9	844.0	16.1	69.9	66	3.5	4	0.9			
Little Prairie Bend	2011	846.5	851.9	23.3	79.1	66	12.0	4	1.6	185.4	3	89.5
Island 14 Bend	2060	855.0	860.3	23.6	97.1	74						
Little Cypress Bend	2061	861.3	866.8	23.0	80.1	72						
Williams Point	2015	873.0	880.9	23.6	87.9	67						
New Madrid Bend	2012	883.0	893.0	20.7	111.9	67	5.9	7	2.4	176.9	2	11.0
Slough Bend	2062	896.4	902.6	18.0	66.9	65	5.6	7	0.7	161.9	1	
Hickman Bend	2013	917.9	923.8	23.6	129.9	62						
Twin Pond	2063	936.6	939.6	33.1	82.0	50						
Wickliffe	2016	950.0	952.9	21.0	73.2	66	17.6	8	2.8	190.2	3	103.3

Table 2. Fish species collected with trotlines (T; N = 1,096) and otter trawls (O; N = 612) in the Lower Mississippi River between RM 250 and RM 953, during 1997-2011. N₁ represents the number of samples in which the species was collected, and N₂ the number of specimens collected. Low water (%) represents the percentage of the samples taken during the low-water period (Jul-Dec). Median length (fork lengths are given for sturgeon species and total lengths for all others) is the length at which 50% of the fish collected were smaller and 50% were larger. Depths represent the minimum and maximum depth at which each species was collected.

Common name	Scientific name	Gear	N ₁	N ₂	Low water (%)	Median length (in)	Depth (ft)	
							min	max
American eel	<i>Anguilla rostrata</i>	T	28	29	48	24.8	8.2	72.8
		O	10	11	55	24.6	10.2	35.4
Paddlefish	<i>Polyodon spathula</i>	T	6	17	18	27.1	15.7	32.2
		O	65	549	8	0.9	3.9	40.7
Pallid sturgeon	<i>Scaphirhynchus albus</i>	T	117	156	24	28.3	6.2	65.9
		O	37	96	21	28.9	6.9	44.0
Shovelnose sturgeon	<i>S. platorhynchus</i>	T	606	3449	21	23.5	6.2	88.9
		O	226	2411	29	23.0	3.3	69.6
Bowfin	<i>Amia calva</i>	T	1	1	100	25.1	18.4	18.4
		O	1	2	100	24.0	25.6	25.6
Longnose gar	<i>Lepisosteus osseus</i>	T	1	1	100	37.6	4.6	4.6
		O	24	40	50	36.3	7.5	38.4
Shortnose gar	<i>L. platostomus</i>	T	3	7	100	24.4	7.5	16.7
		O	11	23	65	24.8	6.9	31.5
Spotted gar	<i>L. oculatus</i>	T	7	11	100	25.2	7.9	27.2
		O	16	57	86	24.4	10.2	38.4
Rainbow smelt	<i>Osmerus mordax</i>	O	1	1	0	2.3	8.9	8.9
Goldeye	<i>Hiodon alosoides</i>	O	53	304	92	3.7	3.9	33.5
Mooneye	<i>H. tergisus</i>	O	7	19	26	1.2	3.6	16.4
Skipjack herring	<i>Alosa chrysochloris</i>	O	28	56	93	3.1	4.9	45.6
Gizzard shad	<i>Dorosoma cepedianum</i>	O	56	502	37	4.1	3.6	45.6
Threadfin shad	<i>D. petenense</i>	O	38	258	98	2.6	3.3	47.2
Bighead carp	<i>Hypophthalmichthys nobilis</i>	O	2	2	50	29.3	11.2	16.1
Silver carp	<i>H. molitrix</i>	T	1	1	100	31.5	20.3	20.3
		O	31	69	72	20.9	6.9	37.4
Grass carp	<i>Ctenopharyngodon idella</i>	O	6	10	100	37.0	10.2	16.1
Common carp	<i>Cyprinus carpio</i>	T	7	8	63	23.6	2.0	72.8
		O	26	51	80	21.4	4.9	38.4
Channel shiner	<i>Notropis wickliffi</i>	O	60	3646	32	1.7	2.3	53.5
River shiner	<i>N. blennius</i>	O	7	30	90	2.2	3.9	26.2
Silverband shiner	<i>N. shumardi</i>	O	37	741	17	2.0	3.3	46.9
Emerald shiner	<i>N. atherinoides</i>	O	7	31	100	1.8	10.2	25.6
Blacktail shiner	<i>Cyprinella venusta</i>	O	4	7	100	2.8	3.6	25.6
Bullhead minnow	<i>Pimephales vigilax</i>	O	16	58	52	1.6	3.6	26.2
Bluntnose minnow	<i>P. notatus</i>	O	5	20	65	1.5	7.2	13.5
Mississippi silvery minnow	<i>Hybognathus nuchalis</i>	O	7	10	70	1.9	4.9	26.9

Pugnose minnow	<i>Opsopoeodus emiliae</i>	O	2	3	33	2.0	3.6	26.2
Silver chub	<i>Macrhybopsis storeriana</i>	T	32	37	32	5.5	6.2	55.8
Speckled chub	<i>M. aestivalis</i>	O	277	5569	62	1.4	2.3	56.4
Sicklefin chub	<i>M. meeki</i>	O	5	6	0	2.2	4.9	18.0
Gravel chub	<i>Erimystax x-punctatus</i>	O	1	1	0	4.3	15.7	15.7
River carpsucker	<i>Carpoides carpio</i>	O	52	143	45	5.1	3.6	43.3
Blue sucker	<i>Cycleptus elongatus</i>	O	14	19	74	23.6	2.3	42.0
Bigmouth buffalo	<i>Ictiobus cyprinellus</i>	T	1	1	100	31.3	14.8	14.8
		O	10	25	60	23.4	6.9	43.6
Smallmouth buffalo	<i>I. bubalus</i>	T	43	60	72	22.6	6.2	56.8
		O	25	99	76	22.8	7.5	38.4
Black buffalo	<i>I. niger</i>	T	10	10	70	27.9	8.5	25.3
		O	16	44	55	25.3	5.2	35.4
Highfin carpsucker	<i>Carpoides velifer</i>	O	4	4	50	10.4	6.9	35.4
Freckled madtom	<i>Noturus nocturnus</i>	O	16	33	45	1.8	5.9	23.0
Stonecat	<i>N. flavus</i>	O	29	171	81	1.0	9.2	35.4
Flathead catfish	<i>Pylodictis olivaris</i>	T	139	197	53	16.6	2.0	72.8
		O	78	184	64	19.3	4.9	38.4
Blue catfish	<i>Ictalurus furcatus</i>	T	874	4386	37	14.9	2.0	72.8
		O	392	10890	73	3.7	3.3	73.5
Channel catfish	<i>I. punctatus</i>	T	310	673	33	15.7	2.6	64.3
		O	350	6954	58	2.4	2.3	69.6
Pirate perch	<i>Aphredoderus sayanus</i>	O	1	1	100	2.8	9.8	9.8
Striped bass	<i>Morone saxatilis</i>	O	12	16	81	5.7	3.6	25.6
White bass	<i>M. chrysops</i>	O	27	63	67	8.2	4.9	37.4
Yellow bass	<i>M. mississippiensis</i>	O	1	1	100	5.2	31.5	31.5
Flier	<i>Centrarchus macropterus</i>	O	1	1	100	3.0	15.1	15.1
Dollar sunfish	<i>Lepomis marginatus</i>	O	1	1	100	3.9	10.2	10.2
Orangespotted sunfish	<i>L. humilis</i>	O	5	16	75	1.7	3.6	25.6
Longear sunfish	<i>L. megalotis</i>	O	1	2	0	2.3	3.6	3.6
Bluegill	<i>L. macrochirus</i>	O	5	13	92	1.5	3.6	26.2
Spotted bass	<i>Micropterus punctulatus</i>	O	1	1	100	7.6	14.1	14.1
Largemouth bass	<i>M. salmoides</i>	O	1	3	0	3.0	4.9	4.9
Black crappie	<i>Pomoxis nigromaculatus</i>	O	4	7	86	2.6	5.2	16.1
White crappie	<i>P. annularis</i>	O	17	49	92	3.3	3.6	25.6
Dusky darter	<i>Percina sciera</i>	O	2	2	100	2.3	4.9	53.5
River darter	<i>P. shumardi</i>	O	29	78	53	1.7	3.6	26.9
Logperch	<i>P. caprodes</i>	O	2	2	100	3.1	4.6	5.9
Brighteye darter	<i>Etheostoma lynceum</i>	O	1	1	100	1.9	22.0	22.0
Sauger	<i>Sander canadense</i>	O	53	207	62	3.3	3.6	37.4
Walleye	<i>S. vitreus</i>	O	3	8	13	0.6	14.1	33.5
Freshwater drum	<i>Aplodinotus grunniens</i>	T	146	228	55	14.5	2.0	88.9
		O	265	7567	45	0.9	2.3	69.6
Striped mullet	<i>Mugil cephalus</i>	T	1	1	100	19.7	21.7	21.7

Table 3. Parameters a and b corresponding to those described in equation 1, according to all species combined (trotline = 19 species; trawls = 63 species), according to individual species meeting minimum sample sizes (≥ 100 specimens collected in ≥ 20 sets or tows), according to low- and high-water periods, and according to gear. Also given are the estimated percentage of the time that fish occupy water deeper than 40 ft during low water ($P_{>40}$) and water deeper than 52 ft during high water ($P_{>52}$). Missing values in a given season indicate sample sizes were too small.

Species	Low				High			
	a	b	r^2	$P_{>40}$	a	b	r^2	$P_{>52}$
Trotline								
All species	-0.060	27.5	0.97	37.7	-0.051	29.4	0.98	27.1
Shovelnose sturgeon	-0.063	26.8	0.98	35.3	-0.058	32.0	0.97	26.8
Pallid sturgeon	-0.067	20.4	0.99	23.6	-0.072	23.0	0.97	11.7
Flathead catfish	-0.062	19.3	0.97	24.1	-0.083	17.7	0.98	5.6
Blue catfish	-0.056	27.9	0.97	39.7	-0.052	26.6	0.97	23.3
Channel catfish	-0.067	12.4	0.96	14.5	-0.061	12.8	0.99	8.6
Freshwater drum	-0.069	15.2	0.98	16.5	-0.069	11.9	0.99	6.0
Trawl								
All species	-0.053	22.8	0.98	33.3	-0.071	14.3	0.97	6.6
Paddlefish	-0.209	14.3	0.96	0.5	-0.201	8.9	0.95	0.0
Shovelnose sturgeon	-0.131	13.6	0.96	3.1	-0.088	18.7	0.97	5.2
Goldeye	-0.141	10.0	0.95	1.5				
Gizzard shad	-0.073	15.0	0.93	15.0	-1.155	16.7	0.92	0.0
Threadfin shad	-0.071	8.0	0.85	9.9				
Channel shiner	-0.072	16.4	0.97	16.7	-0.182	2.9	0.85	0.0
Silverband shiner	-0.213	7.1	0.98	0.1	-1.354	4.1	0.99	0.0
Silver chub	-0.128	8.5	0.95	1.7	-0.080	8.6	0.95	3.1
Speckled chub	-0.117	11.4	0.98	3.5	-0.075	9.5	0.98	4.1
River carpsucker	-0.126	10.9	0.97	2.5	-0.623	17.4	0.94	0.0
Stonecat	-0.112	13.4	0.81	5.0				
Flathead catfish	-0.184	10.9	0.98	0.5	-0.089	20.4	0.91	5.8
Blue catfish	-0.059	22.4	0.99	29.9	-0.091	19.9	0.96	5.3
Channel catfish	-0.070	10.7	0.98	12.1	-0.099	7.5	0.95	1.2
Sauger	-0.128	11.9	0.97	2.7	-0.133	-0.7	0.89	0.1

Freshwater drum	-0.072	24.0	0.97	26.9	-0.094	17.0	0.96	3.6
-----------------	--------	------	------	------	--------	------	------	-----

Table 4. Segment comparison parameters a , b , c , and d corresponding to those described in equation 2, according to low- and high-water periods, and according to data set analyzed. The lower (LCL) and upper (UCL) 95% confidence limits are given for each parameter. The fact that confidence limits around c and d overlap zero indicates no statistical differences occurred between the lower and upper segment of the LMR.

Parameter	Low			High		
	Estimate	LCL	UCL	Estimate	LCL	UCL
Species richness (first appearance)						
a	-0.207	-0.247	-0.167	-0.292	-0.371	-0.212
b	2.9	2.2	3.6	1.4	0.6	2.1
c	0.004	-0.307	0.314	0.160	-0.247	0.567
d	-0.054	-0.119	0.010	0.013	-0.093	0.119
Species richness (last appearance)						
a	-0.065	-0.071	-0.059	-0.112	-0.147	-0.098
b	14.4	13.3	15.5	8.5	7.2	9.8
c	0.095	-0.066	0.114	0.100	-0.289	0.488
d	-0.024	-0.048	0.003	0.032	-0.035	0.082
Catch per line (all species; trotline)						
a	-0.038	-0.043	-0.033	-0.039	-0.043	-0.036
b	25.9	23.6	28.2	36.7	35.0	38.4
c	0.292	-0.017	0.563	0.043	-0.205	0.291
d	-0.002	-0.015	0.011	-0.011	-0.018	0.005
Catch per acre (all species; trawl)						
a	-0.048	-0.057	-0.039	-0.115	-0.132	-0.097
b	12.8	9.9	15.7	6.3	5.3	7.3
c	-0.205	-0.408	0.429	-0.216	-0.045	0.477
d	0.001	-0.011	0.012	0.046	-0.027	0.083

Table 5. FFP reach parameters a , b , c , and d corresponding to those described in equation 3, according to low- and high-water periods, and according to data set analyzed. The lower (LCL) and upper (UCL) 95% confidence limits are given for each parameter. Bolded c values indicate the position of the curve along the depth axis differed between FFP and non-FFP reaches (i.e., LCL and UCL did not include 0); bolded d values indicate the slopes of the cumulative curves differed between FFP and non-FFP reaches.

Parameter	Low			High		
	Estimate	LCL	UCL	Estimate	LCL	UCL
Species richness (first appearance)						
a	-0.236	-0.303	-0.168	-0.123	-0.164	-0.095
b	2.4	1.5	3.4	1.0	-1.0	3.1
c	0.133	-0.475	0.741	0.256	-0.102	0.614
d	0.013	-0.094	0.119	-0.044	-0.092	0.005
Species richness (last appearance)						
a	-0.084	-0.097	-0.072	-0.070	-0.086	-0.054
b	18.7	17.3	20.1	16.9	14.7	19.2
c	1.914	1.107	2.722	0.044	-0.432	0.519
d	-0.086	-0.121	-0.050	0.004	-0.018	0.026
Catch per line (all species; trotline)						
a	-0.061	-0.070	-0.052	-0.062	-0.070	-0.055
b	28.6	26.8	30.4	24.8	23.2	26.3
c	-0.303	-0.717	0.111	0.175	-0.183	0.533
d	-0.002	-0.015	0.011	0.006	-0.005	0.017
Catch per acre (all species; trawl)						
a	-0.058	-0.066	-0.050	-0.094	-0.112	-0.076
b	21.0	19.3	22.8	11.0	9.4	12.6
c	-0.190	-0.508	0.129	-0.263	-0.632	0.107
d	-0.008	-0.022	0.005	0.032	-0.001	0.053

Table 6. Spearman rank correlations (r_L) between fish length and depth according to low- and high-water periods. Also listed are minimum and maximum lengths (in) and the probability (P) of a larger r_L . Fork lengths are listed for sturgeon species and total lengths for all others.

Species	Low				High			
	min	max	r_L	P	min	max	r_L	P
Trotline								
All species	2.5	42.2	0.22	0.33	2.1	41.5	0.47	0.03
Shovelnose sturgeon	11.7	32.0	0.12	0.63	2.1	33.9	0.53	0.02
Pallid sturgeon	17.0	37.1	-0.58	0.04	15.2	38.0	0.64	0.01
Flathead catfish	7.3	42.2	-0.11	0.65	3.9	33.6	-0.54	0.05
Blue catfish	2.7	36.6	0.15	0.51	3.0	41.5	0.29	0.23
Channel catfish	3.9	27.6	0.21	0.44	2.1	28.5	-0.10	0.70
Freshwater drum	7.4	32.0	-0.44	0.08	8.3	25.1	0.60	0.03
Trawl								
All species	0.2	59.1	-0.22	0.35	0.4	49.7	0.53	0.04
Paddlefish	3.3	21.8	-0.30	0.38	0.7	7.0	-0.43	0.02
Shovelnose sturgeon	2.3	38.1	0.10	0.37	1.0	32.7	0.18	0.25
Goldeye	0.3	17.6	0.01	0.96				
Gizzard shad	1.5	16.0	0.03	0.85	0.9	15.9	0.26	0.25
Threadfin shad	0.9	4.8	-0.02	0.89				
Channel shiner	0.8	2.6	-0.08	0.60	1.3	2.6	-0.19	0.42
Silverband shiner	1.4	3.3	0.42	0.06	1.4	3.5	-0.58	0.02
Silver chub	0.9	6.5	-0.02	0.90	0.9	8.5	-0.01	0.93
Speckled chub	0.2	3.9	-0.06	0.50	0.8	5.0	-0.08	0.33
River carpsucker	2.4	8.5	0.53	<0.01	2.7	20.2	0.01	0.95
Stonecat	0.5	3.1	-0.28	0.32				
Flathead catfish	1.5	45.2	0.10	0.54	0.7	30.8	0.22	0.48
Blue catfish	0.6	39.4	-0.24	<0.01	0.4	38.1	0.08	0.45
Channel catfish	0.6	27.6	-0.16	0.05	0.6	33.5	0.13	0.15
Sauger	2.1	16.8	-0.12	0.47	0.9	12.8	0.52	0.03
Freshwater drum	0.4	32.0	-0.21	0.01	0.4	25.1	-0.04	0.71

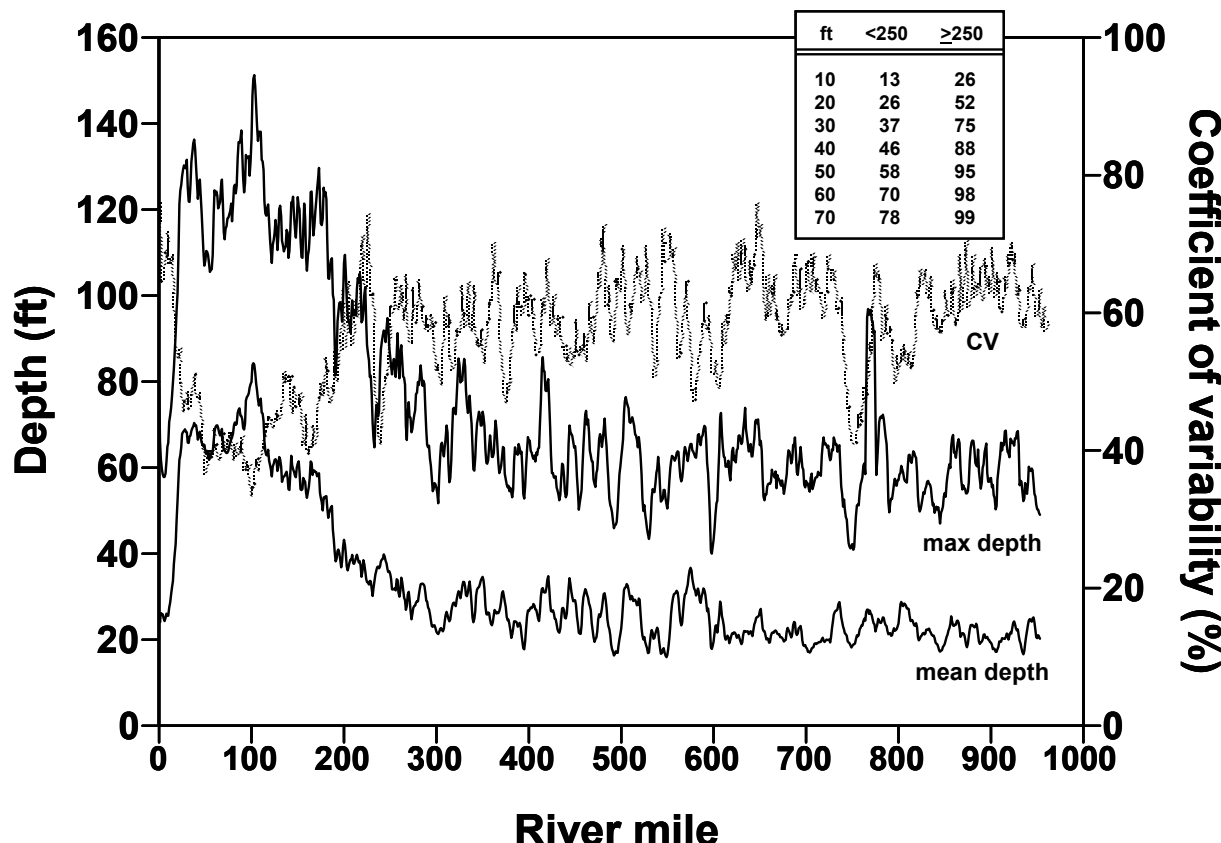


Figure 1. Depth distributions along the Lower Mississippi River between Head of Passes, Louisiana (RM 0) and Cairo, Illinois (RM 953) relative to mean low water reference point. Depth values were obtained from soundings collected approximately every 1.1 yard across transects established perpendicular to the river and spaced out approximately every 330 yards longitudinally along the river. Transect depths were summarized according to river kilometer, and the 6-mile moving averages for mean, maximum, and coefficients of variability (CV, computed as standard deviation/mean) were plotted. The inset table shows cumulative depth distributions (%) at depth increments ranging from 10 to 70 ft for the segment between RM 0 and RM 250, and that between RM 250 and RM 953. In all, values represent 238,251 depth soundings taken in the lower segment and 693,196 depth soundings taken in the upper segment. Data were provided from FFP and obtained from the U.S. Army Corps of Engineers.

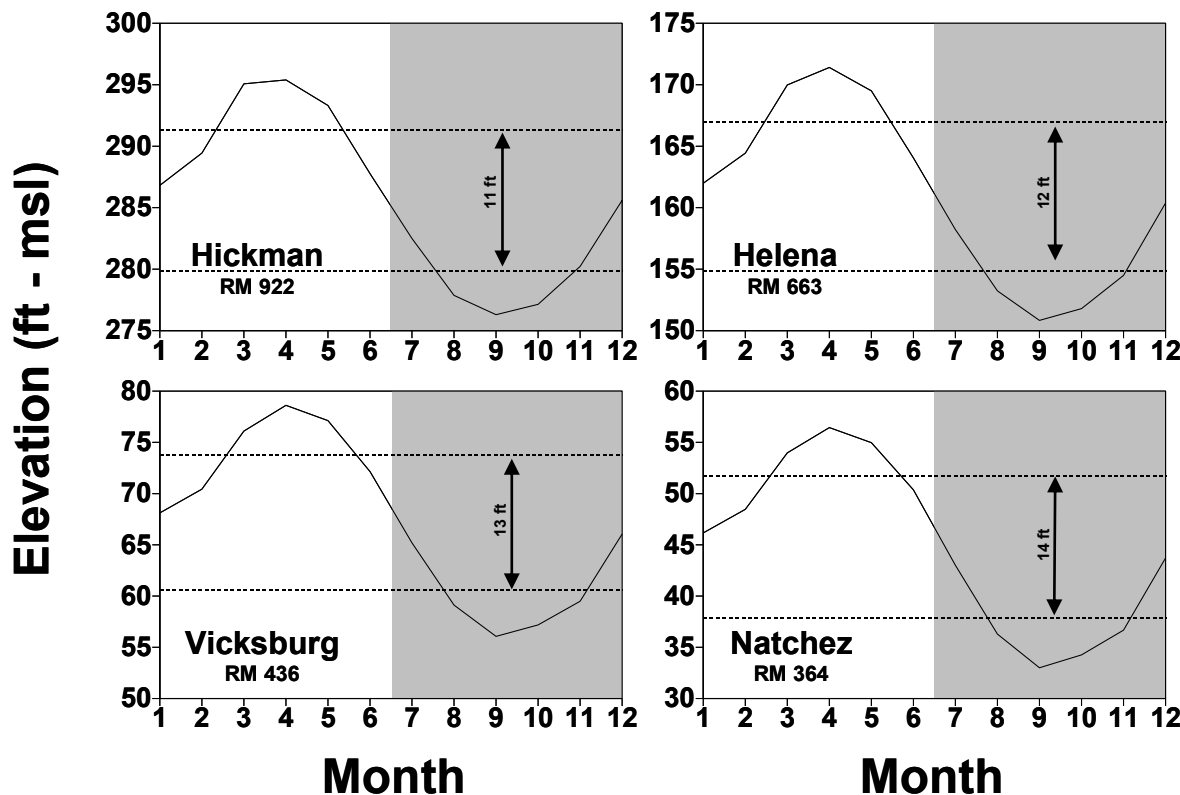


Figure 2. Mean monthly river elevations (feet above mean sea level – msl) at four locations along the Lower Mississippi River. Values represent the mean over a 50-year period between 1961 and 2010 (obtained from www.rivergages.com on 12/12/2011). The shaded areas separate the low-water (Jul-Dec) and the high-water (Jan-Jun) periods. The distance between the dashed lines represent the mean difference in elevation between the high- and low-water periods.

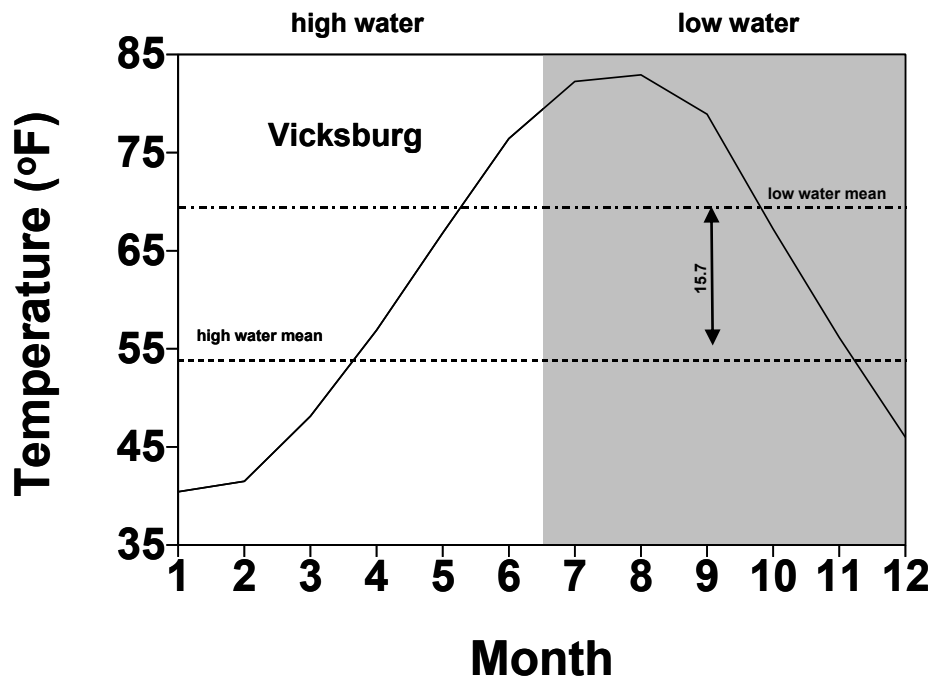


Figure 3. Mean water temperature (°F) at Vicksburg, Mississippi (RM 436). Values represent the mean over a 47-year period between 1963 and 2010. The shaded area separates the low-water (Jul-Dec) and the high-water (Jan-Jun) periods. The distance between the dashed lines represent the mean difference in temperature between the high- and low-water periods. Data provided by U.S. Army Corp of Engineers Research and Development Center, Vicksburg.

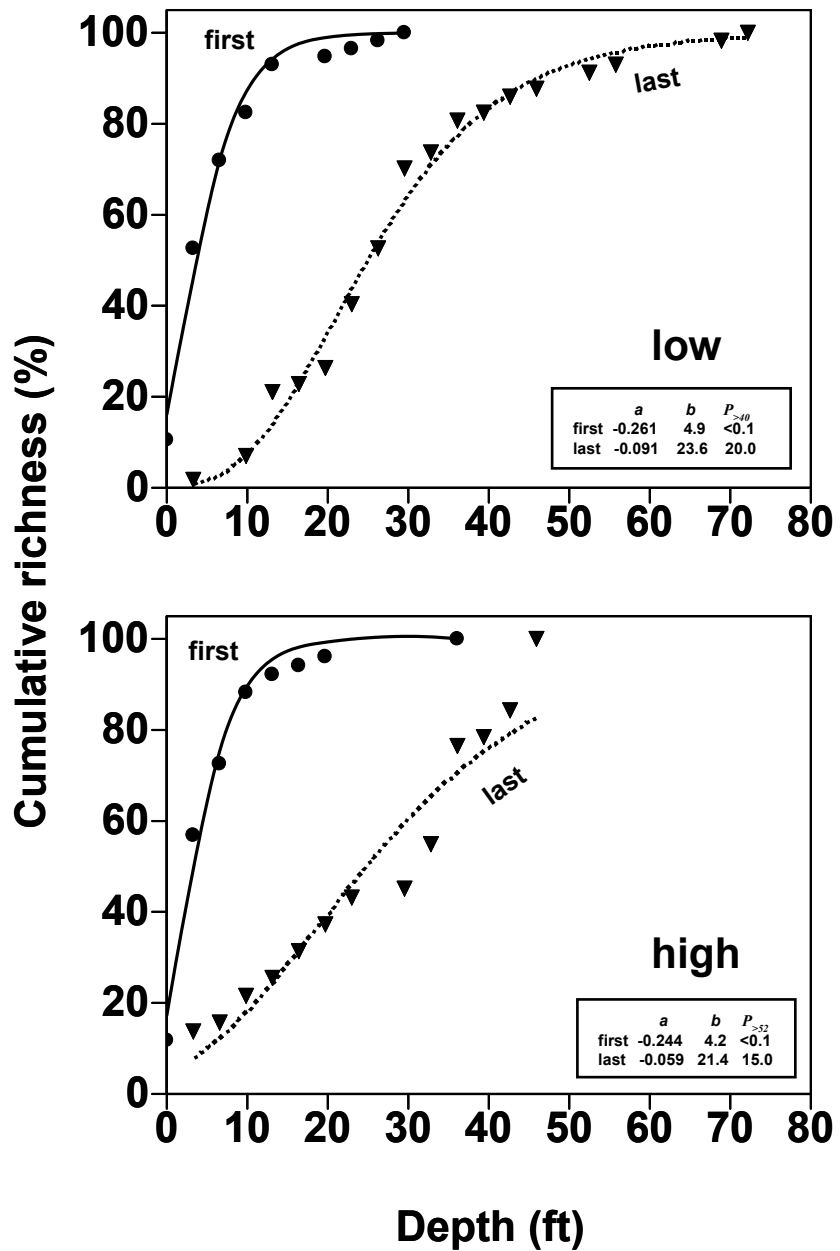


Figure 4. Cumulative number of species collected with trawls along the studied depth gradient in the 703 miles reach of the Lower Mississippi River, during the low-water and high-water periods illustrated in Figure 2. Species were cumulated according to the depths at which they were first collected and depth at which they were last collected. The dashed lines indicate the model fitted with equation 1 using the parameters (*a* and *b*) listed in the boxes. Also given in the boxes are the estimated percentage of species first and last collected in water deeper than 40 ft during low water ($P_{>40}$) and water deeper than 52 ft during low water ($P_{>52}$).

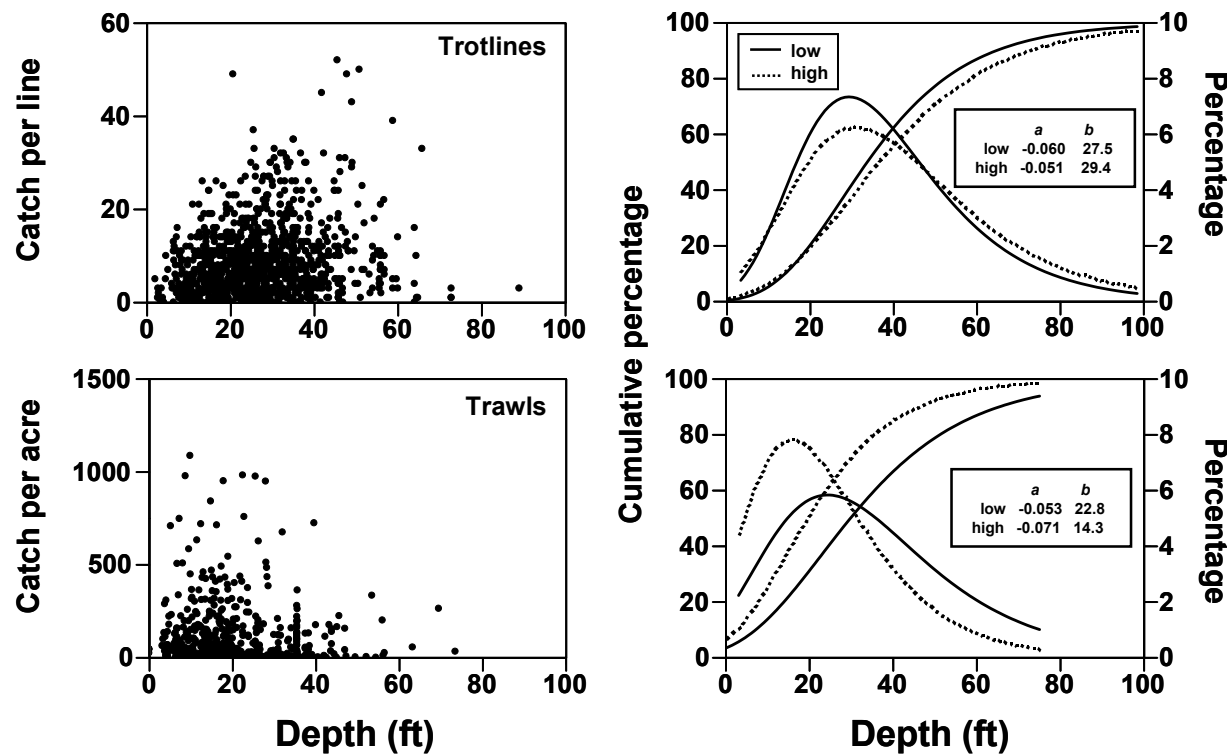


Figure 5. Catch rates of all species combined according to trotlines (19 species) and trawls (63 species). The left panels show the raw catches relative to depth ($N = 1,096$ trotlines and 612 trawls). The right panels illustrate the cumulative percentage curves (y1 axes) fit with equation 1 (a and b listed in boxes). The y2 axes (percentage) were derived from the y1 axes by expressing cumulative percentage in term of percentage increment per 3-ft depth intervals.

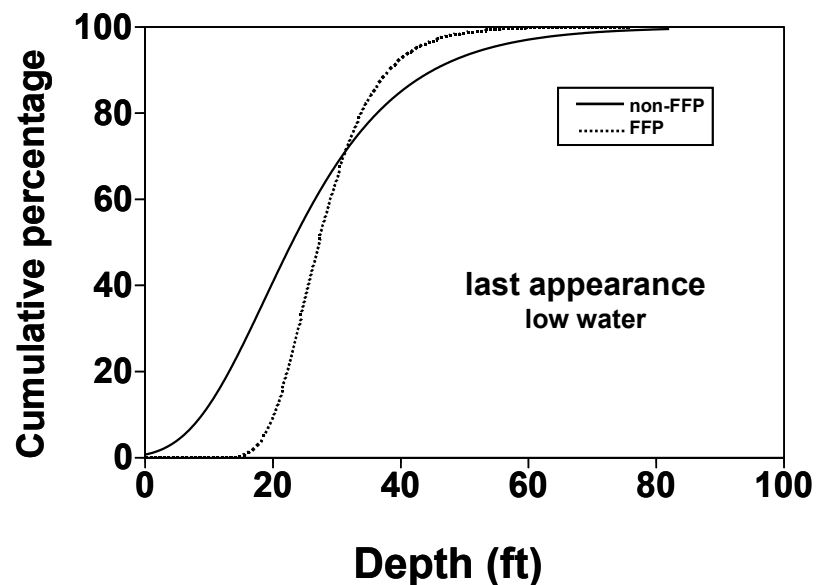
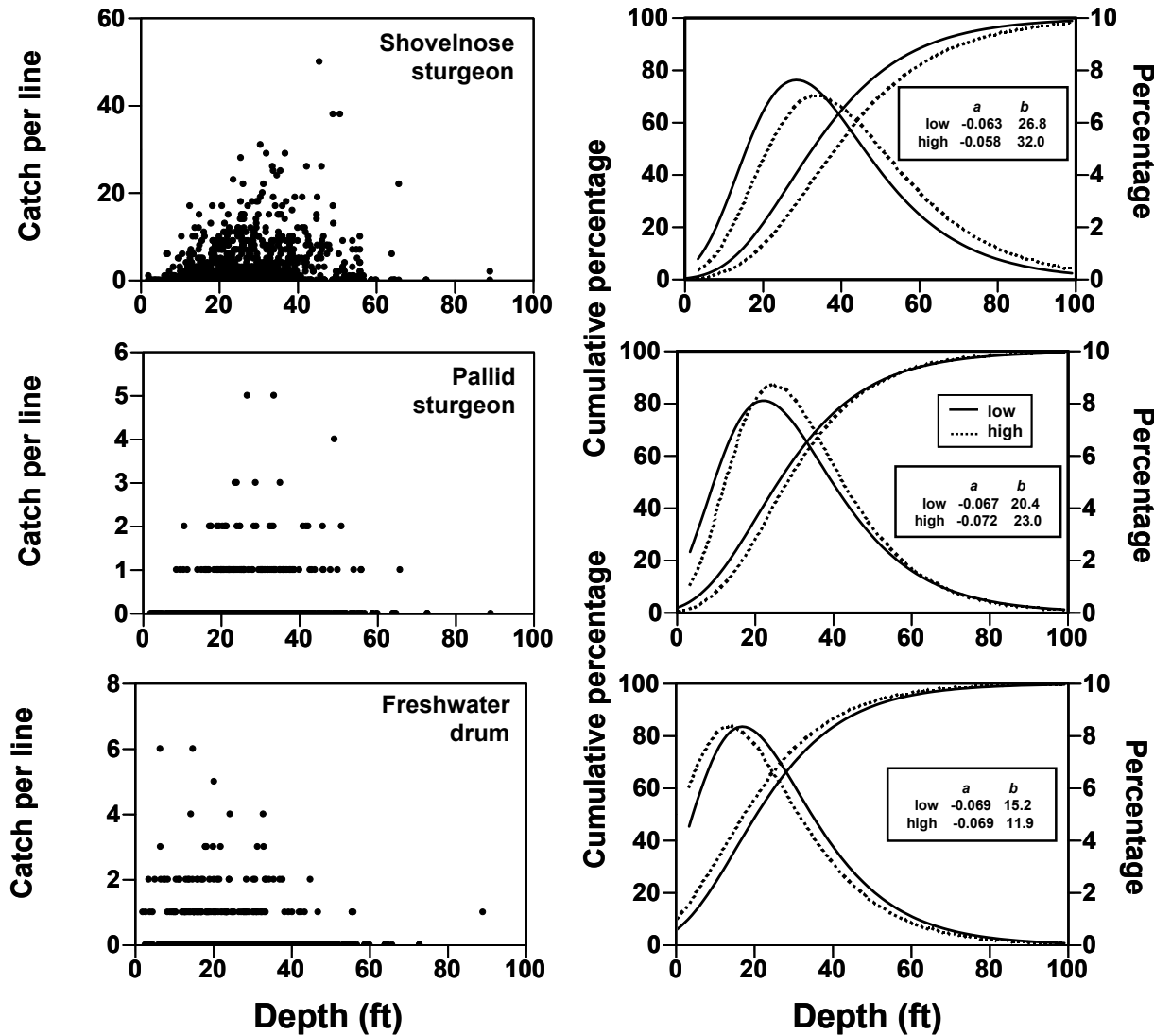
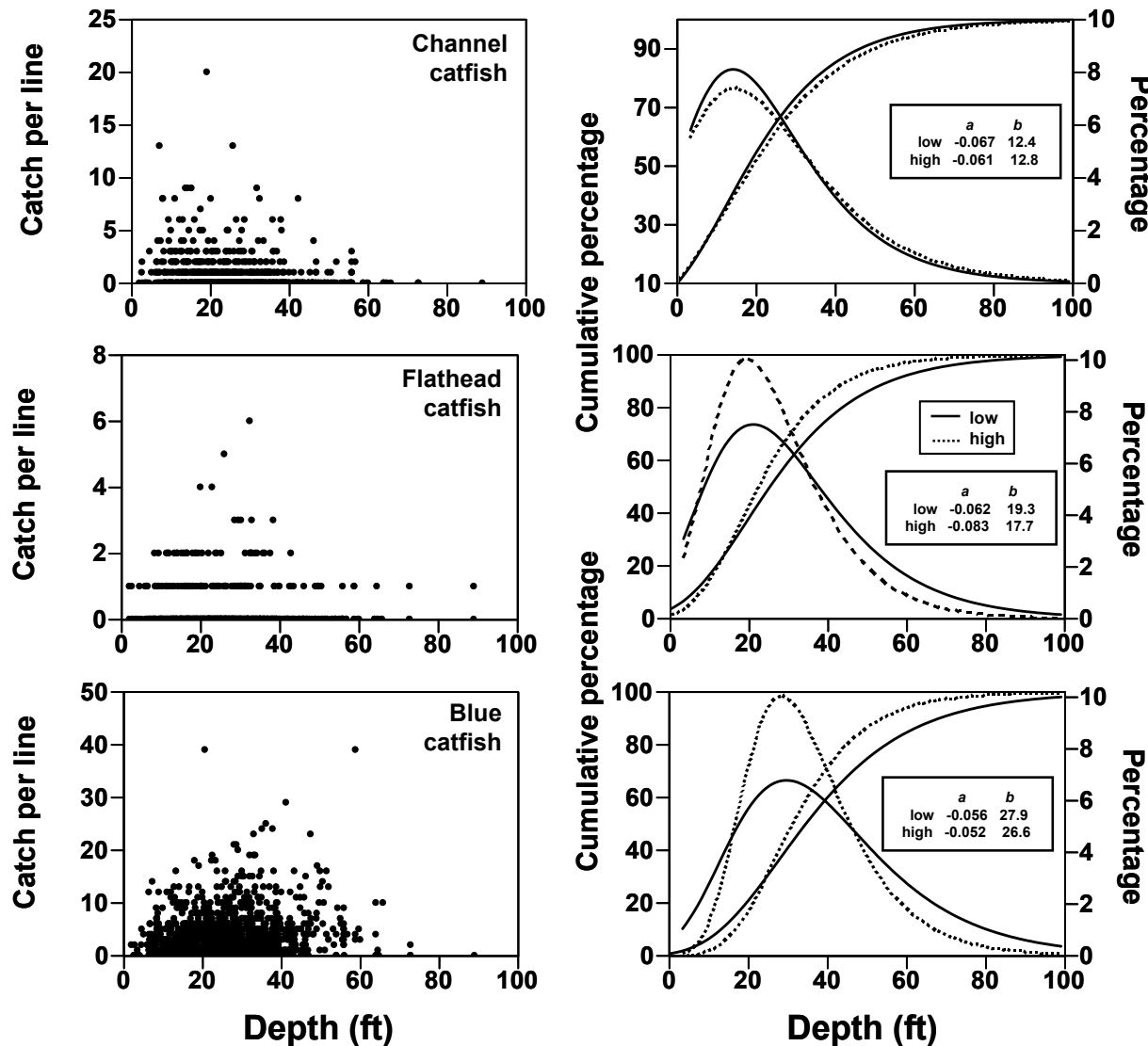


Figure 6. Cumulative species richness according to depths for the models listed in Table 5 as statistically different between FFP and non-FFP reaches.

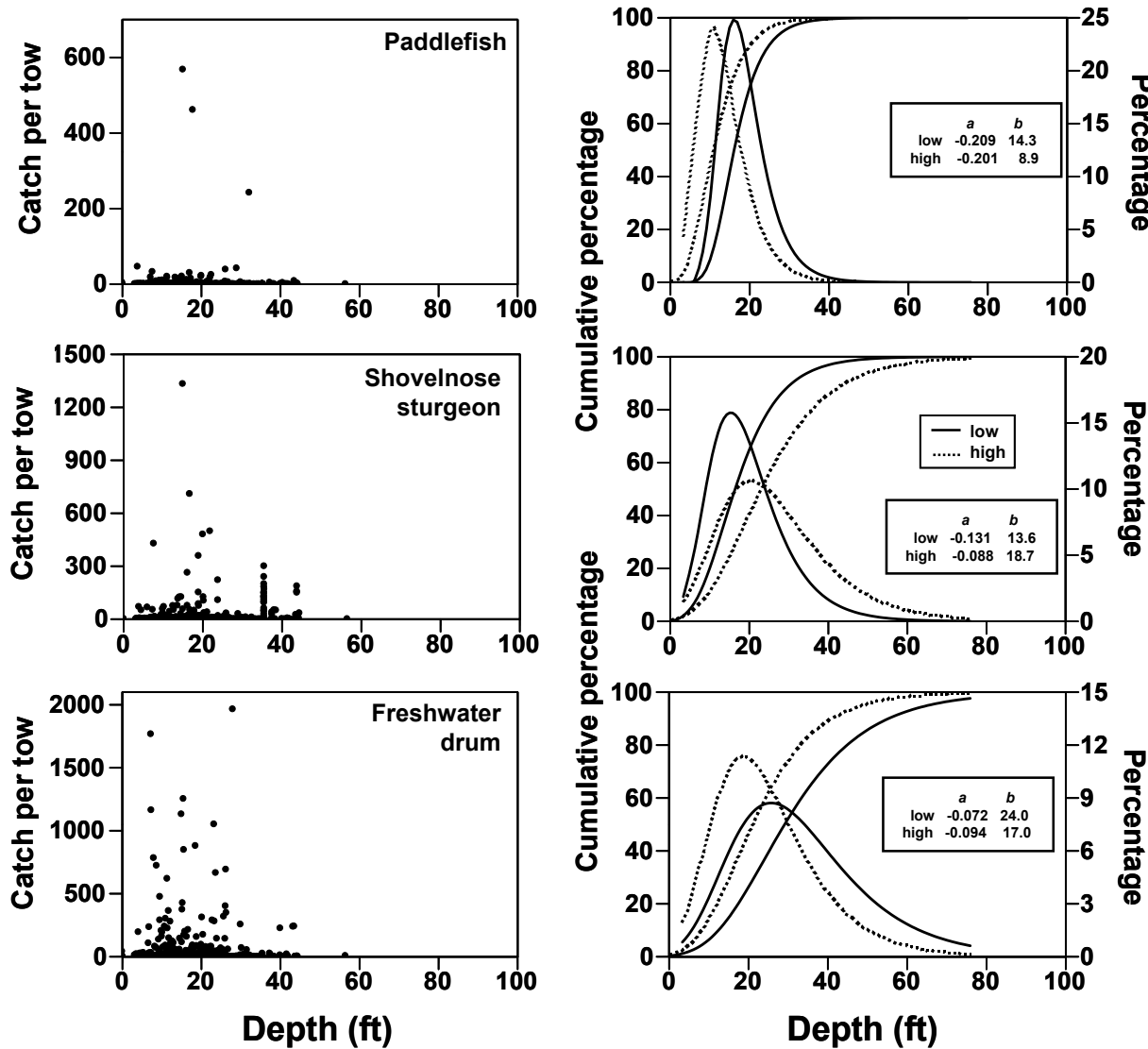
Appendix 1a. Catch rates of selected species collected by trotlines. The left panels show the raw catches relative to depth ($N = 1,096$ trotlines). The right panels illustrate the cumulative percentage curves ($y1$ axes) fit with equation 1 (a and b listed in boxes). The $y2$ axes (percentage) were derived from the $y1$ axes by expressing cumulative percentage in term of percentage increment per 3-ft depth intervals.



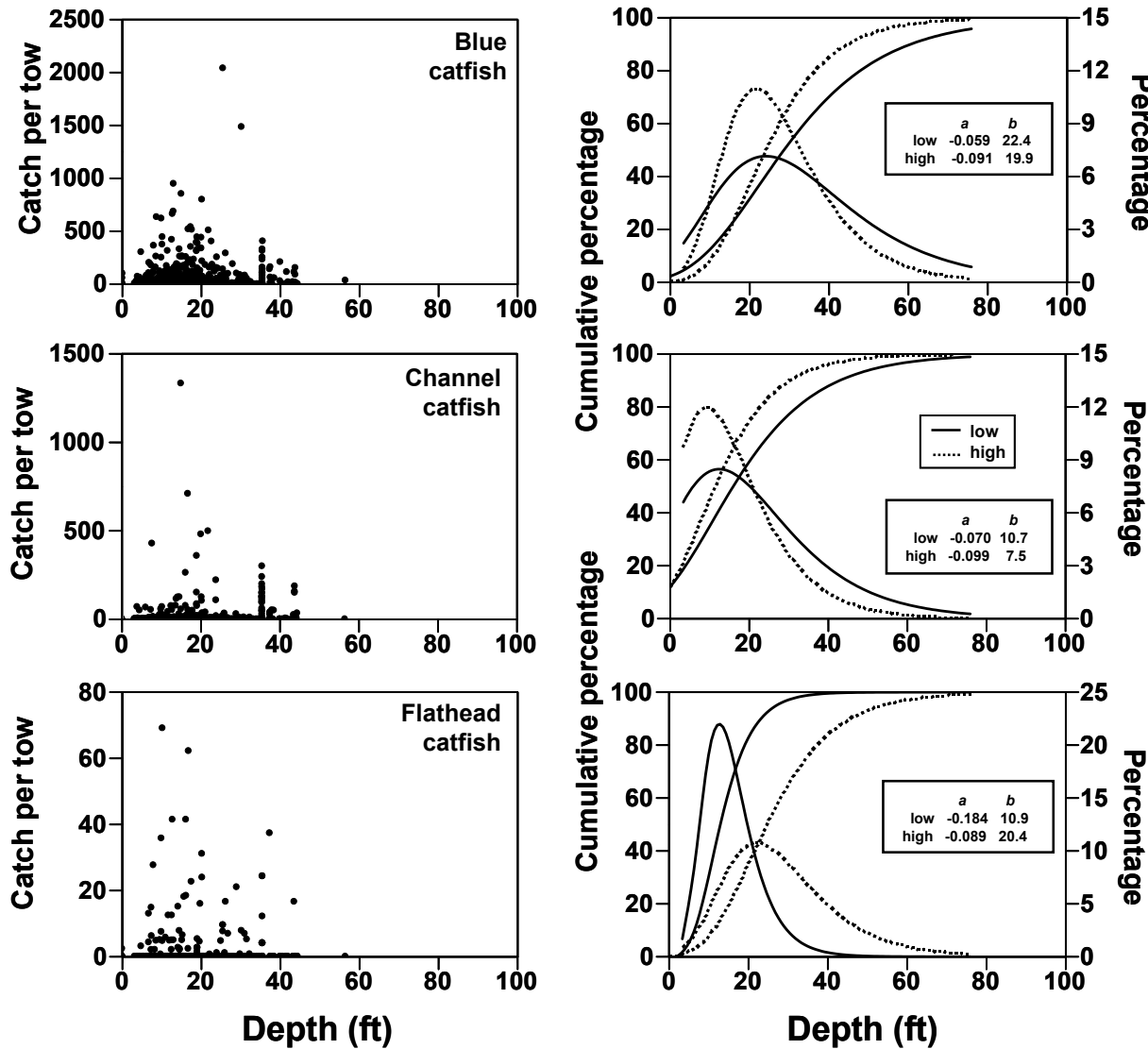
Appendix 1a (continued). Catch rates of selected species collected by trotlines. The left panels show the raw catches relative to depth ($N = 1,096$ trotlines). The right panels illustrate the cumulative percentage curves (y1 axes) fit with equation 1 (a and b listed in boxes). The y2 axes (percentage) were derived from the y1 axes by expressing cumulative percentage in term of percentage increment per 3-ft depth intervals.



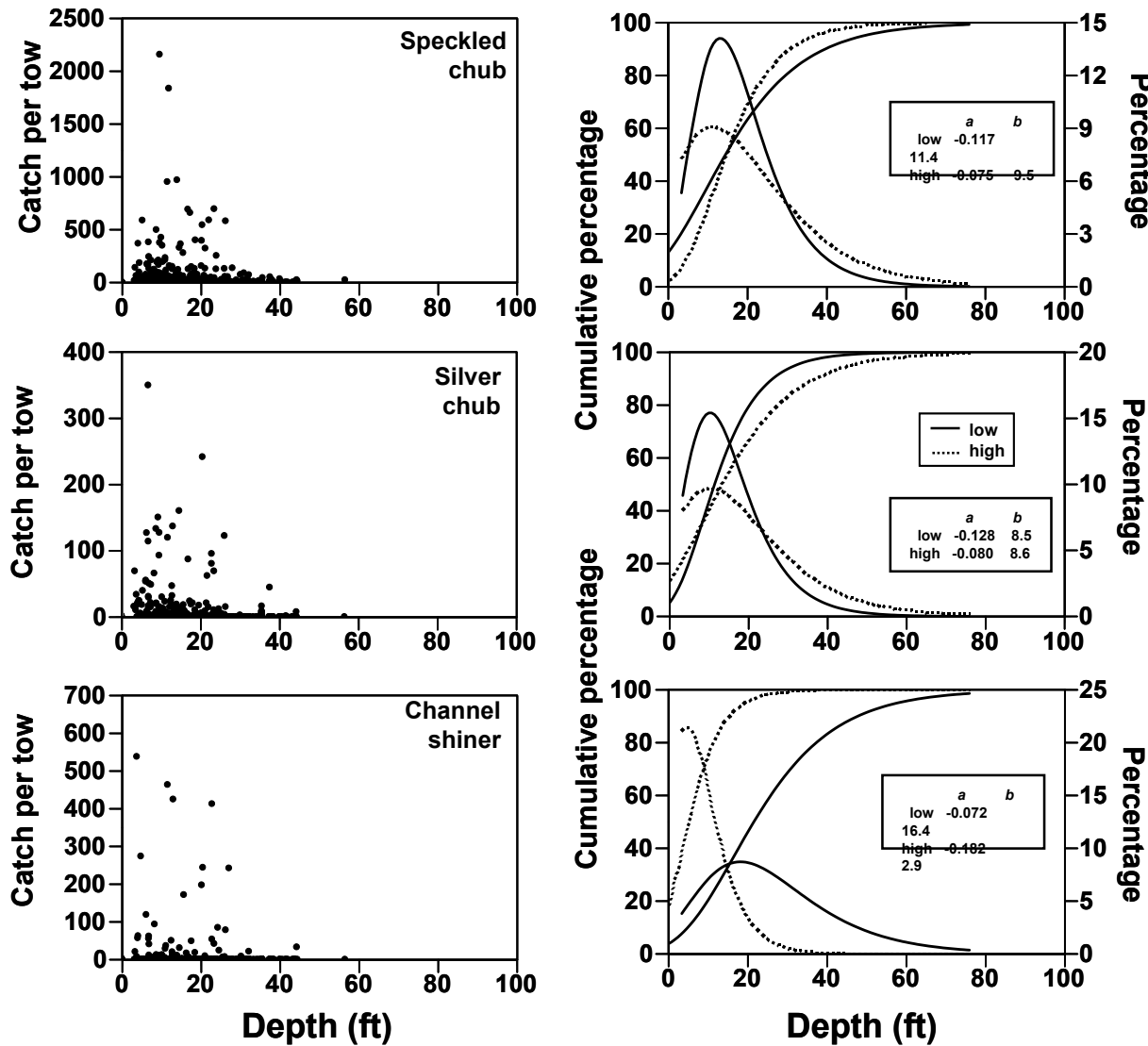
Appendix 1b. Catch rates of selected species collected by trawls. The left panels show the raw catches relative to depth (N = 612 trawls). The right panels illustrate the cumulative percentage curves (y1 axes) fit with equation 1 (a and b listed in boxes). The y2 axes (percentage) were derived from the y1 axes by expressing cumulative percentage in term of percentage increment per 3-ft depth intervals.



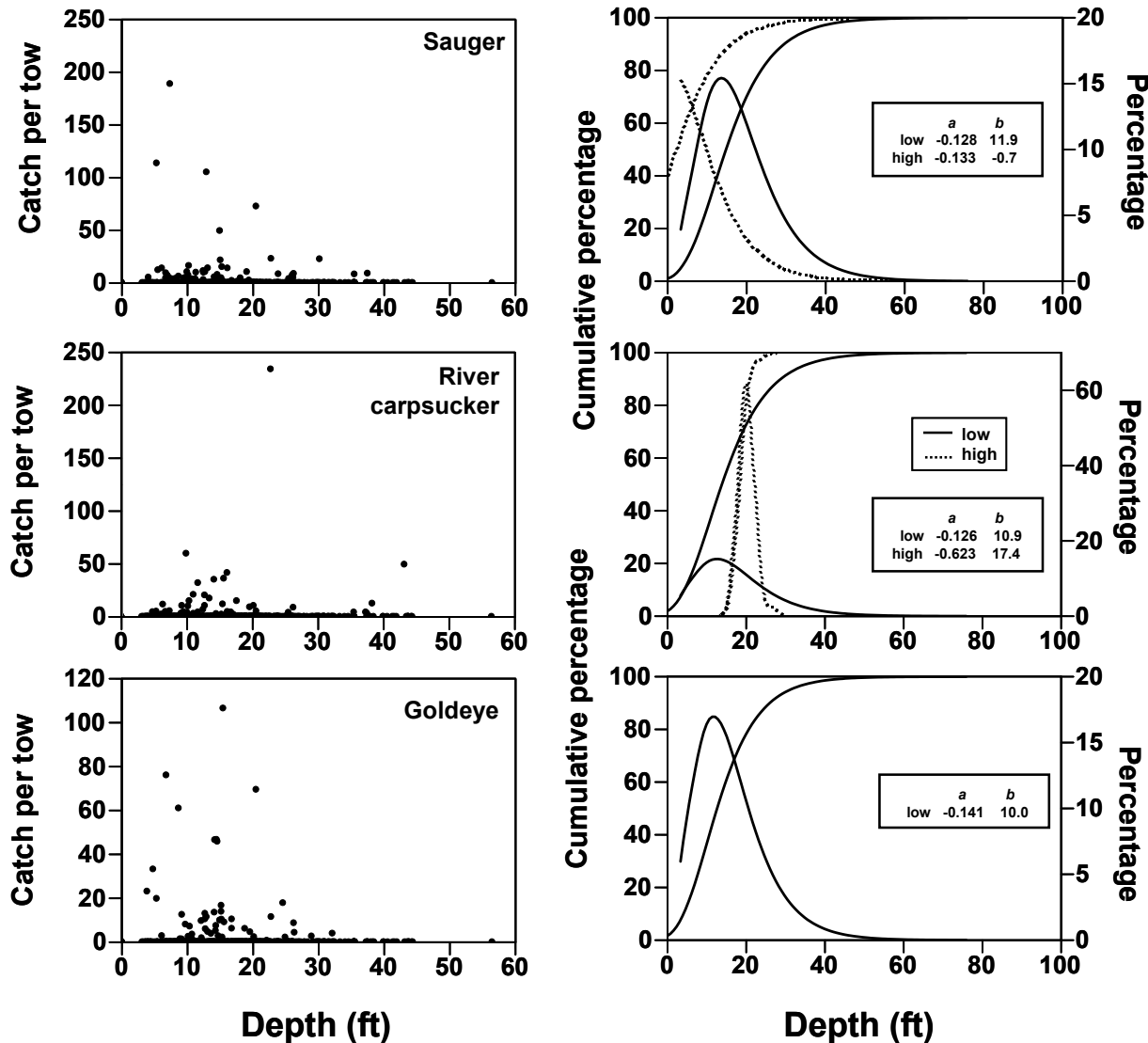
Appendix 1b (continued). Catch rates of selected species collected by trawls. The left panels show the raw catches relative to depth ($N = 612$ trawls). The right panels illustrate the cumulative percentage curves (y1 axes) fit with equation 1 (a and b listed in boxes). The y2 axes (percentage) were derived from the y1 axes by expressing cumulative percentage in term of percentage increment per 3-ft depth intervals.



Appendix 1b (continued). Catch rates of selected species collected by trawls. The left panels show the raw catches relative to depth ($N = 612$ trawls). The right panels illustrate the cumulative percentage curves (y1 axes) fit with equation 1 (a and b listed in boxes). The y2 axes (percentage) were derived from the y1 axes by expressing cumulative percentage in term of percentage increment per 3-ft depth intervals.



Appendix 1b (continued). Catch rates of selected species collected by trawls. The left panels show the raw catches relative to depth ($N = 612$ trawls). The right panels illustrate the cumulative percentage curves (y1 axes) fit with equation 1 (a and b listed in boxes). The y2 axes (percentage) were derived from the y1 axes by expressing cumulative percentage in term of percentage increment per 3-ft depth intervals.



Appendix 10

FISH MONITORING METHODOLOGY



239 Causeway Street
Boston, MA 02114-2103
USA

MAIN: (978) 252-2822
FAX: (617) 367-3372

www.free-flow-power.com

Filename: 2012-06-27_R01_Fish_Population_Insitu_Study_Plan

Subject: In-situ Monitoring Plan for Fish Population

Date	Release Rev	Description
05-01-2012	00	Original
6-27-2012	01	Revisions after initial review

1 Requirements of FERC's Study Plan Determination

- (1) Quantify the blade rotation rate, rotor blade tip speed, shear stress, pressure changes, turbulence, and cavitation associated with the turbine generator using CFD modeling techniques
- (2) Determine the range of fish species in the Mississippi River that may be affected by turbine deployment based on literature review and assessment of fish distribution data collected by the Corps
- (3) Assess the probability of strike-related injuries and mortality for representative species, based on a laboratory-based or *in situ* testing program
- (4) Develop risk-based projections of population effects for several fish species.

From the above requirements, requirements (1), (2), and (3) are not expected to be addressed in the in-situ deployment monitoring as they are not applicable to site test data acquisition. These requirements are addressed in the SPD study report. Requirement (4) is applicable and asks Free Flow Power to monitor how fish interact with the turbine array interface directly and to monitor the population of aquatic life around the turbine throughout the pre and post deployment periods.

2 Methods Executed by Other Companies

2.1 ORPC-Cobscook Bay (P-12711)¹

- ORPC utilized mobile vessel mounted Simrad ES60 echosounder with dual frequency (38KHz and 200 KHz) with a Combi W transducer (single beam 31° x 31°) to monitor overall fish population in the project area.

¹ Ocean Renewable Power Company, 2011. Safe Guard Plans, Final Pilot License Application Cobscook Bay Tidal Project, FERC Project Number 12711. September 2011.

- Coupled with the previously mentioned setup was a DIDSON US300 acoustic imaging unit to survey the upper 10-18m of the site for fish.
- Both of these devices were mounted on a vessel that was anchored over the project site for 24 hours so that two tidal cycles could be monitored.
- For the pre-deployment period, these surveys were done 6 times in that year (2011).
- For the post-deployment period, surveys will be conducted as follows:
 - 2012: 1, 24 hour survey at the project site in March, May, June, August, September, October, and November
 - 2013: 1, 24 hour survey at the project site in March, May, August, and September
 - 2014: 1, 24 hour survey at the project site in May, June, and August
 - 2015-2018: 1, 24 hour survey at the project site in May and September
- Netting efforts were also done to characterize fish population in the project area.
- For the pre-deployment period, netting in the inner, middle, and upper Bay area (project site) were done along with mid-water trawls, benthic trawls, deploying fyke nets, and beach seines to capture and characterize fish in the project area.
- Both the mid-water and benthic trawls took on twenty minutes to complete on average. This timing varied and it was usually resulting from towing in a distance that was too short to conduct a 20-minute trawl in the East and South Bays.²
- Below is a table showing the date and number of mid-water trawls.

Date of Mid-Water Survey	Number of Surveys
May 26th, 2011	2
May 27th, 2011	3
May 28th, 2011	2
June 25th, 2011	1
June 26th, 2011	4
June 27th, 2011	2
June 28th, 2011	2
August 23rd, 2011	2
August 24th, 2011	2
August 25th, 2011	2
August 26th, 2011	2
September 23rd, 2011	2
September 24th, 2011	2
September 25th, 2011	2
September 26th, 2011	2

² Ocean Renewable Power Company, 2012. 2011 Annual Report: Special License Number ME 2011-63-01. February 15, 2012.

- Below is a table showing the date and number of benthic surveys.

Date of Benthic Survey	Number of Surveys
May 26th, 2011	2
May 27th, 2011	3
May 28th, 2011	2
June 26th, 2011	4
June 27th, 2011	2
June 28th, 2011	2
August 23rd, 2011	2
August 24th, 2011	2
August 25th, 2011	2
August 26th, 2011	2
September 23rd, 2011	2
September 24th, 2011	2
September 25th, 2011	2
September 26th, 2011	3

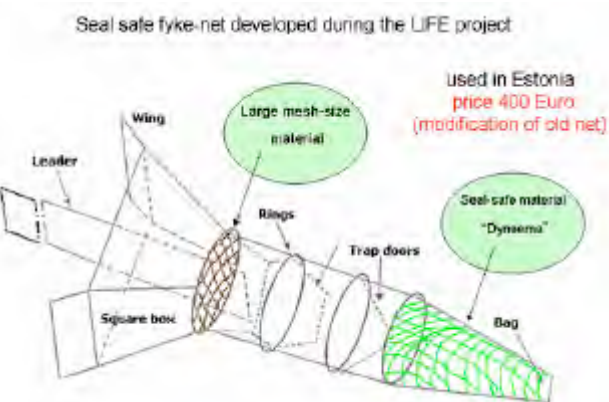
- Below is a table showing the date and number of seine surveys.

Date of Seine Survey	Number of Surveys
May 25th, 2011	3
May 26th, 2011	2
May 27th, 2011	6
May 28th, 2011	2
May 29th, 2011	3
June 24th, 2011	2
June 25th, 2011	7
June 26th, 2011	3
June 27th, 2011	3
June 28th, 2011	5
August 22nd, 2011	3
August 23rd, 2011	3
August 24th, 2011	6
August 25th, 2011	3
August 26th, 2011	2
September 22nd, 2011	7
September 23rd, 2011	4
September 24th, 2011	6
September 25th, 2011	4
September 27th, 2011	4

- Below is a table outlining the number of fyke net deployments and the dates on which they were deployed. Each deployment lasted roughly half an hour.

Date of Fyke Net Survey	Number of Surveys
May 25th, 2011	1
May 26th, 2011	1
May 27th, 2011	2
May 28th, 2011	1
June 24th, 2011	1
June 25th, 2011	1
June 26th, 2011	2
June 27th, 2011	2
June 28th, 2011	1
August 22nd, 2011	1
August 23rd, 2011	1
August 24th, 2011	3
August 25th, 2011	1
August 26th, 2011	1
September 22nd, 2011	2
September 24th, 2011	1

- For the post-deployment period, surveys will be conducted as follows:
 - 2012: mid-water netting in spring, summer, and fall and in May, June, August, and September netting in inner, middle, and upper Bay area (project site) were done along with mid-water trawls, benthic trawls, deploying fyke nets, and beach seines.
 - 2013: mid-water netting in spring, summer, and fall and in May, June, August, and September netting in inner, middle, and upper Bay area (project site) were done along with mid-water trawls, benthic trawls, deploying fyke nets, and beach seines.



2.1.1 Figure 1 - Fyke Net



2.1.2 Figure 2 - Beach Seine

- A Simrad EK60 was mounted to a pile to monitor the environment. The Simrad sensor was outfitted with a Remote Oceans System (ROS) PT-25 that will make it possible to tilt the Simrad. Also installed is a Terrella 6 heading and motion sensor to record the orientation of the mount. The piling is 20 feet high and 195ft from the turbine along the ocean floor.
- An underwater video camera was installed while the turbines were installed to monitor if any fish passed through the turbine. The camera was left monitoring live video for approximately 130 hours on the seabed.

2.2 Verdant (P-12611)³

- An array of split beam acoustic sensors (BioSonics) were installed on the river bank of the project site to record the location of fish in front of their turbines.
- Additionally high definition sonar was used for “near video quality” imaging of fish near the front of the turbine for species identification (DIDSON). The DIDSON system was mounted on a servo (ROS PT-25-FB dual axis heavy duty pan and tilt system) for manual aiming towards the project site.
- This DIDSON system had the following deployment schedule:
 - 3 months prior to deployment for system testing
 - 1 week before the high migratory period (Sept 15th-Dec 1st)

³ Verdant Power, Inc. 2010. Pilot License Application Roosevelt Island Energy Project, Volume 4, RMEE Plans, FERC Project Number 12611. December 2010.

- 3 weeks in the high migratory period (Sept 15th-Dec 1st) with 1 tri-frame installed
 - 6 weeks in the high migratory period (Sept 15th-Dec 1st) with 2 tri-frame installed
- Mobile acoustic surveys using a BioSonics split beam system and a DIDSON sensor were done for 15-17 hours at a time to monitor overall fish population. A total of three surveys were done with the turbines installed.
- Mid-water research trawls were conducted near the shore as studies show that is where most fish populations lie. Trawls will be of standardized length and used to estimate the population of fish around the project site.
- The trawling surveys had the following schedule:
 - First install (2 turbine units)
 - 1 day in May-June
 - 1 day in July-Aug
 - 6 days in Sept-Dec
 - Second install (3 turbine units)
 - Same schedule as first install.
 - Third install (6-12 turbine units)
 - Same schedule as first install.
 - Fourth install (30 turbine units)
 - Same schedule as first install.
- Mobile sonar scans were conducted on a boat to monitor fish populations around the installed turbine and before.
- VEMCO VR2W hydrophones were installed along the banks of the project site to detect fish already tagged (approximately 4,800 fish in the site area).
- The timeline for the monitoring done via the aforementioned hydrophones is below:
 - First install (2 turbine units)
 - April-November
 - Second install (3 turbine units)
 - April-November
 - For the remainder of the installs Verdant has not yet determined if this study will continue.

2.3 SnoPud-Tidal (P-12690)⁴

- Three hydro acoustic surveys were completed in April, August, and November of 2009 to characterize fish density. A fourth study was planned for February 2010. The vessel traveled at 6 knots with a beam angle of 6°. The surveys were done both during the day and during the night to fully characterize the species living in the project site. In each survey there were four "sub-surveys" that will outline the overall project area. Each overall survey takes one day to complete.
- Passive acoustic monitoring of cetacean echolocation was conducted using specialized hydrophones (Chelonia T-Pod and C-Pod) which were deployed on the sea bed. This survey was done from May 2009-mid 2011 where there were two successful recoveries and redeployments of equipment in August 2009 and November 2009.
- An acoustic tag receiver was deployed on the seabed to monitor the location of previously tagged fish (VEMCO VR2W receiver mounted on a SeaSpider). The receiver is on loan from the National Marine Fisheries Service (NMFS) and was deployed in May 2009 to collect data for at least one year.
- With the help of Pacific Ocean Shelf Tracking (POST) fish that had been tagged with acoustic tags were able to be monitored in the project site. Thirteen acoustic tag receivers were put across the inlet just south of the project site to monitor tagged fish as they traveled into and out of the project site
- Video monitoring at the forward face of the turbine was done at the site at EMEC off the coast of Scotland.
- A DIDSON unit was installed in the in-situ site to monitor fish as they moved around and through the turbine. The DIDSON system had the ability to be panned and tilted via a remote control.
- Accompanying the DIDSON was a video camera coupled with a single beam acoustic sensor. The acoustic sensor would trigger the video camera to record once an "event" went through the sonar, such as a fish swimming through the area. Once triggered the video camera would start recording until the acoustic sensor no longer detected the presence of marine life.
- Land based sightings were used to help monitor marine mammals. In conjunction with these land-based surveys SnoPud coordinated with vessel traffic, whose operators were instructed to notify SnoPud when a marine mammal was spotted in and around the project area.
- The bottom of the project site was trawled to obtain population estimates for crustaceans and other bottom dwelling animals. These trawls were done during the pre-deployment stage to characterize the area.

⁴ Snohomish County Public Utility District 1, 2012. Admiralty Inlet Tidal Project, Application for a New Pilot Project License (Minor Water Power Project), Volume 2 Exhibit E, FERC Project Number 12690. February 29, 2012.

- Trawls were also done to estimate the populations of native fish to the project site. Different trawling depths were used to characterize fish species at the different depths of the project site.
- Population information for the project site for various crustaceans and fish species was done by the Washington Department of Fish and Wildlife (WDFW). This survey data helped to estimate the population of various species living in the project site

2.4 SnoPud-Hydroelectric (P-2157)⁵

- In the first year of monitoring, five monthly 24-hour hydro acoustic surveys were conducted.
- Also in the first year of monitoring, four monthly sampling surveys were conducted to monitor the population of various fish species.

2.5 MCT-SeaGen⁶

- Used active sonar systems that monitored the area around the turbines to see how sea life (mostly seals) interacted with the turbine when it was operational.

3 Monitoring Options

Based on previous surveys and the requirements drawn out by the Commission, more than one method of monitoring aquatic life population in the FFP *in situ* deployment site may be useful. Each of the previous companies monitored the overall population of fish, mammals, and in some cases birds to ensure that their installations had no effect on both the population and the location of the populations of the aforementioned. Some of the above also closely monitored biological activity at a very close proximity to their installed equipment with high resolution monitoring equipment to clearly see how aquatic life was interacting with their new installation. Taking into account both the activities of other hydroelectric companies and the requirements stated by the Commission, it can be determined that the types of monitoring useful for FFP's *in situ* deployment are overall population monitoring and close proximity monitoring of aquatic life and how it interacts with FFP's installed turbines.

For purposes of this report, due to the preliminary nature of pricing quotes, the specific identities of vendors referenced here have been redacted by FFP and are referenced herein as "Vendor 1," "Vendor 2," etc.

⁵ Snohomish County Public Utility District 1, 2010. Henry M. Jackson Hydroelectric Project, Fisheries and Habitat Monitoring Plan, FERC Project Number 2157. September 2, 2011.

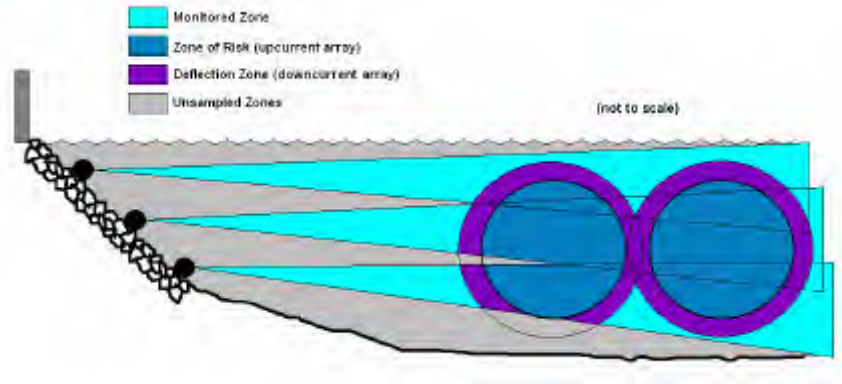
⁶ Marine Current Turbines, 2011. SeaGen Environmental Monitoring Programme, Final Report. January 16, 2011.

3.1 Close Proximity Monitoring

Close proximity monitoring will be useful to characterize fish movement around the front and aft portions of FFP's turbines. The option(s) chosen will be installed after the turbines have been deployed and will monitor the in-situ site for the full twelve months that the turbines are deployed. For close proximity monitoring there are four options:

3.1.1 Acoustic Monitoring

This method calls for an installation of an array of Vendor 16 automated acoustic sensors to monitor the area directly in front of and behind FFP's installed turbines.



3.1.1.1 Figure 3 - Verdant Power Unit Installation

3.1.1.2 Pros

- Vendor 16 is an established company that has worked directly with FERC at a three-day expo that they put on to show FERC the capabilities of hydro-acoustic monitoring. They have been involved in many hydroelectric projects over their 30 years of existence including Verdant Power, river monitoring on the Yukon River, and various surveys of lakes, rivers and dams for environmental groups.
- The automated monitoring system outputs daily counts of fish movement in various areas of the 3-D "electronic grid" established by the acoustic sensors.
- The sensor array notes fish size and direction of travel.

3.1.1.3 Cons

- The sensor array does not identify the species of fish or give a visual image.
- The equipment will be left unattended along the riverbed where it may be stolen.
- With the installation comes a minor disruption of the river environment.

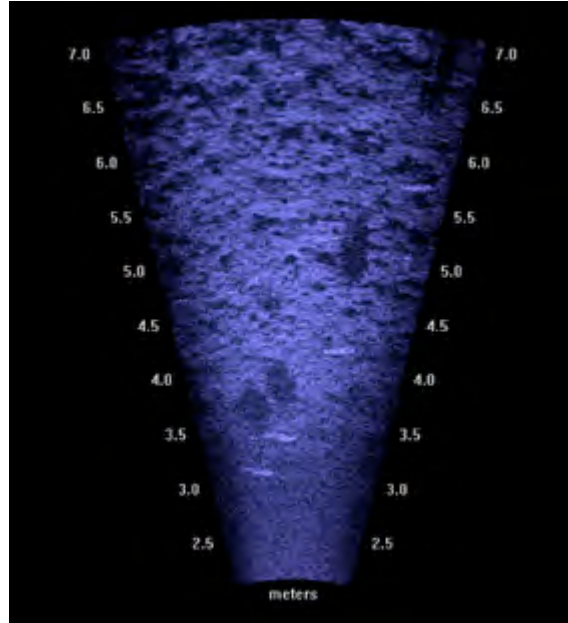
3.1.1.4 Cost

The price for one automated monitoring system is around \$100,000 with one transducer sensor, an Echosounder (surface unit), a data collection laptop with all of the necessary monitoring software, and cabling. Installation costs are \$1,000 per day (usually takes 2-5 days), which does not include any additional costs that may be needed, such as a mounting structure for the sensors. The unit is \$65,000 with only the custom Vendor 16 software on the Echosounder. If more than one transducer is needed for the monitoring effort then each can be bought for an additional cost

of \$20,000. The number of transducers would depend on the proximity to the turbines as the monitoring zone increases with distance. Additional costs could include custom designed housing for the transducer(s). These systems can be rented though it is often more cost effective to buy the system given their long deployment periods for ample monitoring.

3.1.2 High Definition Acoustic Monitoring

This close proximity method calls for the surveillance of the front and aft portions of the turbine with a DIDSON high definition sonar system.



3.1.2.1 Figure 4 - Image of DIDSON profile of a river bottom

3.1.2.2 Pros

- The high image and video quality produced by DIDSON is not affected by murky or turbulent water.
- The image and video quality makes species identification possible.

3.1.2.3 Cons

- The DIDSON is only capable of providing 2D imaging.
- No event counter can be installed on the unit.
- The monitoring range is very short with a maximum range of 30m.
- Video quality degrades as the distance from the sensor increases.
- Installing this system on the riverbed creates minor to moderate river environment intrusion depending on installation location.

3.1.2.4 Cost

The Vendor 17 standard costs are \$74,900, which does not include a mounting device which would be needed for a riverbed installation.

3.1.3 High Resolution Video

This monitoring plan calls for high-resolution video and IR monitoring of the front and the rear of the turbine with BRAVO equipment from Vendor 18.



3.1.3.1 Figure 5 - Picture of Fish Through Vendor 18

3.1.3.2 Pros

- The high-resolution video feed makes it possible for species identification.

3.1.3.3 Cons

- Given the low visibility in the river, this would make this option ill fitted for FFP's monitoring plan.

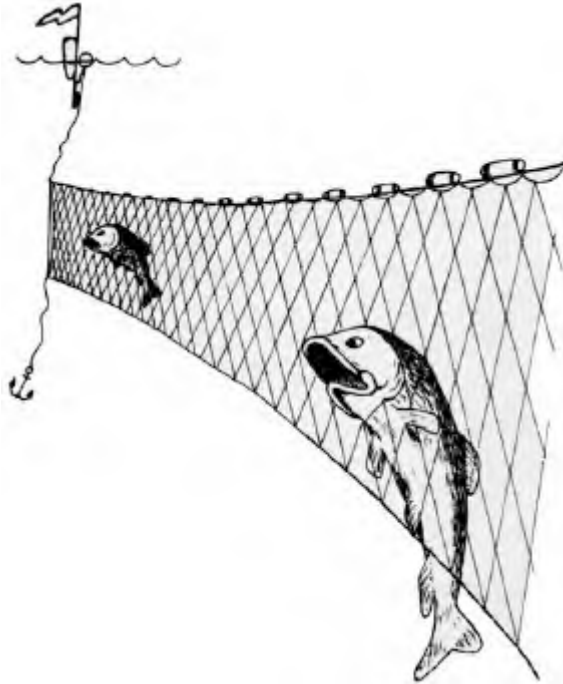
3.1.3.4 Cost

One system with high resolution video sensors and temperature sensors, real-time video broadcast with two computers, cabling, all the necessary software, installation, and online live video hosting for data analysis costs a little over \$18,000. Remote secondary data processing with fish count summaries, species identification, size classifications free for the first year, but \$750/month after.

3.1.4 Net Installation on a Turbine

In this method, netting is installed on the outlet of one of FFP's turbines and periodically retrieved to examine and record the characteristics of the fish trapped inside of them. Initially the nets will be retrieved in short intervals to ensure that the net system is working properly and the appropriate recovery time can be judged. One netting survey will be done in each quarter. The best methodology for deployment and retrieval of the net was determined to be a 100ft long net

with two remotely activated flotation devices that would be attached to the net. These devices would bring the back half of the net up to the surface where an anchored boat would be waiting to retrieve the net. The aft half of the net would be taken off and an inflatable buoy bag would be placed on the aft portion of the forward half of the net.



3.1.4.1 Figure 6 - Picture of a Typical Gill Net Setup

3.1.4.2 Pros

- This system provides full characterization of the fish that pass through the turbine.

3.1.4.3 Cons

- The nets may break and separate from the diffuser and get tangled in the blades of a leeward turbine.
- It may be difficult to prove that fish have not been damaged by the turbine blades as net could damage the fish and cause the trapped fish to bleed to death.
- Given the low visibility conditions of the Mississippi River and the high rate of flow, using divers is not a feasible option for moderate to high flow conditions.

3.1.4.4 Cost

- Vendor 1 was able to provide two estimates in the form of day rates. For a full twelve hour day with a four person crew which they deemed the necessary amount of people for the job the cost would be \$3,460. This would mean that the job would last between 2-4 hours on the water. If the job lasts longer than 4 hours then the rate would be \$5,080. Vendor 1 has a boat equipped with side scan sonar which they would use on FFP's

project site while conducting their work with no additional cost. Vendor 1 has been working on jobs on the Mississippi River for over 35 years and is very experienced in a wide variety of jobs on the river. Their rates would go up significantly (approximately double) if the *in situ* site fell within Army Corps jurisdiction as prevailing wages would be applied. Vendor 1 would only be comfortable diving in low flow conditions.

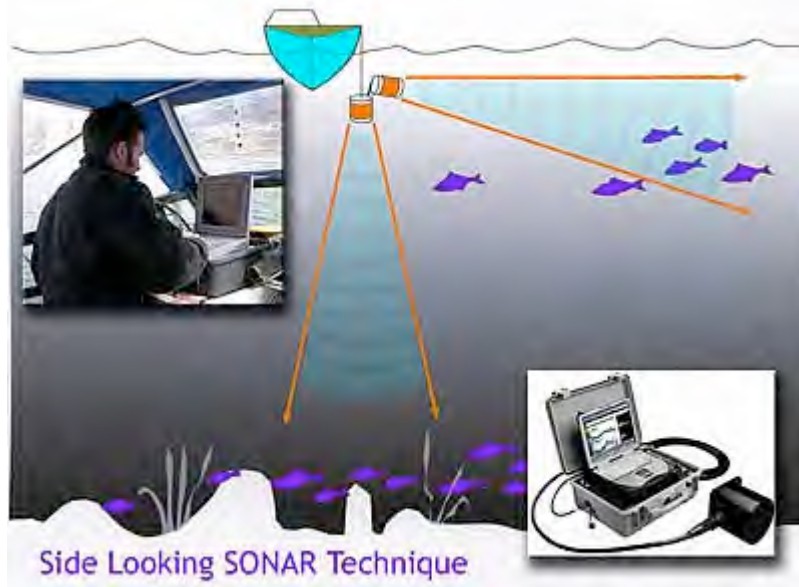
- A possible mechanism to deploy and retrieve the netting would involve the use of underwater winches. Vendor 19 builds customized underwater winches for job specific applications and the prices of these systems go from \$50,000-\$75,000 a piece.
- Vendor 9 has developed remotely inflatable buoyancy devices that can be activated through acoustic, electrical, or mechanical means. Vendor 9 offers three different options that could suit FFP's needs for an underwater flotation bag.
 - One is an acoustic release system where an acoustic transducer sends down a pulse to an acoustic receiver on the float that when actuated sends a signal to the tank attached to the buoy to release the gas and inflate the buoy. The cost for just the acoustic release system would be \$11,000 and the cost for a buoy bag with a 19ft³ canister of gas would be \$2,500.
 - A surface buoy would be deployed that would tether directly to the buoy bags on the net. A boat would then go up to the buoy and transmit an electric pulse that would activate the canisters on the buoy bags to inflate. The cost of this electrical release system would be roughly \$2,000 while the buoy bags would come at \$500 apiece.
 - A surface buoy would be deployed that would tether directly to the buoy bags on the net. A boat would then go up to the buoy and transmit compressed air into the line on the buoy that would inflate the buoy bags directly. The cost for this inflation method would be \$500 while the cost for a buoy bag would be \$500.
- Vendor 4 quoted a 100-foot net for FFP to be used on the back of the turbines for \$8,543. This price did not include a mounting method to the aft portion, which would cost approximately \$1,000 based on an engineering estimate.
- Vendor 8 provided a ballpark estimate for load cells which may be installed on the net to show when the net needs to be retrieved from the river. Given the expected loads on FFP's load cells (<1000 lbs) the load cells would be "S" shaped with an I-bolt connection to the turbine. The cost of a typical load cell for FFP's application would be between \$2,500-\$3000 not including cabling which would cost about \$3/ft. for underwater cables.
- Vendor 6 also makes acoustically actuated systems, though their systems release an already inflated buoy tethered on a rope to the surface by releasing the spool of rope holding onto the buoy. A rough estimate for one of these systems would be between \$6,000-\$7,000. Renting a system could be done through Vendor 7.
- Vendor 10 has release systems that release after a certain time that cost between \$4,000-\$5,500. This system also uses a spool and an already inflated buoyancy bag

3.2 Overall Population Monitoring

The population of the aquatic life living around FFP's deployment site can be monitored to address requirement (4) from the Commission. For overall population monitoring there are five options.

3.2.1 Hydro-Acoustic Surveys

Conduct monthly hydro acoustic surveys with a boat-mounted acoustic sensor (Vendor 16) to determine the fish population during pre and post deployment. Survey area should be 100m upstream of deployment site, 500m downstream and 100m to each side (Total area of 650m x 225m including dimensions of project site). Surveys should be done once every two weeks for both the pre-deployment and post-deployment periods of the *in situ* deployment.



3.2.1.1 Figure 7 - Vendor 16 Hydro-Acoustic Survey Displayed

3.2.1.2 Pros

- With this system there are no permanent installations on the riverbed; minimal environmental impact.
- This method has been used by every river study listed in this document.
- The sensor used in this survey can double as a bathymetry measuring instrument.

3.2.1.3 Cons

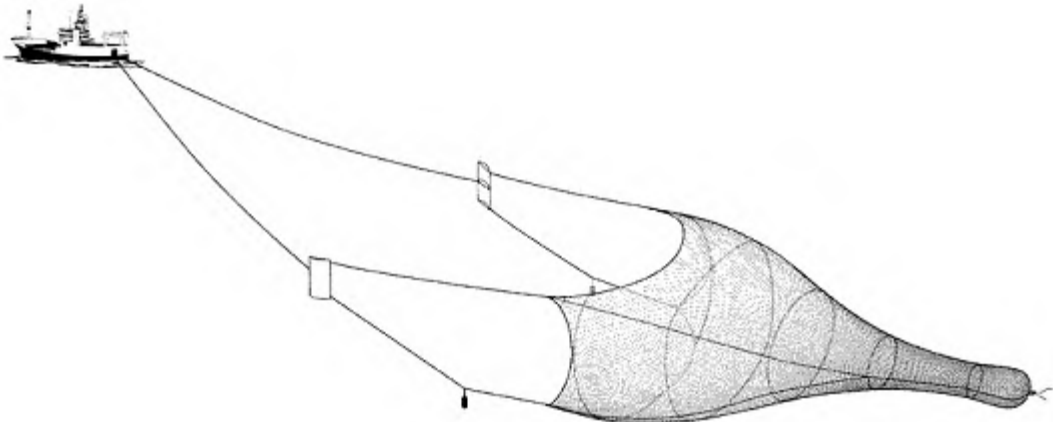
- The fish type cannot be determined using this setup.
- The additional costs of renting a boat and hiring someone to drive it must be factored into this option.
- It is impossible to obtain the fish population level with 100% certainty (may miss some going by as you scan one section of the river and the possibility of counting the same fish multiple times).

3.2.1.4 Cost

- The entire system needed (Vendor 16) to conduct one of these studies costs \$40,000 which includes cabling, an Echosounder, data collection software and a transducer. Additional costs of having to hire someone to drive over the site to do this monitoring must also be factored in.
- Vendor 20 has a similar system that has a high-resolution transducer capable of accurate readings down to 1,000ft. The system has two capabilities, one is that you can tune the system for the size of a certain species of fish and the system will identify these fish and the direction they are swimming in as well as the overall length and size of each fish. The system also has a biomass option that outputs the amount of “fish flesh” per meter of water. This gives the overall mass of fish in a certain volume, but does not provide the number of fish or any type of species identification. This unit costs \$38,000. For an additional \$10,000, a system called the Olex can be added that can determine the height of the river bottom and its contours.
- A day rate was provided by Vendor 2 for conducting a single beam bathymetric survey over FFP’s project site. The pricing for a full day’s work on FFP’s project site is \$3,450.

3.2.2 Netting Surveys

Netting surveys will be used for direct population study using an agency recommended net to trawl for fish in the project site. According to the Miranda report the most effective method would be an otter trawl.



3.2.2.1 Figure 8 - Netting Survey with an Otter Trawl

3.2.2.2 Pros

- The otter trawl allows full characterization of the fish that are caught in its net.
- This method is generally more accurate than a mobile acoustic survey as it does not double count fish and you have less of a likelihood to miss fish swimming through the project area.

3.2.2.3 Cons

- Given the flow rate of the river at FFP's project site, trawling may be difficult.
- The size of the project area as well as its contour may also add to difficulty of trawling.
- This survey has the potential to disrupt river traffic.
- There will be no way to capture fish swimming around the turbines.

3.2.2.4 Cost

Vendor 3 was able to provide costs for an electro fishing effort, but these costs can translate directly to the cost of a netting effort. These costs are seen below:

Develop study plan

bio \$125/hr x 8 hrs = \$1,000

Travel, preparation and sampling

2 techs \$80/hr x 80 hrs = \$6,560

1 tech \$80/hr x 24 hrs = \$1,920

Data entry

tech \$80/hr x 8 hrs = \$640

Report/memo

bio \$125 hr x 8 hrs = \$1,000

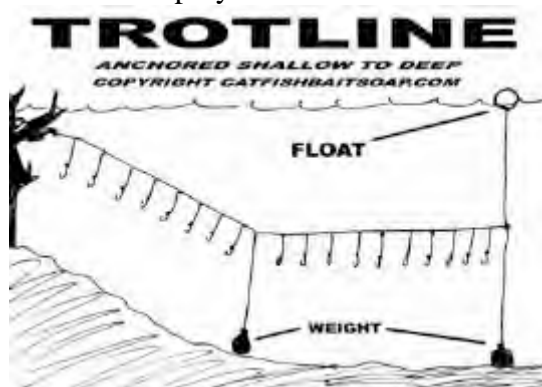
Travel and Boat

Travel and boat expenses = \$2,000

Total: \$13,120

3.2.3 Trotlines

Trot lines will be installed around the deployment site to catch the fish living there.



3.2.3.1 Figure 9 - Trotline Deployed on a River Bottom

3.2.3.2 Pros

- A trotline would allow for the ability to identify the species of fish as well as record its characteristic measurements.

3.2.3.3 Cons

- The trotline may interfere with boat traffic if the line is in danger of becoming tangled in boat propellers or if the floats are deployed in the middle of the river.
- This method is not very effective as fish may swim right by hooks.

3.2.3.4 Cost

- Trotlines typically cost under ten dollars. The cost for deploying a trot line must also be factored in. A typical day rate for a collection effort such as this one would cost \$1,580 (based on day rates from Vendor 2).

3.2.4 Electro fishing

This method utilizes the applications of a small shock to stun the fish and bring them to the surface for collection in a boat.



3.2.4.1 Figure 9 - Electro Fishing on a Small Boat

3.2.4.2 Pros

- This is a safe, very effective way to collect fish. No permit is necessary if there are no threatened or endangered species in the site area.

3.2.4.3 Cons

- With a high river speed at and around FFP's project site, it may be very difficult to corral fish at the surface.
- Depending on the water conductivity level it may not be an effective option (lower water conductivity desirable) as the electricity may not pass through the fish.
- Electro fishing is most effective in shallow water with a low river velocity, which is incompatible with the characteristics of FFP's *in situ* deployment site.

3.2.4.4 Cost

Vendor 3 was able to provide some rough estimates for the costs associated with an electro fishing effort in an area roughly as large as FFP's project site (once FFP's project site is determined they will be able to provide more exact estimates). Vendor 3 recommends electro fishing over a netting operation due to the depth of the river and the overall area of FFP's project site. Electro fishing would involve a one-day study period where FFP's site would be surveyed to determine the best way to conduct an electro fishing operation, a half a day of work to file for the permit through the state, and three days to conduct sampling efforts. Below is a more specific list of the costs of the operation:

Develop study plan

bio \$125/hr x 8 hrs = \$1,000

Determine permitting requirements and obtain permits

bio \$125/hr x 16 hrs = \$2,000

Travel, preparation and sampling

2 techs \$80/hr x 80 hrs = \$6,560

1 tech \$80/hr x 24 hrs = \$1,920

Data entry

tech \$80/hr x 8 hrs = \$640

Report/memo

bio \$125 hr x 8 hrs = \$1,000

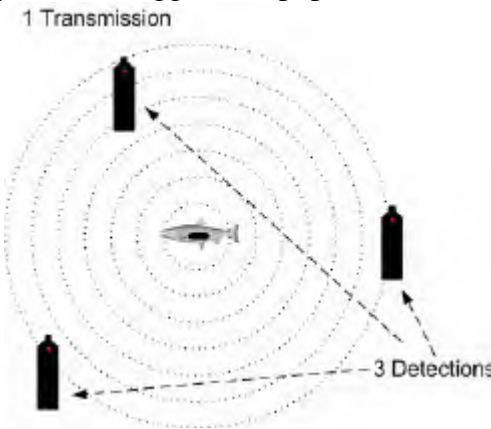
Travel

Travel and boat expenses = \$2,000

Total: \$15,120

3.2.5 Telemetry

Use telemetry to continuously monitor tagged fish population around the *in situ* site.



3.2.5.1 Figure 10 - Image Depicting Telemetry for Aquatic Surveying

3.2.5.2 Pros

- This is an accurate way of tracking fish within project area. For Vendor 21, this accuracy is to within 15 meters on the general model and to within 6 meters on the finely adjusted model, the latter of which also maps in 3D.

- The United States Fish and Wildlife Service (USFWS) and the United States Geological Survey (USGS) are interested in expanding their telemetry survey of pallid sturgeon in the Mississippi River, so coordinating with them maybe possible.

3.2.5.3 Cons

- A tagging effort must be done by FFP in order to track other types of fish species currently not tagged in the Mississippi River.
- It will be impossible to tag every fish in the project site, thus every fish cannot be monitored. This becomes especially detrimental to the monitoring effort if the fish that inhabit the project site are migratory.

3.2.5.4 Cost

- Vendor 21 has two systems that could be deployed:
 - A VR2W receiver which is battery operated acoustic receiver and hydrophone which has a range of 300-400m. The system has not been tested near hydrokinetic turbines so it is not known whether the electrical interference generated from the turbine arrays will take away from the range of the receiver. Data is taken by a blue tooth receiver when you come into close proximity with the receiver. Each receiver costs \$1,460.
 - Vendor 21 is developing a new advanced system that can be powered by cable and accessed by Ethernet tether to extract data. This system can be battery powered and in the event that it is being powered by cable and the cable connection breaks it can seamlessly convert to battery power. This system can also measure fish location in 3D. Data can be emailed to Vendor 21 directly and they will convert it to 3D usable data. The software pack costs \$250 if it is desired that the data be converted directly. The system costs \$3,800 and comes with the sensor and a 5m cable.

Accessories/Notes:

- Individual tags for fish cost between \$330-\$350 generally.
- Advanced tags for fish that allow for 3D tracking cost \$580.
- In order to track fish progress through the project site triangulation would need to be established which would require 4-9 sensors.
- A tag would need to be put in the middle of the river to serve as a reference point for the receivers. This tag would cost \$390.
- Servicing for setting up a triangulated site costs \$5,000.

4 Recommendation

4.1 Close Proximity Monitoring

The following table is a summary of the options reviewed.

	Vendor 16 System	Vendor 17 System	Vendor 18 System	Gill Netting	Comments
Practical for Mississippi River Monitoring?	Yes	Yes	No	Yes	
Is Species Identification Possible?	No	Yes	Yes	Yes	Vendor 17 system is not 100% accurate.
Can the Population of Fish be Quantified?	Yes	No	No	Yes	
Is this Method Harmful to the Environment?	Yes	Yes	Yes	Yes	All involve installing directly on the project site. Gill netting is by far the most harmful as it kills the fish it catches.
Relative Cost	High	Moderate	Low	Moderate	
Relative Risk of Not Achieving Useful Result	Certain	High	Certain	Moderate	The Vendor 16 system on its own will not be able to identify fish species. The Vendor 18 system will not be able to be used to see fish due to the murky water of the Mississippi River. The Vendor 17 system will not be able to distinguish between the two species of pallid sturgeon that will inhabit the area around FFP's project site.

Setting up a net behind one of FFP's turbines is FFPs recommendation (unchanged from previous reports) to monitor fish in a close proximity setting to FFP's turbine. A Vendor 16 system, though effective in detecting fish, would not be able to determine the fish species type through its sensors which is pivotal to FFP's monitoring needs. Given the high cost of a Vendor 16 system, it would not seem cost effective to install to solely monitor the overall fish population in close proximity to the turbine. A Vendor 17 system would be able to identify most fish types, but given the small difference between the American sturgeon and the pallid sturgeon, both of which should be prevalent in FFP's project site, a Vendor 17 system would not be adequate in determining the difference between the two.

Once the turbines have been deployed the most appropriate means to measure and record the fish population that passes through FFP's turbines would be a long, two part 100ft net attached to the turbine with two acoustically inflatable buoys attached to the net. One net would be continually deployed and redeployed on one turbine while the other would be installed on different turbines to determine any close proximity variability in fish population in the project area. Four days of testing the deployment method would be done in the first week of the in-situ deployment with three deployments during three different seasons as well.

4.2 Overall Population Monitoring

The following table summarizes the options reviewed.

	Hydro-Acoustic Surveys	Netting Surveys	Trotlines	Electro Fishing	Telemetry	Comments
Practical for Mississippi River application?	Yes	Yes	Yes	No	No	Telemetry is not practical in tracking the total population of fish in the project area.
Specific Species Identification?	No	Yes	Yes	Yes	Yes	
Is it Harmful to the Environment?	No	No	Yes	No	No	Trotlines are the only method with a permanent installation required in the project area.
Relative Cost	Low	Moderate	Low	Moderate	Moderate	
Relative Risk of Not Achieving Useful Result	Moderate	Moderate-High	High	High	Certain	Vendor 3 said that net surveys would be very difficult over FFP's project site. Trotlines will not be a very effective means of characterizing the fish population in FFP's project site as they will not catch the majority of fish that inhabit FFP's site. It will be very difficult to corral fish at the surface of the river in an electro fishing effort with the speed of the river. With a telemetry survey we would only be able to monitor tagged fish and therefore we would miss lots of species in FFP's monitoring effort, especially migratory fish that travel through FFP's project site.

The mobile survey option, which was conducted by most of the companies listed at the beginning of this document is the most effective option for a population survey. Electro fishing

would be thorough in being able to count all of the fish in the immediate project area but with the flow of the river it would be impractical as fish would be carried down river quicker than they could be corralled. Netting trawls would also be difficult with the bathymetry of the river and it would not be able to quantify the number of fish immediately around the project area.

5 Cost Analysis

The following is a scenario recommended by FFP and is discussed herein for agency consideration and additional consultation, if necessary.

For mobile acoustic surveys to monitor overall fish populations the estimate provided by Vendor 2 will be used. For the pre deployment period there will be 12 surveys conducted in total with a day rate of \$3,450 for a total cost of \$41,400 (these surveys would also be done in conjunction with the hydraulics surveys). For post deployment, surveys would be done at the same frequency of twice a week for the yearlong period for a total cost of \$82,800 (these surveys, too, would be done in conjunction with the hydraulics surveys). For the net installation it was estimated that there would be four days during the first week of deployment where the nets would be continuously deployed and retrieved to ensure that the methodology of doing so was sound. This could cost \$20,320 (four days of 10 hour work on the river with overnight accommodations factored into the cost from Vendor 1 \$5,080/day). FFP outlined that there would be four netting efforts in total, where deployment and retrieval would cost \$10,380 (three days of 10 hour work on the river without over night accommodations factored into the cost from Vendor 1 \$3,460/day). The cost for the nets themselves would be \$17,086 (for two nets from Vendor 4). This price does not include the cost associated with mounting the nets to the turbines which, through an engineering estimate, can be estimated to cost an additional \$1,000. This would be some apparatus (in all likelihood a fixture with ropes attached to the turbine in some fashion) that would connect the front of FFP's hoop net to the diffuser of the turbine.

Activity	Cost	Comments
(Pre-deployment) Bi-weekly single beam acoustic surveys to characterize fish populations.	\$41,400*	Based on day rates from Vendor 2. (\$3,450/day)
(Post-deployment) Bi-weekly single beam acoustic surveys to characterize fish populations.	\$81,800*	Based on day rates from Vendor 2. (\$3,450/day)
(Post-deployment) Install and retrieve two nets behind two turbines a total of four times during the initial week of installation and then three more times at different times of the year (spring, summer, fall) after that	\$99,786	-\$22,000 for two acoustic release systems for the buoys (\$11,000 per buoy) -\$5,000 for the price of two remotely inflatable buoys (\$2,500 per buoy) -\$20,320 (four days of 10 hour work on the river with overnight accommodations factored into the cost from Vendor 1 \$5,080/day) -\$10,380 (three days of 10 hour work on the river without overnight accommodations factored into the cost from Vendor 1 \$3,460/day) -\$17,086 for two nets from Vendor 4. -\$25,000 engineering estimate for a methodology to attach the front half of the net to the turbine.
Total Cost	\$198,986	

*Note on the total cost matrix the cost for the mobile surveys for the hydraulic surveys and the fish population surveys are split between the two, since the same survey boat will be doing the hydraulic and fish population surveys.



239 Causeway Street
Boston, MA 02114-2103
USA

MAIN: (978) 252-2822
FAX: (617) 367-3372

www.free-flow-power.com

Filename: 2012-06-28_R01_Insitu_Netting_Plans

Subject: In-situ Netting Plans

Date	Release Rev	Description
05-04-2012	00	Original
6-28-2012	01	Revisions after initial review

1 Introduction

This document will present various concepts investigated to serve as the netting installation to be used in the in situ deployment. This document will examine each concept, how it was meant to be implemented, and why it was ultimately deemed fit/unfit for the in situ deployment.

2 General Obstacles for Deployment/Retrieval

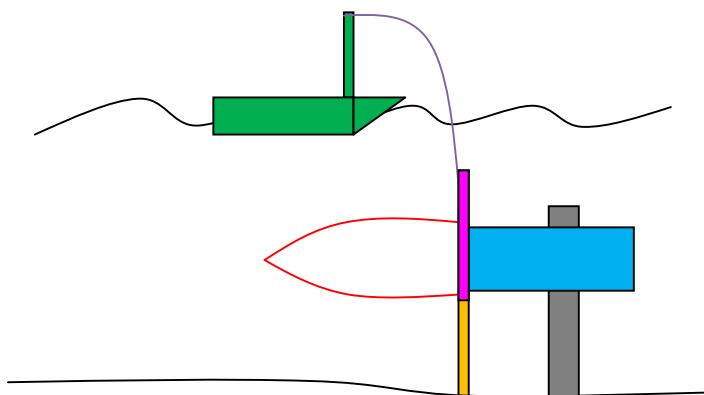
- Divers will not dive in high flow conditions and it is a goal of FFP to conduct at least one turbine entrainment survey in these conditions.
- The torque generated by the high velocity of the river during high flow conditions makes mounting structures that extend above FFP's piling not feasible as they would deform due to the drag force.
- The low visibility of the Mississippi River makes it hard for divers to work in the most ideal conditions that the river presents (low flow rates at low water level).
- Hydraulics would be very challenging to obtain approval for as they could leak chemicals into the waters of the project area.
- Vendor 4 could bring FFP's net size down to a 2.25" mesh, though this would almost double the cost of the net as almost twice as much material is being used. They currently have 4" mesh in stock, were we to order a 2.25" mesh it would take 4-6 weeks to make.
- The removable portion of the net could be moved up or down the net to wherever we wanted it to be placed.

3 Proposed Monitoring Efforts

3.1 Piling Mounted Net System

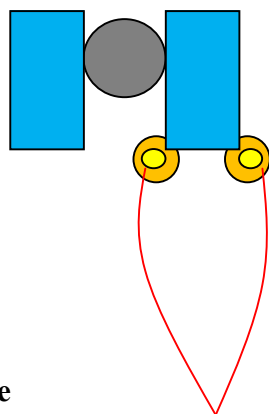
Raise and lower the net on two pilings installed behind the turbine. The net is mounted on a fixture which can slide up and down the two net pilings

SIDE VIEW



Main Piling
Turbine
Net Piling
Net
Boat
Lift Cable
Net Mount to Net Piling

TOP VIEW



Deployment/Retrieval Procedure

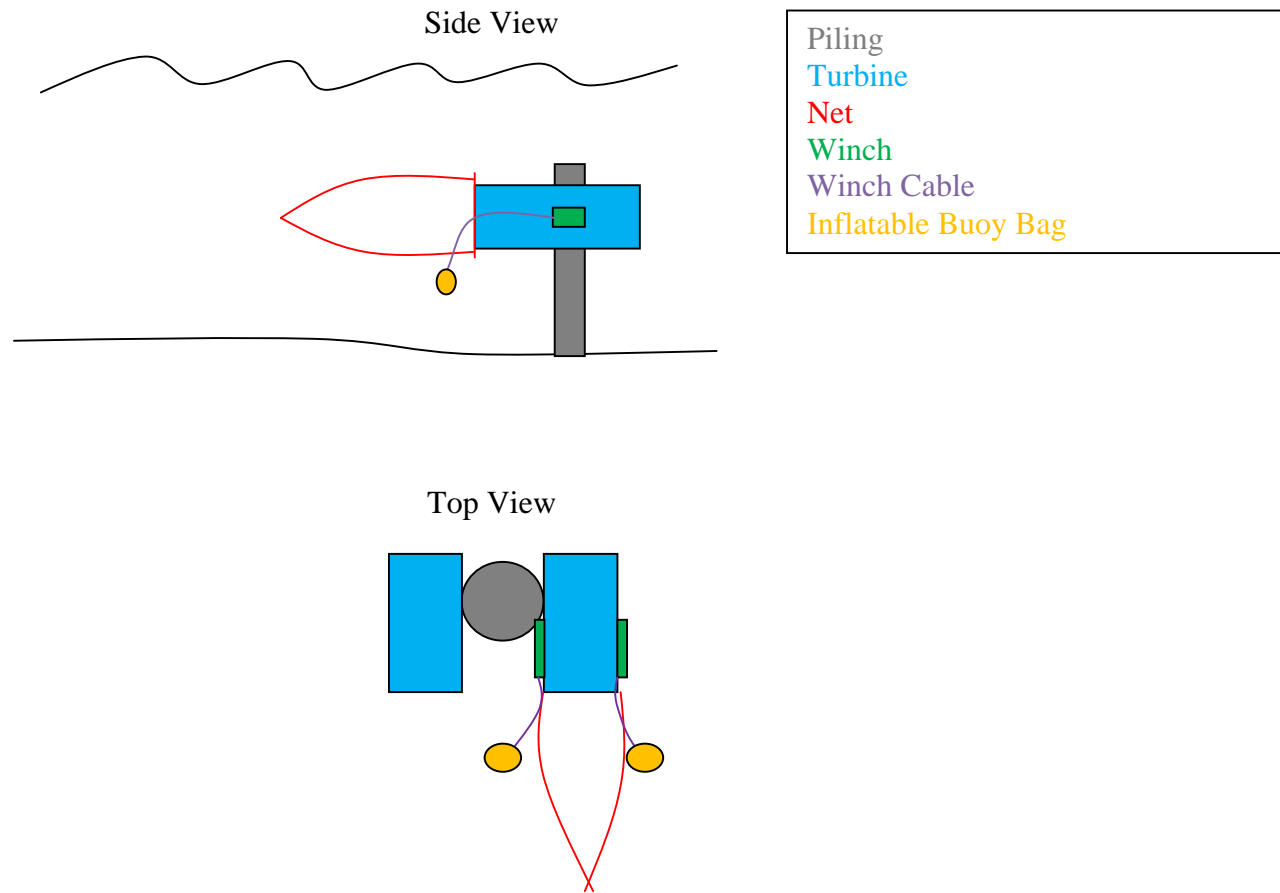
- 1.) A crane would latch onto an eye hook or an equivalent on the net mount and raise the mount and net to the surface.
- 2.) After the fish had been quantified the crane would lower the net its mount onto the pilings until it rested into its appropriate place.

Considerations

- In high water condition the torque generated on the net pilings from the flow would be very high and would cause the net piling to bend.
- Lowering the mount onto the net pilings in high water conditions would be difficult with no visibility.
- Divers could be used in high water conditions, but they are costly and will not dive while the river is flowing at a high rate like that experienced during high water conditions.

3.2 Winch Deployment System

Install two to four winches on the side of the turbine to release and reel in the net to the back of the turbine.



Deployment/Retrieval Procedure

- 1.) Once a boat had made its way to the project site it would remotely activate the inflatable buoy bag to inflate, sending it to the surface.
- 2.) Once the buoy bag was visible on the surface, the winch would be reeled out sending the net up to the surface.

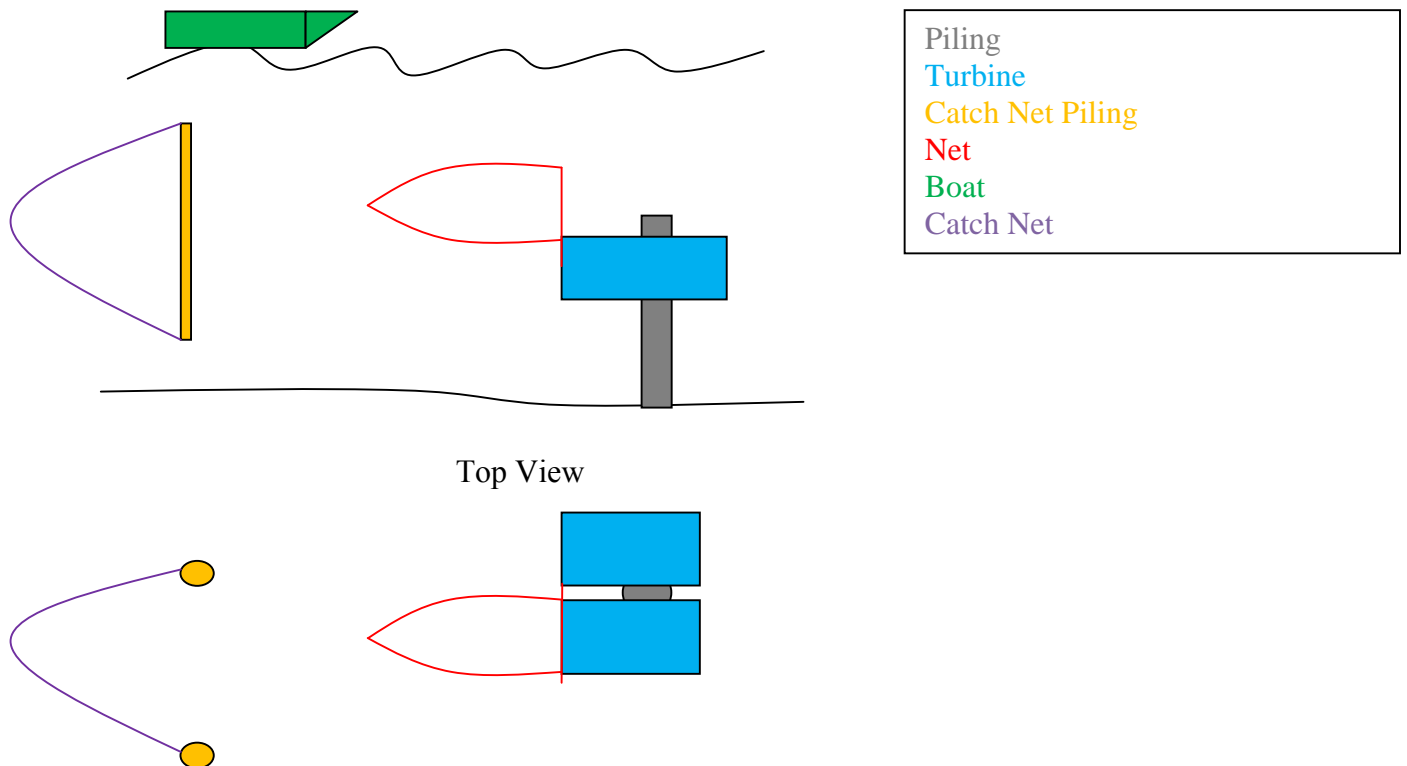
3.) After the net had been cleaned out and a new deflated buoy bag had been installed on the end of the winch cable, the winch would reel in the net until it had reached its proper position behind the turbine.

Considerations

- The cost of an underwater winch cable system from Vendor 19 ranges between \$50,000-\$75,000.
- In sending the net up to the surface and reeling it in through the winch cables there is a possibility that the cables will become tangled in the turbulent flow.

3.3 Release Net Method

In this method the fish would be caught in the net behind the turbine and then the net would be triggered to open up and release the fish into a larger net downstream.



Deployment/Retrieval Procedure

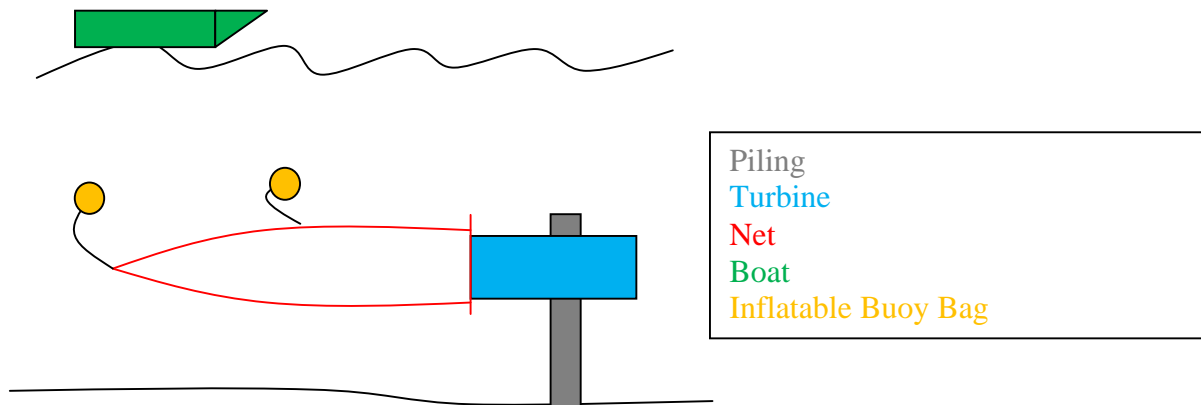
- 1.) Once the net fills with fish it would be actuated by some mechanism to open up from the back and spill its contents into the catch net.
- 2.) A boat would then pick up the net from above.
- 3.) After the net had been cleared of its contents it would be redeployed on the catch net pilings below.

Considerations

- The initial net may not release all of its contents as some fish may get caught in the netting and not spill out into the catch net.
- Redeploying the net would be difficult in high water and would require higher pilings which would be subject to a significant amount of torque from the river flow.
- Retrieving the net and ensuring that no fish spilled out of the net upon retrieval would also be difficult to prove.

3.4 Long Net with Inflatable Buoys

Deploy an approximately 100ft behind the turbine and engage inflatable buoys to raise the back half of the net up above the water. The net would have a throat at the 50ft. mark to ensure that fish who swim into the net would become trapped in the latter half of the net.



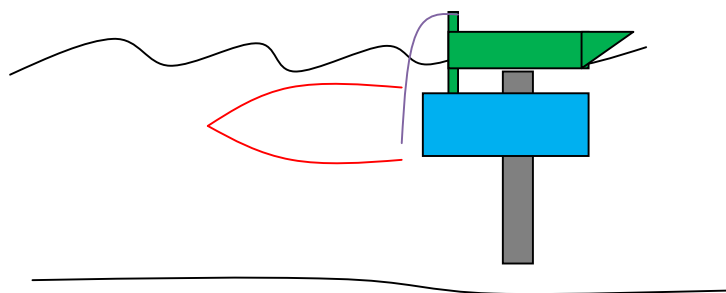
Deployment/Retrieval Procedure

- 1.) When the net is ready to be retrieved the buoy bags are inflated and they will rise to the surface bringing the back half of the net with them. An anchored boat will be waiting above and will pull the net in using the inflatable buoy bags as a reference.
- 2.) Once the back half of the net has been emptied the inflatable buoy bags will be replaced and the net will be redeployed over the side of the boat.

- **Considerations**
- If a small net mesh size is used then the net could tangle itself during retrieval and redeployment.
- Since the net opening remains fixed to the turbine, the net length needs to be sized so it will reach the surface whether at high water (-65 ft) or low water (-20 ft).

3.5 Fishing Boat with a Trawl Net

Using a winch system on a fishing boat lower a trawl net behind the turbine. The boat would have acoustic sensors on board which would help to guide the net down to the turbine.



Piling
Turbine
Net
Boat
Winch Cable

Deployment/Retrieval Procedure

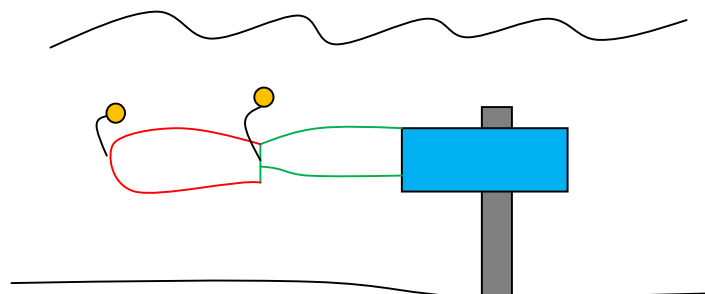
- 1.) The fishing boat would locate the turbine and then deploy a net behind the turbine.
- 2.) After a certain allotted time the net would be retrieved from a winch cable system on the boat and then redeployed in the same manner.

Considerations

- Finding the turbines is going to be difficult and time consuming, Vendor 1 estimated that it would take approximately two hours to find the turbines even with GPS coordinates.
- It will be nearly impossible to determine whether the net is exactly behind the turbine.
- Without fixing the net to the turbine, the net is going to be hard to control.

3.6 Install a Two Part Net Behind the Turbines

A portion of the net will be permanently attached to the turbine while a removable portion of the net will be installed at the end of the attached portion of the net. The permanent section of netting would have a throat to guide fish into the removable portion.



Piling
Turbine
Removable Portion of Net
Permanent Portion of Net
Inflatable Buoy Bag

Deployment/Retrieval Procedure

- 1.) With both portions of the net deployed, the inflatable buoys would be inflated by an overhead acoustic transducer from a boat, raising the back portion of the net.
- 2.) The removable portion of net is then removed and the fish are characterized.
- 3.) If an immediate redeployment is desired the removable portion of net is reinstalled to the permanent portion of netting, otherwise the forward most inflatable buoy bag is deflated and put back into the water attached to the permanent portion of net.

4.) To reinstall the net to turbine, the inflatable buoy bag is inflated in the same manner and when the aft portion of permanent net is risen to the surface and the removable portion of net is attached.

Considerations

- Fish may get trapped in the permanent portion of net and therefore would not be accounted for when pulling the net to the surface.
- There is a significant risk of tangling the net at the surface during retrieval and redeployment.

4 Recommendation

The following tables summarizes the netting options reviewed.

	Piling Mounted Net System	Winch Deployment System	Release Net Method	Long Net with Inflatable Buoys	Fishing Boat with a Trawl Net	Two Part Net Deployment System	Comments
Will this method work in all flow conditions? (high and low flow)	No	Yes	Yes	Yes	Yes	Yes	The torque generated on the pilings would deform them to the point where they would not be usable.
Is this method relatively costly?	Yes	Yes	No	No	No	No	Underwater winches from Vendor 19 cost at a minimum \$50,000 for one system.
Are there major logistical concerns with deployment and retrieval of the net?	Yes	No	Yes	No	Yes	No	Finding the project at the bottom of the river which according to river divers is going to be very difficult and time consuming.

5 Thoughts for Future Designs or Design Modifications

- It may be in FFP's best interest to have several different sections of the removable portion of the net made with different mesh sizes to determine through trial and error which mesh size is most effective in capturing the fish around FFP's *in situ* deployment

site. It should also be recorded how much debris each net captures as this should be minimized as much as possible.

- The permanent portion of the net installed on the turbine may want to be made with a net material that is stronger than the removable portion as it would be installed on the back portion of the turbine for months at a time.
- After consulting with USACE and independent expertise, the range of fish sizes that should be inhabiting the mid water column where FFP's turbines will be deployed is fish ranging from 3 inches (juvenile shad and shiner) to 3 feet (sturgeon and cat fish) in length. A very small mesh size would need to be used in order to obtain this wide array of fish sizes (1/4"-3/4"), but with a small mesh size the load that the net can take is significantly decreased.
- A possible addition to the net system could be load cells to help determine when the appropriate time would be to go and retrieve the nets from the river.
- Vendor 10 makes timed release systems that are roughly \$10,000 cheaper than acoustic releases. These systems could be used instead of the acoustic releases if a proper time for deployment can be established.